PhD. 102050

AIRBORNE GEOPHYSICAL INVESTIGATIONS OF SUBGLACIAL STRUCTURE OF WEST ANTARCTICA

EDWARD JAN JANKOWSKI

A dissertation submitted for the degree of Doctor of Philosophy in the University of Cambridge.

Queens' College

Cambridge

August 1981

CONTENTS

Preface			i
Summary			iii
CHAPTER 1	PREVIOUS GEOLOGICAL AND GEOPHYSICAL WORK IN WEST ANTARCTICA		1
1.1		Introduction	1
1.2		West Antarctica and Gondwanaland	2
	1.2.1	Introduction	2
	1.2.2	Reconstructions of Gondwanaland	4
	1.2.3	Breakup of Gondwanaland	6
1.3		Tectonic evolution of Antarctica	9
1.4		Antarctic Geology	14
	1.4.1	Introduction	14
	1.4.2	East Antarctic Shield	15
	1.4.3	Transantarctic Mountains	19
	1.4.4	Thiel Mountains	26
	1.4.5	Pensacola Mountains	27
	1.4.6	Shackleton Mountains	30
	1.4.7	Ellsworth Mountains	31
	1.4.8	Whitmore Mountains	33
	1.4.9	Marie Byrd Land	34
	1.4.10	Ellsworth Land	36
	1.4.11	Antarctic Peninsula	38
1.5		Geophysical Studies	41
	1.5.1	Introduction	41
	1.5.2	Radio Echo Sounding (RES)	42
	1.5.3	Oversnow Traverses	43

1.5.4 Aeromagnetics 47
1.5.5 Seismological Studies 51
1.5.6 Palaeomagnetic Studies 53
1.5.7 Marine Geophysics 57
1.6 Structure of West Antarctica from Geophysical Studies 60
1.6.1 Subglacial Topography of West Antarctica 60
1.6.2 Upper Crustal Structure 61
1.6.3 Deep Crustal Structure 66
1.6.4 Boundary between East and West Antarctica 67
1.7 Problems to be solved 68

CHAPTER 2 DATA COLLECTION AND REDUCTION 71
2.1 Introduction 71
2.2 Flight Planning 73
2.3 Radio Echo Sounding 77
2.3.1 Equipment 77
2.3.2 Digitisation of Records 80
2.3.3 Navigation Data Recording System 81
2.3.4 Navigation 83
2.3.5 Altimetry 84
2.3.6 Discussion of Errors 86
2.3.7 Compilation of Ice Sheet Surface Map 90
2.3.8 Compilation of Bedrock Map 92
2.4 Magnetics 94
2.4.1 Equipment 94
2.4.2 Geomagnetic Field 95
2.4.3 Regional Field, Secular and Diurnal Variations 95
2.4.4 Compensation of data 101

2.4.5 Sources of error 104

2.4.6 Magnetic Properties of rocks 105

CHAPTER 3 WEST ANTARCTIC ICE SHEET 109

3.1 Introduction 109

3.2 Ice Surface Morphology 110

3.3 Drainage of the West Antarctic Ice Sheet 116

3.4 Grounding Line of the Ronne-Filchner Ice Shelf 121

3.4.1 Isostatic Considerations 127

CHAPTER 4 BEDROCK IN WEST ANTARCTICA 130

4.1 Introduction 130

4.2 Subglacial Morphology 131

4.3 Isostatic Displacement of West Antarctica 137

4.3.1 Theory 139

4.3.2 Application 141

4.3.3 Limitations of Method 146

4.3.4 Discussion 149

CHAPTER 5 ANALYSIS OF MAGNETIC DATA 153

5.1 Introduction 153

5.2 Magnetic Profile Analysis 153

5.2.1 Smoothing of Data 154

5.2.2 Depth to Magnetic Basement 156

5.2.3 Computer Modelling 162

5.2.4 Transformation of Profiles 170

5.2.5 Theoretical Tests of Programs 173

5.3 Areal Approach 183

CHAPTER 6		GEOLOGICAL AND TECTONIC INTERPRETATIONS	185
6.1		Introduction	185
	6.2.1	Cenozoic Volcanic Province	186
	6.2.2	Byrd Subglacial Basin	191
	6.2.3	Ellsworth-Whitmore Mountains	198
	6.2.4	Transantarctic Mountains	204
	6.2.5	Boundary between East and West Antarctica	206
6.3		Implications to the Tectonic History of Antarctica	211
6.4		West Antarctica and Gondwanaland	215
	6.4.1	Gondwanaland Reconstruction	216
	6.4.2	Breakup of Gondwanaland	220
CHAPTER 7		CONCLUSIONS	226
APPENDIX 1		MAGNETIC SUSCEPTIBILITY OF ANTARCTIC ROCKS	230
APPENDIX 2		MAXIMUM DEPTH TO MAGNETIC BASEMENT	235
APPENDIX 3		COMPUTER MODELLING OF ANOMALIES	255
REFERENCES			274

MAPS IN MAP POCKET.

Fig. 2.7 Ice Surface Topography.

Fig. 2.8 Bedrock Topography.

Fig. 5.9 Residual Magnetic Field.

Fig. 5.10 Residual Magnetic Field

Fig. 6.1 Thickness of non-magnetic material overlying magnetic 'basement' in West Antarctica.

PREFACE

The work in this thesis was undertaken with the helpful guidance and encouragement of my supervisor Dr. D.J. Drewry. I also wish to thank Dr. G. de Q. Robin, director of the Scott Polar Research Institute, for making available the facilities of the Institute.

The field work was undertaken during the austral summers of 1977-78 and 1978-79 as part of an International programme in Antarctica in co-operation with the US National Science Foundation and the Technical University of Denmark. I am also indebted to personnel of the Applied Physics Laboratory, Johns' Hopkins University, for installing and operating the magnetometer. I also wish to express my gratitude to the Commander, Executive Officer and all flight crews of US Navy Antarctic Development Squadron Six for their support in the field.

I wish to thank all my colleagues at SPRI for helpful discussions during the course of my work especially Hugh Steed, Ben Millar, Chris Neal, Paul Cooper, Rob Massom and Sue Jordan. I am especially grateful to Dr. J.C. Behrendt and the staff of the USGS Branch of Regional Geophysics in Denver for assistance in analysis of the magnetic data. Dr. C.R. Bentley and Dr. N. Levanon provided valuble unpublished data and I wish to thank Dr. D.H. Elliot, Dr. I. Dalziel and Dr. W. Bossum for helpful discussions during the final writing of this thesis.

I thank the National Environment Research Council for the generous provision of a research studentship for 3 years and to the Institute for financial support to allow completion of my studies.

It would have been impossible to carry out this research without the assistance and co-operation of other members of the SPRI radio echo sounding teams. However, all data reduction, analysis and interpretation, unless otherwise stated, are entirely my own work. I also declare that this thesis does not exceed the regulations on length and has not been submitted for a degree at any other university.

SUMMARY

This thesis reviews the state of knowledge on geology, structure and tectonic evolution of West Antarctica. An airborne geophysical survey in West Antarctica comprising simultaneous Radio Echo Sounding (RES) and magnetics was carried out over ~1 M km^2 of the ice covered area. The collection and reduction of large volumes of RES and magnetic data are described. The first detailed maps of ice sheet surface and bedrock topography were compiled from the RES data and are presented.

The main characteristics of the West Antarctic ice sheet and its stability are briefly discussed including the grounding zone of the Ronne-Filchner Ice Shelf. Calculations for the depression of the crust by the weight of the overlying ice sheet are made and the bedrock topography isostatically adjusted. Detailed comparisons of magnetic profiles with the bedrock topography are made. Depth determinations on the magnetic profiles were performed and selected anomalies are modelled by computer to give quantitative estimates of bedrock magnetisations.

These data together with other pertinent geophysical data are discussed and interpretations of subglacial geology made. Discussion concentrates on defining boundaries between major structural units in West Antarctica and the boundary between East and West Antarctica. The tectonic evolution and position of West Antarctica in Gondwanaland is discussed in the light of these interpretations. West Antarctica is thought to comprise several microcontinental fragments which have moved relative to each other during the breakup of Gondwanaland.

CHAPTER 1 PREVIOUS GEOLOGICAL AND GEOPHYSICAL WORK IN WEST ANTARCTICA

1.1 INTRODUCTION

Antarctica has an area of approximately 14 million Km^2 (~1.5 times the area of the USA) and is roughly centred on the geographic South Pole. The world's largest permanent ice cap occupies 95% of the Antarctic and greatly hinders our knowledge of the continent. Since the International Geophysical Year (IGY) in 1957 there has been a marked increase in the amount of scientific work carried out in the Antarctic. The majority of geological work has been carried out in the Transantarctic Mountains and Antarctic Peninsula where there is good exposure. Most outcrops have been visited although, in many cases, knowledge is purely of a reconnaissance nature. In respect of major geophysical work little has been undertaken over the ice covered area of West Antarctica since the mid 1960's. This thesis describes the first systematic geophysical study of West Antarctica involving both airborne radio echo sounding (RES) and magnetometry.

As early as 1937, Du Toit recognised the importance of Antarctica in reconstructions of the southern continents. Today Antarctica remains the least known southern continent and lack of detailed geological and geophysical information is a major problem in Gondwanaland considerations. The main aim of this thesis, therefore, is to extend knowledge from the scattered bedrock exposures to large ice covered areas. With an improved understanding of geology and structure of West Antarctica several outstanding problems associated with Gondwanaland reconstructions may be solved.

Some of the specific problems of geology, structure and tectonics of West Antarctica are outlined at the end of this chapter following a comprehensive review of current knowledge. Later sections consider i) tectonic evolution and ii) details of bedrock exposures in Antarctica, upon which later interpretations are based. A review of all major geophysical work related to the structure of West Antarctica is also presented. This forms a major source for later chapters of the thesis.

Chapter 2 describes data collection, reduction and some of the principles of both RES and magnetometry. The remaining chapters relate to the analysis and interpretation of the data. The area of interest is shown in Fig. 1.1. The rather ambiguous terms East Antarctica and West Antarctica are used consistently throughout this thesis and will be defined here. East Antarctica is that part of Antarctica facing the Atlantic and Indian Oceans and lying predominantly within the eastern hemisphere. West Antarctica is seperated from East Antarctica by the Transantarctic Mountains, faces the Pacific Ocean and lies within the western hemisphere.

1.2 WEST ANTARCTICA AND GONDWANALAND

1.2.1 INTRODUCTION

The concept of all the southern continents belonging at one time to a single landmass, Gondwanaland has been in existence for many years (Wegener, 1912). One of the first reconstructions, and remarkably still considered one of the best, was presented by Du Toit (1937). In it he recognised the importance of Antarctica to reconstructions of Gondwanaland describing it as a 'key-piece' around which the other continents can be fitted with remarkable precision.

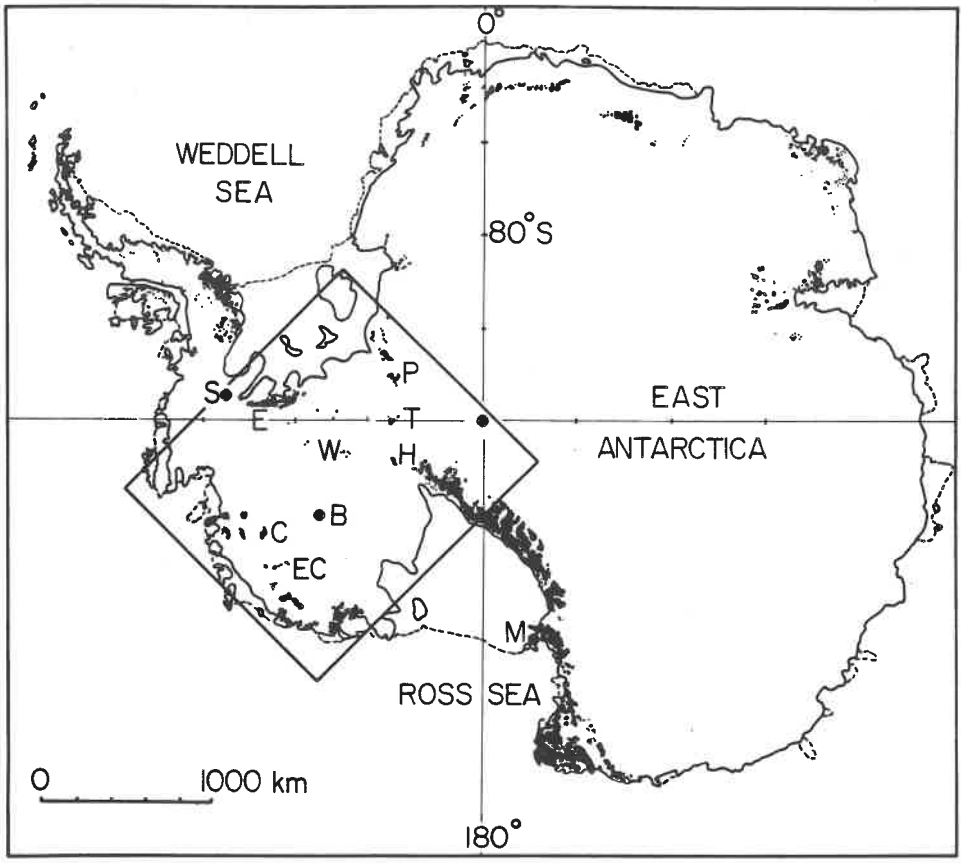


Fig. 1.1 Antarctica showing area of interest.

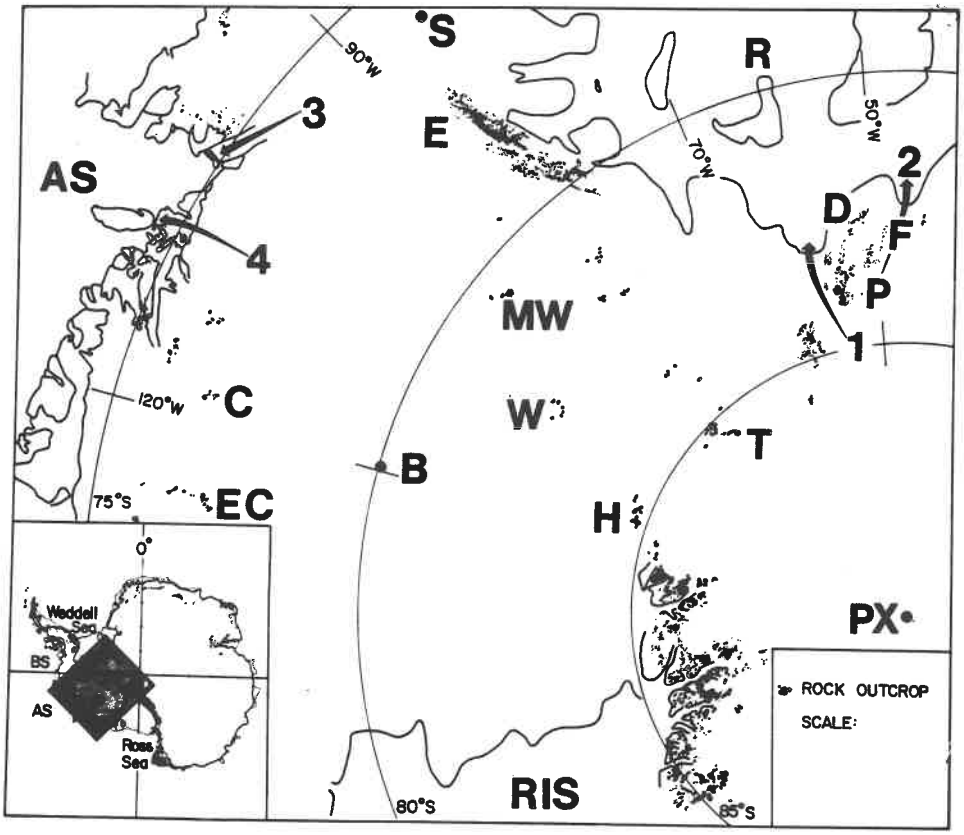


Fig. 1.6 West Antarctica

The early history of Gondwanaland is poorly known but some fragments may have been joined together even in the Archean (Craddock, in press). The main landmass, however, had certainly formed by late Precambrian times and remained largely intact throughout the Palaeozoic and early Mesozoic. During this time the Pacific Ocean edge of the supercontinent formed an active continental margin shown by the late Precambrian, lower Palaeozoic, mid Palaeozoic and early Mesozoic orogenies recognised in Antarctica and other Gondwana continents. What is important to establish for this thesis is the position of Antarctica, and in particular West Antarctica, within Gondwanaland prior to its breakup. The subsequent evolution of West Antarctica within Gondwanaland after the commencement of breakup is crucial to understanding its present day structure.

1.2.2 RECONSTRUCTIONS OF GONDWANALAND

Since Du Toit's 1937 reconstruction of Gondwanaland many reconstructions have been attempted using a variety of methods. There are those produced by bathymetric matching, largely by computer, of continental margins (Dietz and Holden, 1970; Dietz, Holden and Sproll, 1972; Smith and Hallam, 1970). Usually additional information such as palaeomagnetic data or geological trends are used to produce the final fit, often degrading the original geometric reconstruction but producing a tighter geological fit (Barker and Griffiths, 1977; Barron, Harrison and Hay, 1978). Other reconstructions adopt an 'eye ball' technique using like, Du Toit (1937), geological data as the primary constraint to the fit (Elliot, 1972; Ford, 1972a; Craddock, in press). A third catagory of reconstructions are those obtained by the reversal of sea floor spreading magnetic anomalies (eg. Molnar et al, 1975; Norton and Sclater, 1979). The precise relocation of continental fragments by reversing sea floor spreading magnetic anomalies is impossible prior to the Cretaceous due to the lack of anomalies. Consequently such reconstructions for the early Mesozoic must make use of additional data from within the continents (eg. Grindley and Davey, in

press; Griffiths, 1974). New reconstructions of parts or all of Gondwanaland continue to appear in the literature (eg. Harrison et al, 1979; Gordon and Cox, 1980) without any sign of agreement being reached. This is largely the result of the lack of sufficient geological and geophysical data with which to constrain palaeopositions. The lack of data from the Antarctic is one major factor alongside the lack of pre-Cretaceous oceanic magnetic anomalies.

All of the reconstructions fall into two catagories with respect to relative position of West Antarctica within Gondwanaland. Either West Antarctica is considered as being separate from East Antarctica or Antarctica is considered as one complete unit. One unit Antarctica is found mainly in the geometrical reconstructions and a major problem becomes the overlap of South Africa and the Antarctic Peninsula (Dietz and Holden, 1970; Dietz et al, 1972). Barron et al (1978) and Harrison et al (1979) overcome this problem by placing the Antarctic Peninsula alongside the western margin of South America and dismiss any relative motion between East and West Antarctica as insignificant. Dalziel (1980) has strongly criticised this configuration for the Peninsula pointing to the mismatch produced between the Cape Fold Belt of South Africa and their widely accepted equivalents in the Transantarctic Mountains, plus the doubling up of forearc and arc terrains in South America and the Antarctic Peninsula. Smith and Hallam (1970) overcome the problem of overlap by considering the Peninsula to be a post breakup structure. Geological evidence suggests that southern South America and the Antarctic Peninsula were once a continuous cordillera (Barker and Griffiths, 1972, 1977; Dalziel and Elliot, 1971). The origin of the oroclinal bending of the Peninsula is not, however, resolved. Dalziel and Elliot (1971) attribute the bending to disruption and fragmentation of the cordillera during the break-up of Gondwanaland. Barker and Griffiths (1972) however assume that the cuspate shape of the junction between South America and the Antarctic Peninsula existed prior to separation. More recently Dalziel (in press) has rejected the idea that the cuspate shape of the Peninsula is purely

the result of the break - up of Gondwanaland.

The other types of reconstructions are overwhelmingly in favour of some sort of relative movment between East and West Antarctica (Molnar et al, 1975; Norton and Sclater, 1979; Gordon and Cox, 1980) and some split West Antarctica into at least 3 separate units (Elliot, 1972; Stump 1973; Barker and Griffiths, 1977). Molnar et al (1975) require ~500 km of relative movement between East and West Antarctica between 80 and 40 Ma BP. Marie Byrd Land originally lay closer to East Antarctica before under-going rifting in the form of back-arc spreading (Molnar et al, 1975). The low elevations marking the Byrd Subglacial Basin may be evidence of rifting in West Antarctica (Elliot, 1974). Fig. 1.2 summarises some of the more important reconstructions of Gondwanaland.

1.2.3 BREAKUP OF GONDWANALAND

The exact timing of Gondwanaland disruption is difficult to establish although the concensus of opinion would be during the Jurassic (Elliot, 1972; Barron et al, 1978; Craddock, in press; Norton and Sclater, 1979) in association with middle to late Jurassic volcanic activity in the southern Andes and the Antarctic Peninsula. Separation of East Gondwanaland (Madagascar, India, Antarctica, Australia and New Zealand) from West Gondwanaland (South America and Africa) occurred at this time. The rifting of East and West Gondwanaland is associated with the Jurassic dolerites of the Transantarctic Mountains (Elliot, 1975), the Karroo of South Africa, and the Parana, Deccan and Rajmahal traps. Elliot (1972) descibes the developing mid-ocean ridge between Africa and Antarctica as terminating in a transform fault or a series of short ridge segments connected by transform faults which separated East from West Antarctica. This faulting could have rotated the Ellsworth Mountains between East Antarctica and the Mesozoic Orogen of West Antarctica and the Peninsula (Elliot, 1972). Ford

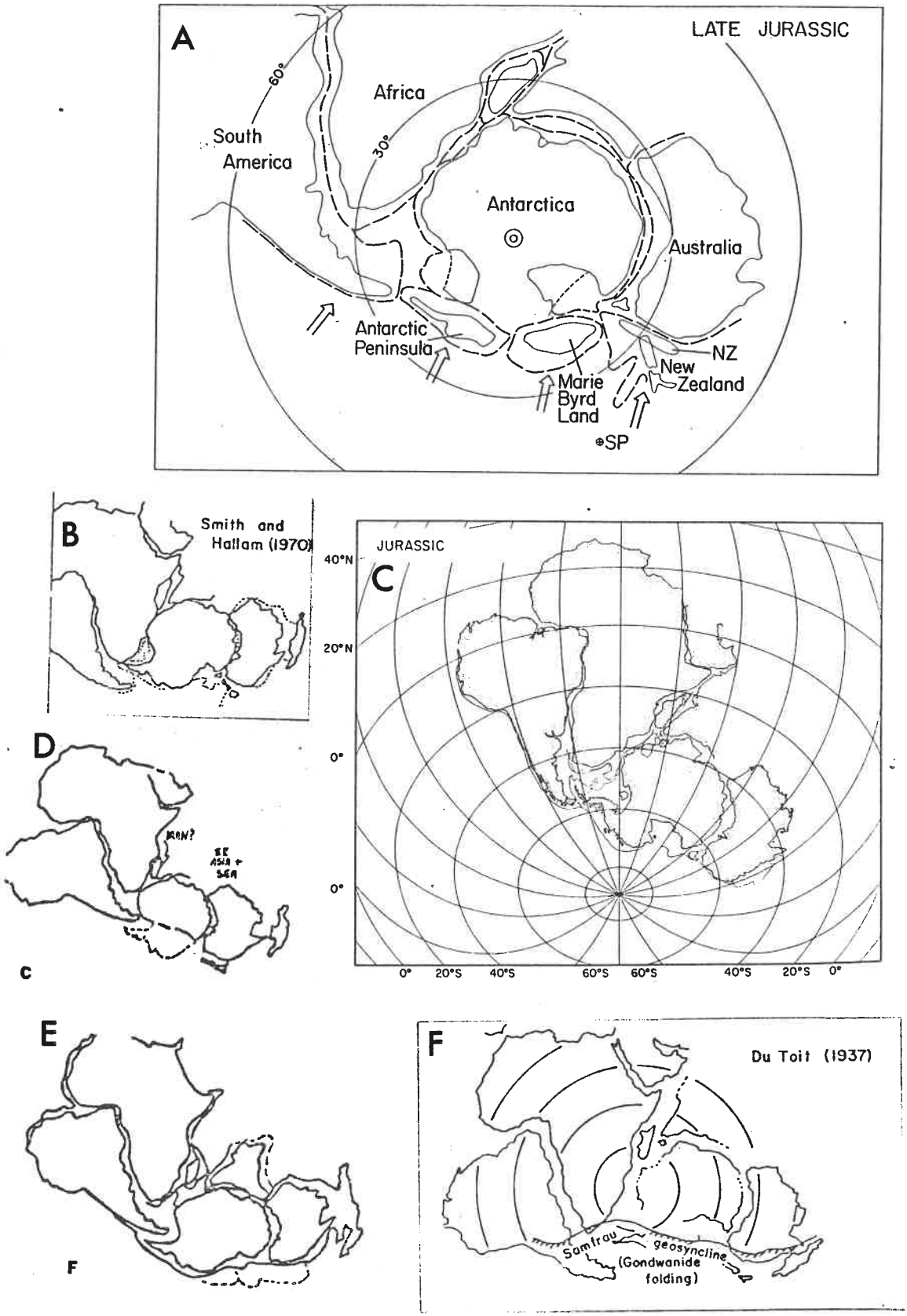


Fig. 1.2 Reconstructions of Gonwanaland.
(A-Elliot, 1972; B-Smith and Hallam, 1970;
C-Norton and Sclater, 1979; D-Tarling, 1971;
E-Barron et al, 1977; Du Toit, 1937).

and Kistler (1980) believe that the large volumes of tholeiitic magma generated in the Transantarctic Mountains relate to an incipient rift system that formed the third arm of a triple junction. This incipient rift lay along the site of the Transantarctic Mountains and was short lived.

In the early Cretaceous (147 Ma BP) the separation of Africa from South America was accompanied by uplift, fracturing and volcanic activity (Herz, 1977). The first sea floor spreading anomalies in the South Atlantic are mid Cretaceous (127 Ma BP) (Norton and Sclater, 1979). Possibly at the same time India separated from Antarctica and Australia. In the late Cretaceous (80-90 Ma BP) Madagascar and India separated resulting in a major reorientation of spreading between India and Antarctica-Australia (Norton and Sclater, 1979).

In the period 81-63 Ma BP rifting occurred between East and West Antarctica in the form of back-arc spreading (Molnar et al, 1975). A triple junction was formed by the spreading in the Tasman sea, the spreading in the South Pacific and the spreading between East and West Antarctica (Molnar et al, 1975). Kellogg (1980) attributes oroclinal bending of the southern end of the Peninsula to movment on a system of ridge sections and connecting transform faults between East and West Antarctica at this time. At 60 Ma BP spreading in the Tasman Sea had stopped and at ~55 Ma BP Australia separated from Antarctica. As a consequence West Antarctica then converged on East Antarctica during the period 63-38 Ma BP (Molnar et al, 1975). The separation of South America from Antarctica may have been the last major event in the breakup of Gondwanaland (Craddock, in press). Prior to this the Antarctic Peninsula had remained fixed to South America while East Antarctica rotated clockwise opening up the Weddell Sea (Barker and Griffiths, 1972). In the early Tertiary, however, the Peninsula transferred from South America to East Antarctica which continued to rotate clockwise thereby opening up the Scotia Sea (Barker and Griffiths, 1972). Dalziel and Elliot (1971) date the bending, disruption and eventual fragmentation

of the South America-Antarctic Peninsula cordillera as either early Cenozoic or else it accompanied spreading in the Drake Passage. Apart from continued spreading in the Drake Passage and the commencement of subduction in the South Sandwich Islands no major changes have occurred in the pattern of spreading between the Gondwana continents. At the present day Antarctica has the unique distinction of being the only continent to be completely surrounded by conservative plate boundaries (see Fig. 1.3).

1.3 TECTONIC EVOLUTION OF ANTARCTICA

The following section draws heavily on the current literature on the geology of Antarctica and also on the tectonic reviews of Stump (1973), Elliot (1975) and Craddock (in press). Emphasis is placed on events affecting West Antarctica and the related margin of the East Antarctic craton.

The East Antarctic Shield has a complex history of deformation and metamorphism, which cannot be adequately described due to the lack of data, but it had probably consolidated by the middle Proterozoic. By the mid Precambrian a sedimentary basin existed along the Pacific margin of the East Antarctic Shield (Elliot, 1975; Stump, 1973; Craddock, in press) occupying the site of the present Transantarctic Mountains. Great thicknesses of greywackes and shales were deposited in this basin derived from the adjacent craton. Towards the top of the sequence felsic volcanics begin to dominate (ie. Fairweather and Wyatt Formations of the central Transantarctic Mountains and Gorecki Rhyolite of the Pensacola Mountains). In the late Precambrian the sediments in the basin were deformed and intruded by batholiths in the Beardmore Orogeny. The deformation and calc-alkaline igneous rocks suggest subduction and a compressive plate margin (Elliot, 1975).

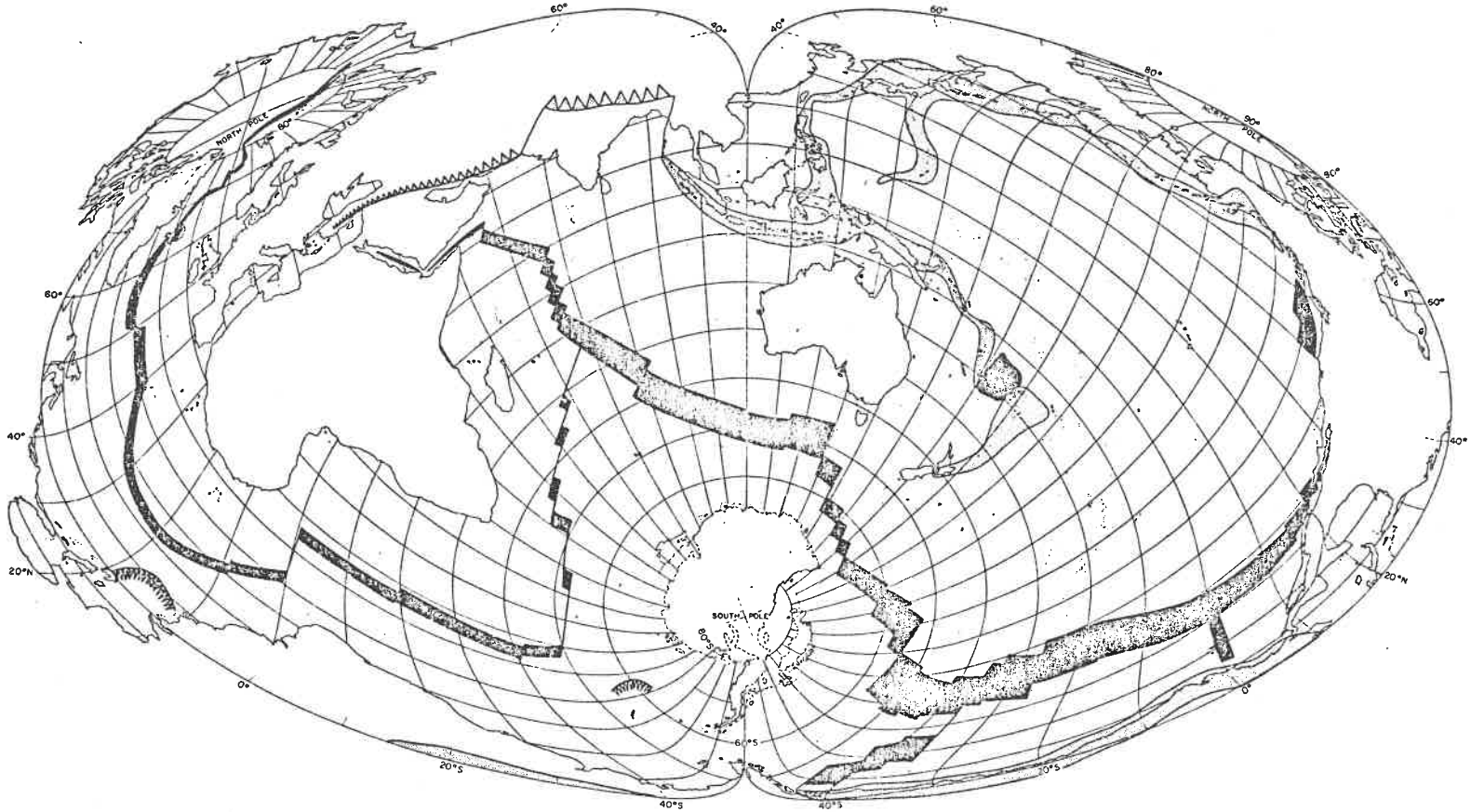


Fig. 1. Equal area map showing crust created during the last 10 million years (black). The shaded region is where the crust is restored to the mantle at island arcs and young mountains. The area of the shaded region corresponds to the distribution of earthquake epicenters deeper than 100 km and presumably is the extent of the plunging crust. The area of new crust and of crust being destroyed is about equal.

Fig. 1.3 Present tectonic configuration of Antarctica (after Menard, 1971).

Widespread erosion followed and in the early Cambrian extensive carbonate sequences were deposited in the central Transantarctic mountains and the Pensacola Mountains while more clastic sequences were deposited in North Victoria Land and the Shackleton Mountains. Eventually the carbonates gave way to more clastic deposits indicating shallowing conditions. The carbonate platform may have extended out into West Antarctica as suggested by marble recovered by the DSDP in the Ross Sea (Hayes et al, 1973). Cambrian carbonates also occur in the Ellsworth Mountains where they form part of a conformable sequence whose base may lie in the Precambrian (?). It would appear that the Ellsworth Mountains have an early tectonic history that is different to the Transantarctic mountains and may not be in the same position relative to East Antarctica as they were in lower Palaeozoic times.

The site of the Transantarctic Mountains was the scene of deformation and intrusive activity during the lower Palaeozoic Ross Orogeny. A ~500 Ma BP thermal event is recorded throughout the continent (Stump, 1973). Sedimentation, meanwhile, was continuous in the Ellsworth Mountains which show no record of this orogenic phase. By mid Palaeozoic times rocks deformed in the Ross Orogeny had been eroded to form the Kukri Peneplain and shallow marine and non-marine sediments were laid down. At this time the Robertson Bay and Bowers Groups of North Victoria Land were intruded by plutons during the 'Borchgrevink' event possibly a late phase of the Ross event (Laird et al, in press; Wright, 1980). A scattering of mid Palaeozoic dates suggest that North Victoria Land, West Antarctica and the Antarctic Peninsula formed part of an active plate margin (Elliot, 1975). Shallow marine Devonian sedimentation continued in the Ellsworth Mountains (Craddock et al, 1964). There followed in the Transantarctic Mountains a long period of non-deposition which is recorded in the disconformity between the Taylor and Victoria Groups. Elliot (1975) relates this to probable uplift in North Victoria and West Antarctica in response to continued orogenesis. During the late Carboniferous and early Permian a major ice sheet was present in the Transantarctic and Ellsworth

Mountains.

Deposition was brought to a close in the Ellsworth Mountains in Permian times with the deposition of shallow marine strata. The late Palaeozoic - early Mesozoic Gondwanian Orogeny followed and strongly deformed rocks in the Ellsworth and Pensacola Mountains. Jurassic intrusives related to the Gondwanian Orogeny occur along the Pacific coast of West Antarctica and in the Antarctic Peninsula. Deposition of Permian flood plain deposits took place meanwhile in the rest of the Transantarctic Mountains although evidence of the Gondwanian Orogeny may occur in a palaeocurrent reversal between Permian and Triassic strata of the Victoria Group (Elliot, 1975). Similarly thick greywacke shale and volcanic sequences of Carboniferous to Permian age were accumulating at this time along the Pacific edge of the Antarctic Peninsula. The geology at this time suggests that the Antarctic Peninsula and the islands of the Scotia Sea were part of a cordillera that linked South America to Antarctica (Dalziel and Elliot, 1971, 1973). Such a reconstruction, however, requires relative movement of parts of West Antarctica (Elliot, 1975). Extensive post Gondwanian orogenic calc-alkaline volcanicity in the Peninsula during the late Jurassic is probably related to crustal subduction. The distibution of compositions of magma would suggest an andesitic volcanic chain in the west with a back-arc volcano-tectonic province to the east (Elliot, 1975). In the Pensacola Mountains the Dufek Intrusion of Jurassic age provides an upper limit to the Gondwanian event. The widespread Jurassic tholeiites of the Ferrar Group are probably comagmatic with the Dufek Intrusion (Ford, 1970; Ford and Kistler, 1980; Kyle et al, 1980) and represent conditions of continental rifting (Elliot, 1974; Ford and Kistler, 1980). This contrasts with the compressive regime suggested by the Jurassic intrusions in West Antarctica that were associated with crustal subduction. Elliot (1974) suggests the extensional tectonic regime is best related to back-arc spreading but within a continental environment (see fig. 1.4).

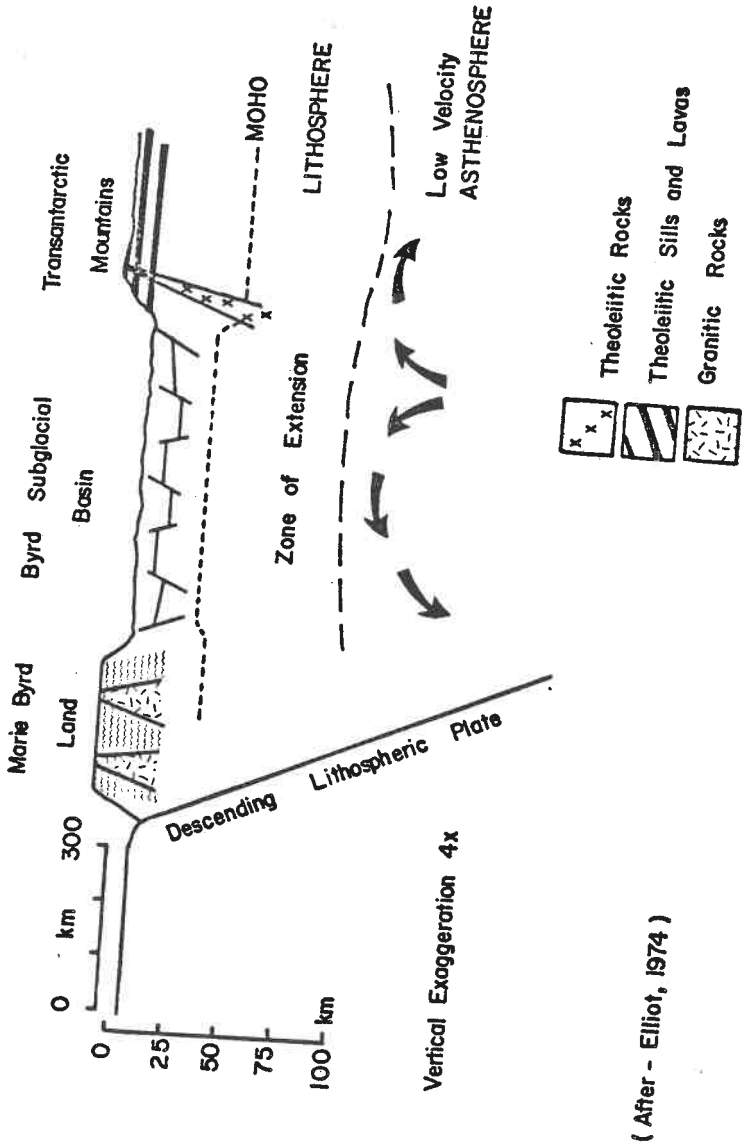


Fig. 1.4 Extensional tectonics in the form of back-arc spreading in West Antarctica (after Elliot, 1974)

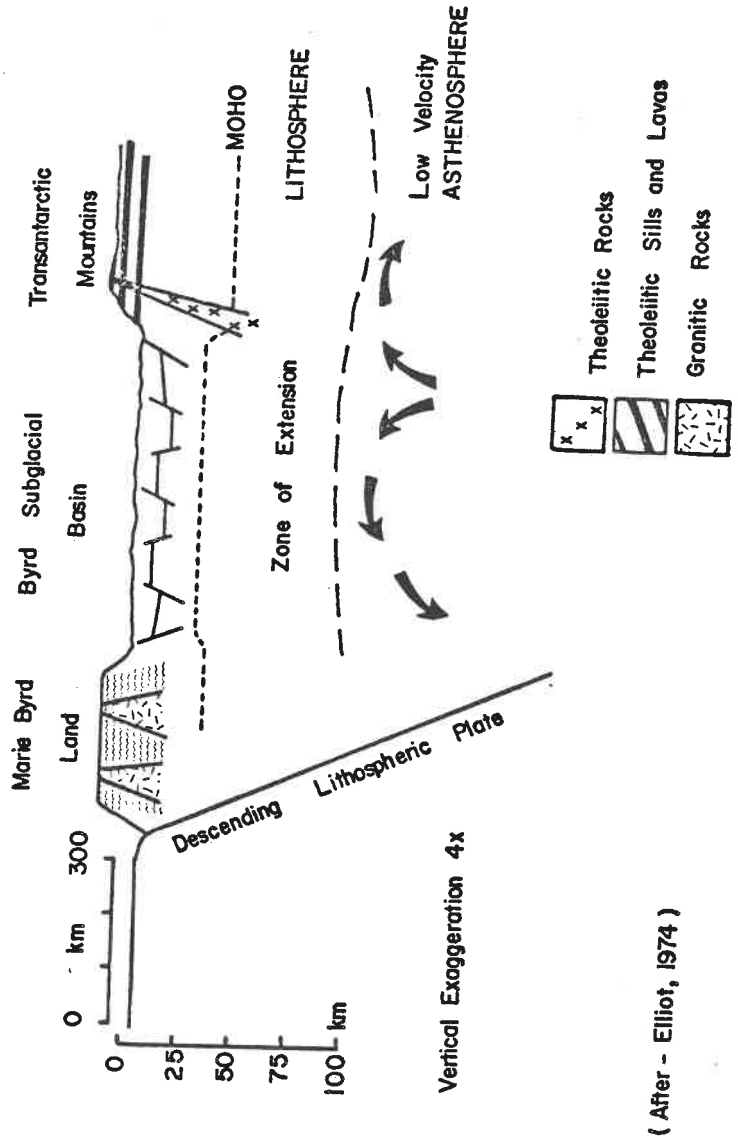


Fig. 1.4 Extensional tectonics in the form of back-arc spreading in West Antarctica (after Elliot, 1974)

In the early Cretaceous Alexandra Island was the site of a depositional trough with shallow marine sediments accumulating towards the craton and deeper water sediments accumulating off shore (Stump, 1973). By the late Cretaceous a shallow marine basin was also located at the northern end of the Peninsula (Bibby, 1966). The Cretaceous was, however dominated by the Andean Orogeny in which plutonism was widespread but crustal shortening confined to South Georgia and to the Jurassic sequences of eastern Ellsworth Land and the Lassiter Coast (Elliot, 1975). Upper crustal tectonism is recorded throughout the late Mesozoic and Cenozoic during which time there were several periods of plutonism, the later episodes being recorded only in the Antarctic Peninsula.

The Cenozoic in Antarctica is dominated by basaltic volcanic activity and vertical tectonics. The mainly alkaline basalts and trachytes in Marie Byrd Land have been related to rift systems such as those in Iceland and East Africa (LeMasurier, 1972; LeMasurier and Rex, in press). At the northern end of the Peninsula the Cenozoic has been marked by the evolution of the Scotia Sea which is still active (Barker and Griffiths, 1972, 1977; Dalziel and Elliot, 1971, 1973). During the Cenozoic uplift also occurred in the Transantarctic Mountains (Drewry, 1975a) and caused faulting in the Ferrar Dolerites (Bradshaw et al, in press). The vertical tectonics have been desribed as the Victoria Orogeny (Gunn and Warren, 1962).

1.4 ANTARCTIC GEOLOGY

1.4.1 INTRODUCTION

In the preceeding sections a brief tectonic history of Antarctica, based largely on study of the ice free areas, and its relations to the other

southern continents was given. However it is important to detail the geological knowledge of those ice free areas in Antarctica that are relevant to the area studied in this thesis. Emphasis will be placed on the exposures in West Antarctica although all bedrock geology will be discussed.

The lack of exposure, 5% at most, and the harsh environment has resulted in a poorer understanding of the geology of the Antarctic than exists in any other continent. Even in many areas of exposure no detailed statigraphies have been determined. In those areas studied in detail the rocks are given local group names which leads to confusion when attempting regional correlations. This is particularly so in the Transantarctic Mountains where the same suite of rocks sometimes has several different group names. Table 1.1 is an attempt to correlate the major rock units. Many of the early radiometric age determinations, particularly K-Ar whole rock isochrons are unreliable and probably give at best minimum ages. Nevertheless almost all outcrops have been described.

In general the Antarctic can be considered of consisting of two parts: 1) East Antarctica, a stable continental shield area. 2) West Antarctica, composed generally of younger rocks that are widely deformed and metamorphosed. (see fig. 1.5).

1.4.2 EAST ANTARCTIC SHIELD

The East Antarctic Shield comprises more than 70% of the area of the present Antarctic continent although less than 3% of it is exposed. Exposure is mostly confined to a narrow coastal strip, except where major glaciers have revealed sections in the interior (eg. Lambert Glacier), and to parts of the Transantarctic Mountains. Hamilton (1964) suggested that

FIGURE 2. Geological sketch map of Antarctica.

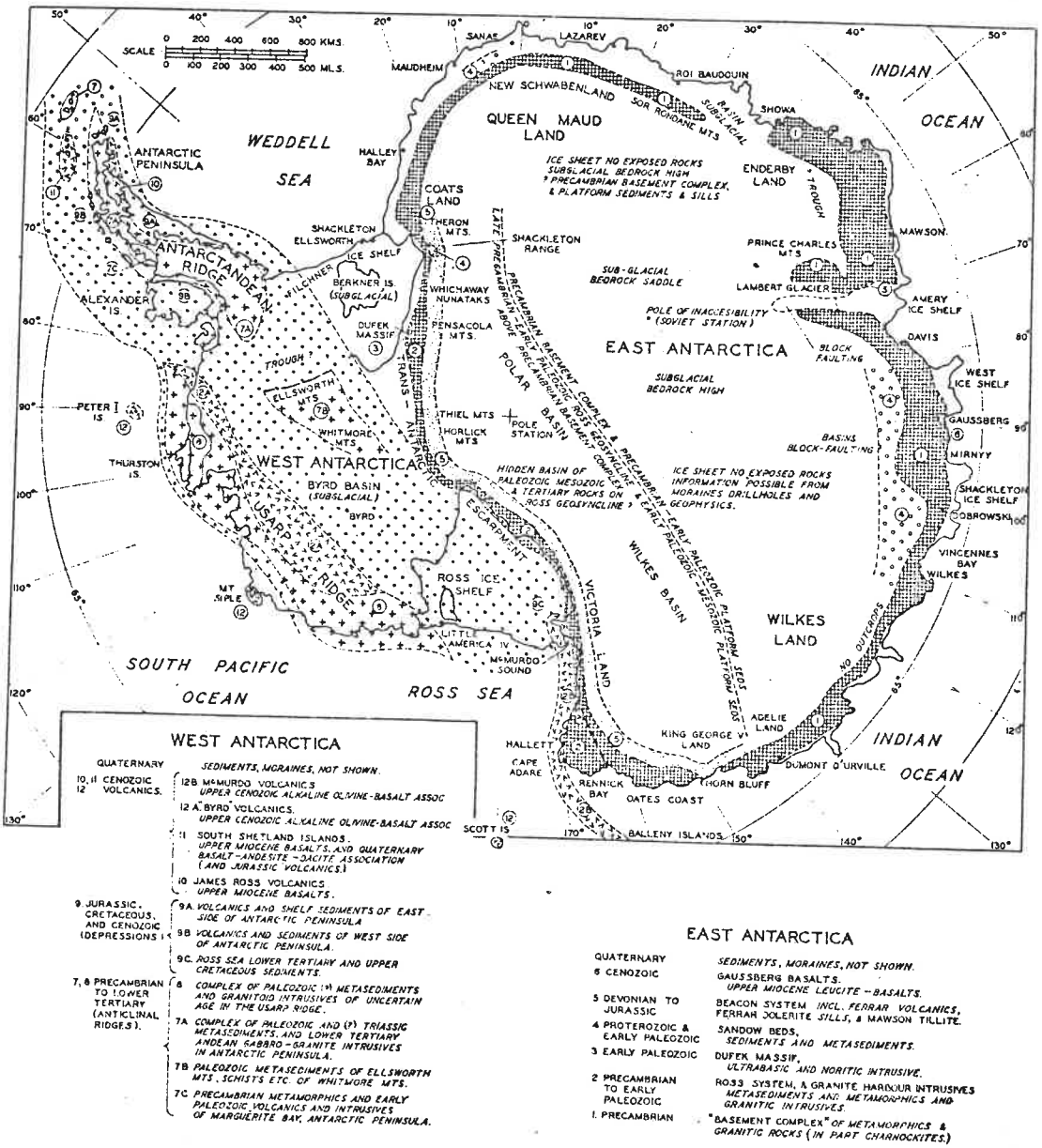


Fig. 1.5 Geological sketch map of Antarctica (after Stump and Fairbridge, 1975).

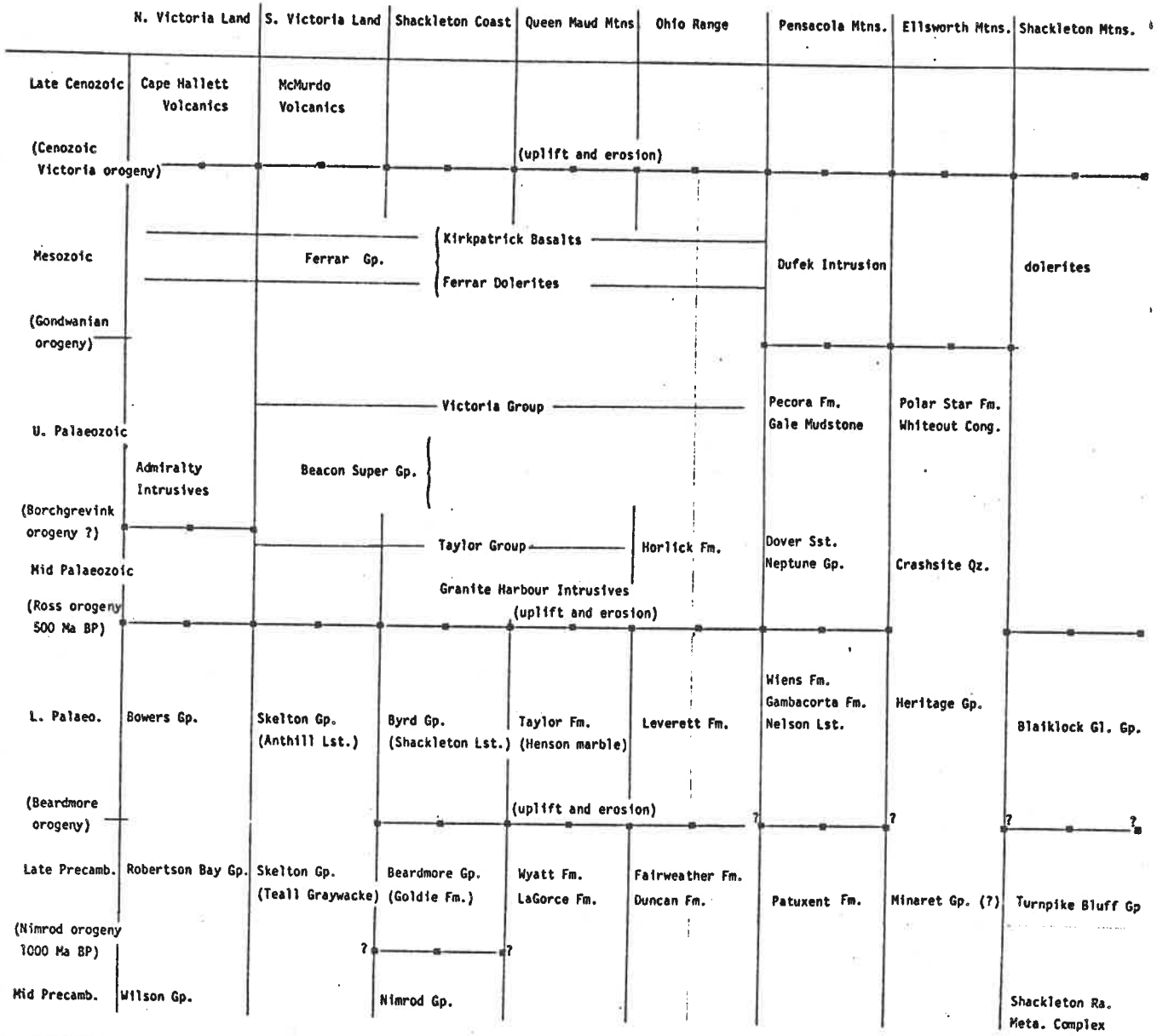


Table 1.1 Correlation of bedrock units in Transantarctic Mtns.

East Antarctica is underlain by a single metamorphic shield. There is no evidence to support or deny this and more recently Ravich and Kamenev (1975) have suggested that the area consists of several smaller but as yet undifferentiated units much as is found in the African Shield.

Ages of rocks in the East Antarctic Shield range from Archean (>2500 Ma BP) to upper Precambrian and Cambrian strata (~600 Ma BP) which are found in the Transantarctic Mountains and at a few coastal localities. Sobotovich and others (1976) report high grade metamorphic rocks from the Fyfe Hills on the west coast of Enderby Land as having Pb isochron ages of >4000 Ma BP, which would make these some of the oldest terrestrial rocks known.

East Antarctica consists of a foundation of metamorphic and igneous rocks which are overlain by a series of relatively flat lying sedimentary and volcanic strata (Craddock, in press). Exposed crystalline basement consists mainly of high grade metamorphics belonging to amphibolite and granulite facies. Gneisses of a wide compositional range are the most abundant rock types but schists, quartzites, marble, and plutonic rocks from gabbro to granite are also common (Elliot, 1975). Charnockites of both igneous and metamorphic origin form the most extensive charnockite province in the world (Craddock, 1972). In Dronning Maud Land, along the George V Coast and along the Knox Coast upper Precambrian to Cambrian detrital sedimentary and some volcanic rocks overlie the metamorphic basement complex. These rocks are relatively flat lying and have experienced little metamorphism (Craddock, 1972). The undisturbed Beacon Supergroup rocks overly these beds and represent the Gondwanian sequence in the Antarctic.

The East Antarcic Shield has undoubtedly undergone a complex history of metamorphism and orogeny (Tingey, 1978) but the stable shield does not appear to have undergone true orogeny, except for some peripheral areas, since the beginning of the Phanerozoic (Craddock, 1972; Elliot, 1975).

1.4.3 TRANSANTARCTIC MOUNTAINS

The Transantarctic Mountains form an almost continuous chain of peaks from Cape Adare to the Horlick Mountains and then continuing as a series of discontinuous mountain ranges through the Thiel, Pensacola and Shackleton Mountains and into Queen Maud Land (see fig. 1.6). These mountains form the margin of the East Antarctic Shield and mark the site of intermittant deformation during late Precambrian and Phanerozoic times. The almost continuous exposure from the Ohio Range at the eastern end of the Horlick Mountains to Cape Adare has been the focus of the most detailed geological work. Many aspects of the geology are common between the different ranges in this sector of the Transantarctic Mountains and will be dicussed collectively leaving discussion of the remaining isolated mountain ranges, related to the study area of this thesis, to later sections.

In general three major rock units are exposed; 1) Middle to late Precambrian - lower Palaeozoic basement complex. 2) Upper Palaeozoic and lower Mesozoic relatively flat lying sedimentary and volcanic strata overlying the basement unconformably. 3) Cenozoic Volcanics with glacial deposits of Miocene to Pleistocene age.

Fig. 1.7 is a sketch section across the central Transantarctic Mountains in the vicinity of the Liv Glacier illustrating the general structure of the central Transantarctic Mountains. The statigraphic division of the basement complex varies from area to area in the Transantarctic Mountains

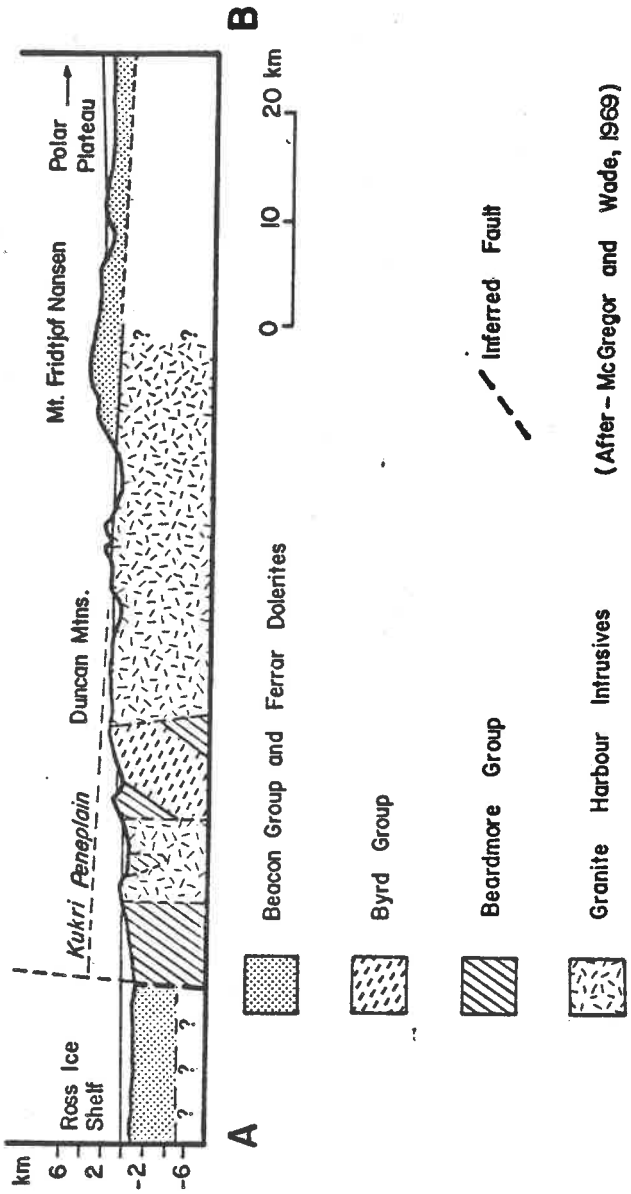


Fig. 1.7 Geological section across Transantarctic Mountains near Liv Glacier (after McGregor and Wade, 1969).

but generally consists of late Precambrian to early Palaeozoic deformed and metamorphosed sedimentary and volcanic rocks that are intruded by a widespread suite of plutonic rocks.

Middle Precambrian

Rocks of this age occur along the Shackleton Coast and belong to the Nimrod Group. The Nimrod Group consists of 3 conformable units separated by a major overthrust from a fourth tectonically higher unit (Adams et al, in press) comprising generally of amphibolite grade schists, gneisses, amphibolites, dolomites, marbles and locally developed skarn deposits (Grindley and Laird, 1969). A sedimentation age of 1800-2000 Ma BP is given for the group from selected non-migmatised paragneisses and other metasediments (Adams et al, in press). Grindley and McDougal (1969) suggest that the Nimrod Group underwent a separate orogeny around 1000 Ma BP termed the Nimrod Orogeny. Little direct evidence now exists, however, for recognition of a separate Nimrod Orogeny in the Transantarctic Mountains based upon new K-Ar age data (Adams et al, in press).

A possible correlation occurs with parts of the Wilson Group in Northern Victoria Land (Grindley and McDougal, 1969) consisting of medium grained regionally metamorphosed biotite and garnet schists grading upwards into gneisses and migmatites (Gair et al, 1969).

Late Precambrian

The Nimrod Group in the central Transantarctic Mountains is overlain by the Beardmore Group consisting of the Cobham Formation (schists, hornfels, quartzite and impure limestone) and the Goldie formation (metagreywackes) (Grindley and Laird, 1969; Elliot, 1975). Similar metasediments (Teall Greywacke) crop out in Victoria Land. Further to the north in Northern Victoria Land equivalent rocks overlie the Wilson Group and comprise the

Robertson Bay Group. This group comprises well bedded hornfels schists and phyllites (Harrington et al, 1967). Wright (1980) found that nowhere, except where in contact with younger intrusives, are rocks belonging to the Robertson Bay Group metamorphosed beyond possible very low grade greenschist facies. In all cases sedimentological evidence indicates that the entire group consists of alternating turbidite deposits and pelagic shale. In the eastern Queen Maud Mountains similar sequences of metagreywackes and phyllites occur in the Duncan Formation (McGregor and Wade, 1969) and the LaGorce Formation (Mirsky, 1969). On the basis of lithology McGregor and Wade (1969) correlate 3300m of metagreywackes in the western Queen Maud Mountains directly with the Goldie Formation of the Beardmore Group.

The late Precambrian strata in the Central Transantarctic Mountains were deformed and intruded by large batholiths in the late Precambrian (Elliot, 1975). The Lonely Ridge granodiorite and possibly others in the Wisconsin Range appear to have crystallised in the late Precambrian (Mirsky, 1969; Elliot, 1975). This is supported by late Precambrian ages (580-650 Ma BP) for rocks in the Nimrod Group (Adams et al, in press).

Lower Palaeozoic

In the central Transantarctic mountains the Beardmore group is unconformably overlain by the Byrd Group consisting of shallow water marine sediments dominated by carbonates (Grindley and Laird, 1969). The 9000m thick Shackleton Limestone is the most prominent and persistent formation in the Byrd Group containing some Cambrian archaeocyathids (Grindley and Laird, 1969). Elsewhere the shallow marine platform is represented by either mixed carbonate-clastic or entirely clastic sequences with or without interbedded volcanic strata. Equivalent rocks are represented in the Queen Maud Mountains by the Henson Marble and Taylor Formation (McGregor and Wade, 1969). Further south in the Ohio Range rocks belonging to the Leverett Formation unconformably overlie the late

Precambrian LaGorce Formation and contains a thick middle Cambrian fossiliferous limestone (Mirsky, 1969; Stump, in press). A Cambrian shallow marine clastic sequence occupies a downfaulted block between the Robertson Bay and Wilson Groups in North Victoria Land. The Bowers Group comprises of a basal coarse polymict conglomerate interbedded with greywackes and overlain by volcanogenic greywackes, argillites, tuffs, agglomerates, limestones, pillow lavas and conglomerates (Dow and Neall, 1972).

The metasediments and metavolcanics described, except the Bowers and Robertson Bay Groups of North Victoria Land were strongly deformed and intruded by a whole suite of plutonic rocks during the Ordovician in the Ross Orogeny (Gunn and Warren, 1962; Elliot, 1975). A 500 Ma BP thermal event is widespread in the Antarctic and is recorded across much of the East Antarctic crystalline basement (Elliot, 1975). The intrusives related to the Ross Orogeny are collectively termed the Granite Harbour Intrusives (Gunn and Warren, 1962; Grindley and Warren, 1964). The intrusives are generally calc-alkaline in composition and include granite, granodiorite, diorite, tonalite and adamellite.

The Robertson Bay - Bowers Group sequence appears to have undergone possible deformation following the deposition of the Bowers Group that is younger than the Ross Orogeny. The sequence is intruded by a number of plutons that have late Devonian - early Carboniferous radiometric ages and has led to the recognition of a mid Palaeozoic event termed the Borchgrevink Orogeny (Craddock, 1970, 1972, in press, Elliot, 1975). More recent work (Wright, 1980) has found no evidence for major forcible injection of these intrusives and suggests that this event is limited to granitic intrusives. The Borchgrevink event may in fact be just a late phase of intrusive activity related to the Ross event. The collective name Admiralty Intrusives has been given by Grindley and Warren (1964) to these younger plutons. Possible extrusive counterparts, the Gallipoli

Porphyries, consisting of porphyritic rhyolites overlie the basement granites at Gallipoli Heights in North Victoria Land (Grindley and Warren, 1964; Gair et al, 1969).

Upper Palaeozoic - Mesozoic

Following the Ross Orogeny the rocks of the Basement Complex were deeply eroded and reduced to low relief forming the widespread Kukri Peneplain (Gunn and Warren, 1962). On this erosional surface rocks belonging to the Beacon Supergroup were laid down. The Beacon Supergroup consists of a flat lying largely non-marine sequence from Devonian, or older, to Jurassic in age and can be divided into two distinct stratigraphical successions, the Taylor and Victoria Groups (Barrett et al, 1972).

The Taylor Group is Devonian, or older in age and comprises generally quartzose sandstones and siltstones. Rocks belonging to the Taylor Group are best developed in South Victoria Land at a locality called Beacon Heights from where the name is derived (Ferrar, 1907). In North Victoria Land the Taylor Group is very thin and erosion of the Kukri Peneplain was probably continuing in this area (Gair et al, 1969). To the south, however, in the Ohio Range the Taylor Group is represented by the Horlick Formation of Long (1964) and contains a rich assemblage of lower Devonian brachiopods, pelecypods, cephalopods and trilobites (Doumani et al, 1965).

The overlying Victoria group is Permian to Jurassic in age and consists of basal glacial beds overlain by a cyclic succession of sandstones, and carbonaceous shales concluded by volcaniclastic deposits (Barrett et al, 1972). A late Palaeozoic disconformity is recognised in most of the Transantarctic Mountains from the Ohio Range to Victoria Land (Mirsky, 1964, 1969). The Victoria Group lies disconformably on the Taylor Group or directly oversteps the basement complex with angular unconformity (Elliot, 1975). A major ice sheet is known to have covered this area during the late

Porphyries, consisting of porphyritic rhyolites overlie the basement granites at Gallipoli Heights in North Victoria Land (Grindley and Warren, 1964; Gair et al, 1969).

Upper Palaeozoic - Mesozoic

Following the Ross Orogeny the rocks of the Basement Complex were deeply eroded and reduced to low relief forming the widespread Kukri Peneplain (Gunn and Warren, 1962). On this erosional surface rocks belonging to the Beacon Supergroup were laid down. The Beacon Supergroup consists of a flat lying largely non-marine sequence from Devonian, or older, to Jurassic in age and can be divided into two distinct stratigraphical successions, the Taylor and Victoria Groups (Barrett et al, 1972).

The Taylor Group is Devonian, or older in age and comprises generally quartzose sandstones and siltstones. Rocks belonging to the Taylor Group are best developed in South Victoria Land at a locality called Beacon Heights from where the name is derived (Ferrar, 1907). In North Victoria Land the Taylor Group is very thin and erosion of the Kukri Peneplain was probably continuing in this area (Gair et al, 1969). To the south, however, in the Ohio Range the Taylor Group is represented by the Horlick Formation of Long (1964) and contains a rich assemblage of lower Devonian brachiopods, pelecypods, cephalopods and trilobites (Doumani et al, 1965).

The overlying Victoria group is Permian to Jurassic in age and consists of basal glacial beds overlain by a cyclic succession of sandstones, and carbonaceous shales concluded by volcaniclastic deposits (Barrett et al, 1972). A late Palaeozoic disconformity is recognised in most of the Transantarctic Mountains from the Ohio Range to Victoria Land (Mirsky, 1964, 1969). The Victoria Group lies disconformably on the Taylor Group or directly oversteps the basement complex with angular unconformity (Elliot, 1975). A major ice sheet is known to have covered this area during the late

Palaeozoic (Stump, 1973).

In most areas the Beacon Supergroup rocks have been intruded and overlain by Jurassic tholeiitic rocks belonging to the Ferrar Group. The Ferrar Group dolerites are massive intrusives (predominantly sills) of tholeiitic quartz dolerite and are related to extrusive flows, the Kirkpatrick Basalts (Elliot, 1972). The Ferrar Group dolerites vary in composition from olivine(rare) to hypersthene and pigeonite tholeiites and exhibit varying degrees of differentiation (Gunn, 1966). The Kirkpatrick Basalts, however, are typical tholeiites and exhibit little variation in composition (Elliot, 1972). These rocks have anomalously high Sr^{87}/Sr^{86} ratios of 0.708-0.714 suggesting crustal contamination (Faure et al, 1972; Kyle and Elliot, 1976; Kyle et al, 1980). The Ferrar Group has been dated radiometrically between 191 and 147 Ma BP (Elliot, 1975). More recent work has shown that the Ferrar Group were intruded over a very short time interval at about 179 ± 7 Ma BP (Kyle et al, 1980).

Cenozoic

Quaternary and possibly later volcanic activity is recorded in parts of the Transantarctic Mountains especially in the McMurdo Sound area. The McMurdo Volcanics consist of alkali-rich volcanic rocks including olivine basalt, trachyte, phonolite, and kenyte with associated pyroclastics (Warren, 1969). These rocks crop out in a N-S coastal belt almost parallel to the Victoria Land ranges and include the present day active volcanos, Mount Erebus on Ross Island and Mount Melbourne (fumarolic) on the mainland. The most southerly exposed volcanic rocks (~87° S) occur on Mount Early in the upper Scott Glacier area (Mirsky, 1969).

The isolated outcrops forming the continuation of the Transantarctic Mountains and the outcrops in West Antarctica form the margin to the area of interest (see fig. 1.1) and consequently will be described in more detail in the following sections.

1.4.4 THIEL MOUNTAINS

The Thiel Mountains lie at approximately 85S 90W about midway between the Ohio Range of the Horlick Mountains and the Patuxent Range of the Pensacola Mountains (see fig. 1.6). They consist of a large nearly flat topped massif joined to a group of high nunataks by a southeast trending ice escarpment along which lie numerous smaller nunataks.

Volcanic rocks form the principal exposure in the Thiel Mountains covering approximately 3000 km^2 (Ford and Himmelberg, 1976) interbedded locally with thin bedded thermally metamorphosed clastics. The sedimentary rocks include some crossbedded quartzites and ripple-marked, mud-cracked argillites (Ford and Aaron, 1962). Late Precambrian isotopic ages of 600-700 Ma BP are reported for these rocks (Schmidt and Ford, 1969) and are similar to rocks in the Wyatt Formation of the Wisconsin Range (Ford and Sumsion, 1971).

Ford and Aaron (1962), Ford (1964), and Schmidt and Ford (1969) originally descibed these rocks as part of a sill-like quartz monzonite porphyry. More recent study however has yielded much textural evidence to support a pyroclastic origin rather than a shallow intrusive origin (Ford and Sumsion, 1971). Hypersthene and cordierite, or their alteration pseudomorphs, chlorite and mica are characteristic of these silicic tuffs. Cordierite is comparatively rare in volcanic rocks and Ford and Himmelberg (1976) believe that the cordierite and hypersthene are refractory and have

been brought up from the site of magma generation. Although no granulites are exposed in the Thiel Mountains the interpretation of these minerals as residuals from partial melting suggests a granulite basement beneath the exposed rocks (Ford and Himmelberg, 1976).

The volcanic rocks are cut by discordant granitic masses belonging to a single or perhaps several related plutons (Schmidt and Ford, 1969). Radiometric ages on the plutonic rocks indicate intrusion during the late Precambrian and early Palaeozoic but with resetting of the older ages during younger Ross Orogeny (Schmidt and Ford, 1969). No younger rocks are exposed in the Thiel Mountains but Ford (1964) on the basis of morainal erratics believes that Beacon type rocks intruded by dolerite sheets are concealed by ice in the escarpments at the southern end of the Thiel Mountains.

1.4.5 PENSACOLA MOUNTAINS

The Pensacola Mountains are a group of ranges and nunataks lying at the southern end of the Ronne-Filchner Ice Shelf (see fig. 1.6) and have a geological history that includes much of the events that affected the whole of the Transantarctic Mountain chain (Schmidt and Ford, 1969).

Late Precambrian

The oldest rocks in the Pensacola Mountains belong to the Patuxent Formation, comprising >10000m of terrigenous turbidites (Schmidt and Ford, 1969). Interbedded with this sequence are numerous basalt flows and pillow lavas The sequence is intruded by dolerite sills and felsic plugs (Gorecki Rhyolite). A Rb-Sr isochron date on the Gorecki Rhyolite gives 1210±76 Ma BP (Elliot, 1975). The Patuxent Formation was intensely deformed and metamorphosed sometime between the intrusion of the Gorecki Rhyolite and

the depostion of overlying unconformable Cambrian limestone (Schmidt and Ford, 1969). The deformation has been tentatively assigned a late Precambrian age and correlated with the Beardmore Orogeny (Elliot, 1975).

Lower Palaeozoic

The Cambrian Nelson Limestone unconformably overlies the Patuxent Formation in the Pensacola Mountains and correlates with the thick Cambrian carbonates (ie. Shackleton Limestone) of the central Transantarctic Mountains. As in the rest of the Transantarctic Mountains the Nelson Limestone is overlain by a volcanic unit, the Gambacorta Formation, comprising rhyolitic flows, breccias, and pyroclastics as well as volcanogenic sandstone and conglomerate (Elliot, 1975). Near the top of the sequence the volcanic unit intertongues with silts and muds of the Weins Formation.

The entire Cambrian sequence and the late Precambrian Patuxent Formation is deformed and intruded by rhyolitic porphyry sills and plugs (Schmidt and Ford, 1969). A Rb-Sr age of 510 Ma BP on a small granite stock intruding the Patuxent Formation (Schmidt and Ford, 1969) correlates with ages obtained for the major Ross Orogeny.

Upper Palaeozoic - Mesozoic

Overlying the Weins Formation unconformably are non-marine and marine sediments of the Neptune Group (Schmidt and Ford, 1969). Disconformably overlying the Neptune Group is the Dover Sandstone comprising of cross-bedded quartzose sandstone of probable upper Devonian age (Elliot, 1975). Partly exposed above the Dover Sandstone is the Gale Mudstone containing scattered fragments of granite, gneiss and rocks from underlying sedimentary strata (Schmidt and Ford, 1969). This unit is described as a tillite and correlates with tillites found in the lower part of the Victoria Group in the rest of the Transantarctic Mountains. The youngest

strata, belonging to the Pecora Formation, crop out in the Pecora Escarpment area and are not seen in contact with the Gale Mudstone (Elliot, 1975). The formation consists of well bedded quartzose sandstones, siltsones, and shales with many interbedded thin coal seams containing abundant Permian glossopterid flora (Schmidt and Ford, 1969). On the basis of lithology these rocks are correlated with the Victoria Group of the Beacon Supergroup (Elliot, 1975).

The entire succession in the Pensacola Mountains except the Permian Pecora Formation in the Pecora Escarpment have undergone folding which is not recognised in the rest of the Transantarctic Mountains. The age of the deformation is regarded as latest Permian to middle Jurassic in age (Elliot, 1975). Following the folding large volumes of mafic magma were intruded into the northern end of the Pensacola Mountains. The Dufek Intrusion is a stratiform gabbroic body exhibiting many similarities of structure and magmatic stratigraphy to the Stillwater and Bushveld Complexes (Ford and Boyd, 1968). The general shape of the intrusion is uncertain although it would appear to be sheet-like in form (Behrendt et al, 1974). The area of the intusion is at least 50,000 km^2 and total thickness of the layered rocks has been estimated at 8-9 km (Behrendt et al, 1980). K-Ar dates of 172$\pm$4 Ma BP on several samples are within the range (163-179 Ma BP) measured for the dolerites of the Ferrar Group in the central Transantarctic Mountains (Ford and Kistler, 1980). Ford (1970) believes the parent magma to be a hypersthene tholeiite similar to the Ferrar Group dolerites. After emplacment, the intrusion was weakly deformed giving it a lopolith-like synclinal form (Behrendt and others, 1974) in response to late Mesozoic and Tertiary contintental movements (Schmidt and Ford, 1969; Ford, 1970).

1.4.6 SHACKLETON MOUNTAINS

The Shackleton Range and the isolated ranges and nunataks extending along the eastern side of the Filchner Ice Shelf into Coates Land form a logical topographic and geological extension of the Transantarctic Mountains (see fig. 1.1).

Precambrian

A Precambrian metamorphic complex underlies the greater part of the Shackleton Range consisting of a lower unit of gneisses, migmatites and granite stocks, and an upper unit of schists, marbles and granite stocks (Clarkson, in press). The only age for the basement complex has been obtained from a granodiorite intruded into one of the granite stocks giving a minimum age of 1446±60 Ma BP (Rex, 1972).

Late Precambrian

In the Read Mountains the basement complex is overlain by rocks belonging to the Turnpike Bluff Group comprising slates and quartzites with minor conglomerates (Clarkson, in press). The true age of the group is unknown but the closest equivalent is the late Precambrian Patuxent Formation of the Pensacola Mountains (Elliot, 1975; ,Clarkson, in press). Structures in the Turnpike Bluff Group trend east-west and are presumed to be Precambrian. This structural trend is approximately perpendicular to the structural trend of the Transantarctic Mountains (Clarkson, in press). The Patuxent Formation of the Pensacola Mountains were first deformed by the late Precambrian Beardmore Orogeny which suggests that the folding in the Turnpike Bluff Group is older than the Beardmore event and as yet undefined (Clarkson, in press).

Lower Palaeozoic

At the northern end of the range, in the Haskard Mountains, rocks belonging to the Blaiklock Glacier Group lie unconformably on the basement complex but are nowhere seen in contact with the Turnpike Bluff Group (Clarkson, in press). The rocks consist of a lower and upper formation of largely clastic rocks separated by an unknown thickness of unexposed strata (Elliot, 1975). The group is thought to be Cambro-Ordovician in age on the evidence of fossiliferous erratics thought to be derived from an intermediate unit of the group (Thompson, 1972). No folding of the Blaiklock Glacier Group has been observed in the field but the dip of the bedding suggests it may be folded into a N-S trending anticline (Clarkson, in press). A similar N-S trend can be seen in some of the older rocks. Clarkson (in press) and Elliot (1975) relate this trend to the Lower Palaeozoic Ross Orogeny. Dykes cutting the schists of the basement complex have been dated at 457±18 Ma BP (Rex, 1972) and are presumably related to the Ross Orogeny (Clarkson, in press). The Turnpike Bluff Group itself is cut by dykes with ages of 297±12 Ma BP (Rex, 1972) and provides a minimum age for the group.

Since the Ross Orogeny there is evidence of regeneration of the E-W trend in the Shackleton Range in the form of major fault zones occupied by large westward flowing outlet glaciers (Clarkson, in press). A small earthquake at 80°S 20°W (Kaminuma and Ishida, 1971; and Kaminuma, in press) further suggests that fault zones may still be active.

1.4.7 ELLSWORTH MOUNTAINS

The Ellsworth Mountains occur at the head of the Ronne-Filchner Ice Shelf about 750 km to the east of Byrd Station. A major eastward flowing glacier, the Minnesota Glacier, bisects the Ellsworth Mountains into two ranges, the Sentinel Range to the north (containing the highest mountain in Antarctica, Vinson Massif 5140 m asl) and the Heritage range to the south.

Lower Palaeozoic

The Heritage group of Craddock (1969) consists of conglomerate, quartzite, sandstone, slate, phyllite and argillite. Limestone beds near the top of the group contain upper Cambrian fossils (Craddock and Webers, 1964; Webers, 1966). The lower part of the succession is dominated by volcaniclastic rocks (Craddock, 1969). The large estimated thickness of the group implies that its base and the underlying carbonate sequence, the Minaret Group, lie within the late Precambrian (Craddock, 1969; Elliot, 1975). Recent field work has cast doubt on the age of the Minaret and Heritage Groups, the Minaret Group may now even overlie the Heritage Group (Spaettstoesser and Webers, 1980). The relations of the Cambrian Heritage Group to other Cambrian beds in the Transantarctic Mountains are unclear. Lying conformably on the Heritage Group are the Crashsite Quartzites comprising cross-bedded, ripple marked quartzites interbedded with minor amounts of argillite, slate, and conglomerate (Craddock, 1969). Probable upper Devonian brachiopods occur in the upper part of the formation (Boucet et al, 1967).

Upper Palaeozoic - Mesozoic

Conformably overlying the Crashsite Quartzite is the glacio-marine Whiteout Conglomerate (Craddock, 1969). Hjelle et al (in press) describe a 1m brown weathered layer at the top of the Crashsite Quartzite and suggest a minor unconformity occurs at the base of the Whiteout Conglomerate. This glacio-marine unit is correlated with the Gale Mudstone of the Pensacola Mountains and with the other late Palaeozoic glaciomarine beds of the Transantarctic Mountains. The Whiteout Conglomerate is conformably overlain by the youngest known formation in the Ellsworth Mountains, the Polarstar Formation, comprising interbedded silty argillites and arenites (Craddock, 1969; Elliot, 1975). Coal beds are also common in the upper part of the formation as well as Permian glossopterid flora (Craddock, 1969; Castle and Craddock, 1975).

The entire Precambrian(?) to Permian sequence of the Ellsworth Mountains were deformed in the early Mesozoic into tight isoclinal folds (Elliot, 1975). This phase of orogeny, the Ellsworth Orogeny (Craddock, 1969) is of a similar age to the Weddell Orogeny of Ford (1972b) that deformed the Pensacola Mountains. Elliot (1975) has correlated the two episodes and termed the event the Gondwanian Orogeny. At the northern end of the Ellsworth Mountains the trend of the folds is north swinging around to NW at the southern end. The northerly trend is almost perpendicular to the trend of folding of a similar age in the Pensacola Mountains. Based on their stratigraphy and structural trends the Ellsworth Mountains appear to be out of position in West Antarctica (Schopf, 1969; Stump, 1973; Elliot, 1975; Clarkson and Brook, 1977).

1.4.8 WHITMORE MOUNTAINS

The Whitmore Mountains lie to the SE of Byrd Station and consist of a series of small mountains and nunataks arranged in an arcuate pattern (see fig. 1.6). The bedrock geology is poorly known having been visited only on a reconnaissance level as part of a larger programme of exploration in West Antarctica (Webers et al, in press). The bedrock consists of predominantly igneous rocks with some metasedimentary horizons.

Metasedimentary rocks comprising altered clastics were found in four exposures by Webers et al (in press). The presence of a large proportion of feldspars (mainly alkali feldspar) and metamorphic rock fragments in the metasedimentary sequence suggest a nearby granitic and metamorphic terrain (Webers et al, in press). Due to insufficient knowledge these rocks have not yet been given formational status.

The entire Precambrian(?) to Permian sequence of the Ellsworth Mountains were deformed in the early Mesozoic into tight isoclinal folds (Elliot, 1975). This phase of orogeny, the Ellsworth Orogeny (Craddock, 1969) is of a similar age to the Weddell Orogeny of Ford (1972b) that deformed the Pensacola Mountains. Elliot (1975) has correlated the two episodes and termed the event the Gondwanian Orogeny. At the northern end of the Ellsworth Mountains the trend of the folds is north swinging around to NW at the southern end. The northerly trend is almost perpendicular to the trend of folding of a similar age in the Pensacola Mountains. Based on their stratigraphy and structural trends the Ellsworth Mountains appear to be out of position in West Antarctica (Schopf, 1969; Stump, 1973; Elliot, 1975; Clarkson and Brook, 1977).

1.4.8 WHITMORE MOUNTAINS

The Whitmore Mountains lie to the SE of Byrd Station and consist of a series of small mountains and nunataks arranged in an arcuate pattern (see fig. 1.6). The bedrock geology is poorly known having been visited only on a reconnaissance level as part of a larger programme of exploration in West Antarctica (Webers et al, in press). The bedrock consists of predominantly igneous rocks with some metasedimentary horizons.

Metasedimentary rocks comprising altered clastics were found in four exposures by Webers et al (in press). The presence of a large proportion of feldspars (mainly alkali feldspar) and metamorphic rock fragments in the metasedimentary sequence suggest a nearby granitic and metamorphic terrain (Webers et al, in press). Due to insufficient knowledge these rocks have not yet been given formational status.

Two granites of differing ages have been recognised by Webers et al (in press) in the Whitmore Mountains. The Mount Seelig Granite is a grey, coarsely crystalline porphyritic granite with a K-Ar age of 190 ±8 Ma BP. The granite intrudes the metasedimentary rocks and is itself cut by a younger granite in the Linck Nunataks. In contrast to the Mount Seelig Granite the Linck Nunataks Granite is a grey equigranular finely crystalline granite with a K-Ar age of 176±5 Ma BP (Webers et al, in press). The radiometric ages in the two granites would suggest that the Whitmore Mountains belong to the same tectonic province as the Ellsworth Mountains (Webers et al, in press).

Scattered nunataks between the Ellsworth and Whitmore Mountains, the Nash, Pirrit, and Martin Hills and Pagano Nunatak all show geological similarities (Craddock and Webers, in press). They consist partly or wholly of mainly felsic intrusive rocks with (except Pagano Nunatak) exposures of deformed metasediments. Radiometric ages lie in the range 163-190 Ma BP and these rocks are likely to be related to the early Mesozoic Gondwanian Orogeny (Elliot, 1975; Craddock and Webers, in press).

1.4.9 MARIE BYRD LAND

Exposures of bedrock in Marie Byrd Land are mainly confined to a coastal region at the east side of the Ross Sea and eastwards towards Thurston Island.

Late Precambrian - Lower Palaeozoic

Based upon minimal evidence late Precambrian-Cambrian metasediments constituting the Swanson Formation crop out in central and southern portions of the Ford Ranges in Marie Byrd Land. The Swanson Formation strata were originally greywackes, sandstones and argillites but have been

deformed and metamorphosed to hornfels, metagreywackes, slates, phyllites, semischists and schists (Wade and Long, in press). The Swanson Formation is associated with an older, highly metamorphosed and migmatised sequence of sediments belonging to the Fosdick Complex (Wade and Long, in press). The Fosdick Complex formed ancestral Fosdick Mountains and supplied sediment for the Swanson Formation. The rocks of the Fosdick Complex show signs of a Precambrian deformation and metamorphism (Wade and Long, in press). The Swanson Formation has many similarites in lithology, deformational pattern and metamorphic history with the Robertson Bay Group of Northern Victoria Land although Wade and Long (in press) favour the suggestion that the two groups are totally unrelated.

Mid Palaeozoic

Evidence of a mid Palaeozoic event is obtained from a Rb-Sr isochron date of 352±21 Ma BP for a granodiorite pluton intruding the Swanson Formation in the Phillips Mountains (Halpern, 1968). Similar plutons in the Ford Ranges give K-Ar ages in the range 301±11 Ma BP to 355±12 Ma BP (Wade, 1972). Elliot (1975) includes the intrusive phase in the Borchgrevink Orogeny. A younger system of folds can be seen affecting rocks of the Fosdick Complex and also the Swanson Formation and has been related to the same orogeny (Elliot, 1975; Wade and Long, in press).

Upper Palaeozoic - Mesozoic

A late Palaeozoic - early Mesozoic event is recorded in intrusives and metamorphic rocks in the Kohler Range on the coast of eastern Marie Byrd Land. A quartz diorite gives a Rb-Sr age of 265±20 Ma BP (Halpern, 1972) and has been included by Elliot (1975) in the early Mesozoic Gondwanian Orogeny. A late Palaeozoic - Mesozoic hiatus occurs in the record since

not one outcrop of sediment of that age has been observed (Wade and Wilbanks, 1972). Deformation and intrusive activity culminated in the middle Cretaceous with the intrusion of numerous granite - granodiorite batholiths over a wide area (Wade and Wilbanks, 1972; Elliot, 1975). Dates fall between 166 and 88 Ma BP and this mainly intrusive event is recorded across much of the Pacific side of West Antarctica and is termed the Andean Orogeny (Elliot, 1975).

Cenozoic

Evidence of Cenozoic volcanic activity is seen in most of the exposed parts of Marie Byrd Land. LeMasurier (1972) has divided the volcanics into a basal unit of sub-horizontal flows with palagonitised tuffs and breccias, overlain by strato-volcanoes comprising flows and pyroclastics and parasitic cones. The basal unit and parasitic cones are largely alkali basalt and the stratovolcanoes consist of felsic flows and pyroclastics of alkaline composition. The flows of the basal unit rests unconformably on the basment erosion surface (Wade and Wilbanks, 1972).

1.4.10 ELLSWORTH LAND

Exposure in Ellsworth Land is restricted to the western coastal area, including Thurston Island, and to mountains in the east at the base of the Antarctic Peninsula.

Palaeozoic - Mesozoic

A series of metavolcanic rocks ranging in composition from basic to acidic form scattered outcrops on Thurston Island. Their age is uncertain, possibly Palaeozoic (Lopatin and Orlenko, 1972) but have been related to the Ross Orogen by Elliot (1975). Igneous and metamorphic rocks between Marie Byrd Land and Thurston Island have yielded whole rock and mineral

not one outcrop of sediment of that age has been observed (Wade and Wilbanks, 1972). Deformation and intrusive activity culminated in the middle Cretaceous with the intrusion of numerous granite - granodiorite batholiths over a wide area (Wade and Wilbanks, 1972; Elliot, 1975). Dates fall between 166 and 88 Ma BP and this mainly intrusive event is recorded across much of the Pacific side of West Antarctica and is termed the Andean Orogeny (Elliot, 1975).

Cenozoic

Evidence of Cenozoic volcanic activity is seen in most of the exposed parts of Marie Byrd Land. LeMasurier (1972) has divided the volcanics into a basal unit of sub-horizontal flows with palagonitised tuffs and breccias, overlain by strato-volcanoes comprising flows and pyroclastics and parasitic cones. The basal unit and parasitic cones are largely alkali basalt and the stratovolcanoes consist of felsic flows and pyroclastics of alkaline composition. The flows of the basal unit rests unconformably on the basment erosion surface (Wade and Wilbanks, 1972).

1.4.10 ELLSWORTH LAND

Exposure in Ellsworth Land is restricted to the western coastal area, including Thurston Island, and to mountains in the east at the base of the Antarctic Peninsula.

Palaeozoic - Mesozoic

A series of metavolcanic rocks ranging in composition from basic to acidic form scattered outcrops on Thurston Island. Their age is uncertain, possibly Palaeozoic (Lopatin and Orlenko, 1972) but have been related to the Ross Orogen by Elliot (1975). Igneous and metamorphic rocks between Marie Byrd Land and Thurston Island have yielded whole rock and mineral

ages between 310 and 355 Ma BP (Wade, 1972; Craddock, 1972) and is further evidence of the effects of a mid Palaeozoic event in West Antarctica at about the same time as the Borchgrevink event (Elliot, 1975). Evidence of the late Palaeozoic - early Mesozoic event, the Gondwanian Orogeny can be found in the Jones Mountains located on the Eights Coast of the Bellingshausen Sea. A basement complex of intrusive and extrusive igneous rocks contains a coarse grained granite with a late Triassic K-Ar age of 199±6 Ma BP (Craddock et al, 1964). The complex is however predominantly Mesozoic in age (Craddock et al, 1964) related to the Andean Orogeny (Elliot, 1975).

Jurassic rocks are the oldest exposed in the mountains in eastern Ellsworth Land and comprise a sequence of sedimentary and volcanic rocks (Laudon, 1972). The volcanics, mainly felsic in composition, crop out in the north of the area and include many dacites and andesites (Laudon, 1972). These rocks were folded during the late Jurassic - early Cre taceous and intruded by mafic dykes (Laudon, 1969). Plutons of diorite, granodiorite, quartz diorite and quartz monzonite, bearing a close genetic relationship to Andean intrusives in other parts of West Antarctica, were intruded into the succession during the middle Cretaceous (Laudon et al, 1969; Laudon, 1972; Elliot, 1975).

Cenozoic

Evidence of Cenozoic volcanics is common in the areas of outcrop in Ellsworth Land. Pliocene olivine basalts occur in the Merrick Mountains of eastern Ellsworth Land (Laudon, 1972) while in the Jones Mountains on the Eights Coast largely flat lying olivine basalt pyroclastics, flows and intrusives overlie the eroded surface of the Jurassic igneous basement (Craddock et al, 1964). Similarly the Hudson Mountains to the south of Thurston Island comprise a group of volcanic cones composed principally of olivine basalts and tuffs (Wade and Wilbanks, 1972).

1.4.11 ANTARCTIC PENINSULA

The Antarctic Peninsula extends from West Antarctica to as far north as 63° S in the form of an arcuate dissected plateau decreasing in height northwards (Barker and Griffiths, 1972). The Peninsula is thought to form the southern end of the Scotia Ridge which comprises a system of submarine ridges and associated troughs forming a loop that extends 1500 km east from the tip of the Peninsula and Tierra del Fuego. Many similarities therefore exist between the southernmost Andes and rocks of the Antarctic Peninsula (Barker and Griffiths, 1972; Dalziel and Elliot, 1971,1973).

Basement Complex

The only extensive outcrop of basement metamorphics reported in the Antarctic Peninsula occurs on the west coast at Marguerite Bay between Adelaide and Alexander Islands (Dalziel and Elliot, 1973). The basement, in contrast to other parts of the Scotia Ridge, consists largely of orthogneiss rather than paraschists. In view of the contrast between the Marguerite Bay rocks and the undoubted pre - Jurassic metamorphic complexes elsewhere in the Scotia Ridge, Dalziel and Elliot (1973) believe that they may be,in part, of Mesozoic age.

Late Palaeozoic Sedimentary Sequences

Rocks assigned to these sequences occur intermittently in the Antarctic Peninsula. The most extensive and northerly exposures occur in the Trinity Peninsula Series. Outcrops on the west side of the Peninsula are sparse south of 64° S though they are reported from Alexander Island (Grikurov, 1978). This series consists largely of graywacke and shale with chert, limestone, various other sedimentary rock types and possi bly mafic metavolcanics (Dalziel and Elliot, 1973). The Cape Legoupil Formation which crops out on the NW coast of the Peninsula bears striking resemblance to the Trinity Peninsula Series. Earlier suggestions of a lower

Cretaceous age for this formation are now incorrect and a Permo-Triassic age accepted (Dalziel, in press, Thompson, 1975). The Legoupil Formation is also considered to be lithologically identical to the Miers Bluff Formation of Livingston Island (Dalziel, in press).

Late Palaeozoic rocks throughout the Peninsula are highly folded and show evidence of polyphase deformation. Dalziel and Elliot (1973) believe that the present isolated areas of outcrop may have resulted from obliteration of one original depositional basin by subsequent early Mesozoic tectonism. This tectonic activity is related to the Gondwanian Orogeny (Elliot, 1975) which is eqivalent to the Weddell Orogeny of Ford (1972) and the Ellsworth Orogeny of Craddock (1972).

Late Mesozoic

The Antarctic Peninsula, associated islands to the east and Alexander Island on the west, show considerable thicknesses of Mesozoic rocks. Palaeontologically dated late Jurassic sequences are known only at Hope Bay and at Ablation Point on Alexander Island (Dalziel and Elliot, 1973). The Hope Bay sequence consists of coarse conglomerate with thin sandstones and mudstones passing up into mudstone and shale with subordinate sandstone (Bibby, 1966). The top of the section includes tuffs and agglomerates that mark the base of the late Jurassic volcanic sequence. The Jurassic volcanics reach their maximum thickness , 3050 m, further south on Oscar II Coast (Adie, 1964). The volcanics are principally andesite lavas and pyroclastics with minor amounts of basaltic and rhyolitic flows (Dalziel and Elliot, 1973). These volcanics probably form much of the main axis of the Peninsula south of Oscar II Coast and Marguerite Bay.

On Alexander Island a sedimentary succesion largely volcanic in origin outcrops at Ablation Point and Belemnite Point while further south at Fossil Bluff a thick related sequence occurs. On the eastern side of the island, however, a considerable thickness of deltaic sandstones and conglomerates overlain by interdeltaic sandstone and mudstone crop out (Dalziel and Elliot, 1973).

Intensive deformation took place in the Cretaceous - earliest Tertiary Andean Orogeny in the Scotia Arc region except in the northern Antarctic Peninsula and the South Shetland and South Orkney Islands (Dalziel and Elliot, 1973). This was preceeded, accompanied and followed by emplacement of the Andean batholithic igneous complex, accompanied locally by thermal metamorphism. The intrusives range in composition from gabbro to alkali granite belonging to a normal calc-alkaline suite (Adie, 1955).

Cenozoic

The Cenozoic is dominated by active volcanism that is part of a widespread volcanic province in West Antarctica. The essentially alkaline volcanism is associated with an extensional tectonic regime that gradually superc eded the Mesozoic calc-akaline activity following the cessation of subduction along the western margin of Antarctica (Barker et al, 1977). There is no proven record of early Tertiary deposits on the Peninsula itself. The only extensive Tertiary sequences occur on the offshore islands to the east (Dalziel and Elliot, 1973).

1.5 GEOPHYSICAL STUDIES

1.5.1 INTRODUCTION

The IGY in 1957 saw a dramatic increase in scientific exploration, especially the earth sciences, in the Antarctic. Much emphasis was placed on examining the geology of the exposed areas of Antarctica and the previous sections of this thesis clearly demonstrate the complexities of Antarctic geology. West Antarctica has experienced several orogenic episodes and there is evidence that parts of West Antartica may not have retained the same position in relation to East Antarctica. The ice sheet in West Antarctica conceals many of the answers to problems concerning tectonic evolution. These problems, short of the ice cap melting, can only be approached using geophysical exploration techniques.

In the years following the IGY the US initiated a programme of oversnow geophysical traverses in West Antarctica. These traverses were, however, very slow and extremely costly to support, and the programme ceased in the mid 1960's. Between 1957 and 1966 the University of Wisconsin flew many thousands of kilometers of aeromagnetic profiles in West Antarctica. These flights however suffered from bad navigation and lack of control on the ice thickness. From the late 1960's airborne Radio Echo Sounding (RES), developed at the Scott Polar Research Institute has been used to study the ice sheet and bedrock of Antarctica. The work described in this thesis represents the first joint use of RES and magnetometry and the only large scale geophysical exploration on mainland Antarctica since the ending of the oversnow traverses and early aeromagnetic flights.

1.5.2 RADIO ECHO SOUNDING (RES)

At suitable frequencies and at low temperatures ice becomes almost transparent to radio waves. This, coupled with the high reflection coefficients of ice/rock and ice/water interfaces enables radio waves to be used for sounding through ice (Robin et al, 1969). The technique of RES, similar in principle to marine acoustic echo sounding, is therefore a rapid means of obtaining accurate and continuous depth profiles through continental ice sheets.

The Scott Polar Research Institute (SPRI) became interested in using radio waves to measure the thickness of ice in the early 1960's (Evans, 1963). During 1967-68 the SPRI undertook its first season of RES in the Antarctic with support from the US National Science Foundation and using a US Navy C-121. This season was mainly for evaluation purposes and was followed in 1969-70 by a fully operational season using this time a C-130F (Robin et al, 1970). Several flights were completed over the Ronne-Filchner Ice Shelf, refueling at Byrd Station but the work suffered badly from navigational inaccuracies that are inevitable with dead reckoning. During 1971-72 an inertial navigational system was used for the first time making it feasible to fly a precise pattern of flights over the featureless interior of the ice sheet. A 100 km rectangular grid of flights was completed in East Antarctica enabling detailed maps of ice sheet surface and more importantly bedrock configuration to be compiled (Drewry, 1975b). During the next season, 1974-75 the SPRI, the Technical University of Denmark (TUD) (with similar experience in Greenland) and the US National Science Foundation entered into co-operation. TUD introduced a new, more powerful radio echo sounder to the Antarctic (Robin et al, 1977). A similar grid, but of side 50 km was completed in Marie Byrd Land in the area between Byrd Station and the Ross Ice Shelf (Rose, 1978). The author was involved in the next two seasons, 1977-78 and 1978-79, when the main objective was to extend this grid to cover the rest of West Antarctica. In

addition to radio echo sounding the aircraft, a C-130R, was equipped with a proton precession magnetometer for simultaneous measurements during both seasons (Drewry and Meldrum, 1978; Drewry et al, 1980).

1.5.3 OVERSNOW TRAVERSES

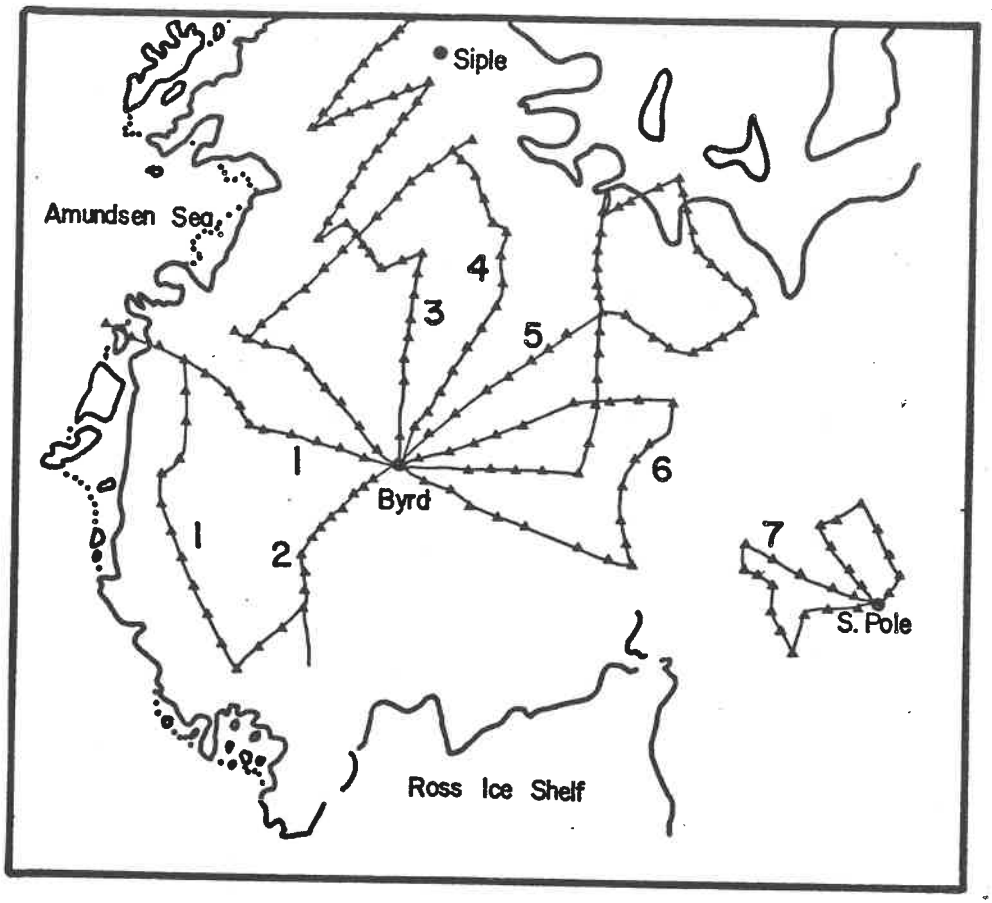
In the years following the IGY the US undertook a programme of geophysical oversnow traverses in West Antarctica. Seismic, gravimetric, altimetric and magnetic observations were made. Fig 1.8 shows the locations of the traverses. In general altimetric, gravimetric, and magnetic observations were recorded every 5.5 km and seismic soundings every 55 km (ie. every 30 minutes of arc).

Altimetric observations

The procedures followed for altimetric measurements were generally the same for all the traverses. Altimeters were carried in two traverse vehicles travelling 5.5 km apart, the rear vehicle occupying successive stations previously occupied by the lead vehicle. This allowed readings from each vehicle to be compared, to give the difference in elevation over the 5.5 km interval. At each stop air temperature and wind velocity were recorded to enable corrections for temperature and for horizontal variations in atmospheric pressure to be applied to the data (Bentley and Ostenso, 1961; Bentley and Chang, 1971). Bentley (1964) estimates the total error relative to a base station for the bulk of the traverses to be 50m with a standard deviation of 25m. The traverses in West Antarctica are on the whole better than average with errors in the range 20-25m (Bentley and Chang, 1971).

Gravimetric observations

The gravity values were chiefly used to provide topographic detail between



US Oversnow Traverse

1	Marie Byrd Land Traverse	1959-60
2	Little America - Byrd Traverse	1956-57
3	Ellsworth Highland Traverse	1960-61
4	Sentinel Range Traverse	1957-58
5	Wisconsin Traverse	1963-64
6	Horlick Mountains Traverse	1958-59
7	South Pole Traverse	1962-63
▲	Seismic Station	

Fig. 1.8 Location of US oversnow traverses in West Antarctica.

seismic stations. The general method adopted is to equate changes in free air anomaly (FAA) relative to a seismic station to changes in ice thickness by assuming that the principal influence on gravity will be due to the density contrast between ice and rock. This difference is then added to or subtracted from the seismic determined elevation of the rock surface relative to sea level (Bentley and Ostenso, 1961; Behrendt, 1964a; Bentley and Chang, 1971). The difference in elevation between the seismic elevation and that obtained from the FAA at the next seismic station may then be distributed lineally over the intervening gravity stations. Using a semi-infinite slab approximation and a density for ice of 900 Kgm^{-3}, and for rock 2670 kgm^{-3} the factor is 13.56 m/mgal. Bentley (1964) estimates that the average error due to topography in determining bedrock elevation from gravity is $\pm$300 m for all Antarctic traverses. However in areas of rough terrain the error is likely to be several hundred meters (Bentley and Chang, 1971). For this reason seismic elevations and not those determined from interpolation using the FAA have been used in this thesis.

Magnetic observations

During early traverses (Bentley and Ostenso, 1961; Bentley and Chang, 1971) magnetic data are of limited value consisting of measurements of vertical intensity only. The readings suffer badly from calibration changes, temperature effects and instrument drift. No corrections were applied for temporal variations because of the long distances from any control station. In a later traverse Behrendt (1964a) adopted a different system of magnetic observations, using two proton precession magnetometers measuring the total field and using an interval method similar to that adopted for altimetric observations. Magnetometers were placed in both the lead and the rear vechicles. Measurements were made on the move at intervals of 0.75 km, the rear vechicle reoccupying the positions of the lead vechicle. At each stop for altimetric observations simultaneous readings of the magnetometers were made by a radio-link. This method allows correction for diurnal change and recognition of magnetic storms. Crossing each anomaly twice adds confidence to the readings (Behrendt,

1964a).

Seismic observations

Every ~55 km on all the traverses seismic reflection measurements were made, primarily to calculate ice thickness to be used for calibrating the FAA. A major source of error arises in the determination of seismic velocity in ice. Bentley and Chang (1971) use a constant negative correction of 30m to account for the velocity gradient in the upper low density 200m. Bentley and Ostenso (1961) and Bentley and Chang (1971) report a low velocity layer at the base of the ice sheet. They adopt a velocity 3850 ms^{-1} through the top 90% of the ice and 3600 ms^{-1} in the remaining 10%. Bentley (1964) estimates the errors of measurement to be $\pm$2% in West Antarctica. Fig. 1.8 shows locations of oversnow traverses with the seismic reflection stations marked.

About three dozen seismic refraction profiles long enough to provide information about seismic velocities beneath the ice have been completed on the Antarctic Ice Sheet, mainly during the programme of oversnow traverses. The results of these measurments are summarised in Bentley and Clough, (1972) and Bentley (1973) and are based on the work of Crary and Van der Hoeven (1961), Bentley and Ostenso (1961), Behrendt (1963), Crary (1963a,1963b), Robinson (1963, 1964a, 1964b), and Chang (1964). Time as well as explosives were in short supply on the oversnow traverses and the profiles are not nearly as complete as would be desirable, several comprising of only a single shot (Bentley, 1973). As a result seismic velocity sections beneath the ice cannot be deduced in detail but Bentley and Clough (1972) have been able to put some definite limits on acceptable geological columns in regions devoid of outcrop.

The only determination in West Antarctica of deep crustal structure from explosion seismology comes from an unpublished refraction profile, 23 km long, at 83°S 70°w near the head of the Ronne-Filchner Ice Shelf (Bentley, 1973). Positions of seismic refraction profiles are shown on fig. 1.9.

1.5.4 AEROMAGNETICS

Between 1958 and 1964 investigators from the University of Wisconsin flew 75000 km of aeromagnetic profiles in Antarctica. The first flights were made by Thiel in 1958-59 and 1959-60. During 1960-61 Behrendt and Wold (1963) flew 14000 km of profile entirely in West Antarctica. Total field measurements were made from a US Navy R4D8 aircraft at altitudes of between 500 and 1000 m above the ice surface. The data were not corrected for diurnal and magnetic storm effects because of the great distances of the flights from Byrd Station (Behrendt and Wold, 1963). Two methods of analysis were adopted by Behrendt and Wold (1963). Anomalies with wavelengths <50 km were studied in profile form since the flight lines were too widely spaced to permit correlation from one line to another. Peter's (1949) half-slope method was used on selected anomalies to obtain an estimate of maximum depth to magnetic basement. Fig. 1.10 shows the location of flight tracks in West Antarctica with the positions of depth estimates by Behrendt and Wold (1963) shown. For the longer wavelength anomalies an areal approach was adopted using the method of Mack and Haubrich (1961) in which eleventh- and third-degree least squares polynomial surfaces were fitted to the data and a residual anomaly map produced by the subtraction of the lower degree fit from the higher (Behrendt and Wold, 1963). The error at cross over points was then distributed by a least squares method. Fig. 1.11 is taken from Behrendt and Wold (1963) and shows residual anomalies contoured at 100 nT intervals.

Fig. 1. Locations of seismic refraction profiles (numbered points) and cross-sections (heavy lines) superimposed on a map of subglacial topography. Open circles indicate profiles not included in the cross-sections. Subglacial topographic contours are shown by light lines, solid where above sea-level, dotted where below. The heavier dashed line indicates the approximate position of the pre-glacial shoreline.

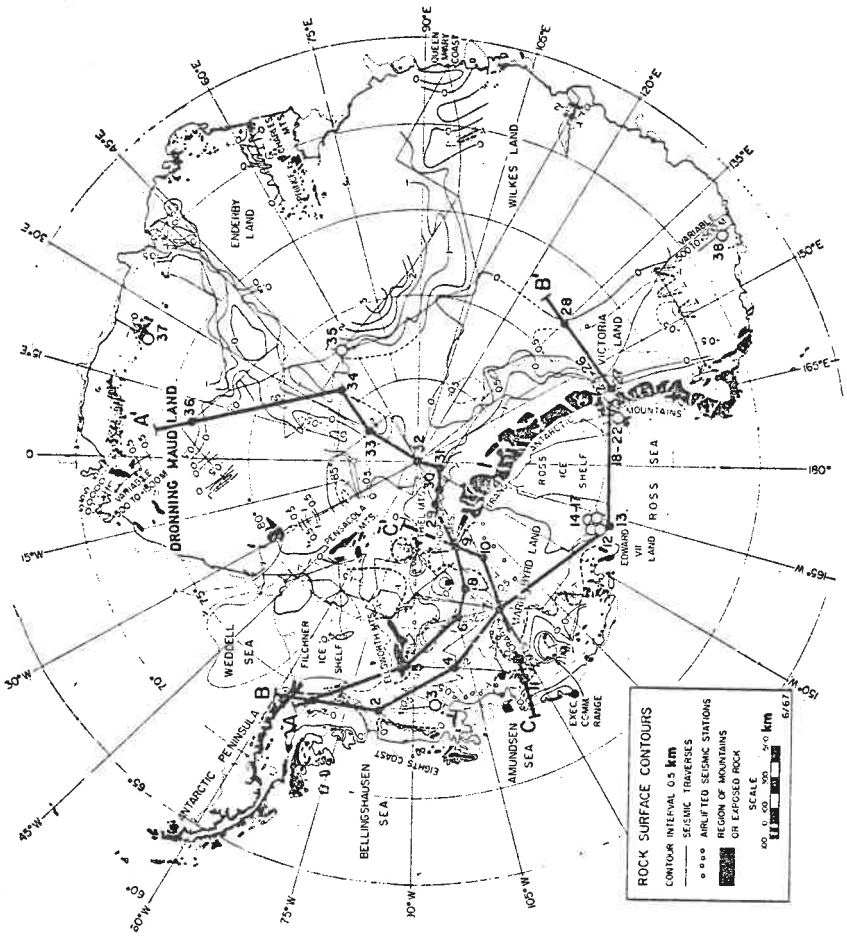


Fig. 1.9 Location of seismic refraction profiles (after Bentley and Clough, 1972).

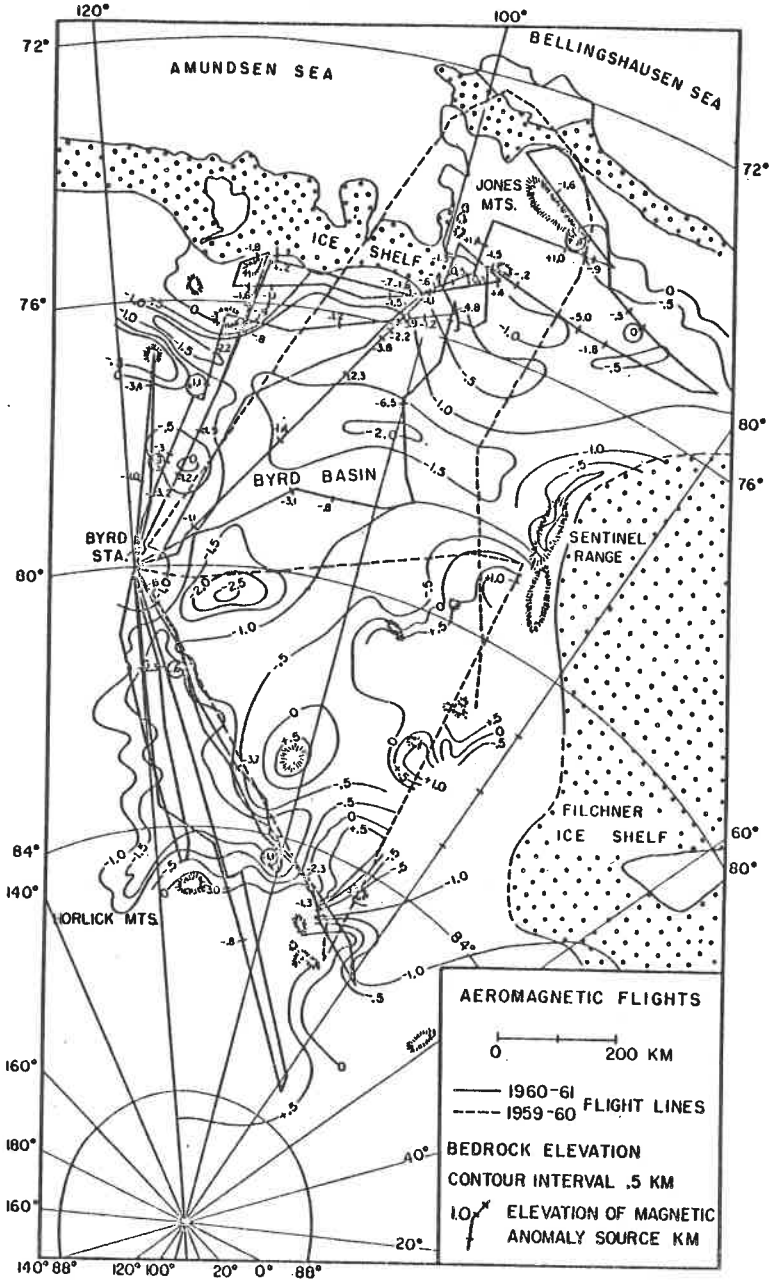


Fig. 4 Bedrock elevation map showing calculated depths to sources of magnetic anomalies.

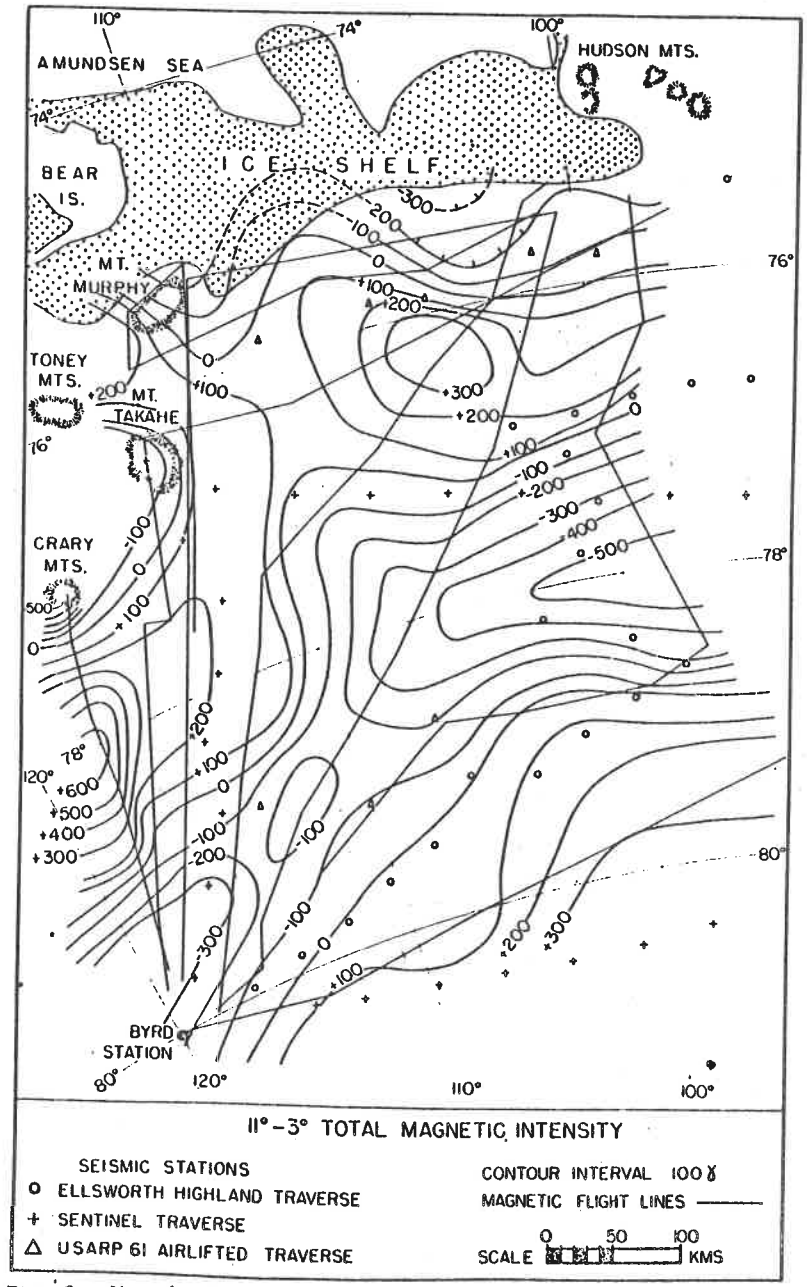


Fig. 9 Map showing difference between 11° and 3° surfaces.

Fig. 1.10 Aeromagnetic flights and depths to magnetic basement.

Fig. 1.11 (top) Residual anomaly map of West Antarctica. (after Behrendt and Wold, 1963).

During 1963-64 a further 48000 km of profile were completed in Antarctica (Behrendt, 1964b). About 28000 km of track were flown over the Transantarctic Mountains and the remaining 20000 km concentrated to the east of Byrd Station over the northern Pensacola Mountains, Berkner Island, the Ronne-Filchner Ice Shelf and the Ellsworth Mountains. Measurements were made at altitudes again ranging from 500-1000 m above the ice surface. Behrendt (1964b) has taken all the aeromagnetic data plus 13000 km of data collected during Project Magnet (US Naval Oceanographic Office, 1963, 1965) and constructed an anomaly density map showing the distribution of anomalies with widths <50 km.

One of the 1963-64 flights flew into the Dufek Massif and Forrestal Range of the Pensacola Mountains and first recorded the high amplitude magnetic anomalies associated with these ranges. The Dufek Massif was known to be formed of statiform gabbro (Neuberg et al, 1959; Aughenbaugh, 1961). The Forrestal Range had not been visited but on the basis of the magnetics it was assumed to be similar in composition to the Dufek Massif. This led to a large scale scientific survey in 1965-66 of the Pensacola Mountains (Huffman and Schmidt, 1966). The results described in detail by Behrendt et al (1974), included aeromagnetic measurements from a US Navy LC117 at a constant barometric elevation of 2100 m.

A severe limitation to all previous aeromagnetic work in the Antarctic has been the lack of control on the bedrock elevation beneath the ice surface. This prevents direct comparison between bedrock profile and magnetic anomalies. Behrendt and Wold (1963) used the maximum depth to magnetic basement, determined by Peter's (1949) graphical half-slope method, to provide an upper limit on the thickness of ice beneath the anomaly. However magnetic basement does not always occur at the ice/rock interface. This thesis descibes the first survey in which aeromagnetics have been combined with RES . The main advantage of this method is to allow elevation of magnetic basement to be compared with the elevation of the ice/rock

interface. Succeeding chapters detail the reduction, analysis and interpretations of this work.

During 1978-79 the author was also involved outside the immediate work of this thesis in a joint programme with the US Geological Survey to revisit the Dufek Intrusion in the Pensacola Mountains. A further 4200 km of track were completed (Behrendt et al, 1980, 1981). (see fig. 1.12)

1.5.5 SEISMOLOGICAL STUDIES

At the beginning of the IGY in 1957 reliable seismographs were installed in Antarctica for the first time. The technique of using dispersive earthquake waves for earth exploration was then applied to problems of Antarctic structure. Earthquakes in general generate surface waves of Love and Rayleigh type which are dispersed in a layered earth in which the elastic parameters vary with depth (Adams, 1972). For earth models in which the variations of seismic velocity and density are known with depth it is theoretically possible to produce dispersion curves showing the relationships between velocity of travel of the wave and its period. At the time of interest in dispersive wave studies in Antarctica rapid digital computers were not available and it was inpractical to investigate models with more than two or three layers (Adams, 1972). Another handicap to the study of Antarctic structure is the lack of major earthquakes on the continent (Bentley, 1973). It has, therefore, been necessary to make use of surface waves from earthquakes at a considerable distance from Antarctica and to make corrections for the non-Antarctic segments of the paths. Although additional dispersion studies have been made in East Antarctica the mean crustal thickness estimate for West Antarctica is still based primarily on Love wave group velocities from a single earthquake at periods between 20 and 30 seconds (Bentley, 1973).

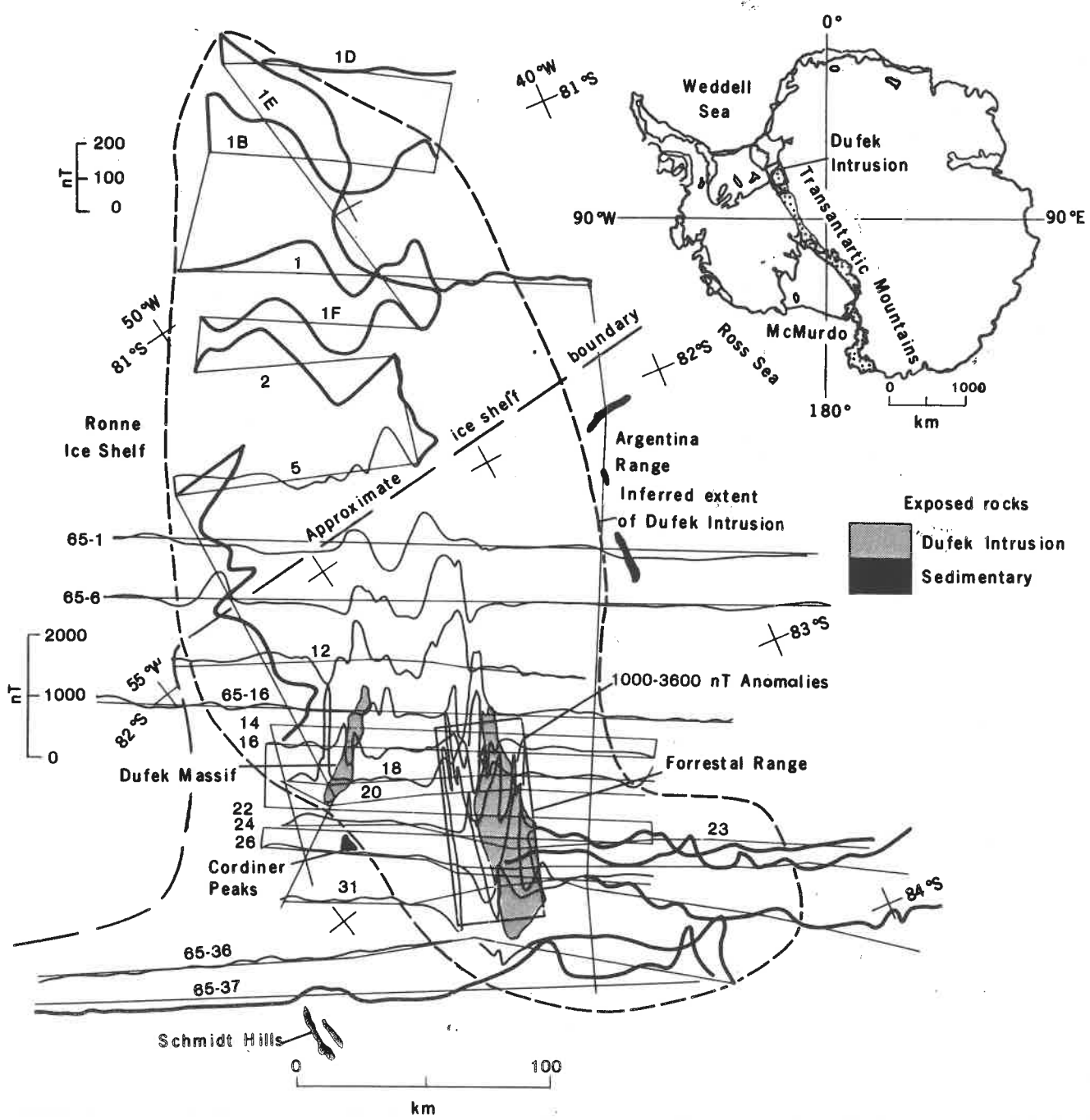


Fig. 1.12 Aeromagnetic flights in the Dufek Massif, Pensacola Mountains.
(after Behrendt et al, 1981)

1.5.6 PALAEOMAGNETIC STUDIES

Palaeomagnetic studies on orientated rock samples in Antarctica have been concentrated in the Antarctic Peninsula, Ellsworth Land and the coast of Marie Byrd Land. Palaeomagnetic studies have also been reported from various localities in the Transantarctic Mountains, mainly on Jurassic dolerites. Fig. 1.13 shows the positions of relevant palaeomagnetic sites.

Early studies of palaeomagnetism suffered from poor dating of samples making precise conclusions difficult. Blundell and Stephenson (1959) collected eight orientated samples from dolerite sills and dykes in the region of Theron Mountains, Shackleton Range and Whichaway Nunataks. Precise age of the rocks is uncertain, but probably Jurassic, and give a palaeo-pole of 54°S 136°W. Turnbull (1959) collected 23 orientated from Cenozoic volcanics at Cape Hallet, 57 samples of Jurassic Ferrar Dolerite from the Ferrar Glacier as well as a few samples of the Beacon Sandstone from the same locality. The oval of confidence about the palaeo-pole for the Cenozoic volcanics only just fails to include the present pole, but this difference is of doubtful significance (Turnbull, 1959). 21 of the samples were reversely magnetised. All of the samples of Ferrar Dolerite were normally magnetised with a mean direction rather different to the present field (Turnbull, 1959). Based on a geocentric dipole model for the earth's magnetic field they give a palaeopole at 58°S 142°W. In the main the samples of Beacon Sandstone were too weakly magnetised for significant measurement (Turnbull, 1959). A further 13 samples of Jurassic Ferrar Dolerite were studied from the Beardmore Glacier area by Briden and Oliver (1963). Their tests indicate a stable direction of magnetisation and give the Jurassic palaeo- pole as 59°S 139°W. This agrees fairly closely with the results of Turnbull (1959) and Blundell and Stephenson (1959) on similar rocks.

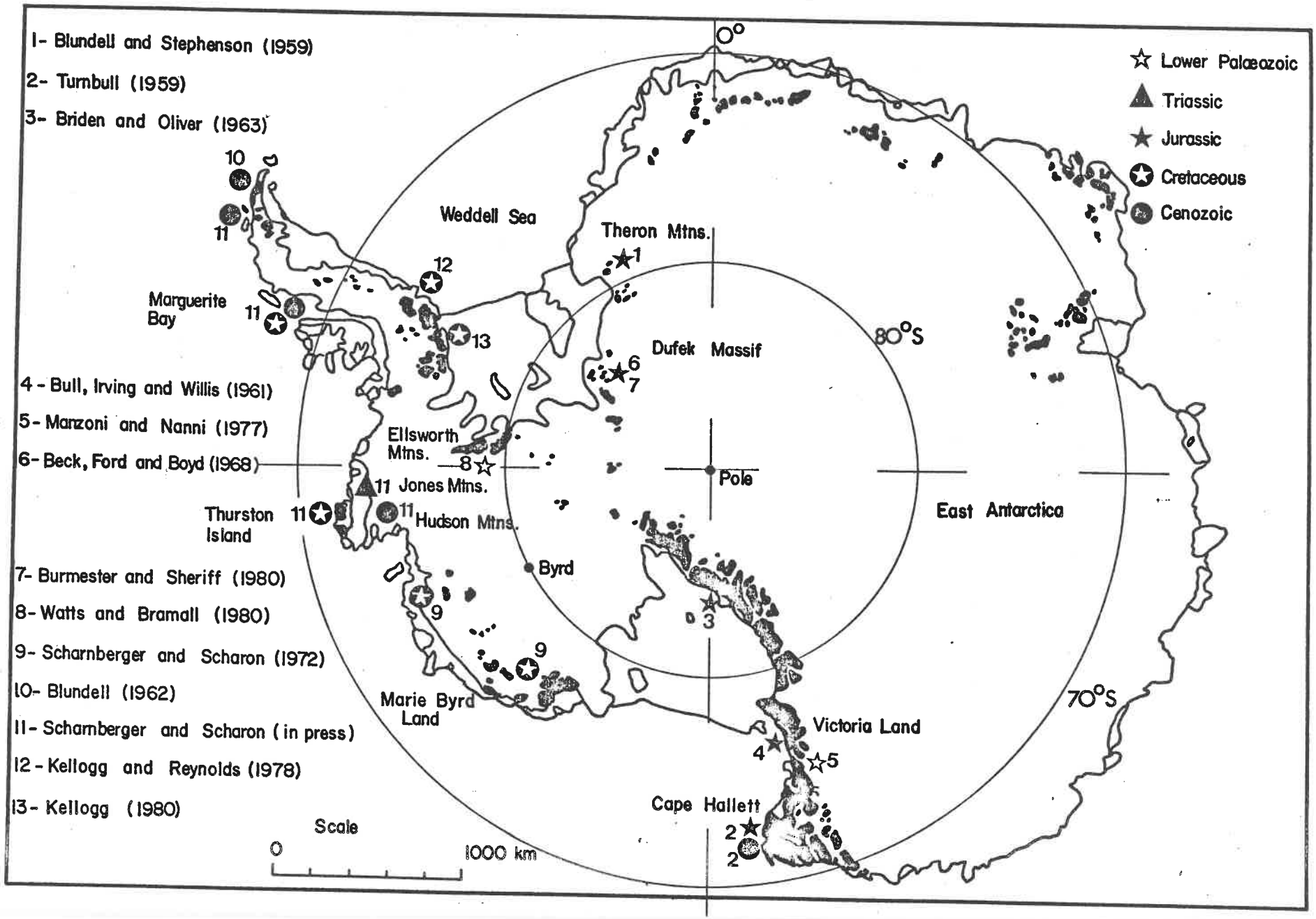


Fig. 1.13 Palaeomagnetic sites in West Antarctica and the Transantarctic Mountains.

More recently Beck, Ford and Boyd (1968) collected 57 samples at 43 different sites scattered throughout the exposures of the stratiform Dufek Intrusion in the Pensacola Mountains. The Dufek Intrusion is thought to be co-magmatic with the Ferrar Dolerites of the Transantarctic Mountains (Ford, 1970; Ford and Kistler, 1980; Kyle et al, 1980). The average palaeomagnetic pole position for the Dufek Intrusion 47°S 164°W (Beck, Ford and Boyd, 1968). This is not within the cluster of poles which have been calculated for the Ferrar Dolerites and may indicate that the two are not precisely contemporaneous. Five sites were reversely magnetised in a arrangement that could be explained either by cooling of the intrusion through a reversal of the earth's field or by mineralogically controlled self reversal (Beck, Ford and Boyd, 1968). Recent aeromagnetic work favours cooling through reversals of the earths field (Behrendt et al, 1980,1981). Burmester and Sheriff (1980) have recalculated the palaeopole for the Dufek Intrusion, assuming no tectonic correction is needed, to be 60°S 223°E.

Palaeomagnetic studies outside the Transantarctic Mountains are concentrated in and at the base of the Peninsula, in the Ellsworth Mountains and in the coastal outcrops of Marie Byrd and Ellsworth Lands. Orientated samples were collected from 27 sites in granitic plutons and from 5 sites in basaltic dykes cutting the plutons in Marie Byrd Land (Scharnberger and Scharon, 1972, see fig. 1.13). Absolute ages on two of the granites indicate lower Cretaceous dates for the intrusive activity. Scharnberger and Scharon (1972) determined the Lower Cretaceous palaeomagnetic pole at 36°S 116°E. The basic dykes are younger than the granites and define a polar wandering path across the southern Indian Ocean (Scharnberger and Scharon, 1972). When compared with the middle Jurassic palaeo-poles for the Transantarctic Mountains there is a striking contrast and Scharnberger and Scharon (1972) interpret this as indicating that East and West Antarctica were separate entities in lower Cretaceous times.

Preliminary results from the Ellsworth Mountains indicate that mean declinations of palaeomagnetic vectors for late Cambrian - early Ordovician rocks are ~90° different from those of the east Antarctic craton (Watts and Bramall, 1980).

In the Peninsula region Blundell (1962) reports on a study of 400 samples collected at 104 different sites in Graham Land situated at the northern end of the Antarctic Peninsula. Palaeomagnetic poles are only given for the Cretaceous Andean Suite and for the Cenozoic volcanics as the intrusion of the Andean Suite has effectively destroyed the original magnetism in older rocks (Blundell, 1962). The results show that the Cretaceous and Cenozoic rocks both lie close to the axial dipole field and are consistent with the hypothesis that the earths magnetic field has remained constant, in Graham Land, apart from secular variation, since the beginning of the Tertiary. Similar results are obtained by Scharnberger and Scharon (in press) from 47 sites in Graham Land and 22 in Ellsworth Land. These results contrast with the middle Jurassic poles from the Transantarctic Mountains and the lower Cretaceous poles from Marie Byrd Land. They indicate that Ellsworth Land is part of an Antarctic Peninsula tectonic unit and that this area, Marie Byrd Land and the Transantarctic Mountains formed 3 separate tectonic plates during Mesozoic times (Scharnberger and Scharon, in press).

Further evidence for little movement of the Antarctic Peninsula in the last 100 Ma BP is reported by Reynolds and Kellogg (1974) and Kellogg and Reynolds (1974, 1978) from 290 samples at 64 sites on the Lassiter Coast at the southern end of the Peninsula. The upper Cretaceous plutons and dykes of the Lassiter Coast give palaeo-poles of 83°S 131°W (Kellogg and Reynolds, 1978). More recently Kellogg (1980) has reported on palaeomagnetic work from further south on the Orville Coast and in eastern Ellsworth Land. Results on upper Cretaceous plutons and dykes define an average palaeomagnetic pole at 71°S 165°W (Kellogg, 1980). The mean

declinations of Andean Intrusives elsewhere in the Peninsula are orientated towards the north while those on the Orville Coast and in eastern Ellsworth Land have mean declinations rotated 51° from north (Kellogg, 1980). Although the 95% confidence level is large (±27°) Kellogg (1980) concludes that the southern part of the Peninsula has undergone major oroclinal bending since the late Cretaceous.

1.5.7 MARINE GEOPHYSICS

Much of the marine geophysical studies in the southern oceans around Antarctica concentrated on the ocean basins and the processes of sea-floor spreading. The amount of data collected is impossible to review in the specific context of this thesis. Much of the data and their bearing on Antarctica is used in Gondwanaland reconstructions discussed earlier (eg. Molnar et al, 1975; Barker and Griffiths, 1977; Norton and Sclater, 1979). The results of many cruises in southern waters by the US research vessel Eltanin are reviewed by Hayes (1973) and more detailed studies in the Scotia Sea area by Barker and Griffiths (1972,1977), Barker (1979), Hill and Barker (1980), Barker et al (in press), and Dalziel and Elliot (1971,1973). Of more interest to the work of this thesis are the results of the Deep Sea Drilling Project (DSDP) obtained during cruises of the Joint Oceanographic Institutions for Deep Earth Sampling (JOIDES) research vessel Glomar Challenger. During four legs of DSDP, legs 28, 29, 35, and 36, 31 sites were drilled in Antarctic and sub-Antarctic waters (fig. 1.14). The results of these four legs are reviewed by Drewry (1976) and for completeness those sites on the Antarctic continental shelf will be described here.

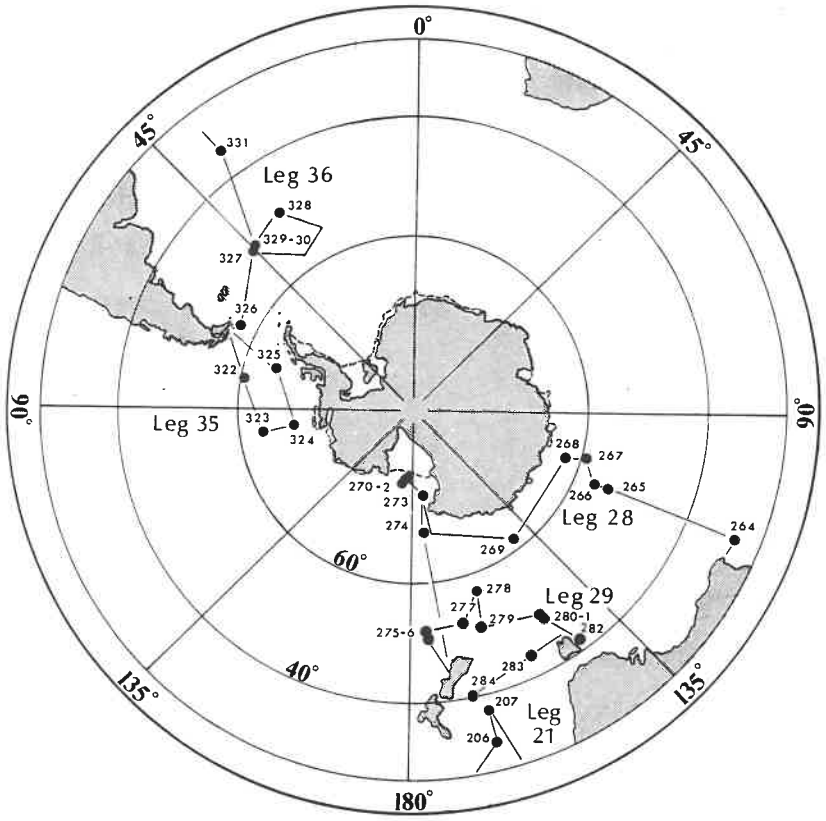


FIG 1. JOIDES deep-sea drilling sites in Antarctic and sub-Antarctic waters, legs 28, 29, 35 and 36.

Fig. 1.14 DSDP sites in Antarctic and sub-Antarctic waters (after Drewry, 1976).

During leg 28 four sites were occupied in the Ross Sea with the purpose of sampling the basment on the Antarctic continental shelf. Basement was successfully cored at site 270 and consisted of calc-silicate gneiss, schist and impure marble similar to rocks of the Skelton Group exposed in the Transantarctic Mountains adjacent to McMurdo Sound and to Cambrian limestones (Shackleton limestone) exposed in the central and southern Transantarctic Mountains (Ford and Barrett, 1975). Much of the Ross Sea beneath the Ross Ice Shelf may be floored by early Palaeozoic granitic and metamorphic rocks similar to those of the basement complex of the Transantarctic Mountains (Drewry, 1976). Hayes and Davey (1975) suggest that the western Ross Sea contains evidence of minor rifting between East and West Antarctica, which could be related to a short lived spreading centre (Drewry, 1976).

Two sites (324 and 325) were drilled on the Antarctic continental shelf in the Bellingshausen Sea during leg 35. Unfortunately basement was not reached at either site. Leg 36 drilled 6 sites on the Falkland Plateau. The Falkland Islands, which are an exposed part of the plateau, comprise a presumed Precambrian basement overlain by a thick sequence of marine and terrestrial Palaeozoic sediments and some Mesozoic diabase intrusives (Drewry, 1976). Only site 330, at the eastern end of the Falkland Plateau, sampled the basement which comprised Precambrian gneisses and granites (Barker et al, 1974). The establisment of the Precambrian continental nature of the Falkland Plateau has important consequences on Gondwanaland reconstructions ruling out any overlap of the Antarctic Peninsula with the plateau, as shown in Smith and Hallam (1970).

Recent work completed in the Weddell Sea area should provide valuble information in an almost inaccessible and consequently little known area of Antarctic waters which may have important implications to the evolution of West Antarctica (Fossum et al, in press, Barker and Jahn, 1980). Reconnaissance work by Barker and Jahn (1980) revealed magnetic

lineations trending north of east and small offset fracture zones in the eastern Weddell Sea. They conclude, however, that the quality of the data set is, as yet, inadequate and are unable to provide an unambiguous age for the Weddell Sea.

1.6 STRUCTURE OF WEST ANTARCTICA FROM GEOPHYSICAL STUDIES

1.6.1 SUBGLACIAL TOPOGRAPHY OF WEST ANTARCTICA

In a continent where 95% of its area is hidden by ice knowledge of the topography of the bedrock beneath the ice is naturally not well known but of geological interest. Before the advent of RES the only information on bedrock elevations were obtained by seismic and gravity measurements on oversnow traverses. Maps depicting the subglacial topography are presented by Thiel (1961), Bentley and Ostenso (1961), Bentley (1962), Bentley (1964), Woollard (1968), Bentley and Chang (1971) and Heezen, Tharp and Bentley (1972). The amount of data that the subglacial topography maps are based on is shown in fig. 1.8. The contouring of rock elevations is very subjective and must be treated with a degree of caution because the traverse tracks are too widely spaced to permit positive interpolation of minor features (Bentley, 1964). However several major conclusions about the nature of the bedrock topography were reached;

1) The subglacial topography of West Antarctica is extremely rugged.
2) The subglacial topography of West Antatctica contrasts strikingly with that in East Anatrctica. Whereas the subglacial floor of East Antarctica would be nearly everywhere above sea level after allowing for isostatic readjustment, much of West Antarctica would lie below sea level.
3) A great subglacial basin exists between the Ross Sea and the

Bellingshausen - Amundsen Seas beneath the ice of West Antarctica. Depths within this basin reach 2500 m below sea level (Bentley, 1964).

4) There is no major channel or depression connecting the Ross and Weddell Seas as originally thought.

5) Prior to the formation of the ice cap, West Antarctica consisted entirely of islands with no land connection with the main part of the continent. Evidence suggests a number of small islands plus four large ones: Marie Byrd Land, the Eights Coast, the Antarctic Peninsula and the Ellsworth Mountains.

Fig. 1.15 shows the subglacial topography of West Antarctica as known before RES.

1.6.2 UPPER CRUSTAL STRUCTURE

The structure of the upper crust has been determined largely from seismic refraction studies with additional information from aeromagnetics and from gravity and magnetic observations on oversnow traverses. The seismic refraction profiles (Bentley and Clough, 1972) are summarised in fig. 1.16.

Section A-A' of Bentley and Clough (1972) is shown in fig. 1.9 and runs from the base of the Peninsula along the mountainous spine of West Antarctica through the Horlick Mountains past the South Pole and into Dronning Maud Land. Column 1 in fig. 1.16 is located at the base of the Peninsula and the velocity structure is typical of granitic intrusives probably belonging to the Andean Intrusive Suite overlain by possible Mesozoic sediments (Bentley and Clough, 1972). Column 5 is close to nunataks at the western end of the Ellsworth Mountains. The 1.3 km thick layer of velocity 5.2 kms^{-1} probably corresponds to Palaeozoic metasediments cropping out in the nunataks. This layer is underlain by

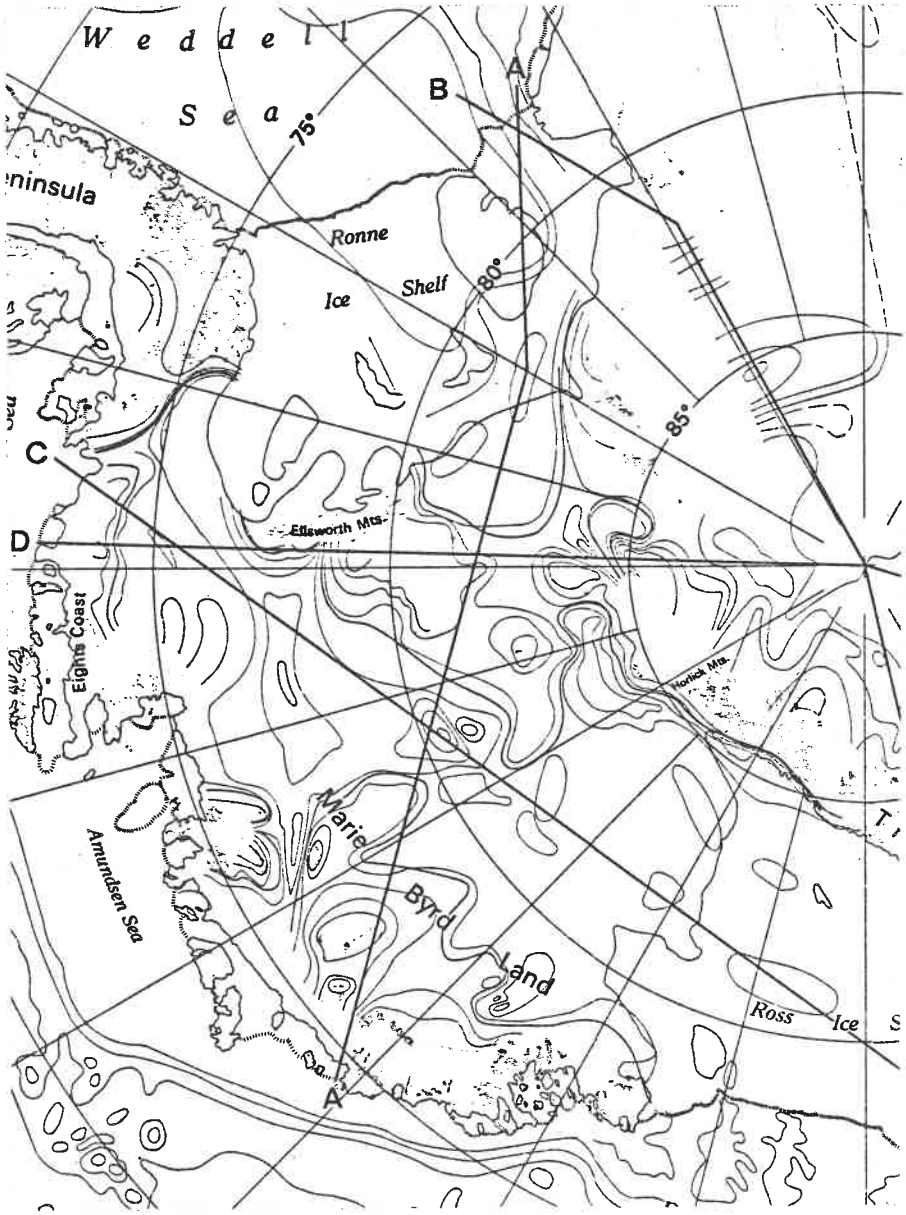


Fig. 1.15 Subglacial topography of West Antarctica (after Heezen et al, 1972).

strata with a velocity of 6.1 kms^{-1} which Bentley and Clough (1972) believe must represent Precambrian basement that is no where exposed in the Ellsworth Mountains. Magnetic data would suggest that similar terrain extended north to the track of the Antarctic Peninsula Traverse (Behrendt, 1964a). Colunm 6 is on the eastern edge of the Byrd Subglacial Basin and is essentially the same as column 5. This is supported by early magnetic data which show an area of few magnetic anomalies extending west from the Sentinel Range about half the distance to Byrd Station and probably represents subglacial extension of the thick metasedimentary section exposed in the Ellsworth Mountains (Behrendt, 1964a; Behrendt and Wold, 1963). Just north of the Whitmore Mountains, in column 8, the layer with velocity 5.3 kms^{-1} probably represents a combination of the same Palaeozoic rocks and felsic volcanics that crop out in the nearby mountains (Bentley and Clough, 1972). Column 9 lies just north of the downfaulted front of the Ohio Range. The 5.5 kms^{-1} layer probably represents granitic basement that is exposed in the mountains, while the 4.4 kms^{-1} layer corresponds well with sediments belonging to the Beacon Supergroup (Bentley and Clough, 1972). The remaining columns indicate velocities consistent with East Antarctic basement.

Section B-B' (see fig. 1.16) again starts with column 1 at the base of the Peninsula and on the similarity of seismic velocities Bentley and Clough (1972) suggest that the 'Antarct-andean' structure can be extended at least as far as column 2. Column 4 is very interesting being situated above what should be typical of the deep part of the Byrd Subglacial Basin. The rocks overlying the basement appear to be distinctly different from the Ellsworth Mountains Palaeozoic strata and from granitic intrusives. Likely possi bilites include Cenozoic volcanic rocks and unmetamorphosed Palaeo-Mesozoic rocks of almost any kind (Bentley and Clough, 1972). Depth determinations on short wavelength anomalies show the absence of a significantly thick sedimentary cover within and to the north and west of the Byrd Subglacial Basin (Behrendt and Wold, 1963). The Byrd Subglacial Basin appears to define the dividing line between different geologic

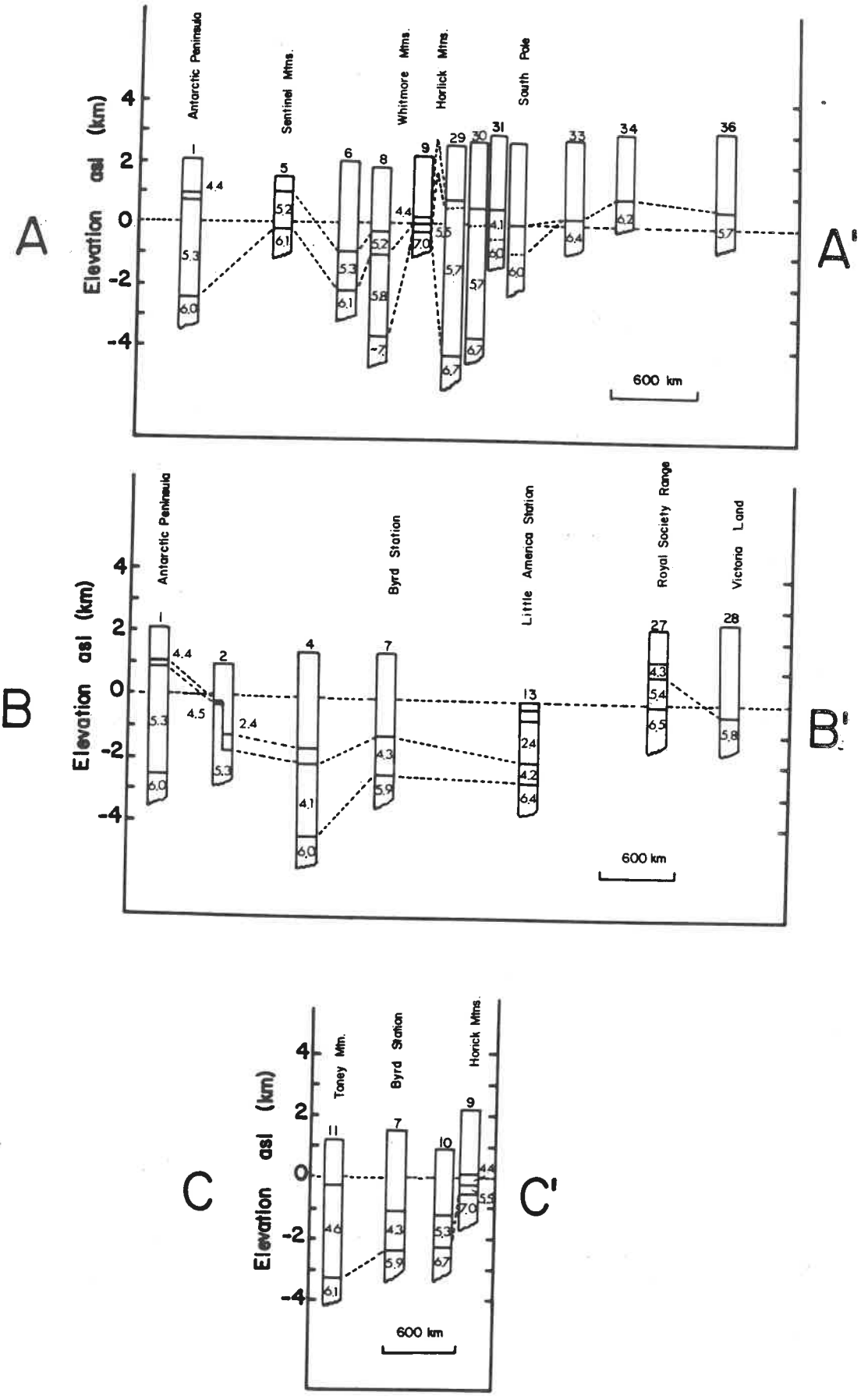


Fig. 1.16 Seismic refraction results

(after Bentley and Clough, 1972)

provinces, with volcanics to the NW and sedimentary rocks and granites to the SE (Bentley and Ostenso, 1961; Behrendt and Wold, 1963; Bentley and Clough, 1972). The section near Byrd Station in column 7 contains similar strata (Bentley and Clough, 1972). Column 13 lies close to Little America and within the extension of the Byrd Subglacial Basin to the Ross Sea. Again rocks similar to those in the deeper part of the basin overlie the basement but are here overlain by 1 km of probable Cenozoic sediments. The section B-B' then crosses the Transantarctic Mountains and continues into East Antarctica. Column 27 lies in the Royal Society Range and shows a seismic structure with velocities typical of Beacon Supergroup rocks, granites and the Ferrar Dolerites.

Section C-C' (see fig. 1.9 and 1.16) is a short north-south profile across the Byrd Subglacial Basin from Toney Mountain to the Horlick Mountains. Column 11 lies on the flank of Toney Mountain and the 4.6 kms^{-1} layer corresponds unambiguously with andesitic-basaltic flows (Bentley and Clough, 1972). This column lies within the Cenozoic volcanic province that characteristically has a shallow magnetic basement (Behrendt, 1964b). On the basis of the magnetics the Flood Ranges do not appear to be part of the Cenozoic volcanic province but rather the plutonic and metamorphic province of the Ford Ranges (Bentley and Chang, 1971). Again the distinct change in seismic structure on crossing the Byrd Subglacial Basin is apparent and further evidence that the Basin represents a major boundary between geological provinces.

In general Behrendt and Wold (1963) recognised a striking correlation between bedrock elevations and residual magnetic anomalies. The magnetics cannot be related to the topography alone as this would require too high susceptibilities but is probable that the residual magnetic and topographic contours are both related to the tectonic pattern of the area (Behrendt and Wold, 1963).

provinces, with volcanics to the NW and sedimentary rocks and granites to the SE (Bentley and Ostenso, 1961; Behrendt and Wold, 1963; Bentley and Clough, 1972). The section near Byrd Station in column 7 contains similar strata (Bentley and Clough, 1972). Column 13 lies close to Little America and within the extension of the Byrd Subglacial Basin to the Ross Sea. Again rocks similar to those in the deeper part of the basin overlie the basement but are here overlain by 1 km of probable Cenozoic sediments. The section B-B' then crosses the Transantarctic Mountains and continues into East Antarctica. Column 27 lies in the Royal Society Range and shows a seismic structure with velocities typical of Beacon Supergroup rocks, granites and the Ferrar Dolerites.

Section C-C' (see fig. 1.9 and 1.16) is a short north-south profile across the Byrd Subglacial Basin from Toney Mountain to the Horlick Mountains. Column 11 lies on the flank of Toney Mountain and the 4.6 kms^{-1} layer corresponds unambiguously with andesitic-basaltic flows (Bentley and Clough, 1972). This column lies within the Cenozoic volcanic province that characteristically has a shallow magnetic basement (Behrendt, 1964b). On the basis of the magnetics the Flood Ranges do not appear to be part of the Cenozoic volcanic province but rather the plutonic and metamorphic province of the Ford Ranges (Bentley and Chang, 1971). Again the distinct change in seismic structure on crossing the Byrd Subglacial Basin is apparent and further evidence that the Basin represents a major boundary between geological provinces.

In general Behrendt and Wold (1963) recognised a striking correlation between bedrock elevations and residual magnetic anomalies. The magnetics cannot be related to the topography alone as this would require too high susceptibilities but is probable that the residual magnetic and topographic contours are both related to the tectonic pattern of the area (Behrendt and Wold, 1963).

1.6.3 DEEP CRUSTAL STRUCTURE

The deep crustal structure of West Antarctica has been studied using seismological observations (mainly surface wave dispersion techniques) and from a consideration of gravity and elevation data.

Crustal structure has been measured directly using explosion seismology at one locality in West Antarctica. A refraction profile 23 km long at the head of the Ronne-Filchner Ice Shelf (83°S 70°W) by Manfred Hochstein obtained distinct reflections with travel times of 8.5-9.3 s on all shots (Bentley, 1973). He calculates the depth to the reflector as 24 km and correlates it with the MOHO. The majority of information however has come form surface wave dispersion methods. Press and Dewart (1959) concluded from their work that although East Antarctica is underlain by a continental type crust West Antarctica is not, being intermediate between continents and ocean basins. A re-analysis by Kovach and Press (1961) indicated a mean crustal thickness of 35 km for Antarctica but with a thicker crust beneath East Antarctica. General agreement would put the thickness of crust in West Antarctica as 25-30 km compared to 35-40 km for East Antarctica (Bentley, 1964; Adams, 1972).

This conclusion is supported by gravitational and elevation data. Adams (1972) gives an average crustal thickness of 32 km everywhere in West Antarctica except beneath the Filchner and Ross Ice Shelves where the thickness is 28 km. Behrendt (1964a) estimated that the crust was 31 km thick at the base of the Peninsula, several kilometers thicker than that beneath Ellsworth Land.

An important consideration is whether West Antarctica with its thinner crust is in isostatic equilibrium. Such a question has been considered by Bentley and Robertson (in press) who have calculated isostatic anomalies from a mean FAA map based on gravity observations on oversnow traverses. They conclude that major areas of West Antarctica including the Byrd Subglacial Basin are not detectably out of isostatic eqilibrium. However positive anomalies occurring at the base of the Peninsula and on the eastern flank of the Ellsworth Mountains are tentative indications of uncompensated crustal thinning (Bentley and Robertson, in press).

1.6.4 BOUNDARY BETWEEN EAST AND WEST ANTARCTICA

In the preceeding sections geological and geophysical evidence all indicate that East and West Antarctica are two fundamentally different areas: but the nature of the boundary between the two is unknown. The boundary is of considerable importance in defining the boundary between tectonic provinces and in assessing the geological evolution of Antarctica in particular and Gondwanaland as a whole. Robinson (1964a) describes a marked Bouguer anomaly gradient between East and West Antarctica in the region of the Transantarctic Mountains. Two dimensional modelling of the gravity data by Robinson (1964a) resulted in the conclusion that a major fault separates East from West Antarctica, extending right through the crust, and across which there is an abrupt change in crustal thickness. Evidence of major surface faulting occurs only in the Ohio Range of the Horlick Mountains, at Cape Surprise near the Beardmore Glacier and in the southern Pensacola Mountains. A boundary fault system of large magnitude (~3000 m) occurs between the Ohio Range and the bedrock of West Antarctica to the NW (Long, 1965).

Behrendt,Meister and Henderson (1966) discussed a similar regional gravity anomaly in the Pensacola Mountains explaining it as the result of crustal thickening across the transi tion between East and West Antarctica. The same strong gravity gradient is described by Smithson (1972) in the Dry Valley's area of the Transantarctic Mountains. Smithson (1972) concluded that a young fault cutting surface rocks or a deep fault or step in the MOHO is insufficient to explain the high gradient. The best model that fits the data is the crust thickening from 27 to 40 km from west to east with a 8 km thick slab of dense basaltic material in the upper crust to the west of the Transantarctic Mountains. This indicates that the crust in West Antarctica is not only thinner but more mafic and fundamentally different to East Antarctica and could represent an ancient subduction zone (Smithson, 1972). Behrendt et al (1974) discuss the gravity gradient in the Pensacola Mountains in more detail. Two explanations fit the data best, (see fig. 1.17), either the crust is abnormally thin in West Antarctica (taking into account seismic data, Bentley, 1973) or the crust has the accepted thickness for West Antarctica of 30 km and a steep faultlike step extends from the MOHO to the surface (Behrendt et al, 1974). They conclude that one might expect a steep discontinuity at the crust mantle interface if this steep gravity gradient marks the edge of the continent at the time of separation from Gondwanaland.

1.7 PROBLEMS TO BE SOLVED

Numerous problems concerning the West Antarctic ice sheet and the geology, structure and tectonics of the bedrock have been raised in the preceeding sections. The problems that this thesis attempts to answer can be listed as;

West Antarctic Ice Sheet

1) The surface topography of the West Antarctica ice sheet is poorly

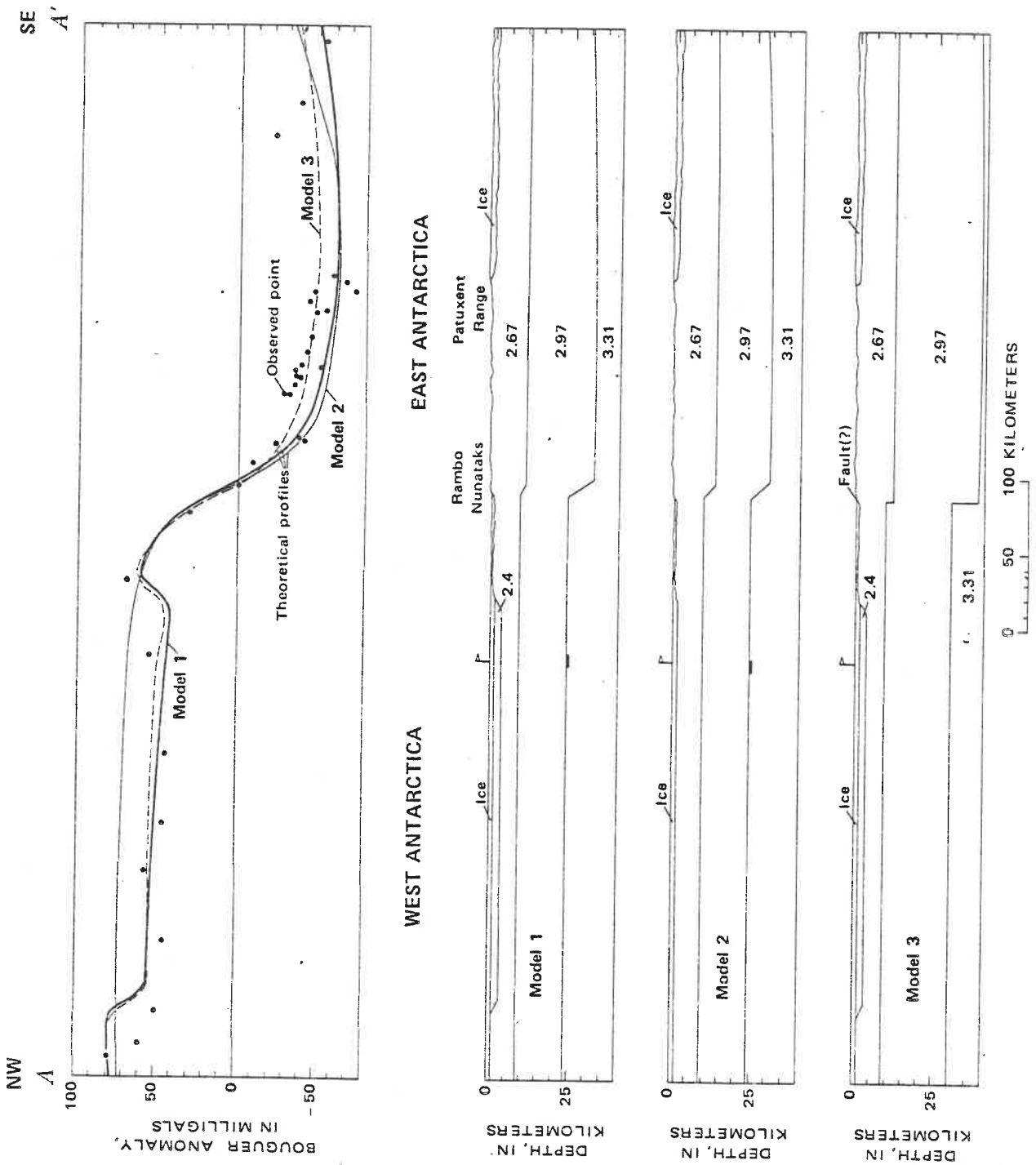


Fig. 1.17 Bouguer anomaly profile and theoretical crustal models across boundary between East and West Antarctica (after Behrendt et al, 1974).

The mass effect of ice has been included in the Bouguer reduction. Densities in models are in gcm^3. Flag indicates location of deep seismic reflection station; bar in models 1 and 2, the reflection itself.

known, being based on a limited number of measurements from US oversnow traverses.

2) Delineation of the major drainage basins of West Antarctica.

3) The flow of ice into the Ronne-Filchner Ice Shelf is not well understood.

4) The grounding line of the Ronne-Filchner Ice Shelf between the Ellsworth and Pensacola Mountains is also poorly known, the area being beyond the coverage of LANDSAT satellite imagery (~80°S).

5) Thickness of ice in many parts of West Antarctica is unknown.

Bedrock

1) The bedrock topography, like the ice sheet surface, is poorly known. Early maps of the bedrock topography can only resolve the largest of features leaving many unidentified.

2) Allowing complete deglaciation and isostatic recovery what would be the distribution of land and sea areas in West Antarctica.

3) Geology of the ice covered areas of West Antarctica is largely unknown.

4) Identification of major structural units in West Antarctica. This has not been possible with the data previously available.

5) The location of the boundary between East and West Antarctica. This boundary is known to be important to the tectonic evolution of Antarctica but its position is poorly known in the ice covered area between the Horlick Mountains and the Pensacola Mountains.

6) Has Antarctica always retained its present outline or has there been relative motion between parts of Antarctica?

7) If it was, at one time, more than one plate how is West Antarctica subdivided?

8) How can reconstructions of Gondwanaland be improved using the conclusions derived from this work?

CHAPTER 2 DATA COLLECTION AND REDUCTION

2.1 INTRODUCTION

The data presented in this thesis were collected during the austral summers 1977-78 and 1978-79 by a team from the Scott Polar Research Institute (SPRI). The author was actively involved in the collection of data during both seasons but gratefully acknowledges the valuable assistance of the other members of the team.

This work was part of an International programme of Radio Echo Sounding (RES) in Antarctica in co-operation with the US National Science Foundation Division of Polar Programmes (NSF) and the Electromagnetics Institute of the Technical University of Denmark (TUD) (Robin et al, 1977). During the two seasons magnetic measurements were made simultaneously with the RES. The magnetometry was carried out in co-operation with the Applied Physics Laboratory of Johns' Hopkins University, Baltimore. All equipment was mounted in a specially configured C-130R Hercules aircraft provided by NSF and operated by US Navy Antarctic Development Squadron Six.

This chapter describes the collection and reduction of the RES and magnetic data. Due to the large amounts of data collected all data reduction was carried out on the University of Cambridge IBM 370/165 computer. The techniques used to reduce the RES data are similar to those employed by Rose (1978) and Steed (1980) and are outlined in fig. 2.1. Reduction of the magnetic data involved standard aeromagnetic methods.

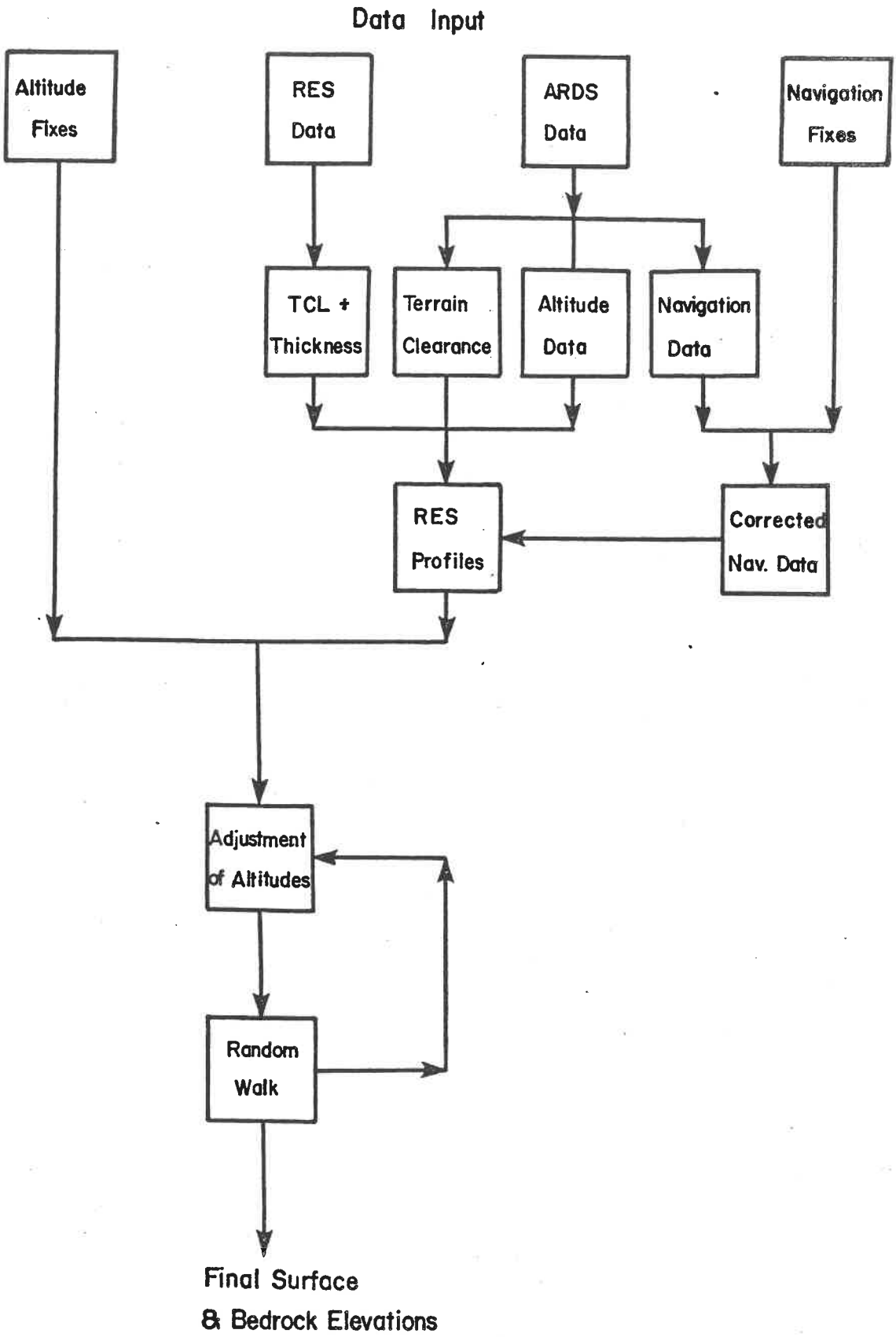


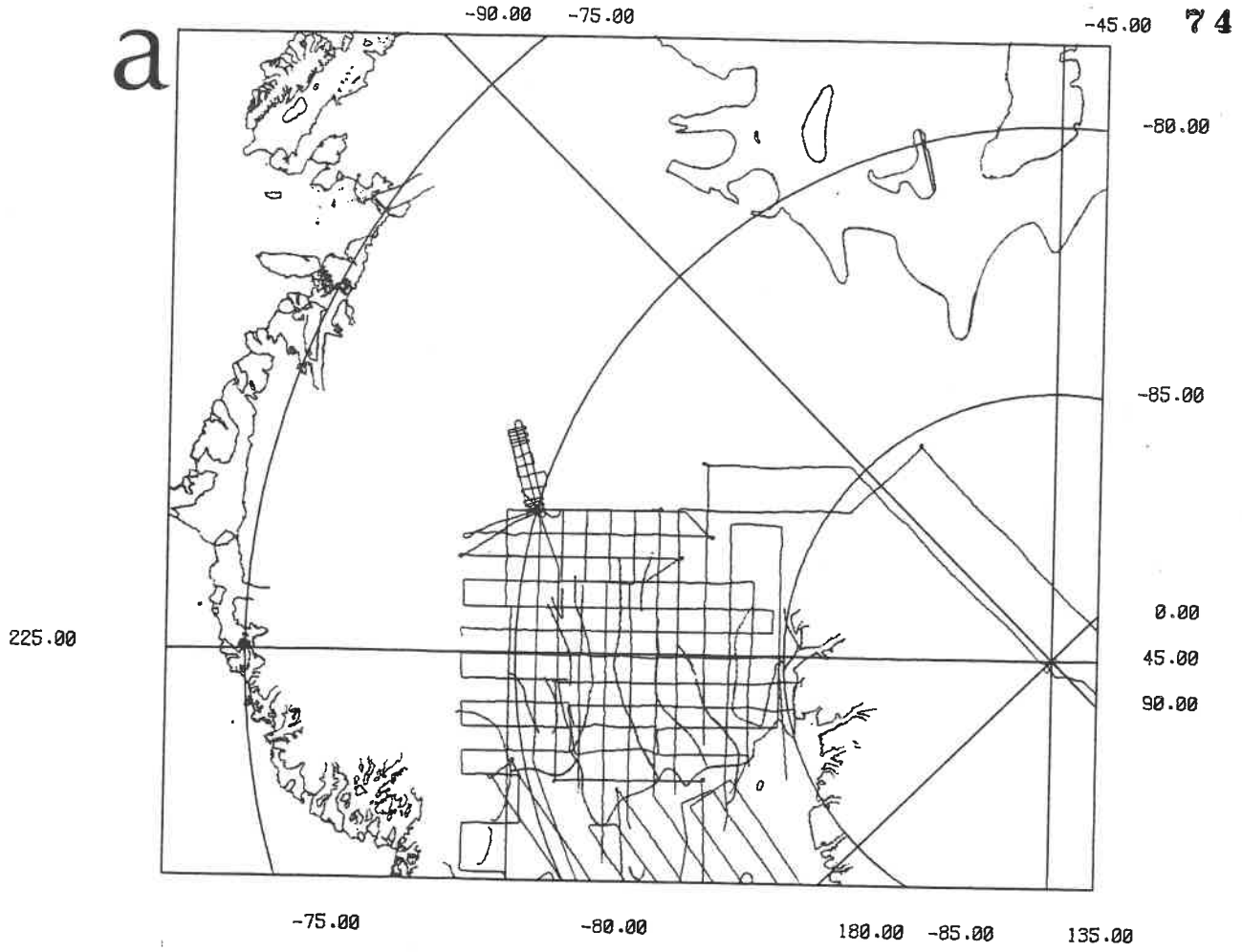
Fig. 2.1 Outline of RES data reduction.

Presentation of the RES data includes data from an earlier season, 1974-75. These data are fully described in Rose (1978) and is included here in discussions of the structure of West Antarctica. Data collected during 1977-78 and 1978-79 seasons have not been previously reduced or analysed except by the author.

2.2 FLIGHT PLANNING

The first systematic study of West Antarctica was made during the 1974 -75 field season. Flights were designed to form a rectangular grid of side 50 km orientated parallel to the 45° E - 135° W meridian, with an intersection over Byrd Station (Rose, 1978). The West Antarctic grid is rotated through 45° with respect to the existing East Antarctic grid (Drewry, 1975a). This orientation was chosen so as to follow ice flow lines and ice surface contours. Fig. 2.2a shows the flights completed in 1974-75 that have been incorporated into this thesis. Flights during 1977-78 and 1978-79 were designed to continue this grid network to cover the rest of West Antarctica (fig. 2.2b). Fortuitously the orientation of the early flights lay roughly parallel to and perpendicular to the tectonic grain of West Antarctica.

All flights operated out of McMurdo Station on Ross Island (see fig. 1.1). Due to the long distances to be flown before reaching the area of interest (> 2000 km) the majority of the flights made use of South Pole Station and Byrd Station, or both, for refueling. All flights were planned by the author prior to the commencement of each season. However weather conditions, mechanical failures, and varying aircraft performance meant that some of the completed flight tracks bore little relation to the ones planned. Consequently, as changes quite often had to be made in-flight it was essential to avoid repeating any parts of the grid that had been flown before. A 50 km rectangular grid orientated parallel to the 45° E - 135° W



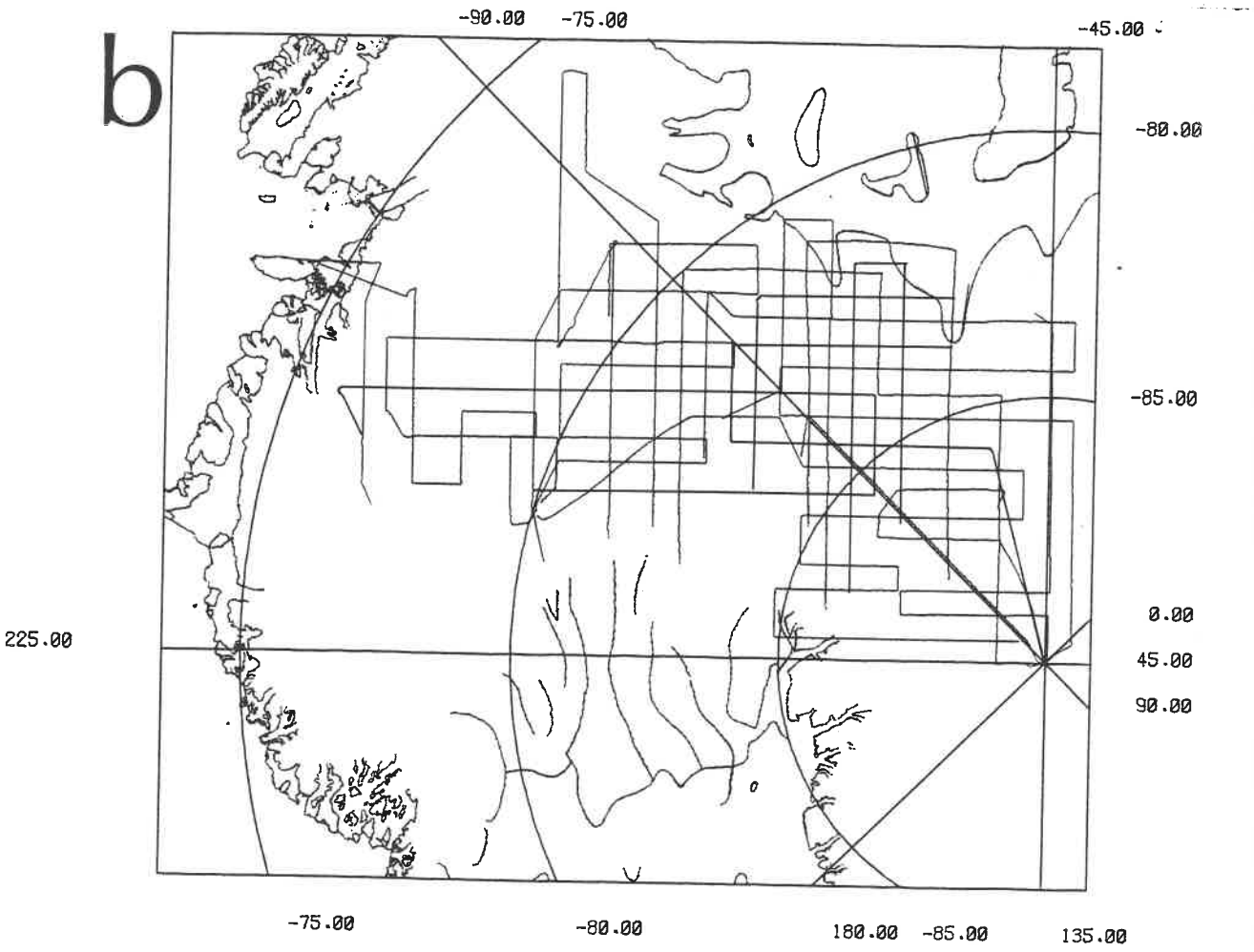


Fig. 2.2 RES flight lines a)1974-75 (after Rose,1978)
b)1977-78, 1978-79

meridian, centered on Byrd Station, was generated by computer and the crossing points output as latitude and longitude. This removed the need to calculate latitude and longitude from air navigation charts whilst in-flight. Instead simple grid co-ordinates could be used and these then looked up in a directory to provide the necessary latitude and longitude. Using this method a completely new flight could be planned, but conforming to the overall grid pattern, in a matter of minutes reducing the chances of error by misreading map co-ordinates.

Flights were planned to use the maximum amount of fuel available for RES. The fuel weight available was calculated by subtracting the gross weight of the aircraft, crew and equipment from the maximum taxi and take-off weights allowed (see Table 2.1). These figures differ according to the form of take-off (ie. wheeled or ski) and on the condition of the surface used for the runway. Wheeled take-off is only possible at McMurdo during the early part of the season (ie. up to about mid December) when the sea ice in McMurdo Sound is thick enough to take the weight of the aircraft. All other take-offs and landings were made on skis from a prepared ski-way on the McMurdo Ice Shelf. Specific Range Charts (NATOPS, 1975) for the LC-130R were then used to calculate fuel burn rates at various altitudes and true airspeeds. Table 2.1 shows the figures used for planning flight tracks.

The aircraft did not always perform in accordance with the published specific range charts. This varied to some extent with the experience of the flight crew but can largely be accounted for by the drag effects of the RES antennae. The aircraft was flown at high altitude (~8500 m) to the area of interest and then descended to the operating altitude which was usually about 300 m above the ice surface. The aircraft would then maintain a constant pressure altitude in order to simplify both RES and magnetic data reduction. Altitude was changed in steps when necessary. Changes in altitude would be necessary for several reasons:

1) Topographic obstruction in the flight path.

BASIC FLIGHT PLANNING INRUT DATA

	(lbs)	
1 Aircraft weight	85 521	BASIC WEIGHT
2 Oil	360	
3 Galley equipment	50	
4 Polar survival equipment	495	
	86 426	
5 Augmented crew (9) + baggage	1 800	
	88 226	OPERATING WEIGHT
6 RES pallet and equipment	2 900	
7 ARDS pallet and operatives	2 300	
8 Vertical camera	490	
9 RES crew	600	
	94 516	GROSS WEIGHT

Aircraft maximum taxi and T/O weight (K lbs)

	NZCM	NBY	NPX	Siple
1 Wheels	155	-	-	-
2 Ski	147	135	135	135

Standard ramp fuel load (for XD03) (K lbs)

1 Wheels	61	-	-	-
2 Ski	54	41	41	41

Fuel required for taxi and T/O = 1 klb

Fuel required overhead destination = 7 klbs

Fuel Burn rates.

High Altitude (25 000 feet asl) 4.5-4.6 klbs/hr (5.5 in first hour)

Low Altitude (10 000 feet asl) 5.5 klbs/hr

(5 000 feet asl) 6.0 klbs/hr

High altitude no-wind True air speed = 275 knots

Low altitude " " " " = 235 knots

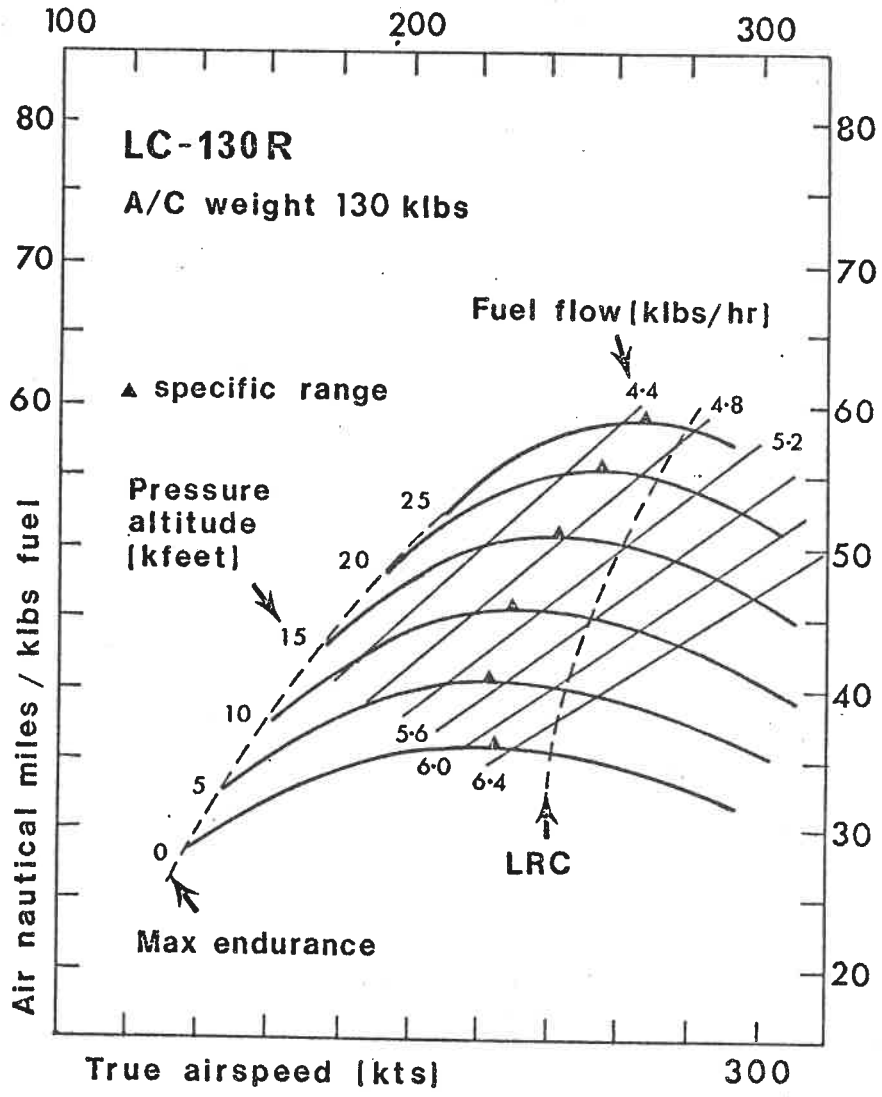


Table 2.1 Flight Planning data (after NATOPS, 1975).

2) Low cloud (RES antennae had no de-iceing circuits and build up of ice on leading edges of antennae could make aircraft unstable)

3) Noise on magnetometer record. High frequency noise was sometimes a problem with the magnetometer and was usually associated with flying through low cloud when the engine de-ic ing circuits cut in.

4) Loss of a return from the bedrock. This occured when either terrain clearance increased producing loss of power by increased geometrical losses or alternatively thickness of ice increased thereby increasing absorption in the ice column, or both occurred.

2.3 RADIO ECHO SOUNDING

2.3.1 EQUIPMENT

During both seasons downward looking pulse modulated radar systems operating at centre frequencies of 60 MHz and 300 MHz were used. The radar systems were designed and built by TUD in co-operation with SPRI (Christensen, 1970; Skou and Sondergaard, 1976). The 60 MHz radar provided the majority of the data for this thesis and was usually operated with a pulse length of 250 ns and had a total system performance of 212 dB (Skou and Sondergaard, 1976). The antennae for the 60 MHZ radar were mounted 1/4 wavelength apart (ie. 1250mm) beneath the starboard wing and consisted of 4 in-line dipoles. These were mounted in fibre-glass reinforced balsawood neutral aerofoils (Skou and Teilgaard, 1978). This configuration produced a beamwidth of 120° fore and aft and 20° sideways. The 300 MHZ is very similar to the 60 MHZ radar but has a system performance about 3 dB down ie. 209 dB (Christensen, 1970) transmitting through 4 backfire antennae producing a beamwidth of 20° fore and aft as well as sideways. In areas of rugged topography the 60 MHz radar becomes confused with numerous hyperbolic echoes which are almost absent on the 300MHz

system due to the much narrower beamwidth. As absorption is however frequency dependent, the 300 MHz radar is less satisfactory in areas of thick ice (Robin et al, 1977) (see fig. 2.4).

As in previous seasons data were recorded on 35 mm film in 3 different modes (see fig. 2.3). The 'Z' scope record is a differentiated range profile displaying echo delay time on the y-axis and time on the x-axis. 'A' scope records are produced at regular intervals and display received power against echo delay time. The third mode of recording gives a continuous display of echo strength (ESM) of the bedrock echo (see Neal, 1977, for all details). 'A' scopes were also recorded on 8 mm (super 8) movie film at regular intervals or if desired in 10s bursts at 54 frames/sec. In addition to the 35 mm film 60 MHz 'Z' scope records were produced by a Honeywell 1856-A fibre optic oscillograph producing a high quality profile on heat sensitive dry-silver paper. This form of recording has many advantages over the 35 mm film, one being the almost real time profile produced. This enabled aircraft altitude to be changed rapidly when bedrock returns became weak thereby helping to maintain a continuous RES profile.

All the 35 mm film was annotated automatically with timing marks which contained the date, time(hr,min,sec), flight number, coded information on the settings of the radar equipment and a time parameter. This time parameter, referred to as a CBD number, is derived from a crystal oscillator and is incremented by 1 every 15 seconds. Every 16 CBD (ie. 4 mins) time calibration marks are flashed on to all the displays in the form of 2 micro-second pips. These were used when digitising to calculate range in air and ice.

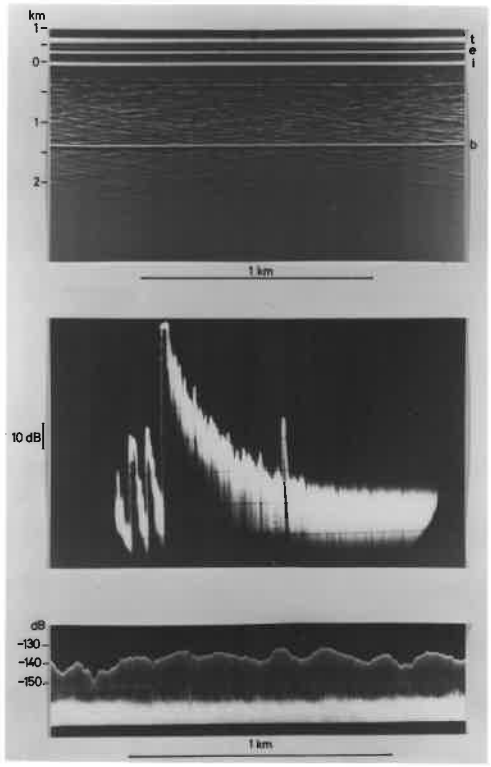


Fig. 2.3 Example of RES records a)60 MHz 'Z-scope'
b)60 MHz 'A-scope'
c)ESM

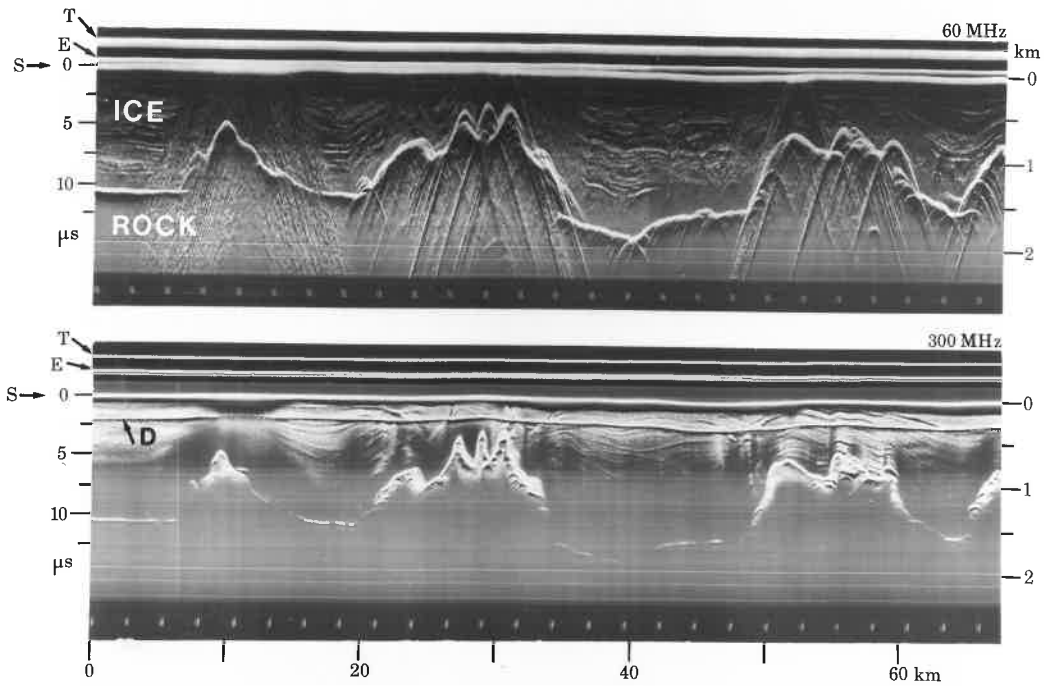


Fig. 2.4 Comparison of 60 and 300 MHz 'z-scopes'

2.3.2 DIGITISATION OF RECORDS

The 1977-78 data were digitised from a back projected image of the 60 MHz 'Z' scope, on 35 mm film, using a PCD X-Y digitiser. A moveable cursor was used to measure the distance between transmission pulse, ice surface and bedrock returns every CBD (ie 15 s or ~1.7 km on the ground). The digitised data were output on to 8-track paper tape. Digitised distances in mm on the film record were then converted to delay times using the time calibration marks. Aircraft terrain clearance were calculated using ice surface echo delay and velocity in air of 300 m/usec, remembering that measured echo delays represent 2-way travel times. Similarly ice thickness was calculated from the echo delay and using a velocity of radio waves in ice of 168 m/usec (see Robin, 1975; Johari and Charette, 1975; Glen and Paren, 1975). A complicating factor in determining ice thickness is the top of the ice column consisting of compacted snow (firn) which has a lower density than ice. The velocity of radio waves in the firn layer is slightly higher than in ice and, therefore, echo delay times for the bedrock reflection are slightly shorter. A standard thickness of 10 m, adopted by Robin et al (1969), was added to the calculated ice thickness to correct for this effect.

The method of digitisation discussed above proved to be very slow and consequently a different approach was used for the 1978-79 data. Use was made of the high quality Honeywell oscillograph output and a flat bed X-Y digitiser. Instead of digitising the transmitter pulse, ice surface and bedrock returns at regular intervals each return was digitised in turn in sections of about 100 CBD, thereby utilising to maximum effect the integrating qualities of the profiles. A moveable cursor was used to digitise the two end points of the transmitter pulse (which is always a straight line) and the time calibration marks. The cursor was then moved along the surface pulse from one end

of the profile to the other producing an almost continuous stream of X-Y co-ordinates. The bedrock return was digitised in a similar fashion. A computer program then produced an array of CBD number and terrain clearance and then an array containing CBD number, terrain clearance and ice thickness. The program then took the latter array, which is random in time, and by linear interpolation produced a new array of CBD number, terrain clearance and ice thickness at regular time intervals (ie. every 3 s or ~360m on the ground). Where two or more values of ice thickness occurred at the same CBD number (obtained as a result of digitising hyperbolic echoes) the program retained the value with the minimum delay. Fig. 2.5 shows an example of oscillograph record and digitised profile.

2.3.3 NAVIGATION DATA RECORDING SYSTEM

One of the most important aspects of a survey of the form conducted in Antarctica is the necessity to reconstruct flight tracks at a later date for interpretative purposes. For this the Airborne Research Data System (ARDS) was used during both seasons. The ARDS was installed by the US Naval Weapons Center, China Lake, California and operated by them during 1977-78 season. During 1978-79 season personnel from the Applied Physics Laboratory (APL) of Johns' Hopkins University, Baltimore took over operation of the system.

The ARDS is capable of recording up to 100 channels of 6 digit data at a rate of 8 scans/sec on magnetic tape in both digital and analogue form. In addition all channels are output at selected time intervals on a high speed printer as a back up facility. During both seasons only 38 channels were used (see Table 2.2 in Steed, 1980). During 1977-78 the data were recorded at the maximum rate of 8 scans/sec. This meant that more than one tape per flight was required

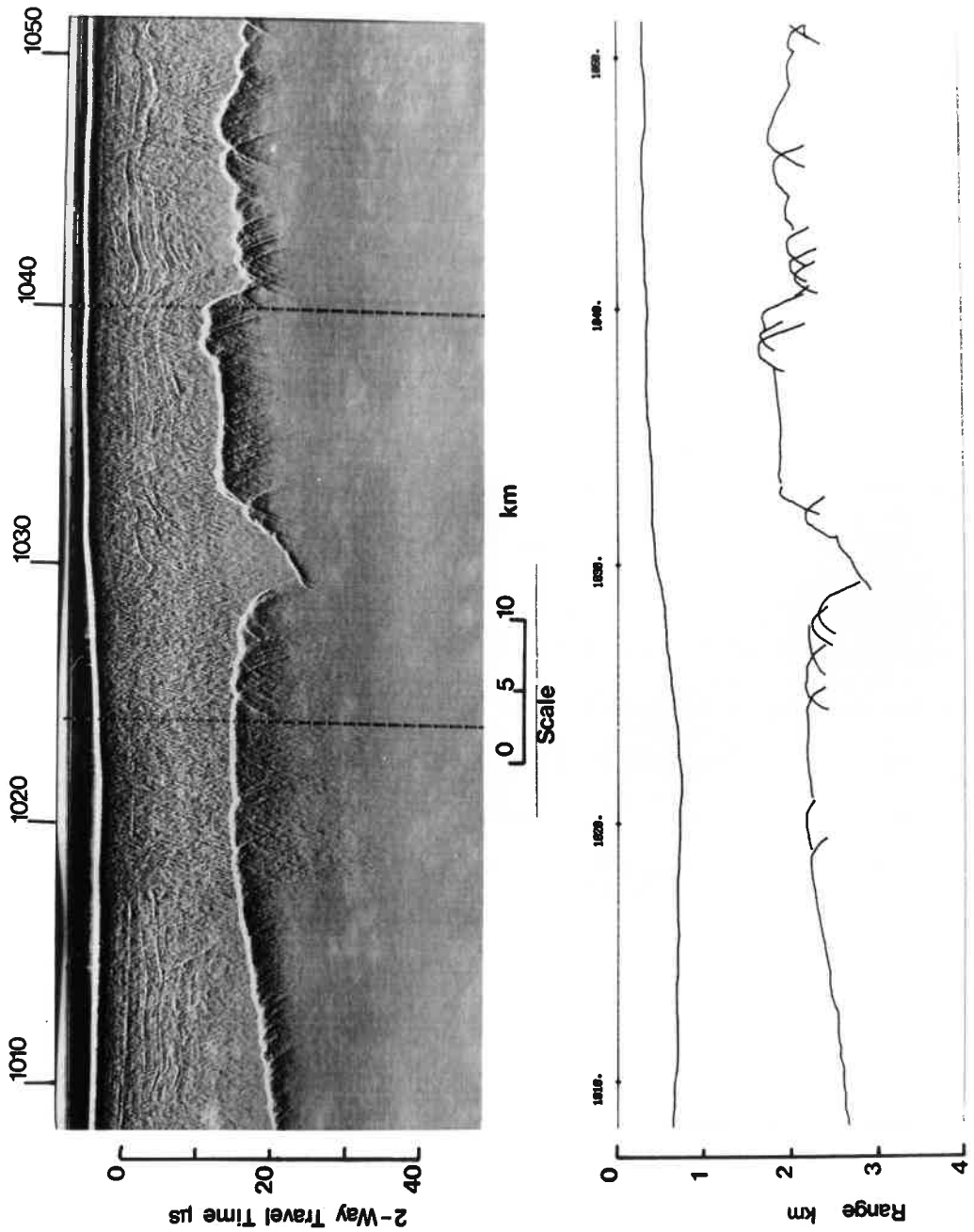


Fig. 2.5 60 MHz 'Z-scope' and digitised profile.

resulting in a short gap in the data (~15 mins) which had to be filled using printer output. For this reason it was decided to slow the recording rate down to 4 scans/sec for the 1978-79 season. This allowed all the data to be accommodated on one tape or allowed tapes to be changed while the plane was refueling at outlying stations.

2.3.4 NAVIGATION

During both seasons navigational control was provided by a Litton LTN-51 inertial system (INS). The system is fully described in Rose (1978). INS suffer not only from linear drift, but also a cyclic drift whose period is 84.4 min (referred to as the Schuler frequency). Rose (1978) compared the output from two INS operating simultaneously during the 1974-75 season. He reported a maximum difference of 7.3 km after several hours with a RMS deviation of 5.2 km. Only one INS was available during 1977-78 and 1978-79 and the drift has been treated as linear. The cyclic variations are small compared to the spacing of flight lines (~50 km) and are not, therefore, thought to be significant.

In-flight fixes were provided by i) oblique photographic resections on known topographic points, for eg. mountain ranges, nunataks, or by overflying them. Photographic fixes were obtained using a hand held camera on the flight deck. At the exact instant of the photograph INS position was recorded by the ARDS with an event mark appearing on the 35 mm RES film. Geographical co-ordinates were obtained from the photographs using a vanishing point method (Imhof and Dolittle, 1966). In 1977-78 additional photographs were taken with 2 side looking oblique cameras that were hard mounted to the aircraft mainframe. These, however suffered badly from vibrations and were generally unusable. In 1978-79 they were replaced by a Wild large

format (9inch x 9inch) vertical camera mounted in the belly of the aircraft. Photographs from this camera were only useful when overflying isolated features: the generally low terrain clearances resulted in a very limited field of view. ii) The positions of outlying bases (ie. South Pole, Siple and Byrd) were also used for navigational control. Positional errors were then distributed lineally along the flight track using computer methods. Navigational errors are discussed in 2.3.6.

2.3.5 ALTIMETRY

Altitude of the aircraft was measured with a Garrett pressure transducer with a precision of 0.001 mB and calibrated to give readings correct to ~24 mm. The measurement of altitude by barometry suffers from errors that are due to variations in the shape of constant pressure surfaces which depend on weather systems. During the 1967-68 field season synoptic maps of pressure surfaces in the Antarctic were compiled using available weather data and show that the height of constant pressure levels can vary by up to 140m over several hundred kilometres. Rose (1978) went to great lengths to attempt to correct for these effects by calculating the changes in pressure in a horizontal direction but producing only a slight improvement in the accuracy of altitude determination. Consequently it was decided not to attempt this more rigorous approach with the 1977-78 and 1978-79 data.

format (9inch x 9inch) vertical camera mounted in the belly of the aircraft. Photographs from this camera were only useful when overflying isolated features: the generally low terrain clearances resulted in a very limited field of view. ii) The positions of outlying bases (ie. South Pole, Siple and Byrd) were also used for navigational control. Positional errors were then distributed lineally along the flight track using computer methods. Navigational errors are discussed in 2.3.6.

2.3.5 ALTIMETRY

Altitude of the aircraft was measured with a Garrett pressure transducer with a precision of 0.001 mB and calibrated to give readings correct to ~24 mm. The measurement of altitude by barometry suffers from errors that are due to variations in the shape of constant pressure surfaces which depend on weather systems. During the 1967-68 field season synoptic maps of pressure surfaces in the Antarctic were compiled using available weather data and show that the height of constant pressure levels can vary by up to 140m over several hundred kilometres. Rose (1978) went to great lengths to attempt to correct for these effects by calculating the changes in pressure in a horizontal direction but producing only a slight improvement in the accuracy of altitude determination. Consequently it was decided not to attempt this more rigorous approach with the 1977-78 and 1978-79 data.

Flights were flown at constant pressure altitude with step changes being made when necessary. Altitude fixes are obtained by overflying points of known surface altitude (ie. outlying stations, topographic features etc.). Altitude was also corrected when over-flying over open water or floating ice shelf (assuming simple hydrostatic equilibrium, see Crary et al, 1962), or when crossing the line of one of the US oversnow traverses. The error at fixes was distributed lineally along the flight track using a method described in Rose (1978). If the difference in elevation between successive fixes was <200m the error was distributed with respect to time otherwise it was distributed with respect to change in elevation. Altitude errors are discussed in section 2.3.6.

All the altitude fixes rely on accurate knowledge of the aircraft terrain clearance. As already mentioned this can be measured off the RES film. An independent measurement, however, is provided by the aircraft APN-194 radar altimeter which has a precision of ~24 mm. The radar altimeter has a frequency in the cm wavelength band: higher than the RES equipment. Consequently it has a much narrower beam-width and is therefore more sensitive to changes in the ice surface elevation. A corrected terrain clearance was obtained by comparing the two determinations of terrain clearance over a window of 11 readings and obtaining a mean difference. The mean difference was then added to the value of the radar altimeter at the centre of the window.

After correcting the data in this way the elevation of the ice surface was compared at flight crossing points. In theory the value of ice surface should be the same for both legs, however this is not usually the case due to the simple treatment of the altimetry data. To make the survey internally consistent the error at crossing points was lineally distributed throughout the grid. For this a computer

Flights were flown at constant pressure altitude with step changes being made when necessary. Altitude fixes are obtained by overflying points of known surface altitude (ie. outlying stations, topographic features etc.). Altitude was also corrected when over-flying over open water or floating ice shelf (assuming simple hydrostatic equilibrium, see Crary et al, 1962), or when crossing the line of one of the US oversnow traverses. The error at fixes was distributed lineally along the flight track using a method described in Rose (1978). If the difference in elevation between successive fixes was <200m the error was distributed with respect to time otherwise it was distributed with respect to change in elevation. Altitude errors are discussed in section 2.3.6.

All the altitude fixes rely on accurate knowledge of the aircraft terrain clearance. As already mentioned this can be measured off the RES film. An independent measurement, however, is provided by the aircraft APN-194 radar altimeter which has a precision of ~24 mm. The radar altimeter has a frequency in the cm wavelength band: higher than the RES equipment. Consequently it has a much narrower beam-width and is therefore more sensitive to changes in the ice surface elevation. A corrected terrain clearance was obtained by comparing the two determinations of terrain clearance over a window of 11 readings and obtaining a mean difference. The mean difference was then added to the value of the radar altimeter at the centre of the window.

After correcting the data in this way the elevation of the ice surface was compared at flight crossing points. In theory the value of ice surface should be the same for both legs, however this is not usually the case due to the simple treatment of the altimetry data. To make the survey internally consistent the error at crossing points was lineally distributed throughout the grid. For this a computer

iterative random walk technique was used (see Rose, 1978). A mathematical matrix is constructed of the cross-over points and the changes in elevation to neighbouring points. Control points are included in the matrix consisting of elevations of outlying stations, floating ice shelf and open water. Bentley and Chang (1971) estimate the error in determination of surface altitudes to be 20-25 m on West Antarctic traverses. This is considered rather an optimistic figure for all the traverses used here and an error of 50 $\pm$ 25 m quoted by Bentley (1964) is thought to be more realistic. For this reason the elevations at cross-over points on US traverses were not thought to be accurate enough to include as control points in the random walk calculation. Each 'walk' by the computer through the matrix starts and ends at one of the control points taking a random path between them, and then distributing the error back along the path taken. After many tens of thousands of 'walks' the elevations change little during successive 'walks' and the program is terminated. Each flight is then refixed using the new elevations of crossing points as altitude fixes. (see fig. 2.6 for details of random walk grid).

2.3.6 DISCUSSION OF ERRORS

Radio Echo Sounding

Errors are introduced to the ice surface and bedrock elevations in the digitising of the data and in the navigation and altitude corrections. Random errors occur in the digitising of the transmission pulse, ice surface and bedrock returns. Steed (1980) estimated that the RMS deviation in measuring the distance of a displacement on the projected image for the 1977-78 data was equivalent to a delay of 0.17 us, equivalent to 25.5 m in air, or 14.3 m in ice. Using the high quality oscillograph output for the 1978-79 data and the flat bed X-Y digitiser improved the precision giving a

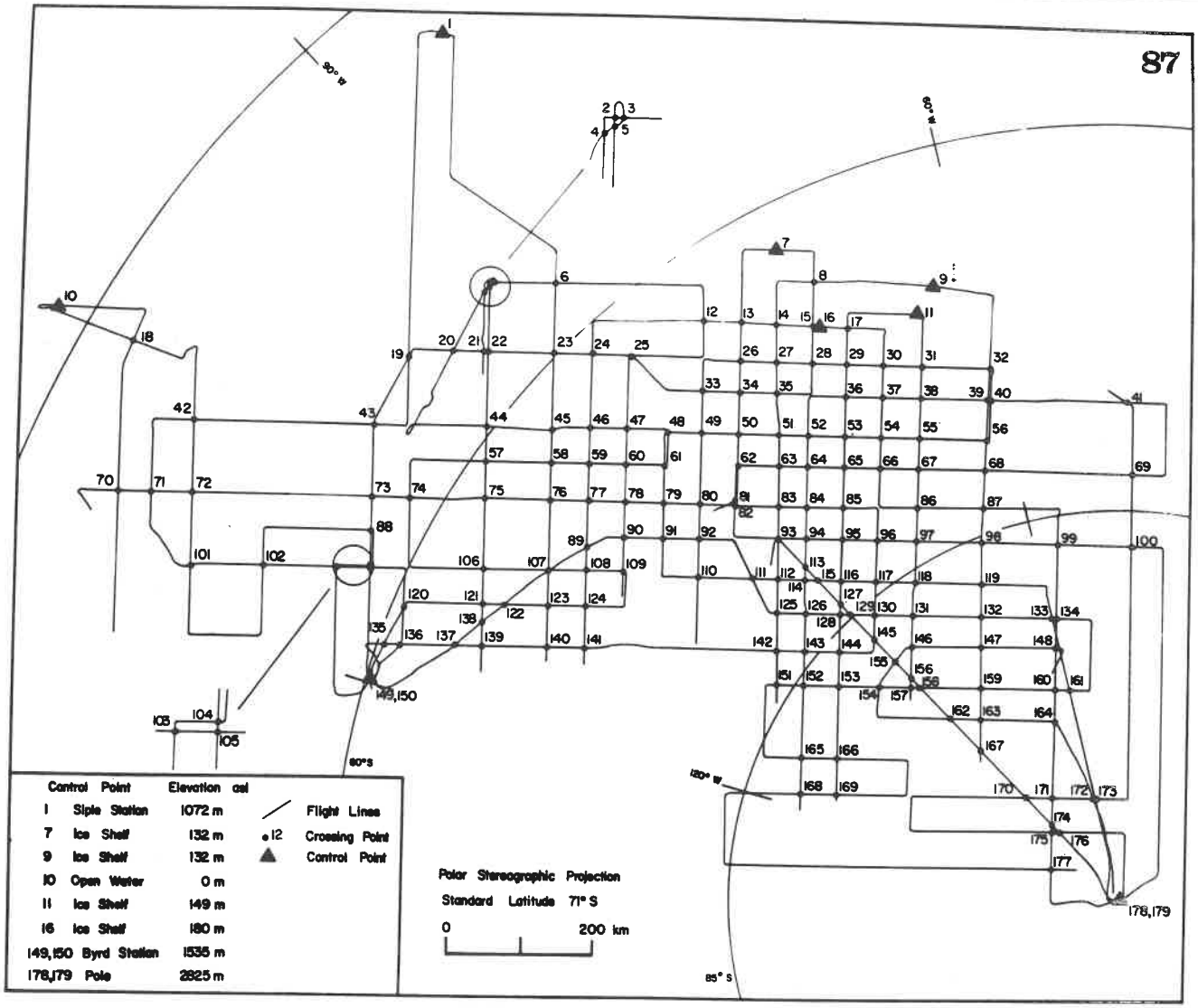


Fig. 2.6 Randomwalk grid used for distributing final altitude errors.

NAVIGATION ERRORS

	Mean Closure Error (km)	Standard Deviation	Mean Error for all fixes (km)	Standard Deviation
1977-78	4.7	2.27	5.25	2.18
1978-79	3.95	2.38	3.11	1.63

ALTITUDE ERRORS

	Mean Error for all fixes (m)	Standard Deviation
1977-78	189	81
1978-79	74	88

Table 2.2 Navigation and Altitude errors.

RMS deviation of 0.12 us or 18 m in air and 10.1 m in ice. Random errors were reduced by averaging the digitised terrain clearance over 3 data points, assuming that variations in the ice sheet surface elevation are linear over several kilometres. As mentioned in 2.3.5 the smoothed RES terrain clearance was combined with the radar altimeter terrain clearance to give a corrected value.

Another source of error connected with RES records is introduced by the very nature of attempting to display a 3- dimensional world in the form of a 2-dimensional profile. The antennae are designed so as to produce as narrow a beamwidth as possible, but inevitably the record is confused by echoes not lying vertically below the recording point. This problem has already been mentioned in section 2.3.1 and use of the narrow beam 300MHz radar is one solution to the problem. An alternative approach to the problem was tried by Harrison (1970), who migrated echo profiles to produce real space profiles. A similar approach would involve substantial extra digitising of the RES film and is only important when the exact nature of the bedrock surface is required. For our purposes the change in elevations are insignificant when compared with the large scale plotting and contouring of the data. Also an experienced digitiser, aware of these problems can avoid spurious echoes and tails of hyperbolae. For this reason all flights were digitised personally by the author.

Navigation

Systematic errors are introduced by the simple approach taken in correcting the navigation data. The Schuler frequency has been ignored and drift assumed to be linear. The error also depends on the accuracy of the navigational fix used. The position of the stations have been determined by geoceiver, which calculate position using radio transmitters in orbiting satellites, and are accurate to better than 10 m. As mentioned in 2.3.4 in-flight fixes were obtained either

by directly overflying a feature or from oblique photographs. For 1977-78 the track was fixed to these points to within 0.5 of a CBD (ie 7.5 s or ~900m on the ground) and for the 1978-79 data positions were fixed to within 0.1 of a CBD (ie 1.5s or 180m). Using the vanishing point method of photographic resection (Imhof and Dolittle, 1966) errors are likely to be better than 1km provided photographs are chosen with features widely distributed about the central line (see p37 Rose, 1978). All these errors are small compared to the flight line spacing. Closure errors after a flight of ~10 - 12 hrs were in the order of 5 km. Table 2.2 lists closure errors for all flights aswell as mean error and standard deviation for all navigation fixes used.

Altitude

Aircraft altitude is liable to errors as discussed in section 2.3.5 due to the complex nature of pressure surfaces and the general lack of control points. Corrections to the altitude are also liable to the same error as the determination of terrain clearance. Surface elevations determined on oversnow traverses have a total error of ~50 m (Bentley, 1964) while geoceiver elevations of stations corr ected for the geoid (King Hele, 1975) are better than 10 m.

Gross systematic errors are quite large, in the order of 189 m for 1977-78 and 74 m for 1978-79 (see table 2.2). However after correction of altitudes, elevations at crossing points were compared and gave a mean error of 46.5m with a standard deviation of 44m. This error was lineally distributed throughout the grid by the random walk method as described in 2.3.5. The total error for elevations is difficult to assess. Ice surface elevations determined by an independent method (ie. from the Tropical Wind Energy Reference Level Experiment, TWERLE) are accurate to ~60 m (Levanon et al, 1977). The ice surface topography drawn from these elevations is in general

agreement with that shown in fig. 2.7 and lends support to the reliability of the data used here.

2.3.7 COMPILATION OF ICE SHEET SURFACE MAP

The corrected ice surface elevations were plotted by computer on a map at a scale of 1:2188800 with polar stereographic projection (standard latitude 71° S). This scale was chosen so as to be compatible with US air navigation charts and previous RES maps compiled at SPRI (see Drewry, 1975a; Rose, 1978; and Steed, 1980).

The coastline for this map has been taken from the 1:5000000 topographic map of Antarctica (American Geographical Society of New York, Sheet 13, 1970). The grounding line of the Ross Ice Shelf has been determined from Landsat satellite imagery and RES data (see Rose, 1978). Similarly the grounding line of the Ronne-Filchner Ice Shelf and the ice rises within it have been determined up to 80° S by Landsat imagery and RES data (Swithinbank, Doake and Crabtree, 1976; Crabtree and Doake, 1980). Further south the grounding line of the Ronne-Filchner Ice Shelf is one of its least known margins and has been determined from RES data collected by the author (Drewry, Meldrum and Jankowski, 1980) and is discussed in detail in chapter 3.

The ice surface elevations were hand contoured at 100m intervals from the RES data using values 15s apart (ie. ~1.7km on the ground) and incorporating all available data on surface elavation from oversnow traverses (Bentley and Ostenso, 1964; Behrendt, 1964a; Bentley and Chang 1971; Bentley, personal commun.; American Geographical Society of New York, Sheet 13, 1970). Data collected and compiled by Rose (1978) have been incorporated in the map (see fig. 2.7 and large scale

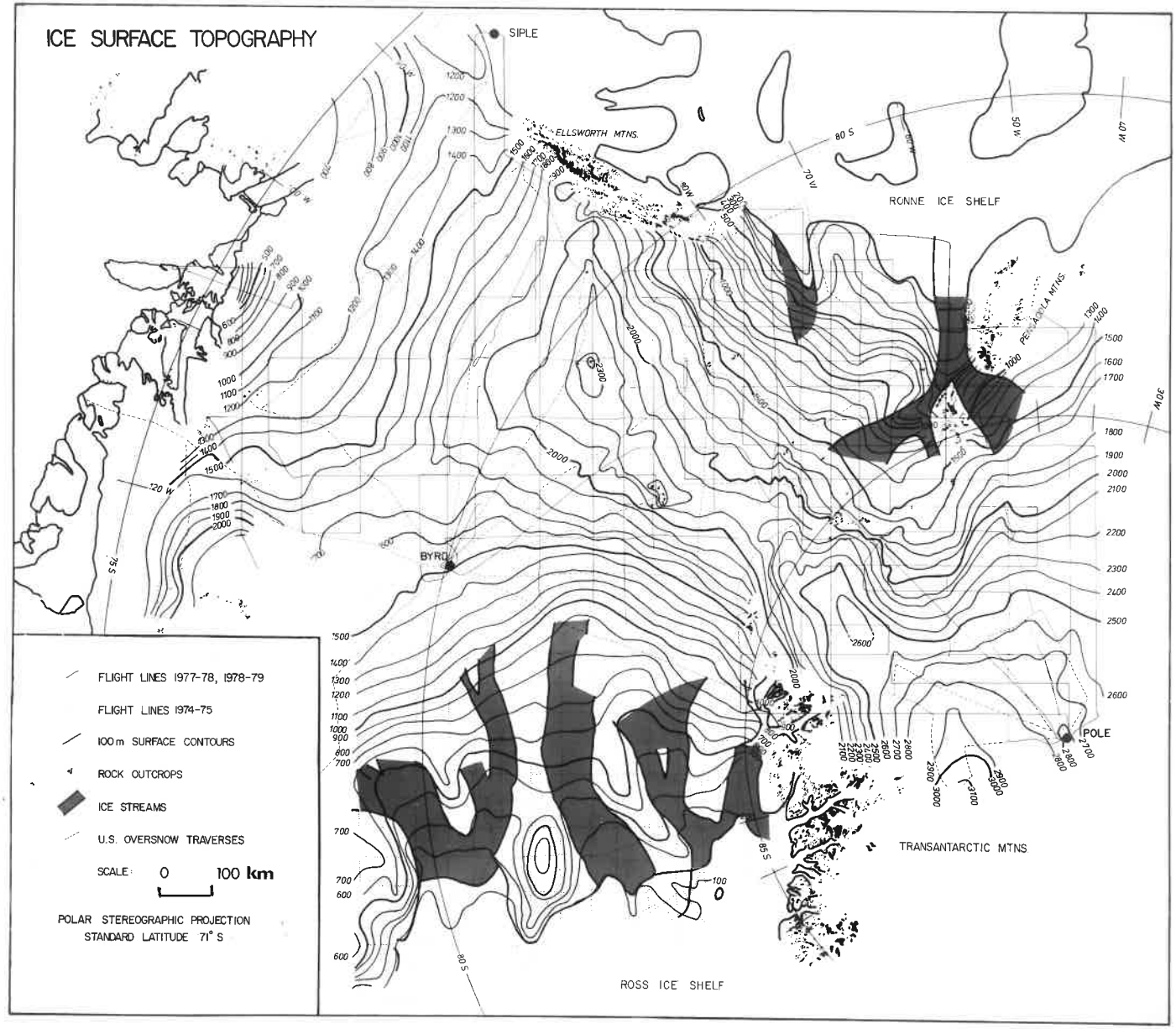


Fig. 2.7 Ice Surface Topography

map in back pocket). Computer contouring routines were not used as they usually require an evenly spaced grid of data. It would have been necessary to either generate new data by interpolation or throw some data away to get the RES data in the right form. Some routines will accept randomly spaced data and fit a surface to it before contouring the best fitting surface, but these were considered to give unreliable results. Discussion of the ice sheet surface and the identification of major ice streams shown on fig. 2.7 can be found in chapter 3.

2.3.8 COMPILATION OF BEDROCK MAP

Bedrock elevations were plotted in a similar fashion as the ice surface data but have been contoured at an interval of 250m. The much rougher nature of the bedrock surface does not allow contouring at a smaller interval and many features can not be resolved by the spacing of the flight lines (see fig. 2.8 and large scale map in back pocket).

Shading has been added to the large scale map in the back pocket to assist with interpretation, showing areas below -1000m asl. In fig. 2.8 shading has also been added to areas with bedrock elevations above 500 m asl. No attempt has been made to contour in detail in areas of rock outcrop. In addition to RES data all available seismic data from US oversnow traverses have been considered (Bentley and Ostenso, 1964; Behrendt, 1964a; Bentley and Chang, 1971; Bentley, personal commun.; American Geographical Society of New York, Sheet 13, 1970) Once again data from Rose (1978) has been included in fig. 2.8.

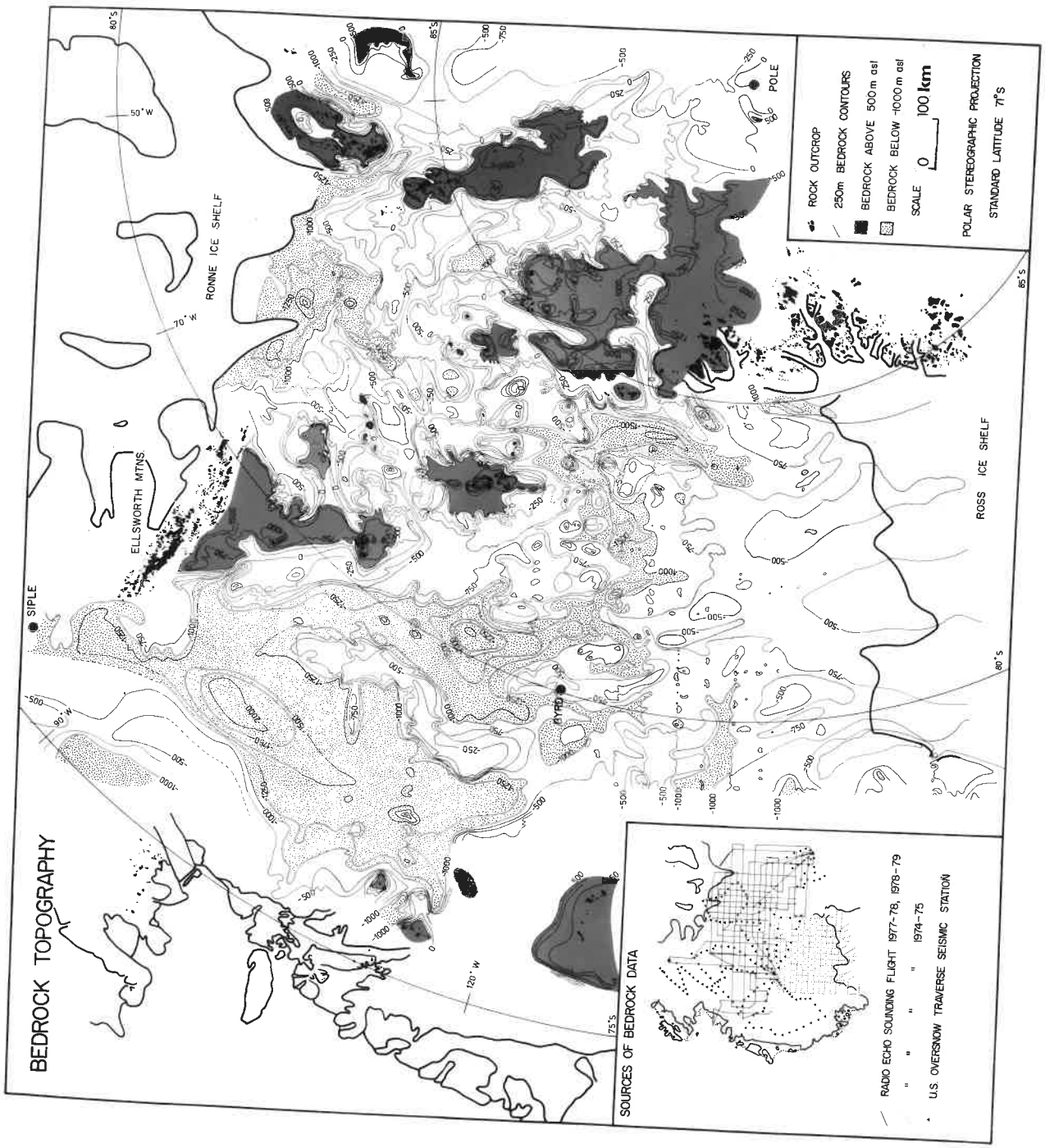


Fig. 2.8 Bedrock Topography

2.4 MAGNETICS

2.4.1 EQUIPMENT

Total field magnetic readings were obtained using a Geometrics G803 proton precession magnetometer with a resolution of 1 nT (1 nT = 1gamma = 10^{-5}oesteds). The principles of this type of magnetometer can be found in most applied geophysical textbooks (eg. Dobrin, 1976; Telford, Geldart, Sheriff and Keys, 1976). The sensor for the magnetometer was mounted near the end of a 3 m long stinger extending out of the tail of the aircraft. This was to minimise, but by no means eliminate the magnetic effects of the aircraft. A knowledge of the field direction is required to compensate the scalar readings for the disturbances due to the aircraft (see section 2.4.4). For this purpose a Devolco 9200C vector magnetometer was included to measure the 3 components of the field. This instrument has an accuracy of about 500 gammas and a resolution of 100 gammas. The vector magnetometer was mounted in the stinger well forward of the sensor for the scalar magnetometer. A heater was incorporated into the vector magnetometer to protect it from extreme cold temperatures. Enough power was dissipated from the scalar magnetometer sensor for it not to need additional heating elements.

Output from the magnetometers was recorded on magnetic tape by the ARDS. During 1978-79 the data was also displayed on a chart recorder. The scalar magnetometer had a cycle time of 0.75s.

2.4.2 THE GEOMAGNETIC FIELD

Measurements of the earth's magnetic field have been made for many centuries and it is well established that the geomagnetic field can be divided into 3 parts (Dobrin, 1976; Nettleton, 1976; and Telford et al, 1976).

1) A main field, regarded roughly as equivalent to a simple, though not quite uniformly polarised sphere. This field is relatively large, is of internal origin and varies slowly with time (ie. secular variation).
2) A relatively small external field which varies rapidly and somewhat erratically in time but occurs approximately in daily cycles. At times however relatively strong short period disturbances occur and are the results of solar induced magnetic storms.
3) Variations of the main field which are constant in time and location, and which are due to magnetic inhomogeneities in the earth's crust.

It is these latter variations of the main field that are of importance to this thesis. Before attempting, however, to interpret any anomaly field in terms of geology the effects of the other two parts of the geomagnetic field must be removed from the recorded data. This problem is discussed in the following section.

2.4.3 THE REGIONAL FIELD, SECULAR AND DIURNAL VARIATIONS

Spherical harmonic analyses of the observed near surface magnetic field have shown that at least 99% is due to sources within the earth and the remaining 1% due to external sources (Runcorn, 1956; Jacobs, 1974; Telford et al, 1976). The present theory on the origin of the internal field suggests that it is caused by a combination of complex mechanical motion

in the liquid outer core and electric currents flowing through it (Telford et al, 1976).

The geomagnetic field can be completely defined by its magnitude, F, its inclination, I (the angle between the horizontal and the direction of the earth's field at that point), and by its declination, D (the angle between geographic north and the field direction). The field is a vector quantity and can be represented by a vertical component (Z) and a horizontal component (H), which itself has two components X and Y in the horizontal plane (see fig. 2.9).

As a result of hundreds of years of observation the geomagnetic field is known not to be permanent but to undergo slow changes referred to as secular variation. The source of these variations is not well understood, but is thought to be internal, possibly connected with changes in convection currents in the core, in the core-mantle coupling and in the rotational speed of the earth (Telford et al, 1976).

In relation to the Antarctic field data discussed in this thesis the earth's main field and its secular variation have been subtracted from the data using a spherical harmonic model (Peddie and Fabiano, 1976). A computer program written by N. Peddie of the US Geological Survey and modified by the author was used. The mathematical model (AWC-75) of the near surface geomagnetic main field and its secular variation is composed of two parts.

1) A model of the 1975.0 geomagnetic main field consisting of a degree 12 spherical harmonic series of 168 internal source terms.
2) A model of the geomagnetic secular variation for the interval 1967 to 1974 consisting of a degree 8 spherical harmonic series of 80 secular variation terms.

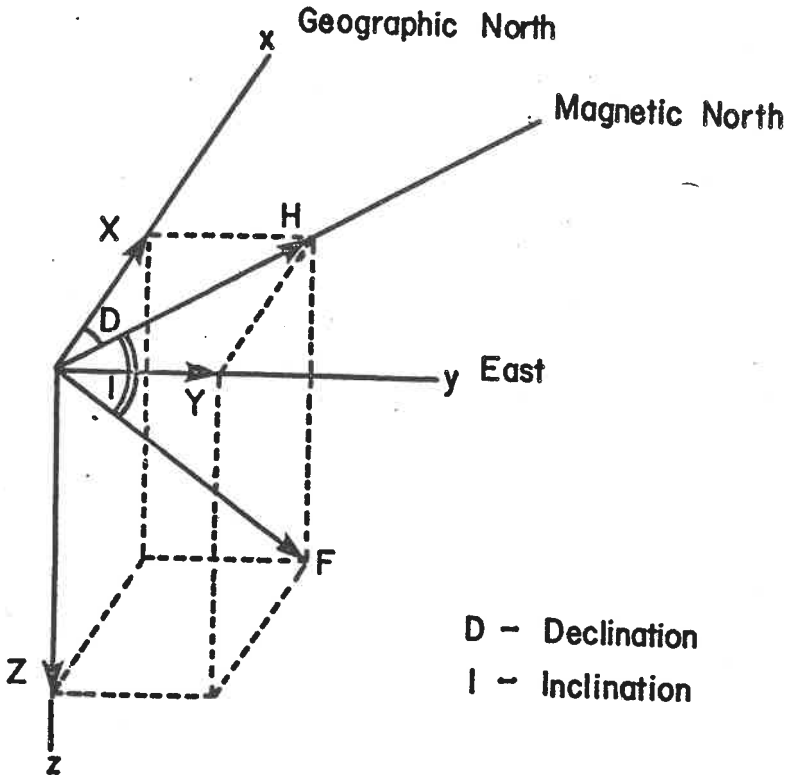


Fig. 2.9 Elements of the Earth's magnetic field

L = 33 nT

T = 10

V = -4

60,000 (TL + LT) = 15

(VT + TV) = 0

60,000 (LV + VL) = -7

60,000 (VV - LL) = -51

60,000 (TT - LL) = -55

60,000 (VV) = -11

60,000 (TT) = -15

60,000 (LL) = 40

Table 2.3 Compensation coefficients for 1977-78 data (after Finkel, 1978).

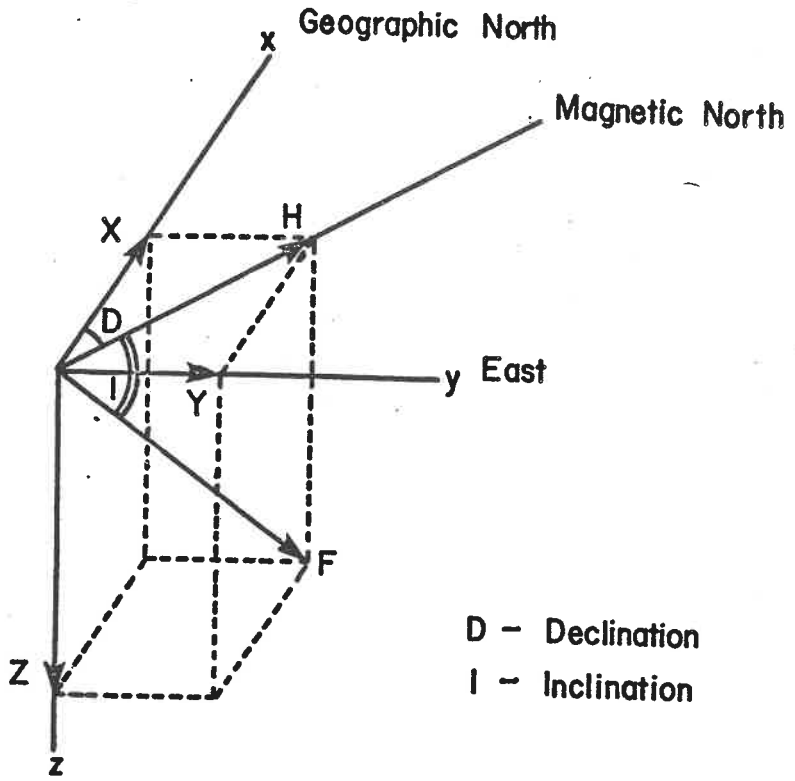


Fig. 2.9 Elements of the Earth's magnetic field

$$L = 33\ nT$$

$$T = 10$$

$$V = -4$$

$$60{,}000\ (TL + LT) = 15$$

$$(VT + TV) = 0$$

$$60{,}000\ (LV + VL) = -7$$

$$60{,}000\ (VV - LL) = -51$$

$$60{,}000\ (TT - LL) = -55$$

$$60{,}000\ (VV) = -11$$

$$60{,}000\ (TT) = -15$$

$$60{,}000\ (LL) = 40$$

Table 2.3 Compensation coefficients for 1977-78 data (after Finkel, 1978).

Full details of the model are decribed in Peddie and Fabiano (1976). The model was updated to the date of the surveys by linear extrapolation (fig. 2.10 shows examples of the observed field and residual field).

The remaining 1% of the geomagnetic field that originates outside the earth is associated with electric currents in the ionized layers of the outer atmosphere. Variations in time of this field are far more rapid than the secular variation of the dipole field. Of these variations the solar diurnal variations are of most significance having a periodicity of about a day and an amplitude of about 25-30 nT. These variations vary with latitude and season and are probably controlled by action of the sun on ionospheric currents (Telford et al, 1976).

It is common practice in magnetic surveys to make continuous readings at a base station within the survey area in order to identify and then subtract the diurnal variations from the data. No diurnal variation correction could be applied to the 1977-78 or 1978-79 data for the following reasons:

1) Remoteness of the survey area. It was logistically impossible to set up a base station.
2) The large area covered by the survey (~0.5 M km^2) would have made it difficult or even impossible to apply the corrections to the whole of the grid even if a remote base station could have been set up.

This is not thought to be too serious a handicap for a reconnaissance survey of this nature because:

1) Duration of flights was generally less than ~12 hrs., and thus less than the period of the diurnal changes.
2) The majority of anomalies studied are an order of magnitude greater than the magnitude of the diurnal variation. Smaller anomalies can still be studied with a certain amount of confidence because of the speed of the aircraft. An anomaly of wavelength 50 km is crossed in only ~7 min.

The diurnal variations are all relatively small in amplitude, but at times

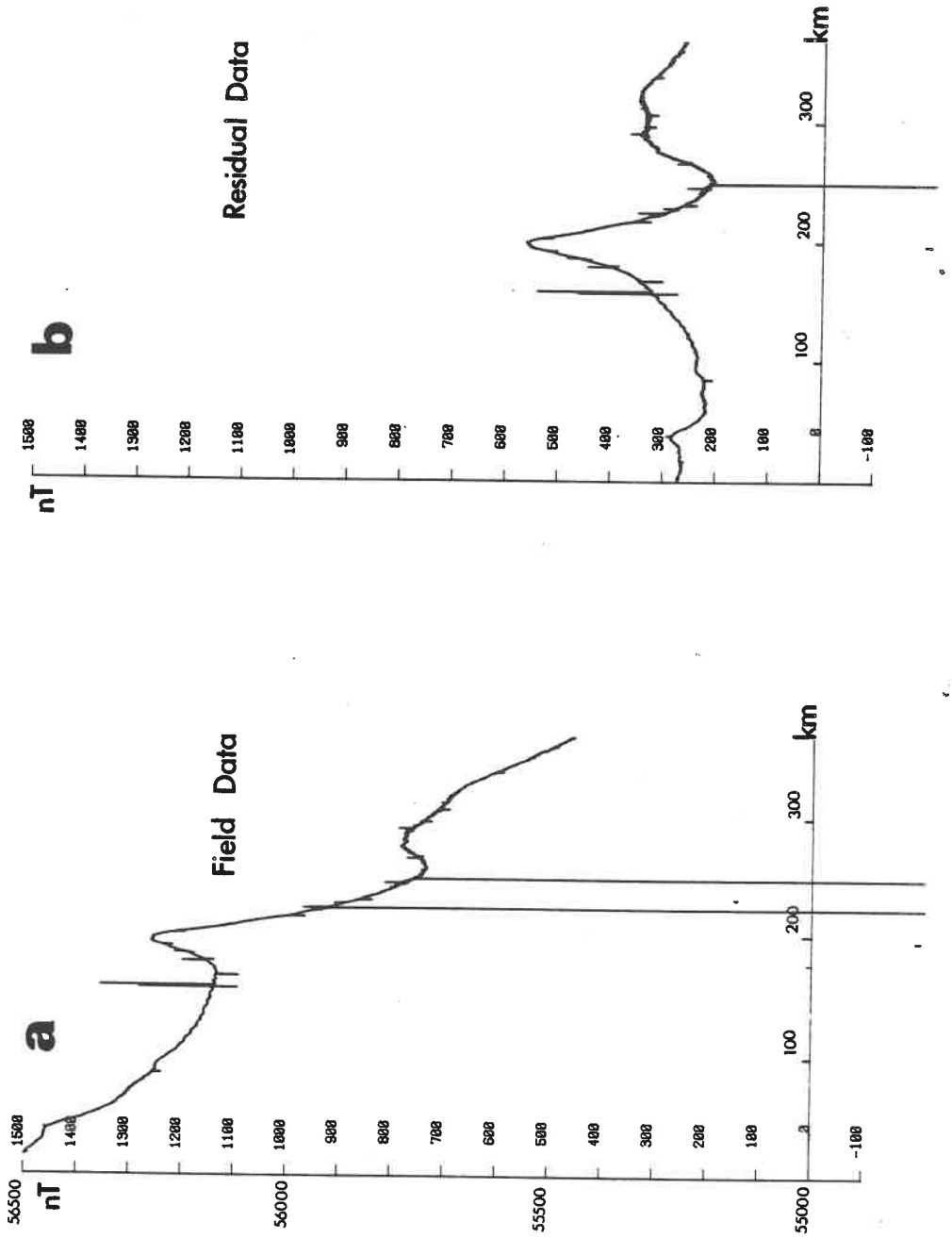


Fig. 2.10 a) Observed total magnetic field.
b) Residual field (after removal of AWC-75).

the geomagnetic field becomes highly disturbed during what are described as magnetic storms. Magnetic storms are rather erratic but appear to occur at intervals of ~27 days, the period correlating with sunspot activity (Telford et al, 1976). Magnetic storms can be particularly violent in high latitudes due to channelling of charged particles towards the geomagnetic poles, where they are accompanied by other manifestations such as usually bright and extensive auroral displays and interruptions to radio communication systems. The area of survey is well within the auroral zone (circular belt of constant dipole latitude 67°). (Jacobs, 1974; Akosofu, 1978).

It is generally believed that magnetic storms and the aurora are caused by gas ejected from time to time by the sun in the form of streams or clouds. The gas is neutral but ionized, consisting mainly of protons and electrons. Magnetic storms, the aurora and other phenomena occur when the earth becomes immersed in such a solar cloud or stream, which have dimensions greatly exceeding those of the earth (Akosofu and Chapman, 1961).

Variations in the geomagnetic field during such storms can be as great as 1000 nT in low to mid latitudes and even higher in polar regions. Consequently magnetic measurements become totally unreliable during a magnetic storm.

Prior to each flight the state of the geomagnetic field was assessed from the continuously recording vector magnetometer at Scott Base (part of New Zealand Antarctic Research Programme) on Ross Island. Although the area of survey was over 2000 km from Scott Base magnetic storms would be experienced in both places almost simultaneously (the actual level of variations experienced however are likely be completely different). At no time during both seasons was the field too highly disturbed, varying by several hundred nT between successive readings, for a flight to be

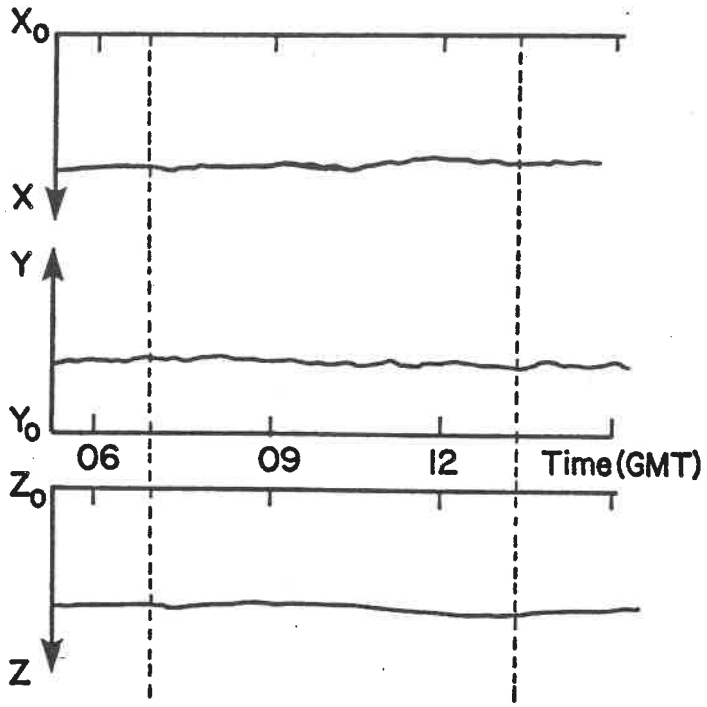
cancelled. Each season the flying was restricted to about a 14 day period during which luckily no major storms occurred. Copies of the magnetograms from Scott Base have been examined for both seasons to assess the reliability of the measurements made during each flight. Fig. 2.11 shows examples of the Scott Base data.

2.4.4 COMPENSATION OF DATA

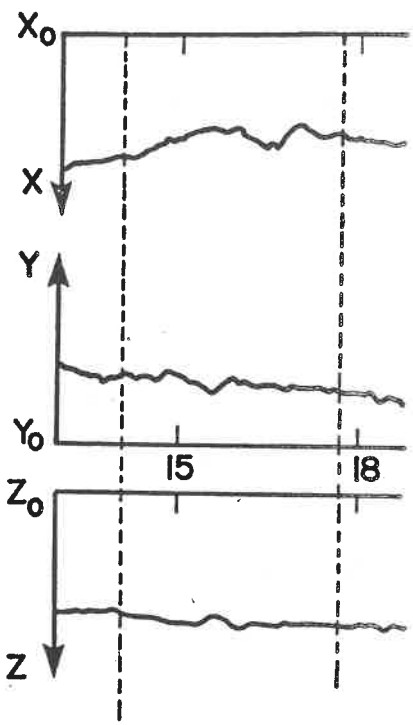
The sensor for the scalar magnetometer was mounted near the end of a tail stinger so as to minimise the effects of the aircraft. Ideally the sensor would have been mounted in a 'bird' and towed well behind the aircraft, however this was not logistically possible with the LC130-R. Since the sensor could not be isolated completely from the aircraft the data were compensated using the technique originally developed by Leliak (1961). Compensation of the data was carried out by Applied Physics Laboratory of Johns' Hopkins University, Baltimore (Finkel, 1978; Hickerson, 1979).

Exact treatment of this problem can be found in Leliak (1961), however a brief description of the three sources of magnetic interference due to the aircraft and the derivation of compensation coefficients will be given here.

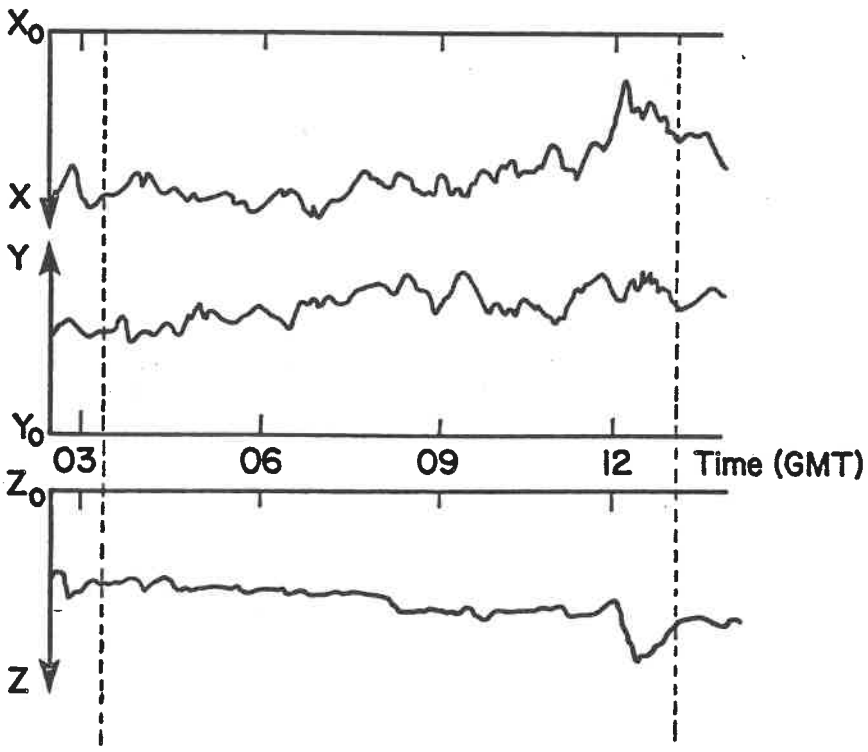
1) The aircraft behaves as a large bar magnet possessing a permanent magnetic field. This field can be expressed in terms of 3 components, one parallel to the longitudinal axis of the aircraft, one parallel to the transverse axis and the third vertically downwards This field is fixed in relation to the aircraft, so when the aircraft turns this field changes its direction in relation to the earth's magnetic field thereby causing a change in the magnetic field around the sensor.
2) The aircraft also acts as an induced magnet. Each component of the



Flight 2
15 Jan 1978



Flight 4
16 Jan 1978



Flight 32
18 Dec 1978

Scales:

SVx = 22·6 nT/mm
SVy = 27·3 nT/mm
SVz = 29·9 nT/mm

Fig. 2.11 Examples of vector magnetometer records from Scott Base, Ross Island.

earth's field induces a magnetic effect at the aircraft which in turn produces 3 field components at the sensor. The induced field is not fixed in relation to the aircraft but its polarity and magnitude are determined by the direction and magnitude of the earth's field.

3) The permanent and induced effects are all due to translational motion. During manoeuvres the aircraft undergoes rotational motion. Various parts of the aircraft cut across flux lines at different rates thereby generating potential differences and eddy currents. These currents then produce field changes at the sensor.

It is necessary to solve an overdetermined system of equations relating to 16 sources of magnetic interference due to the permanent, induced and eddy current fields of the aircraft (Leliak, 1961). All 16 sources of interference can be related to the aircraft manoeuvres and the equations can be developed from data received during sinusoidal manoeuvres of the aircraft.

The general procedure for compensation involved the use of a vector magnetometer whilst performing a series of standard compensation manoeuvres. The standard manoeuvres comprised $\pm 5^{o}$ pitchs, $\pm 10^{o}$ rolls and $\pm 5^{o}$ yaws at periods of 5s flown along the four cardinal magnetic directions. Table 2.3 gives the compensation coefficients determined by APL for the 1977-78 data relating to the permanent and induced fields only (Finkel, 1978). To simplify computation the rotational effects have been ignored because during survey flying most of the motion is translational and the rotational effects are minimal.

During the 1978-79 season time constraints only allowed one set of compensation manoeuvres to be performed. In addition the quality of the manoeuvres was poor, the scalar measurments suffered from noise, and hardware problems with the vector magnetometer, make the coefficients for 1978-79 very unreliable (Hickerson, 1979). For this reason it was decided not to compensate the data (see section 2.4.5 for discussion of errors).

2.4.5 SOURCES OF ERROR

Errors in the residual total field magnetic data used later in this thesis are difficult to assess quantitatively. The recorded total field data is recorded with a precision of 1 nT but errors arise from

1) Inadequate or no compensation of the data for the effects of the aircraft.
2) Diurnal changes.
3) Inadequate model of the earth's regional field in Antarctica.

1) Compensation of the data for the magnetic effect of the aircraft was undertaken by the Applied Physics Laboratory of John's Hopkins University. Due to a combination of circumstances the compensation coefficients calculated are not thought to be reliable for both seasons. For this reason the 1978-79 data were not compensated. The corrections calculated for the 1977-78 data proved to be relatively small (< 20 nT) for those sections of flight where the aircraft was maintaining constant pressure altitude and performing no manoeuvres. For this reason anomalies occurring on sections of flight where the aircraft was changing altitude or turning have not been used in any further analysis. For sections of straight level flight the magnetic effect of the aircraft results in a small largely constant offset.

During the 1978-79 season time constraints only allowed one set of compensation manoeuvres to be performed. In addition the quality of the manoeuvres was poor, the scalar measurments suffered from noise, and hardware problems with the vector magnetometer, make the coefficients for 1978-79 very unreliable (Hickerson, 1979). For this reason it was decided not to compensate the data (see section 2.4.5 for discussion of errors).

2.4.5 SOURCES OF ERROR

Errors in the residual total field magnetic data used later in this thesis are difficult to assess quantitatively. The recorded total field data is recorded with a precision of 1 nT but errors arise from

1) Inadequate or no compensation of the data for the effects of the aircraft.
2) Diurnal changes.
3) Inadequate model of the earth's regional field in Antarctica.

1) Compensation of the data for the magnetic effect of the aircraft was undertaken by the Applied Physics Laboratory of John's Hopkins University. Due to a combination of circumstances the compensation coefficients calculated are not thought to be reliable for both seasons. For this reason the 1978-79 data were not compensated. The corrections calculated for the 1977-78 data proved to be relatively small (< 20 nT) for those sections of flight where the aircraft was maintaining constant pressure altitude and performing no manoeuvres. For this reason anomalies occurring on sections of flight where the aircraft was changing altitude or turning have not been used in any further analysis. For sections of straight level flight the magnetic effect of the aircraft results in a small largely constant offset.

2) Diurnal changes were discussed in section 2.4.3 and the likely error shown not to be crucial to a survey of this nature. The amplitude and period of solar induced variations alters considerably depending on the state of the geomagnetic field at the time. This was always checked before each flight and since the field work was completed. At no time was the field so highly disturbed as to render the data unusable. Errors could be ~30 nT on a quiet day and considerably more on a disturbed day. It is futile to attempt to quantitatively assess the error for each flight from the distant base station records.

3) The spherical harmonic model used for the regional field was the AWC-75 field updated to the date of the surveys by linear extrapolation. Such models are based on magnetic records from around the earth and naturally are more accurate in lower latitudes where there is more data input. There are only a few sources of input from Antarctica. Nevertheless AWC-75 is believed to be the best available, having used data from West Antarctica to generate the model (Peddie, personal commun.). The model adequately removed the regional trend from the data presented in this thesis (see figs. 5.9 and 5.10). Any remaining regional gradient however can be adequately defined by one or more straight line segments or a splined curve and removed from the data if necessary before further analysis.

2.4.6 MAGNETIC PROPERTIES OF ROCKS

The residual anomaly field that is of interest to this thesis is generated by irregularities in the distribution of magnetised material in the upper crust. The main source of local magnetic anomalies in rocks are ferrimagnetic minerals, particularly magnetite. Other ferrimagnetic minerals include titanomagnetite, ilmenite and pyrrhotite. Although in many cases the magnetism of rocks depends mainly upon the present strength of the ambient geomagnetic field and the magnetic mineral content, in

practise residual magnetism often contributes to the total magnetisation in rocks both in amplitude and direction (Telford et al, 1976). Remanent magnetisation effects are very complex depending on the magnetic history of the rocks involved. In the area studied in this thesis remanent magnetisation effects are expected to play a significant part.

As with density in gravitational work the main variable in magnetic studies is susceptibility. Magnetic susceptibility is defined in Appendix 1. Numerous attempts have been made to establish a quantitative relationship between rock susceptibility and their Fe_3O_4 concentration (Lindsley et al, 1966). An extremely rough linear dependence is shown but the scatter is large. Table 2.4a is taken from Dobrin (1976) and illustrates some representative values of susceptibility for several different kinds of rocks and minerals. Note that many of the measurements were made with a field of 1 Oe or more and there is some question how applicable such values are (Dobrin, 1976). More reliable results are obtained by multiplying the volume percentage magnetite in a particular rock by the susceptibility of magnetite (ie 0.3 cgs). Table 2.4b shows the range of susceptibility, given by Dobrin (1976), for given rock types using this method.

Although there is a great variation in the susceptibility values for a particular rock, and a wide overlap between different types, sedimentary rocks have the lowest average susceptibility and basic igneous rocks the highest. Ideally possible source rocks exposed within a survey area would be sampled and their bulk susceptibility measured or estimated so as to provide control for subsequent modelling studies. This is extremely difficult in the area surveyed in this thesis due to the lack of exposed bedrock. Susceptibility measurments on the few exposed rocks are not well reported and for this reason samples of exposed rocks in West Antarctica, belonging to the collection of C. Craddock at the University of Wisconsin, were examined. Susceptibility measurments on 24 mm diameter cores from

these rocks can be found in Appendix 1.

a

MATERIAL	k x 10^{-6} cgs	at H, Oe
Magnetite	300,000-800,000	0.6
Pyrrhotite	125,000	0.5
Ilmenite	135,000	1
Franklinite	36,000	
Dolomite	14	0.5
Sandstone	16.8	1
Serpentine	14,000	30.5
Granite	28-2700	1
Diorite	46.8	1
Gabbro	68.1-2370	1
Porphyry	47	1
Diabase	78-1050	1
Basalt	680	1
Olivine-diabase	2000	0.5
Peridotite	12,500	0.5-1.0

b

MATERIAL	MAGNETITE CONTENT AND SUSCEPTIBILITY, (cgs)						ILMENITE AVERAGE	
	MINIMUM		MAXIMUM		AVERAGE			
	%	k x 10^{-6}	%	k x 10^{-6}	%	k x 10^{-6}	%	k x 10^{-6}
Quartz porphyries	0.0	0	1.4	4,200	0.82	2,500	0.3	410
Rhyolites	0.2	600	1.9	5,700	1.00	3,000	0.45	610
Granites	0.2	600	1.9	5,700	0.90	2,700	0.7	1000
Trachyte-syenites	0.0	0	4.6	14,000	2.04	6,100	0.7	1000
Eruptive nephelites	0.0	0	4.9	15,000	1.51	4,530	1.24	1700
Abyssal nephelites	0.0	0	6.6	20,000	2.71	8,100	0.85	1100
Pyroxenites	0.9	3000	8.4	25,000	3.51	10,500	0.40	5400
Gabbros	0.9	3000	3.9	12,000	2.40	7,200	1.76	2400
Monzonite-latites	1.4	4200	5.6	17,000	3.58	10,700	1.60	2200
Leucite rocks	0.0	0	7.4	22,000	3.27	9,800	1.94	2600
Dacite-quartz-diorite	1.6	4800	8.0	24,000	3.48	10,400	1.94	2600
Andesites	2.6	7800	5.8	17,000	4.50	13,500	1.16	1600
Diorites	1.2	3600	7.4	22,000	3.45	10,400	2.44	4200
Peridotites	1.6	4800	7.2	22,000	4.60	13,800	1.31	1800
Basalts	2.3	6900	8.6	26,000	4.76	14,300	1.91	2600
Diabases	2.3	6900	6.3	19,000	4.35	13,100	2.70	3600

Table 2.4 Magnetic Susceptibilty for commom rock types and minerals (after Dobrin, 1976).

CHAPTER 3 WEST ANTARCTIC ICE SHEET

3.1 INTRODUCTION

About 95% of Antarctica is covered by ice. In the process of collecting geophysical data on bedrock in West Antarctica much valuble information on the surface morphology and thickness of the West Antarctic ice sheet has been obtained. Although the ice sheet is not directly related to this thesis, and can in fact be considered as a major hindrance, it is nevertheless thought useful to provide a brief resume of some glaciological details.

The broad structure of the ice sheet was generally known from previous surface work, mainly US oversnow traverses (Bentley and Ostenso,1961; Bentley, 1964; Behrendt, 1964a; Bentley and Chang, 1971). The data now available from RES represents a major advance in our knowledge of the West Antarctic ice sheet allowing improved delineation of many features including ice drainage basins of West Antarctica. The part of the ice sheet west of Byrd Station, supplying ice to the Ross Ice Shelf, has been fully described by Rose (1978,1979) and will only be mentioned briefly. The area of the ice sheet to the east of Byrd Station, however, is less well known and this thesis has resulted in better definition of ice streams and a modification of the grounding line of the Ronne-Filchner Ice Shelf (Jankowski and Drewry, 1981).

A major contemporary issue in glaciology at present is the stability of the West Antarctic ice sheet. Mercer (1978) warned that increasing levels of CO_2 in the atmosphere may lead to climatic warming due to the greenhouse effect which could result in the demise of Antarctic ice shelves and the inevitable collapse of the West Antarctic ice sheet. The

flow of ice northwards from West Antarctica into the Amundsen-Bellingshausen Seas is of crucial importance and data were collected from the Thwaites Glacier, one of the main outlet glaciers in this region.

3.2 ICE SURFACE MORPHOLOGY

The ice surface in West Antarctica is shown in fig. 2.7 (and in map in back pocket). Contours have been drawn at 100m intervals as described in section 2.3.7.

The RES results confirm earlier studies of the surface morphology of West Antarctica (eg. Bentley,1964). A major ice divide runs from inland of the Transantarctic Mountains through a gap between the Horlick and Thiel Mountains towards the Ellsworth Mountains. A further ice divide crosses from the Executive Committee Range (passing to the NE of Byrd Station) to join the first divide in the vicinity of Mt. Woollard. West Antarctica is thus effectively divided into a series of drainage basins feeding ice into the Ross Ice Shelf, Ronne-Filchner Ice Shelf and the Amundsen-Bellingshausen Seas (Jankowski and Drewry, 1981). Catchment areas and flow directions have been determined by careful visual inspection of the ice surface contours (see fig. 3.1). Additional detail is provided from recent work (Drewry et al, in press). The Ross Ice Shelf is a major area of outflow from West Antarctica. Ice flows into the ice shelf via five major ice steams which follow subdued bedrock troughs (Rose, 1978). To the NE of Byrd Station the Amundsen Sea is similarly a major area of outflow. The third major drainage basin of West Antarctica lies to the south of the Ellsworth Mountains at the head of the Ronne-Filchner Ice Shelf. Scattered nunataks (eg. Nash and Pirrit Hills) and rugged bedrock topography (see fig. 2.8) in this area result in a more complicated flow pattern.

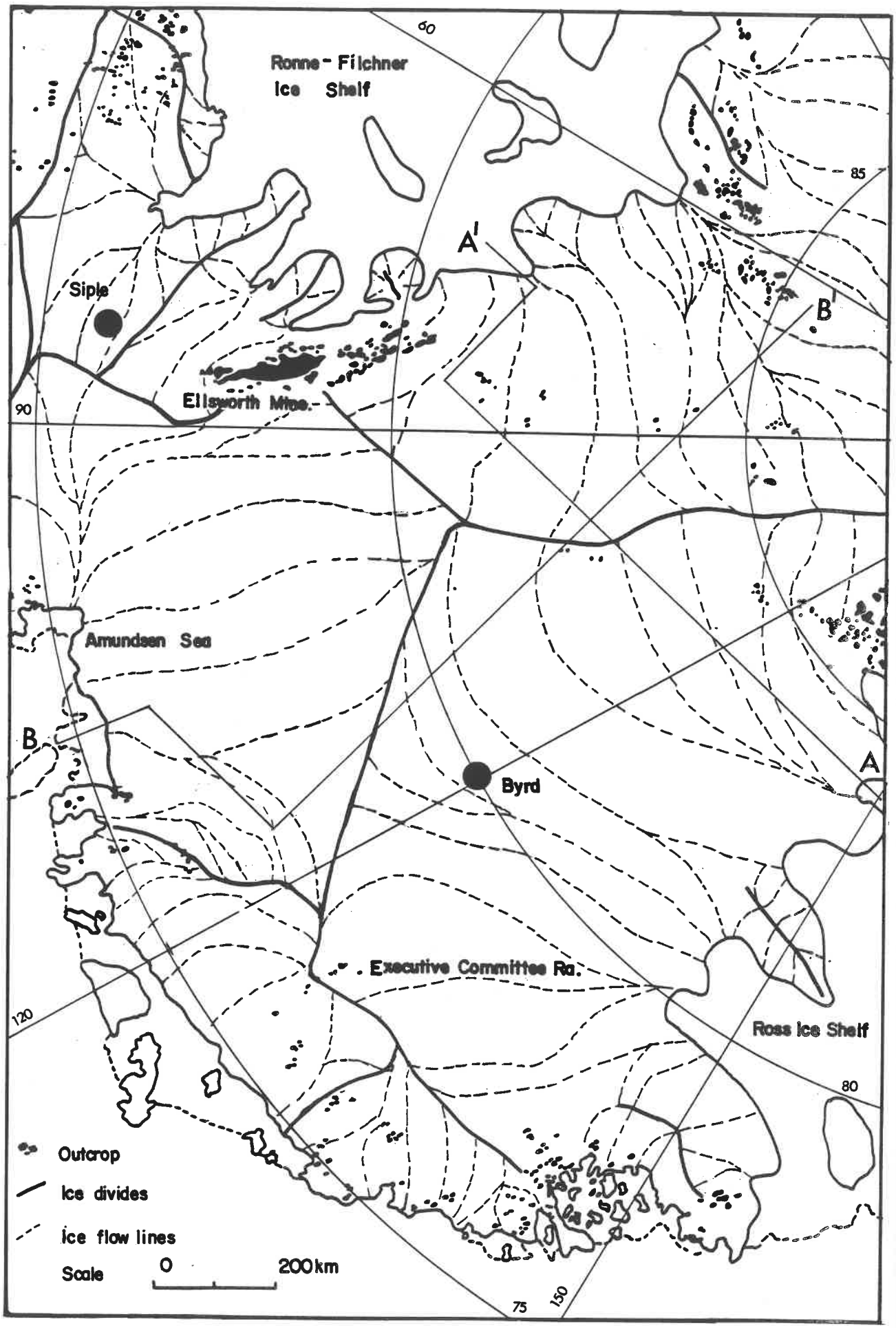


Fig. 3.1 Catchment areas, ice divides and flow lines for the West Antarctic ice sheet.

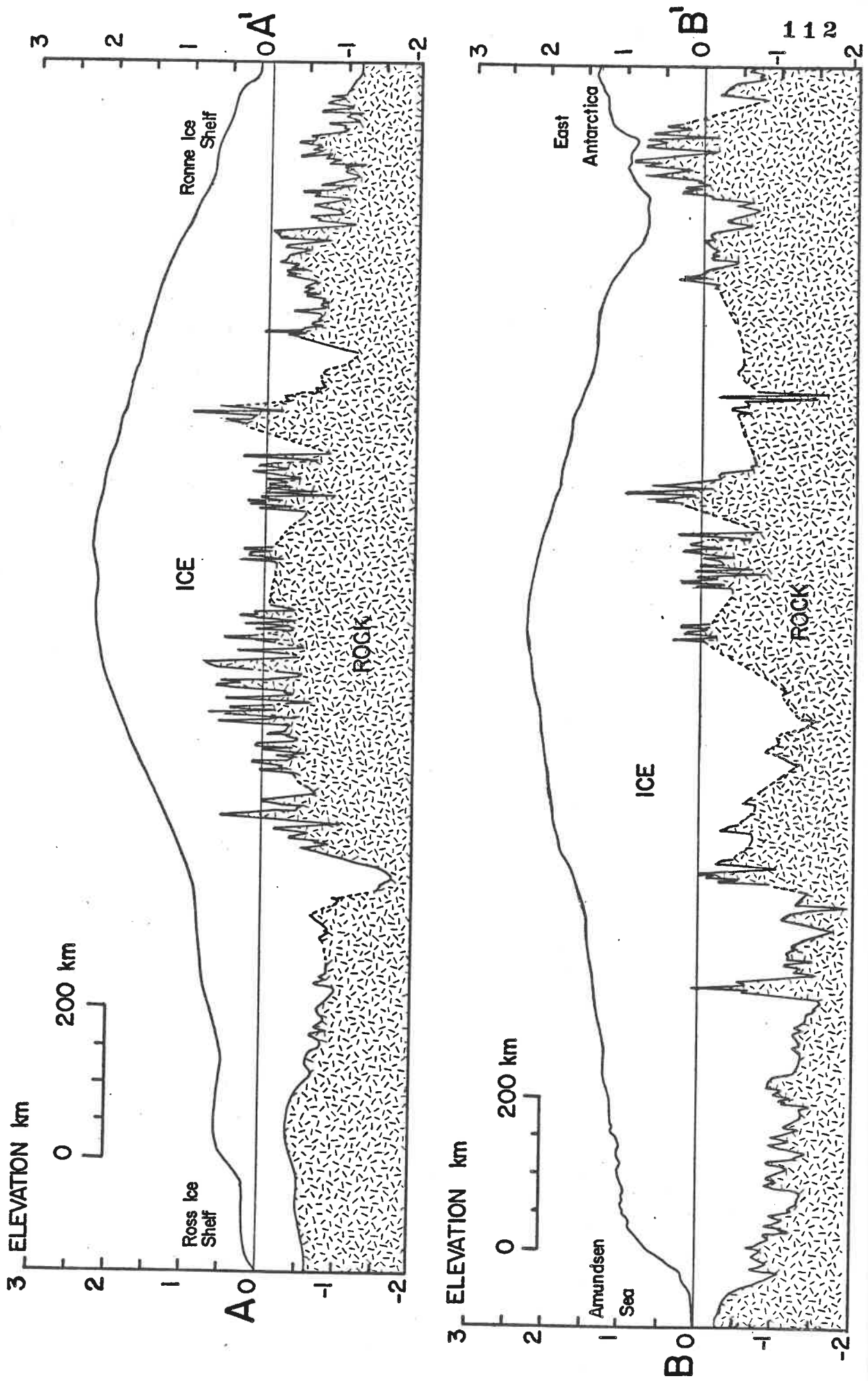


Fig. 3.2 Profiles through the West Antarctic ice sheet (see fig. 3.1 for locations).

The West Antarctic ice sheet is bounded on two sides by large floating ice shelves which locally run aground forming ice rises (ie. Berkner Island, Roosevelt Island). The ice shelves have a buttressing effect on the outflow of ice from West Antarctica (Thomas et al, 1979). Fig. 3.2 shows two sections across the ice sheet running approximately E-W and N-S. (locations of profiles shown in fig. 3.1). A better impression of the surface topography is obtained from fig. 3.3. Here the West Antarctic ice sheet is viewed from two directions from two imaginary points high above the Pacific Ocean. The Ellsworth Mountains are not shown in full so as to allow view of the ice sheet.

An additional source of ice surface data for the Antarctic has recently become available. During the austral summer of 1975 many constant density balloons launched in the southern hemisphere as part of the Tropical Wind, Energy conversion and Reference Level Experiment (TWERLE) eventually traversed the Antarctic (Levanon et al,1977). The balloons, floating at an altitude of 12.5 km, transmitted altimetric data once a minute to the orbiting satellite NIMBUS-6. Levanon et al (1977) estimate the positional accuracy to be 5km and the accuracy of the surface elevations to be $\pm$60m. These data have been shown to be of great use in areas where other forms of surface data are unavailable (Levanon and Bentley,1979). All TWERLE data have been made available by kind permission of N. Levanon and were plotted and contoured at an interval of 200m (fig. 3.4 shows location of all TWERLE data points within the area of interest). There is broad correspondance between the TWERLE data and Fig. 2.7 based on RES and oversnow traverse measurements, although the RES does allow better resolution of surface features. It is clear, however, that TWERLE data will enable contours to be drawn in areas that lack any RES coverage (Drewry et al, in press).

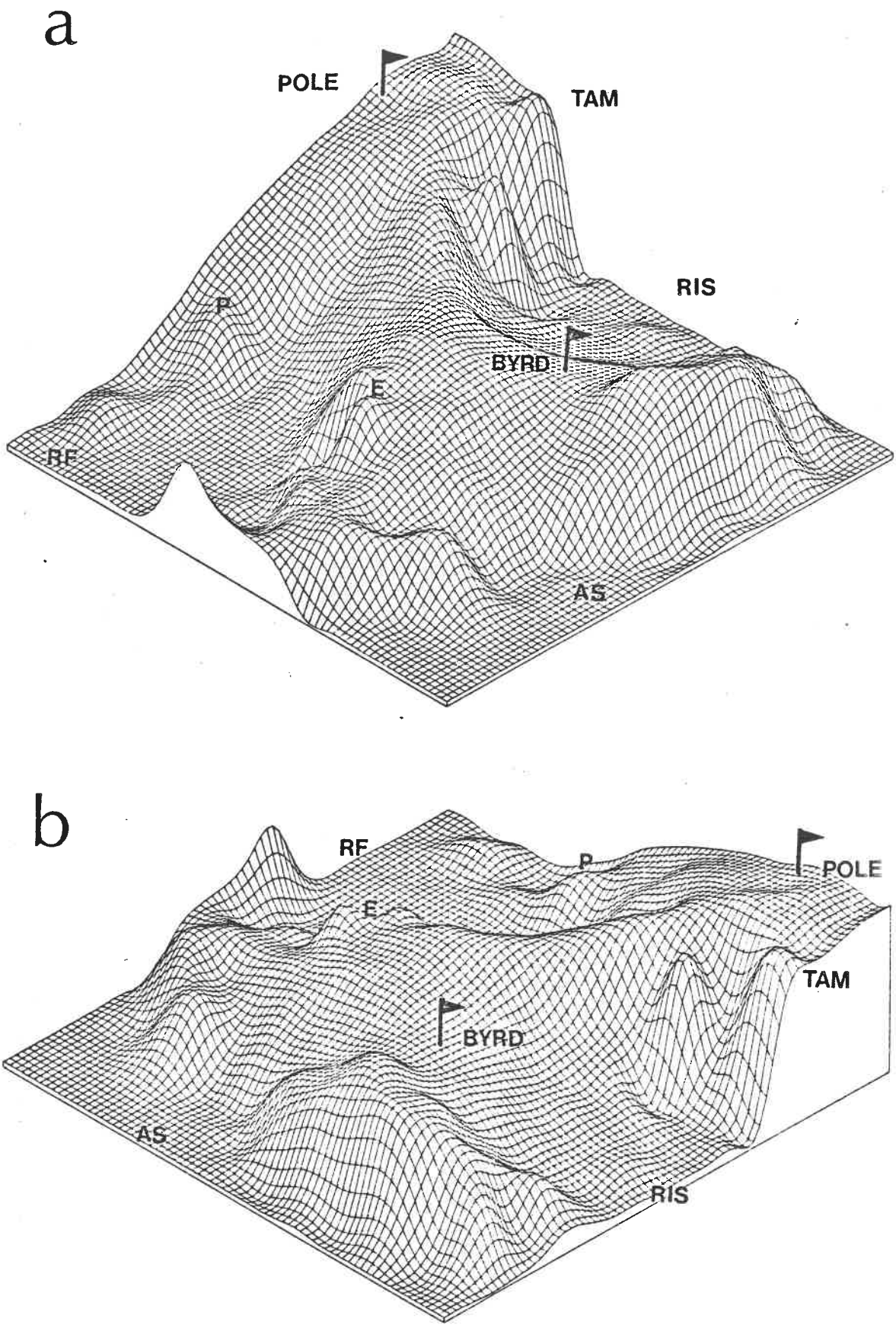


Fig. 3.3 3-D view of West Antarctic Ice Sheet.
(TAM-Transantarctic Mtns. P-Pensacola Mtns.
E-Ellsworth Mtns. RF-Ronne-Filchner Ice Shelf
RIS-Ross Ice Shelf AS-Amundsen Sea).

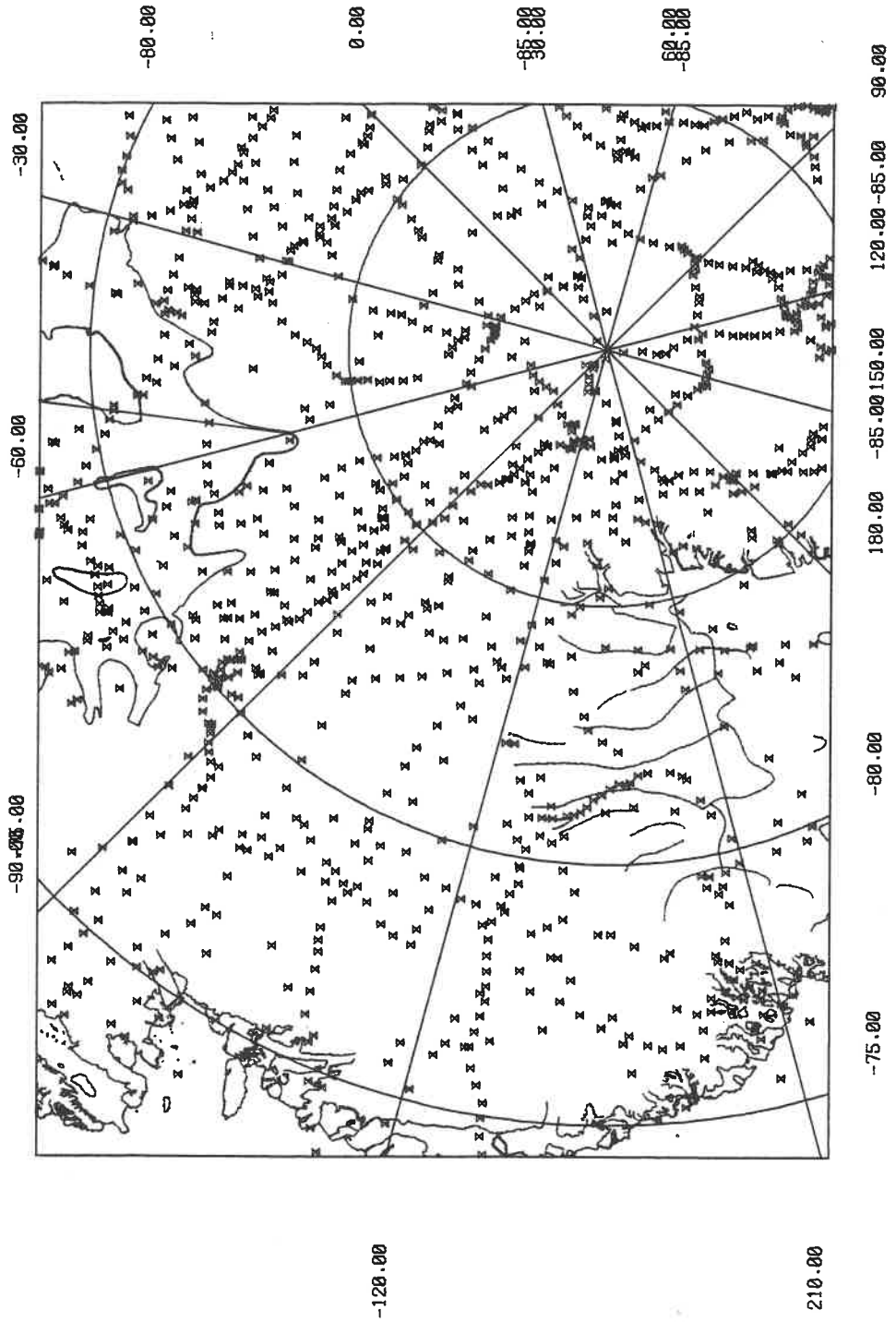


Fig. 3.4 Location of TWERLE elevation points in West Antarctica.

3.3 DRAINAGE OF THE WEST ANTARCTIC ICE SHEET

The surface morphology of West Antarctica is dominated by major ice streams and glaciers feeding ice into the Ronne-Filchner and Ross Ice Shelves and the Amundsen Sea. The major ice streams are shown shaded on fig. 2.7 and on map in back pocket. Two major glaciers, the Thwaites and Pine Island Glaciers, feed ice into the Amundsen Sea but have not been delineated due to a lack of data. No data were collected on the Pine Island Glacier and only one longitudinal and transverse section are available on the Thwaites Glacier.

The ice streams have been delineated by presence of clutter on the RES records produced by surface crevassing. Unlike sastrugi and other surface irregularities which produce weak hyperbolic echoes originating at or near the surface, intense surface crevassing produces strong hyperbolic returns, often obscuring internal reflections and the bottom return. Fig. 3.5 (after Rose,1979) clearly illustrates this property. Rose (1979) used such characteristics plus trimetragon photography and satellite imagery to map the inland boundaries of the ice streams feeding the Ross Ice Shelf. He identified 5 major ice streams (A-E) up to 100km wide and extending inland some 400km from the grounding line. The ice streams are seen to follow subdued troughs in bedrock separated by ridges and domes that are frozen to the bed (Rose,1979). The ice streams feeding ice into the Ronne-Filchner Ice Shelf have been delineated using the same criterion of clutter produced by surface crevassing. Satellite imagery (from LANDSAT) is not available below 80°S and the aircraft was not equipped with a trimetragon camera array as in 1974-75. However all boundaries marked were observed visually in the field and then checked against the RES records for characteristic hyperbolic echoes.

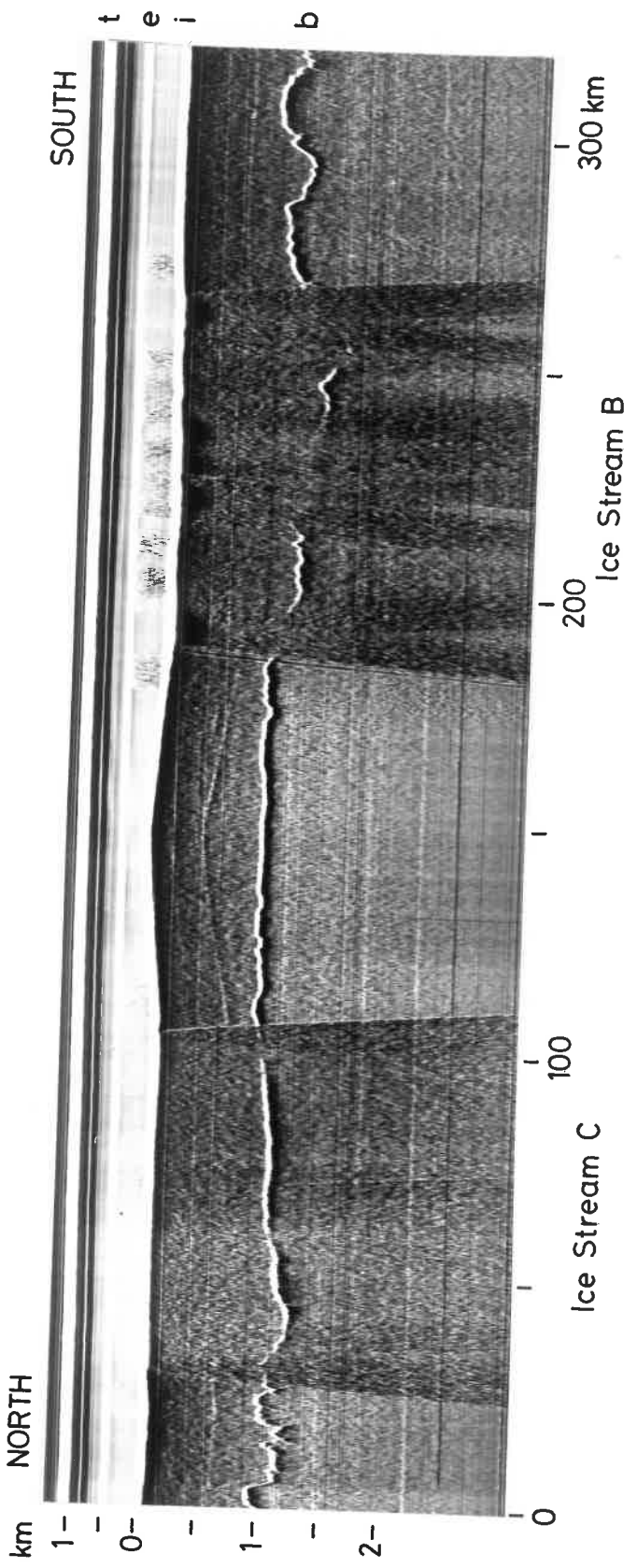


Fig. 3.5 RES profile across ice streams C and B illustrating hyperbolic echoes from surface crevassing. (t=transmitter pulse, e=end of suppression, i=ice surface, b=bedrock) (After Rose, 1979)

The Foundation Ice Stream, running along the west side of the Pensacola Mountains, is already known in general (Hughes,1977) but additional detail from RES shows it to be a major feature of West Antarctic drainage. In its upper reaches the Foundation Ice Stream branches into two around the Patuxent Range of the Pensacola Mountains. The two branches are referred to as the Patuxent Ice Stream and the Academy Glacier. The Foundation Ice Strea (and the Academy Glacier) is associated with a deep (>-1250m asl) narrow bedrock trough (see fig. 2.8). A similar trough runs along the eastern side of the Pensacola Mountains and underlies another major ice stream (not depicted on fig. 2.7 due to insufficient data), the Support Force Glacier. These two deep troughs running along two sides of the Pensacola Mountains are unlikely to be the result of glacial erosion alone and must be tectonically controlled (see fig. 3.6).

About 250km to the NW of the Foundation Ice Stream another ice stream (unamed) is less well pronounced, its boundaries lack strong definition but are nevertheless displayed on RES records and were observed from the air. The ice stream extends inland for only two hundred kilometres. The area between this ice stream and the Foundation Ice Stream forms a peninsula and remains one of the least known margins of the Ronne-Filchner Ice Shelf.

The Thwaites and Pine Island Glaciers feed ice northwards into the Amundsen Sea but do not have large buttressing ice shelves and ice rises. They have been considered crucial to the stability of the West Antarctic sheet (Thomas et al,1979). During 1978-79 one flight was diverted from the grid network to obtain a longitudinal and transverse section of the Thwaites Glacier. Unlike the other major ice streams in West Antarctica the Thwaites Glacier is not associated with any pronounced bedrock channel (see fig 3.7).

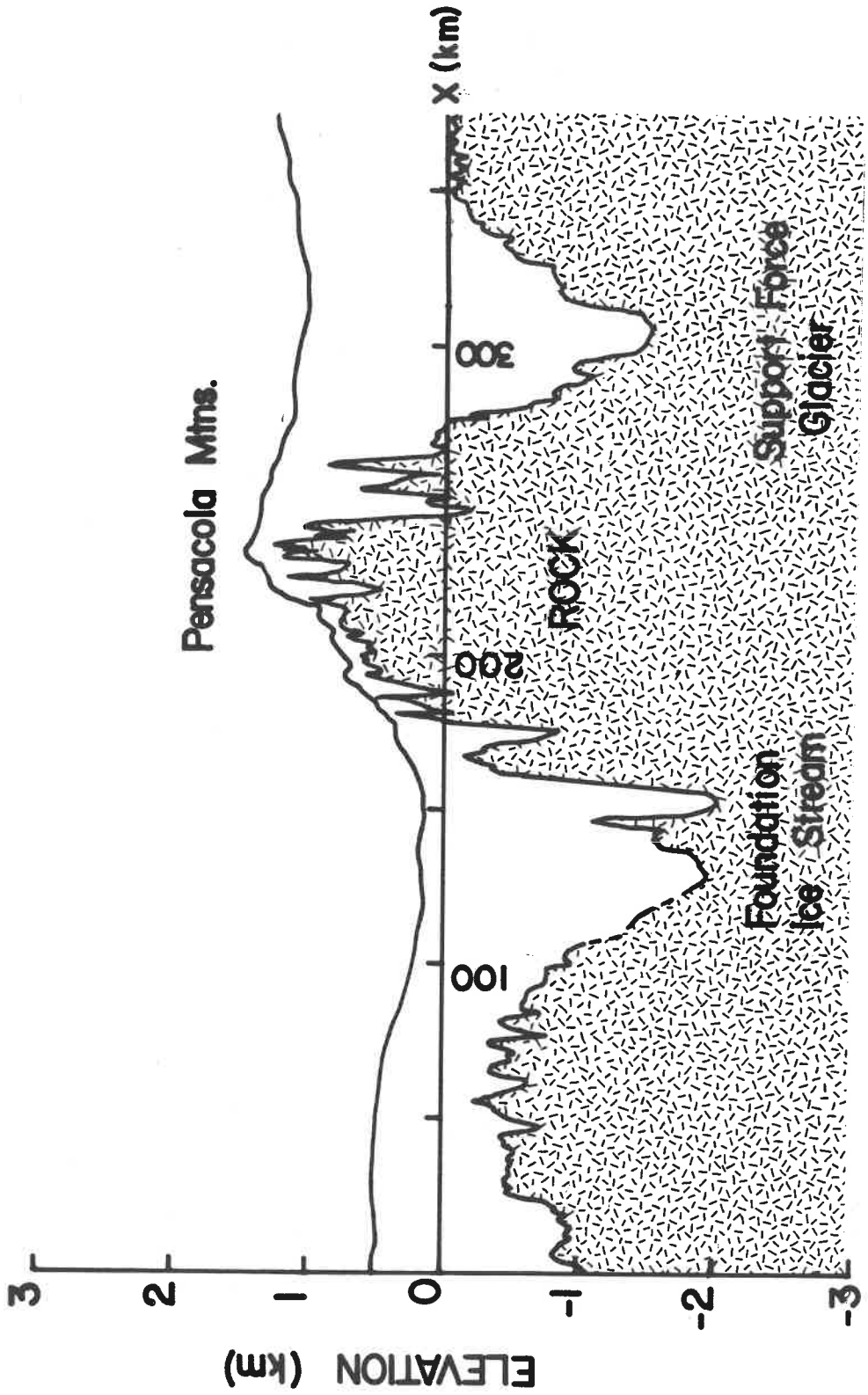


Fig. 3.6 Profile across Foundation Ice Stream and Support Force Glacier.

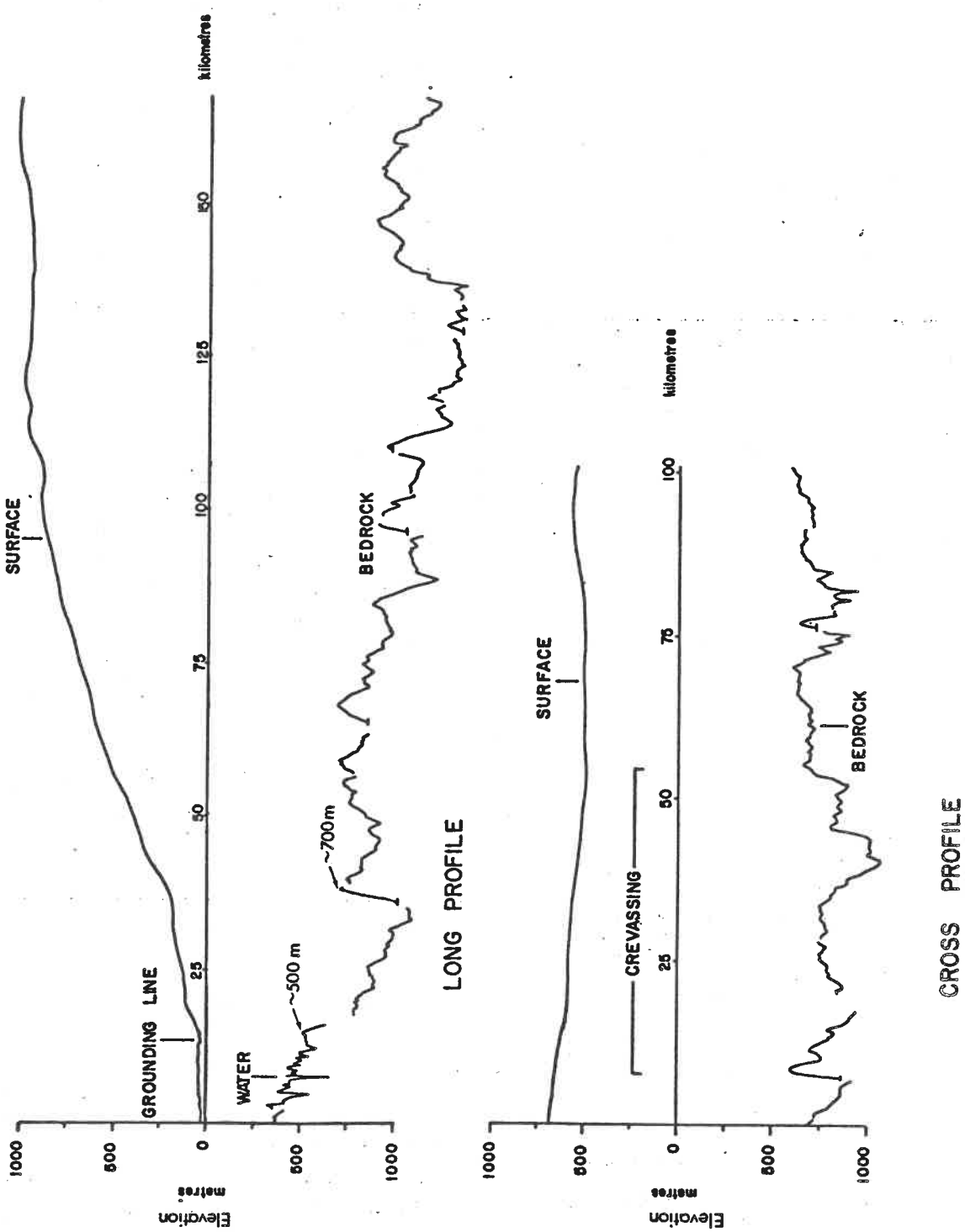


Fig. 3.7 Longitudinal and cross profiles of the Thwaites Glacier.

Thomas et al (1979) believe that unless these major northward flowing glaciers have high bedrock sills they may react more rapidly to climatic changes For completely unrestricted ice shelves Thomas et al (1979) estimate the critical depth below sea level of the bedrock sills to be 400-500m. Fig. 3.7 shows that the Thwaites Glacier has a sill at the grounding line around -500 m asl and a second further inland at about -700 m asl. Clearly further work on these glaciers is required before we will be able to assess whether Thwaites Glacier is in a precarious state of equilibrium or not. The lack of a prominent erosional channel, like the other ice streams of West Antarctica, suggests that the glacier may be a relatively young or a transient phenomenon.

3.4 GROUNDING LINE OF THE RONNE-FILCHNER ICE SHELF

Up to 80°S the grounding line on the Ronne-Filchner Ice Shelf has been determined with reasonable accuracy (Swithinbank et al, 1978; Crabtree and Doake, 1980) using LANDSAT satellite imagery. The area of the grounding line below 80° lying between the Ellsworth Mountains and the Foundation Ice Stream is largely unknown. Several flights during 1977-78 and 1978-79 crossed the grounding line in this area and provide data which greatly alter the previous grounding line position (fig. 3.8). Rose (1978) determined the position of the grounding line of the Ross Ice Shelf by locating the point at which the ice thickness and surface elevation ceased to fulfill the condition of hydrostatic equilibrium using the expression derived by Crary et al, (1962);

$$\text{elevation} = 0.108h + 15.6 \text{ m}$$

where h=thickness of ice

A similar method has been employed to locate the position of the grounding line of the Ronne-Filchner Ice Shelf in the absence of any data other than

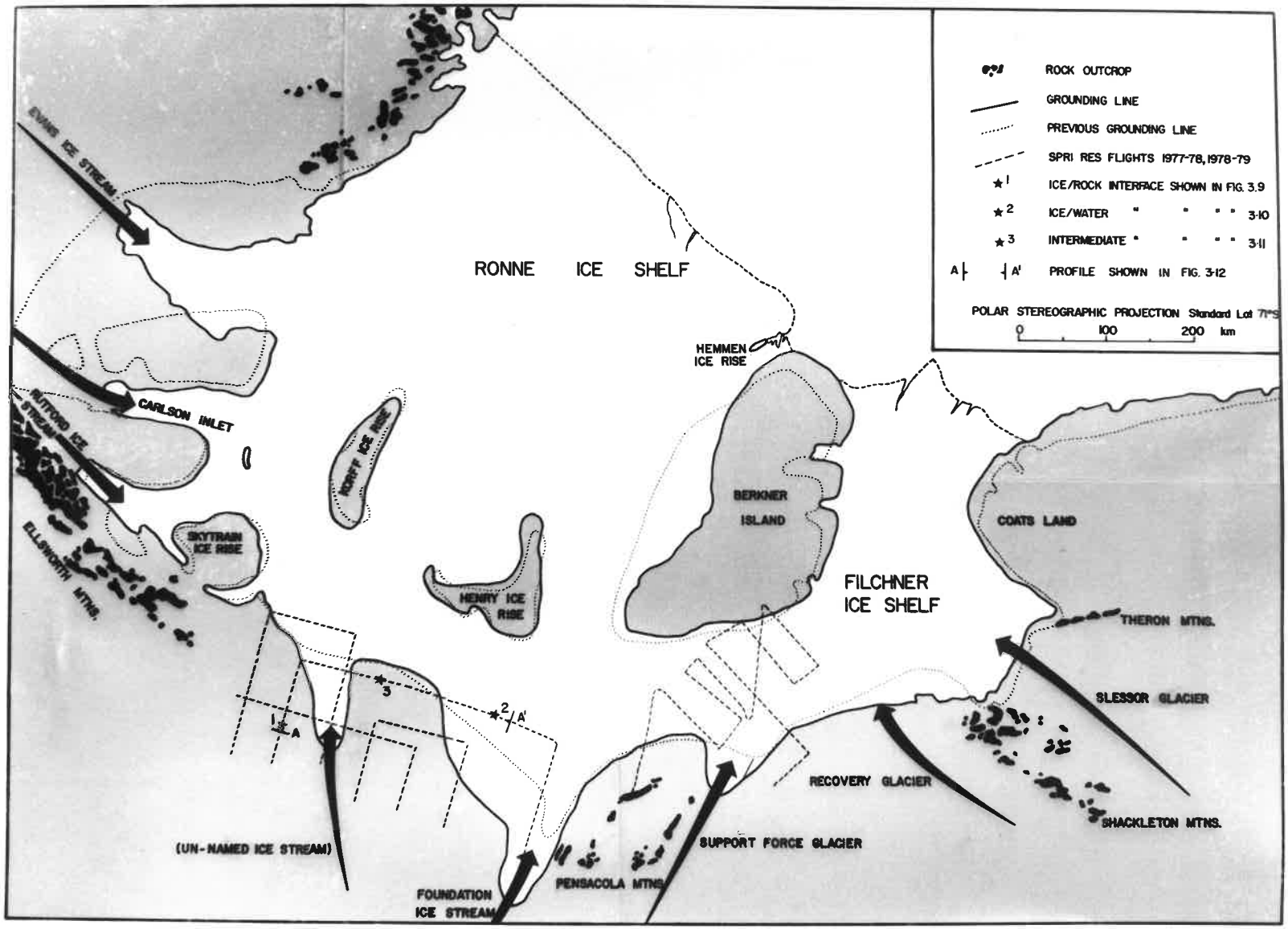


Fig. 3.8 Ronne- Filchner Ice Shelf.

RES. In addition to testing for hydrostatic equilibrium it is often possible to locate the grounding line from careful inspection of the reflections on the RES records. Ice/rock interface reflections typically exhibit rapid fluctuations in instantaneous returned power and appear as shown in fig. 3.9. In contrast ice/water interface reflections are usually characterised by high returned power with little variation over 10's of kilometres resulting in RES records as shown in fig. 3.10. The echo appears very strong and smooth on the 'z-scope' records. Quite often the base of the ice shelf is crevassed giving rise to strong hyperbolic echoes originating at or near the bottom of the ice.

The peninsula area between the Foundation Ice Stream and the ice stream to the NE gives rise to bottom reflections that are 'intermediate' in nature (see fig. 3.11). On 'z-scope' records the bottom return appears much as that of an ice/water interface except for a lack of bottom crevasses. The ESM, however clearly shows that although the returned power is high the nature of the reflecting surface is unlike that of a good ice/water interface. In addition surface elevations and ice thicknesses indicate that the area is well out of hydrostatic eqilibrium. The signs are clearly in favour of the ice being grounded but with water present at the base. A likely explanation of this would be if the ice were grounded on water-saturated sediments; a similar phenomenon to that observed by Soviet Glaciologists on the Lazarev Ice Shelf (Korotevich et al,1978). A study of Soviet 'Meteor' weather satellite photographs indicates that unlike other parts of the Ronne-Filchner Ice Shelf this area does not have a clear grounding line shadow. This lack of relief/reflectivity further suggests that this 'intermediate' area possesses a diffuse grounding line.

This intermediate area is well illustrated in profile A-A' in fig. 3.12 (see fig. 3.8 for location). At about CBD 1010 on fig. 3.12 the bottom return is characteristic of ice/rock interface. A band of surface crevassing occurs just after 1040 and again at 1080. The area between the

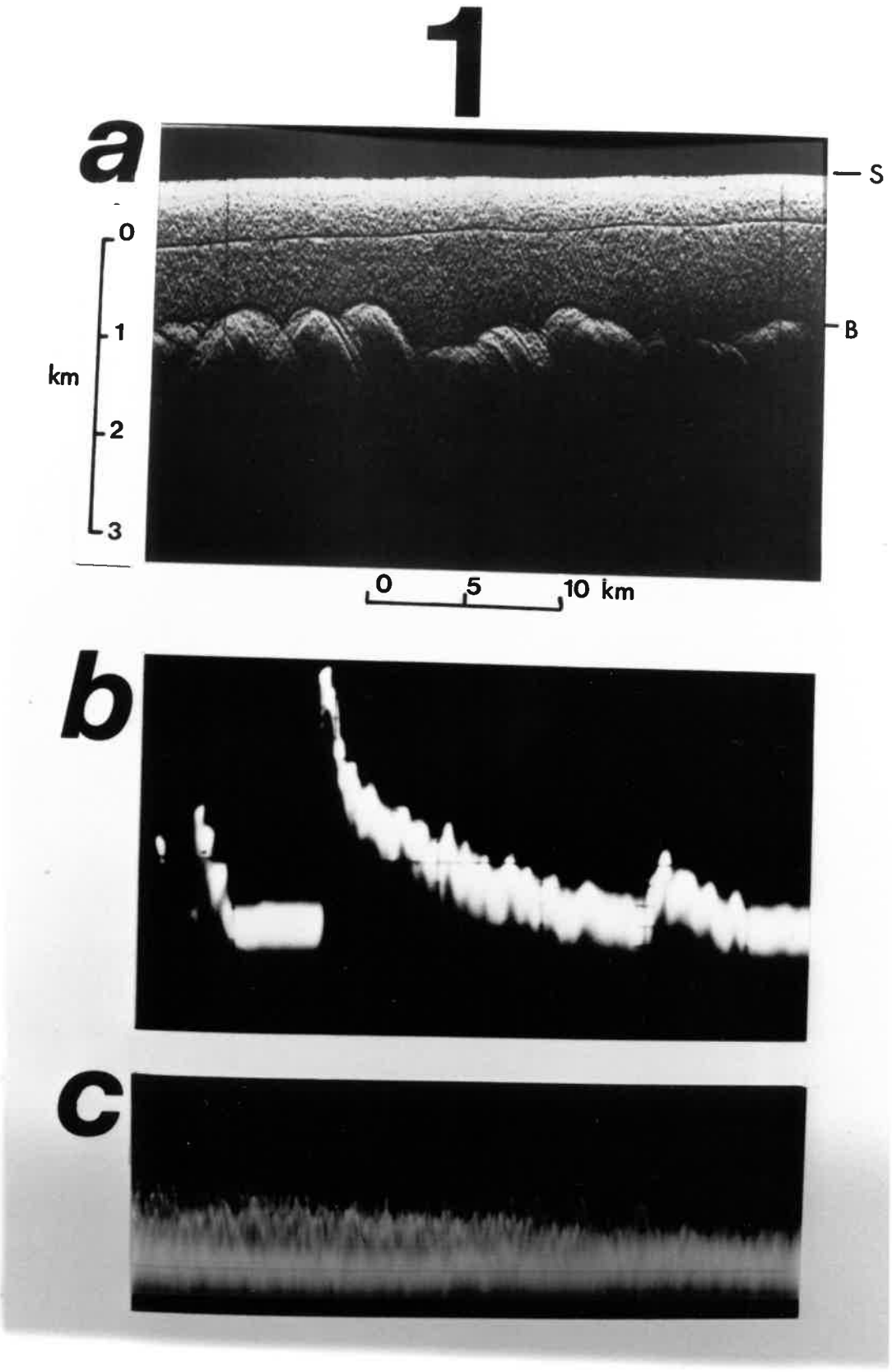


Fig. 3.9 Ice/rock interface. a)60 MHz 'Z-scope'
b)60 MHz 'A-scope'
c)ESM

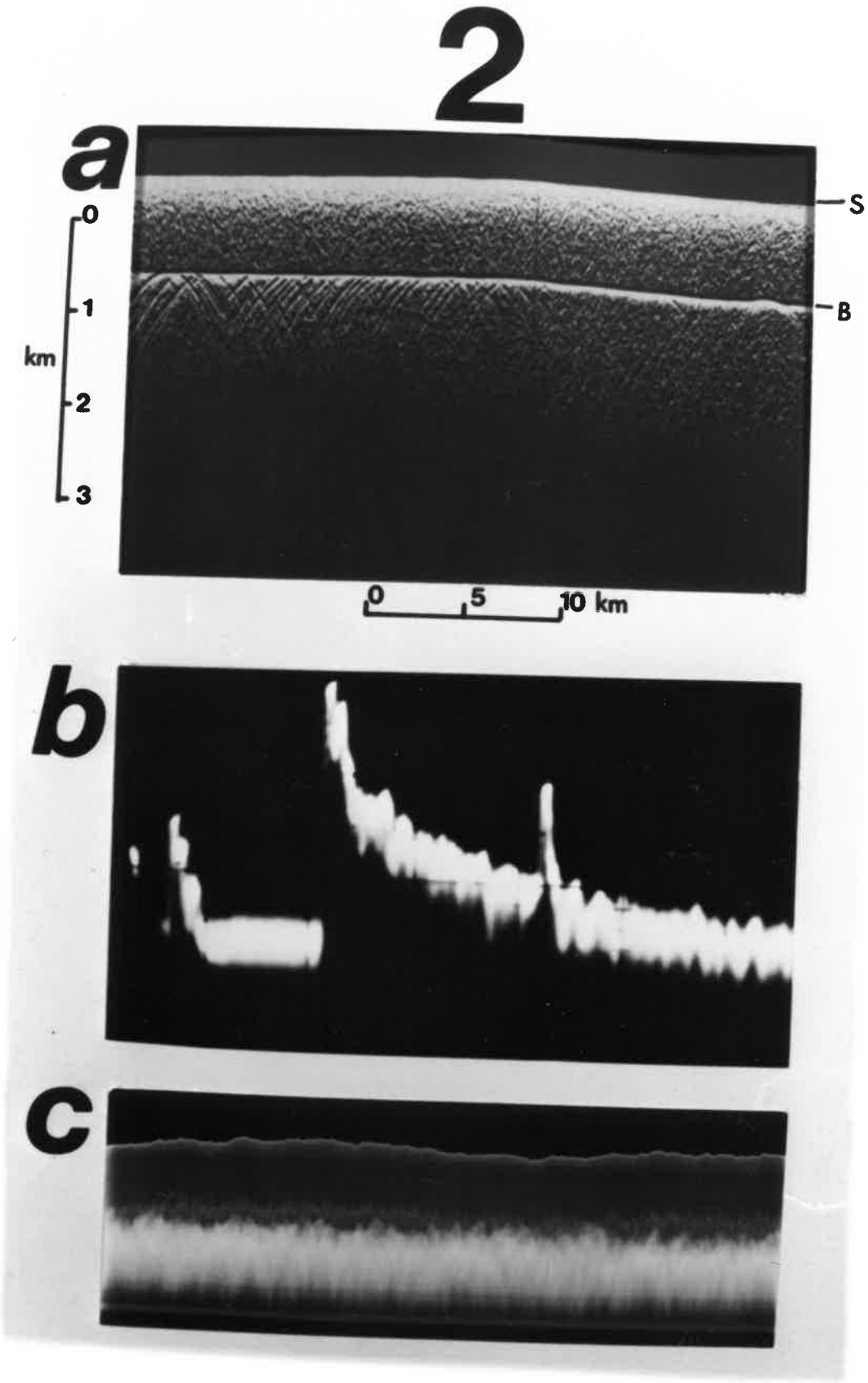


Fig. 3.10 Ice/water interface. a)60 MHz 'Z-scope'
b)60 MHz 'A-scope'
c)ESM

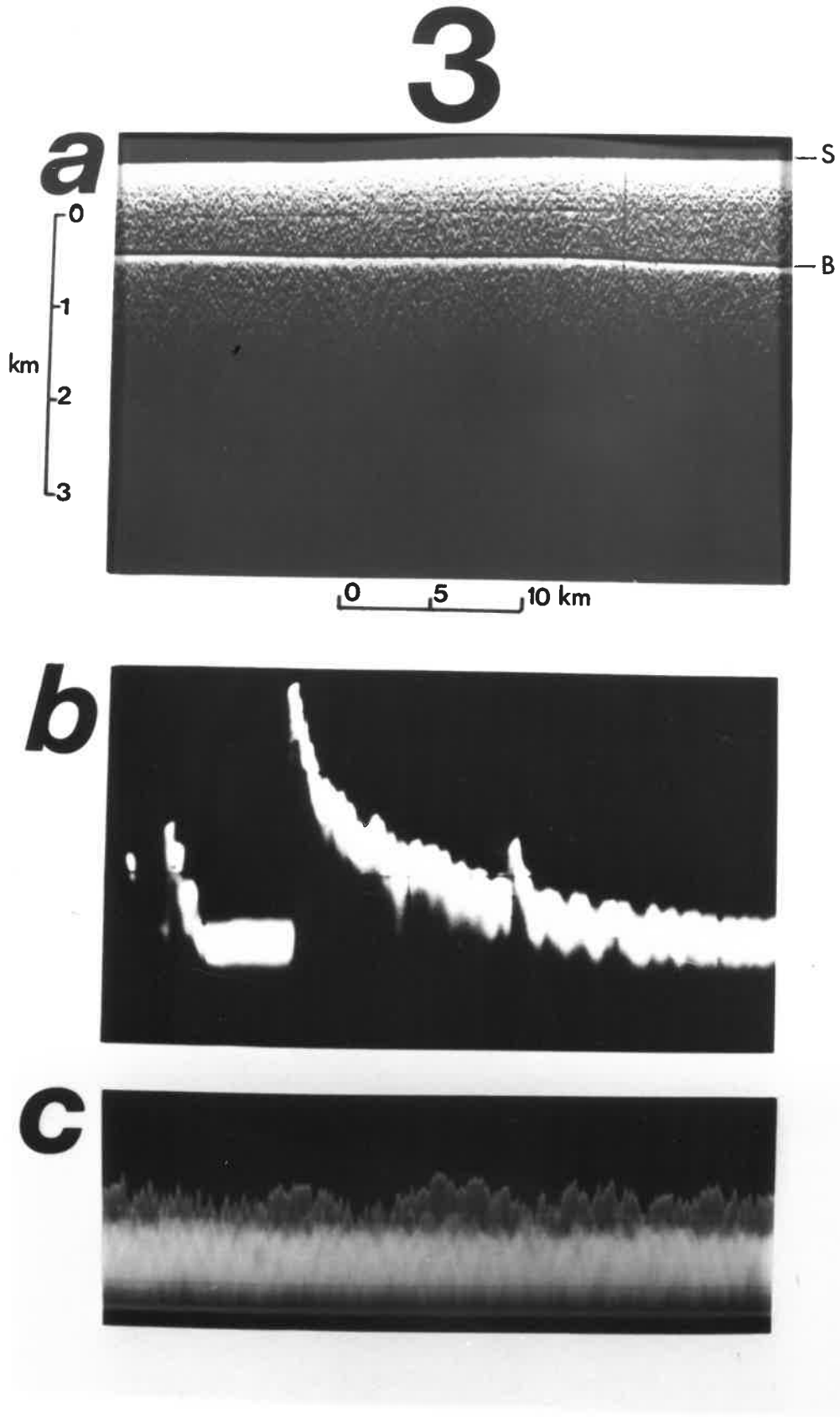


Fig. 3.11 'Intermediate' interface a)60 MHz 'Z-scope'
b)60 MHz 'A-scope'
c)ESM

two zones of crevassing belongs to the minor ice stream and has a strong bottom return with characteristic bottom crevasses at ~1070. The ice surface elevation/ice thickness relation indicates this area to be in hydrostatic eqilibrium. The grounding line can be seen clearly around 1040. After 1080 and until ~1140 the bottom return belongs to this 'intermediate' area. This area is well out of hydrostatic equilibrium. There is no apparent change in the bottom return in fig. 3.12 after 1140 except for the return of bottom crevasses again at ~1180. The ESM records and the hydrostatic test, however clearly indicate a move back onto floating ice shelf.

There are several possible mechanisms which could produce the phenomenon observed in the 'intermediate' area. The bedrock may have been uplifted either in response to isostatic adjustments following deglaciation, or in response to tectonic movements or possibly in response to increased sedimentation out of the ice shelf. On the other hand the ice shelf may have thickened until it grounded itself. This could have occurred as a result of greater accumulation, or increased discharge or more likely that strain rates decreased in response to grounding and pinning back of the flow further out in the ice shelf. A third possible mechanism could involve fall in sea level lowering the ice shelf until it touched the bottom. Of these possibilities perhaps isostatic uplift, lowering of sea level or confinement of flow are the most likely mechanisms with the truth possibly a combination of all these.

3.4.1 ISOSTATIC ADJUSTMENTS

The case for some isostatic adjustment in this area is quite strong. Orheim and Elverhoi (1981) report overconsolidated sediments from the continental edge in the Weddell Sea some 300-400 km from the present ice front, dated to <30 000 years BP. The sediments experienced ice loading

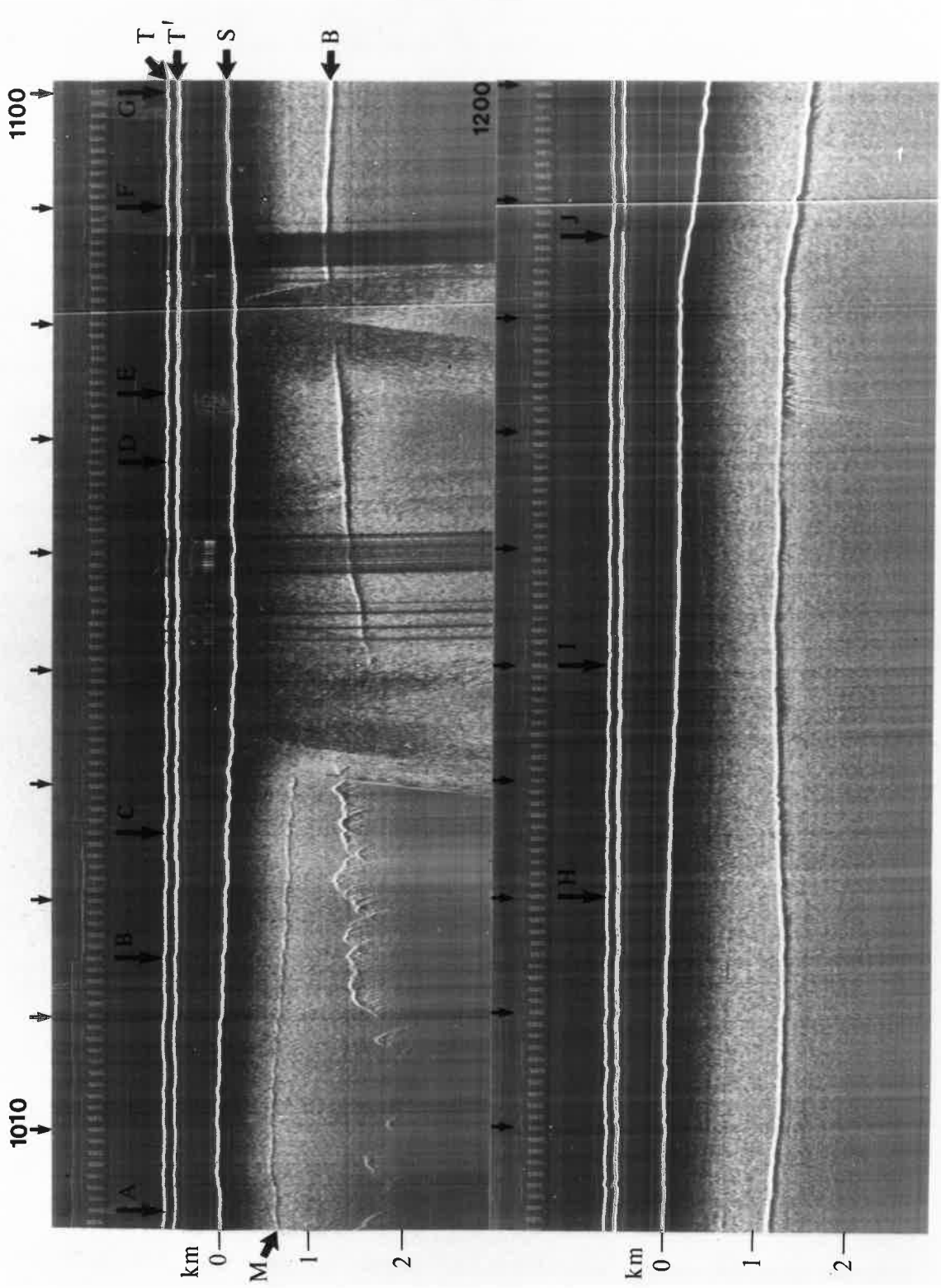


Fig. 3.12 RES profile across 'intermediate zone'

(see Fig. 3.8 for location)

and are evidence of a former advance of the ice sheet to the edge of the continental shelf during the Wisconsin. Former ice levels and the timing of deglaciation are difficult to assess. Moraine levels in the Dufek Massif and the Forrestal Range indicate a maximum of 400m for the greater thickness of the ice sheet (Boyer,1979). A conservative figure of 300m has been assumed for the area between the Ellsworth and Pensacola Mountains (Rutford et al,1980). Using these data deflection of the crust has been determined assuming uniform loading by a circular ice sheet (radius=300km) of uniform thickness 300m using equation (8) of Brotchie and Silvester (1969). Such an extra ice load would result in ~70m deflection of the crust (assuming the density of the mantle =3300 Kgm^{-3}, poissons' ratio =0.25 and lithospheric thickness = 110 km). Deglaciation probably commenced ~15000 years BP (Stuiver et al, 1981) but may have taken several thousand years before affecting the area of interest. Uplift has been assumed to be exponential with a relaxation time of 5000 years (Bott, 1971). Uplift still remaining at the present day is listed below for various times of deglaciation.

	Onset of deglaciation (ka BP)		
	15	10	5
Uplift Remaining (m)	4	9.5	25

Isostatic anomalies in West Antarctica indicate broad isostatic equilibrium at the present day (Bentley and Robertson,in press). The time of grounding and the age of this 'intermediate' zone is unknown but relatively recent isostatic uplift is certainly a viable mechanism for explaining the observed bottom reflections.

The effects of complete deglaciation and isostatic uplift will be discussed in the next chapter.

CHAPTER 4 BEDROCK IN WEST ANTARCTICA

4.1 INTRODUCTION

The map presented in Fig. 2.8 and in the back pocket is the first detailed and systematic study of bedrock in West Antarctica using RES (see Rose,1978; Jankowski and Drewry, 1981). Many features were known in general from previous maps based upon seismic soundings and interpretation of free air gravity anomalies (Heezen et al,1972; Korotkevich et al, 1977). Fig 2.8 is based on some 56000 RES determinations of bedrock elevation and ~250 seismic elevations.

The most striking feature of the map (and in particular the profiles) in comparison to previous work, however, is the considerable improvement in topographic detail. The subglacial topography is divided into several 'terrain units' which are here descibed in detail. The geological interpretation of the bedrock data, however will discussed in a later chapter.

The weight of the ice sheet in West Antarctica has considerable effect on the bedrock elevations depressing them well below their otherwise normal level. This problem is considered here and calculations are made to reconstruct West Antarctica allowing complete deglaciation and isostatic adjustment. The isostatically adjusted elevations are then compared with the present bedrock elevations.

4.2 SUBGLACIAL MORPHOLOGY

The area mapped can be divided into several parts (see fig. 4.1) some of which have been known in general from earlier work. Locations of profiles are shown in fig. 4.2.

1) At the head of the Ross Ice Shelf terrain is very smooth with subdued ridges and troughs marking the positions of the ice steams draining ice into the ice shelf. This area has been fully described by Rose (1978).

2) To the north-east, area (1) is terminated by an extensive subglacial basin (Byrd Subglacial Basin, see fig. 2.8). This large subglacial basin, reaching elevations below sea level of ~2500 m was known from previous work (Bentley and Ostenso, 1961). RES, however, allows much better delineation of the basin (compare fig 2.8 with fig. 1.15). Fig 2.8 shows the floor of the basin to be relatively smooth but this may be a function of the lack of data across the centre of the basin. The large thickness of warm ice over the Byrd Subglacial Basin is a major contributing factor to the poor RES results obtained in this area. A series of subglacial basins continue from the main part of the Byrd Subglacial Basin south, towards the front of the Transantarctic Mountains and terminate abruptly.

3) A completely new feature is the sinuous ridge running across the centre of the Byrd Subglacial Basin. This feature was not described on previous maps (Heezen et al,1972). The ridge is prominent on RES records, especially near Byrd Station standing ~1000 m above the floor of the basin (see fig. 4.3).

4) At the northern margin of the basin Cenozoic volcanic rocks crop out in the Crary Mountains, Executive Committee Range etc. RES records

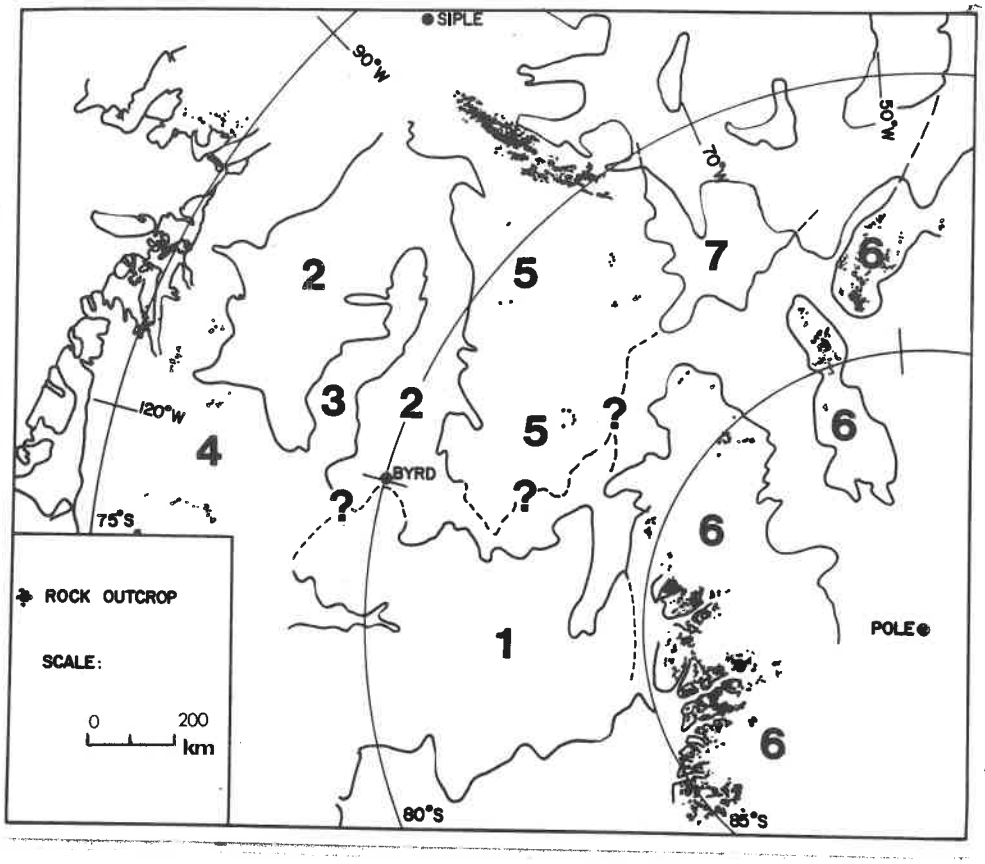


Fig. 4.1 Terrain Units

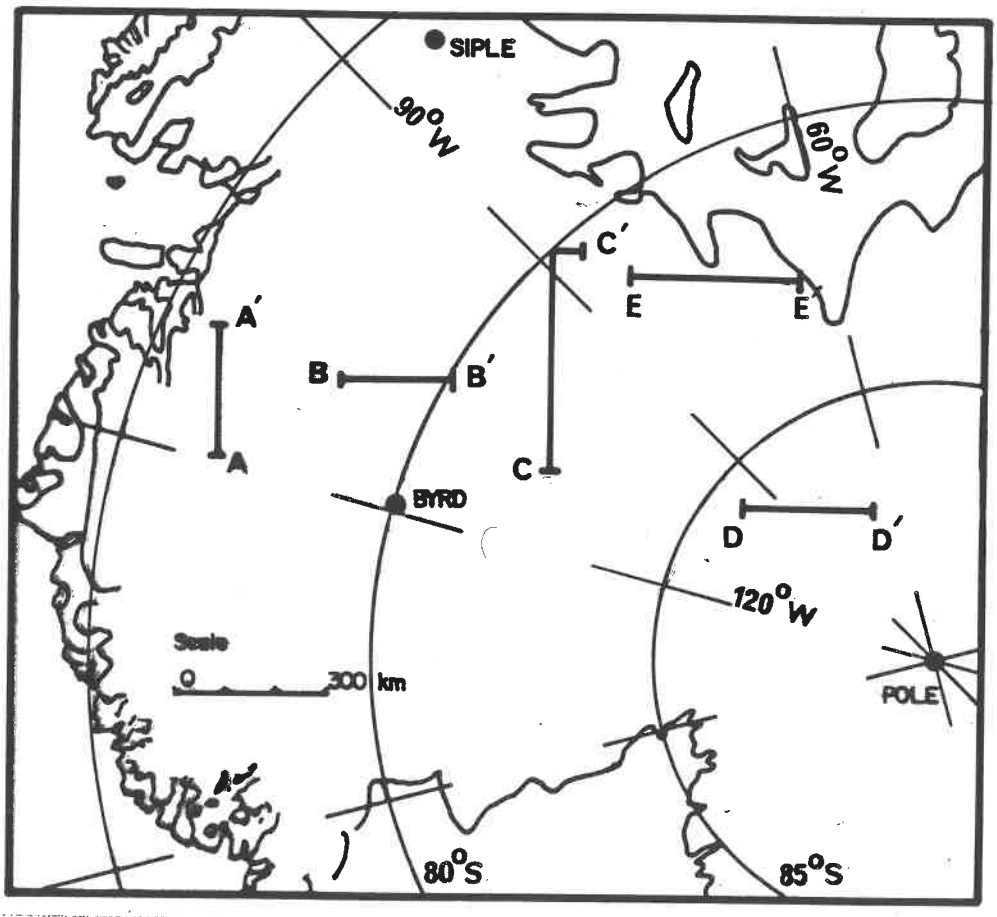


Fig. 4.2 Location of Bedrock Profiles

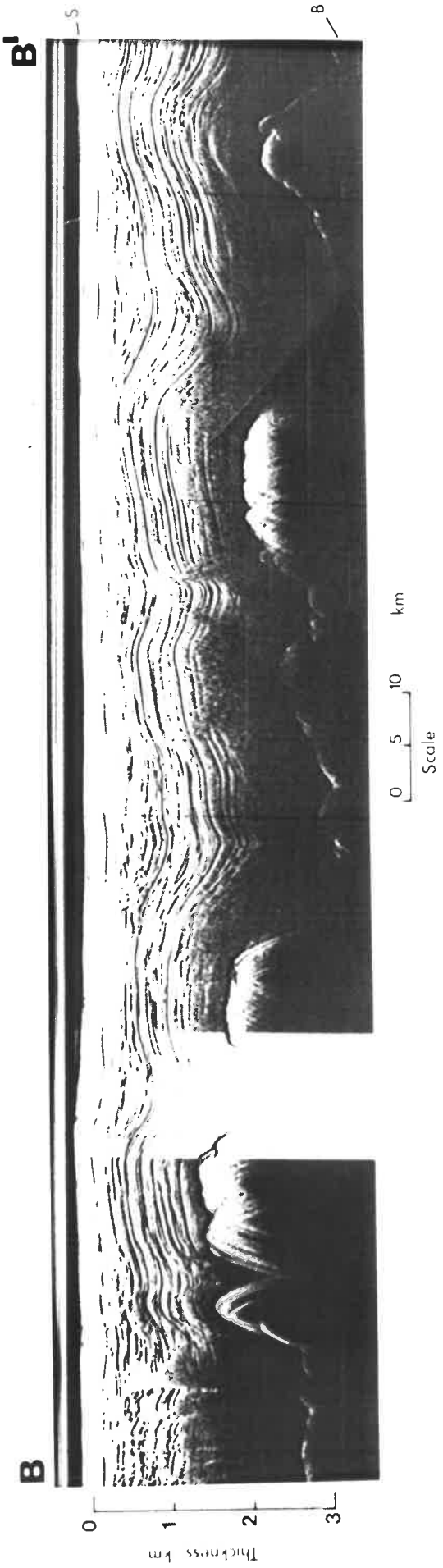


Fig. 4.3 RES Profile across Ridge in Byrd Subglacial Basin.

show these areas to be steep sided and separated by deep narrow troughs, ~50 km wide and with elevations below -1000 m asl (see fig.4.4). Such troughs exist between the Crary Mountains and Toney Mountain and Toney Mountain and Mount Takahe. Bentley and Chang (1971) show a narrow trough between the Crary Mountains and Toney Mountain reaching elevations of 2000 m below sea level based on the interpretation of free air gravity anomalies. However, only seismically derived elevations from previous work have been considered as being sufficiently reliable to include in fig. 2.8. Consequently this trough is not as prominent as on previous maps.

5) A major highland area extends westwards from the exposed Ellsworth Mountains. Terrain is extremely rugged, possessing a relief amplitude of up to ~2 km, a feature not apparent in previous maps. The spacing of flight lines does not allow adequate resolution of this rugged terrain which is clearly apparent on the profiles and consequently this fact is not emphasised on fig. 2.8. An example of this rugged terrain can be seen in fig. 4.5. There is a well defined boundary between this highland area and the Byrd Subglacial basin. The Whitmore Mountains form a steep sided upstanding massif and although separated from the Ellsworth Mountains by a narrow trough probably belong to the same mountainous "terrain region". Similarly the scattered outcrops of the Nash,Pirrit,Martin and Hart Hills to the south of the Ellsworth Mountains appear to be part of the same area.

The Whitmore Mountains are connected to the Thiel Mountains by an area of extremely rugged terrain that is almost cut through by a narrow trough extending from the main subglacial basin to the west.

6) The Transantarctic Mountains constitute a separate highland area and form a semi-continuous chain of mountains across Antarctica. The edge of this area,in the vicinity of the Horlick Mountains is very marked with elevations changing rapidly over ~2000 m (see fig. 6.2). The

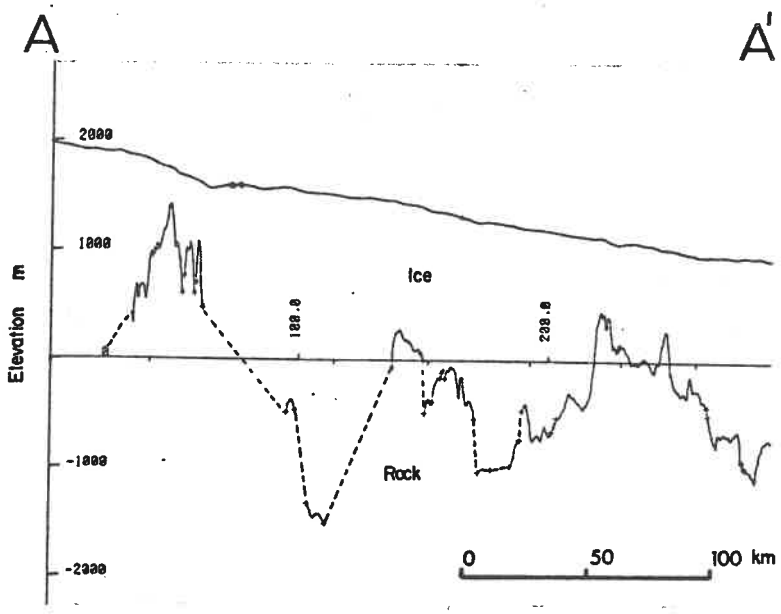


Fig. 4.4 Profile across Cenozoic volcanic outcrops in Marie Byrd Land.

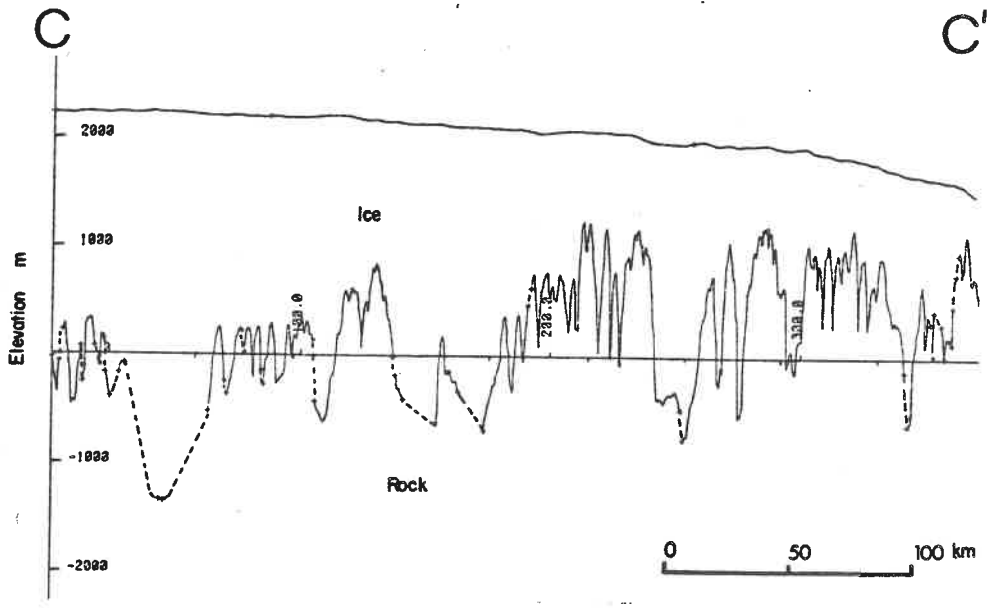


Fig. 4.5 Profile showing rugged topography in the Ellsworth Mtns. 'structural unit'

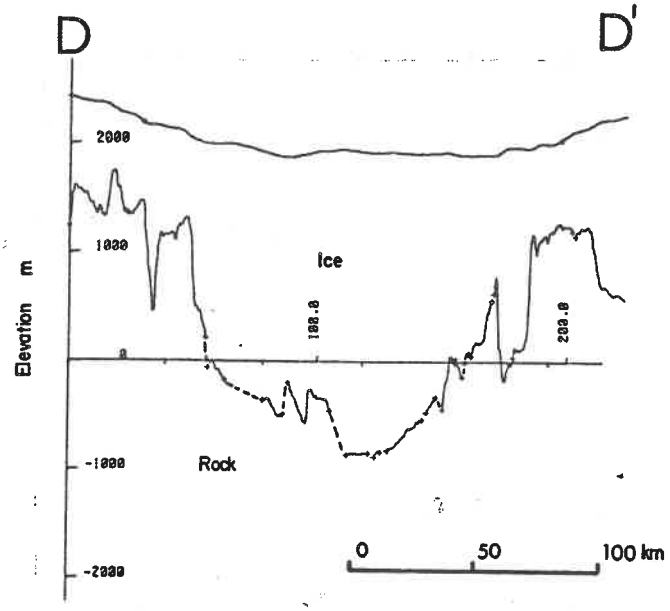


Fig. 4.6 Profile across trough between the Patuxent Range and the Thiel Mtns.

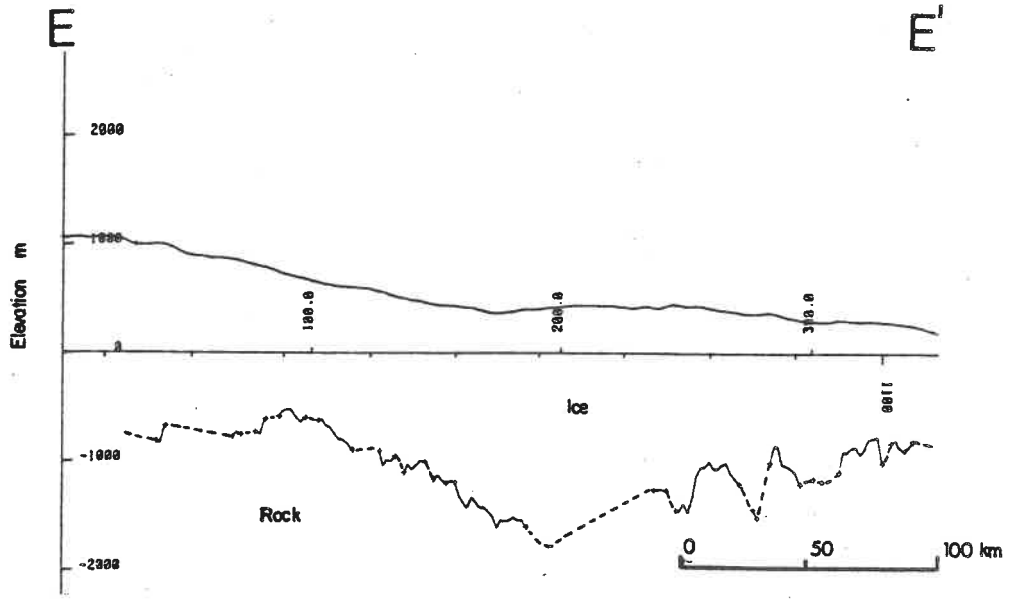


Fig. 4.7 Profile across bedrock low at head of Ronne-Filchner Ice Shelf.

Horlick Mountains themselves are almost severed from the rest of the Transantarctic Mountains by two deep valleys. The main part of the Pensacola Mountains is bounded on two sides by narrow troughs that are occupied by major ice streams, the Foundation Ice Stream and the Support Force Glacier (see fig. 3.6). The Foundation Ice Stream separates the main part of the Pensacola Mountains from the southern end of the mountains, the Patuxent Range. An area of rugged subglacial terrain can be seen extending several hundred kilometers south of the exposed Patuxent Range. This area is separated by a broad N-S trough from the rest of the Transantarctic Mountains (see fig. 4.6).

7) At the head of the Ronne-Filchner Ice Shelf between the Ellsworth Mountains and the Transantarctic Mountains the bedrock forms a deep subglacial depression that appears to widen out into the ice shelf (see fig. 4.7). This depression is known to continue up to Berkner Island along the ice shelf side of the Pensacola Mountains (Behrendt et al,1974).

4.3 ISOSTATIC DISPLACEMENT OF WEST ANTARCTICA

The idea of isostasy has been known since the 1740's when the French geophysicist, Bouguer noted that the horizontal attraction on a plumbline of the Andes Mountains was less than expected. There followed, in 1855, two explanations of this phenonenon. Pratt (1855) suggested that the crust was divided into vertical columns that have the same mass above a certain level known as the depth of compensation and that columns higher than sea level must have a lower density. Airy (1855), on the other hand, proposed that the uppermost layer of the earth is a low density 'crust' which overlies a higher density substratum. This low density 'crust' is of variable thickness and differences in elevation are accompanied by differences in thickness of this outer 'crust'. Isostasy is best described as the application of Archimedes' principle to the outermost layers of the

earth (Bott,1971).

It follows that any load on the crust must be balanced by an equivalent compensating mass deficiency beneath the surface feature if the crust is to be in equilibrium. In this study the earth is treated as a uniform, elastic, thin spherical shell enclosing a viscous liquid (ie. similar to the Airy hypothesis). If the crust were of zero stiffness then uplift due to removal of a load would be in proportion to the ratio of the density of ice to that of the mantle. This simple approach was adopted by earlier work in West Antarctica (Bentley and Ostenso,1961; Bentley,1964; Bentley and Chang,1971). This is a major over simplication and a model involving the flexural stiffness of the crust has been adopted in this study (Brotchie and Silvester,1969). The outer elastic shell is taken to be the lithosphere which encloses the viscous fluid asthenosphere. The boundary between the two is defined by a change in viscosity and lies well below the MOHO (McKenzie,1967). Walcott (1970) has given values for the thickness of continental lithosphere of 110 km and oceanic lithosphere of ~75 km. It has already been shown that the depth to MOHO in West Antarctica is ~10 km less than in East Antarctica (Adams,1972). The difference, if any, in lithospheric thickness between East and West Antarctica is unknown. A value intermediate between oceans and continents of 93 km may be more appropiate but the nature of the transi tion from East to West Antarctica is uncertain. For this study a value of 110 km has been used in the absence of any information on lithospheric thickness in West Antarctica.

The method adopted is similar to that of Rose (1978) and Steed (1980) but the application of the theory was completed independently and slightly more rigorously. The method is applicable if West Antarctica is considered to be in isostatic equilibrium. This assumption is supported by Bentley and Robertson (in press), who state that extensive regions of West Antarctica including the Byrd Subglacial Basin and the basin between the Ellsworth and Pensacola Mountains are not detectably out of isostatic

equilibrium.

4.3.1 THEORY

Brotchie and Silvester (1969) show that for a concentrated load the crustal deflection is equal to;

$$w(x) = \frac{P\ell^2}{2\pi D} \cdot \text{kei}(x) \qquad 4.1$$

where

$w(x)$ = deflection

x = r/ℓ

r = distance from centre

ℓ = radius of relative stiffness = $\left[\frac{D}{(ET/R^2) + \gamma_m}\right]^{\frac{1}{4}}$

D = flexural rigidity = $\frac{ET^3}{12(1-\nu^2)}$

E = Youngs' modulus

T = Thickness of lithosphere

R = radius of lithospheric shell

γ_m = density of mantle

ν = Poissons' ratio

kei(x) = Kelvin function of zero order

Equation 4.1 defines a bell shaped function as shown in Fig 4.8. The value of the radius of relative stiffness of the crust (for T=110 km, v=0.25, density of mantle=3300 Kgm^{-3}, E=8.35 x 10^{10} Nm^{-2} and R=6244 km) is equal to 130 km. Downward deflections can be seen to extend over a distance of 4

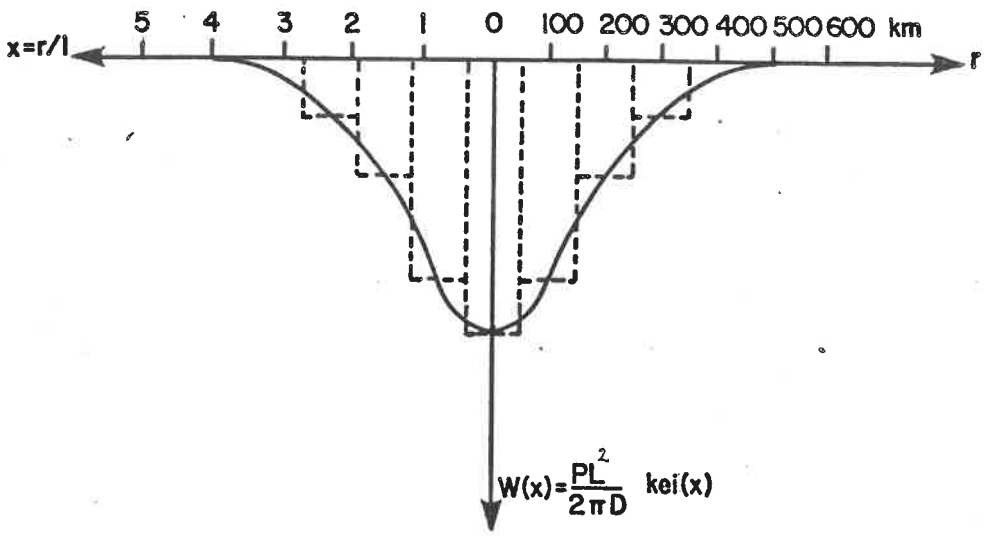


Fig. 4.8 Deformation Function W(x).

0·003	0·007	0·011	0·013	0·011	0·007	0·003
0·007	0·015	0·024	0·027	0·024	0·015	0·007
0·011	0·024	0·041	0·051	0·041	0·024	0·011
0·013	0·027	0·051	0·064	0·051	0·027	0·013
0·011	0·024	0·041	0·051	0·041	0·024	0·011
0·007	0·015	0·024	0·027	0·024	0·015	0·007
0·003	0·007	0·011	0·013	0·011	0·007	0·003

Table 4.1 Array of deformation coefficients.

times the radius of relative stiffness (ie. 520 km) from the centre of the load.

4.3.2 APPLICATION

An exact analytical approach to the problem is not possible due to imprecise knowledge of the dimensions of the ice sheet and also not practical because of the large amount of computational time required. A similar method to Steed (1980) has been used in which West Antarctica is considered as a series of blocks 100 km square which are free to move independently (see fig. 4.9). Using equation 4.1 the deflection due to a load of ice on a 100 km square is;

$$w(x)_{ice} = P_{ice} \cdot \frac{\ell^2}{2\pi D} \cdot \text{kei}(x) \qquad 4.2$$

where $P_{ice} = A.h_{ice} \cdot \rho_{ice} \cdot g$

A = area of block = 10^{10} m^2

h_{ice} = thickness of ice

ρ_{ice} = density of ice = 920 kgm^{-3}

g = acceleration due to gravity = 9.81 ms^{-2}

Each square will respond to the removal of ice by moving vertically so as to emplace asthenospheric material of the same weight. However, the response of each square will be affected by its neighbouring squares as defined by the deformation function. Removal of the world's ice would result in a eustatic sea level rise of ~65 m (Flint,1971) which after isostatic adjustment between the ocean basins and continents would reduce to ~45 m (Steed,1980). The ice burden on each square would therefore be replaced, in the first instance, by a water burden acting over the same

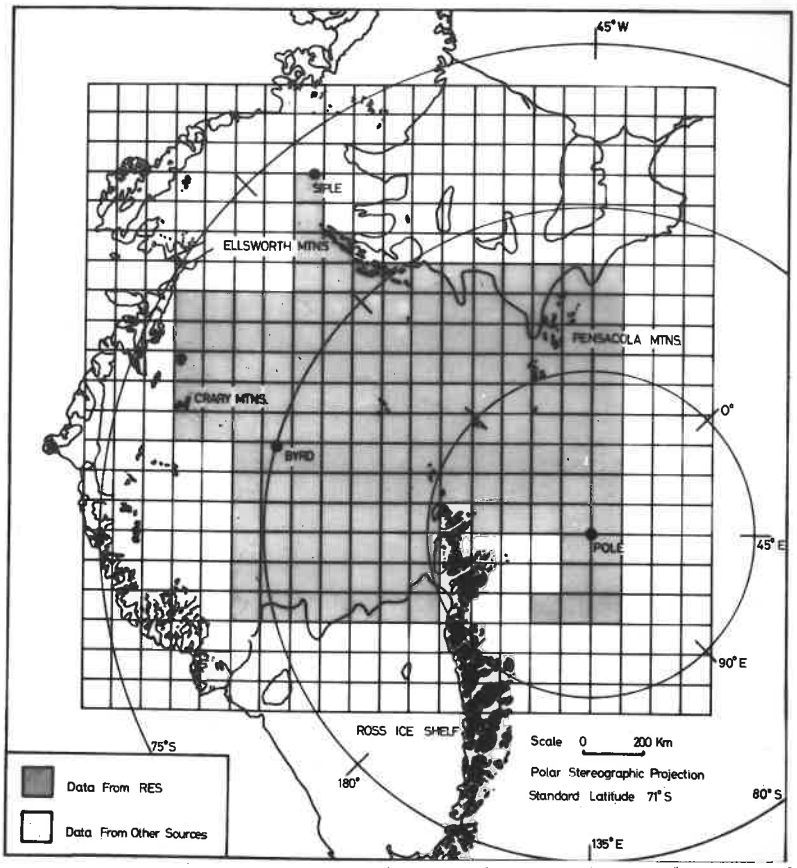


Fig. 4.9 100 km grid superimposed over West Antarctica for calculation of ice load.

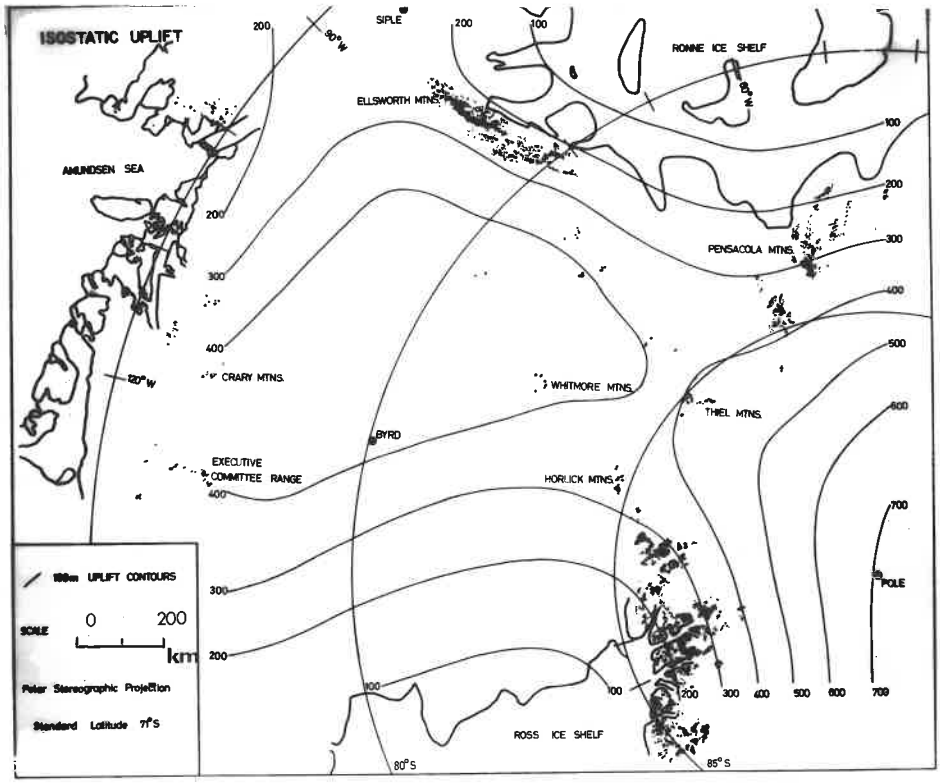


Fig. 4.11 Isostatic uplift in West Antarctica.

area. The deformation due to this water burden is;

$$W(x)_w = P_w \frac{\ell^2}{2\pi D} \cdot \cdot \cdot kei(x) \qquad 4.3$$

where $P_w = A \cdot h_w \cdot \rho_w \cdot g$

h_w = depth of water

ρ_w = density of sea water = 1030 kgm^{-3}

The initial uplift is obtained from a consideration of the change in load on each square. The uplift resulting from this change in load would then reduce the water burden acting on each square which in turn would cause a slight isostatic imbalance. Consequently the calculation is repeated until isostatic equilibrium is reached.

In order to apply the deformation function to the whole area it too was expressed in the form of a 100 km square array. Discrete values were obtained over an area of 700 km x 700 km by averaging the deformation function over each 100 km square. The function was not evaluated beyond the 700 km square as the contribution at the edges becomes insignificant. Coefficients of deformation were obtained from the function by considering the change in load experienced by each square;

$$W(x) = W(x)_{ice} - W(x)_w$$

$$= (\rho_{ice} h_{ice} - \rho_w h_w) \frac{\ell^2}{2\pi D} \cdot kei(x) \cdot A \cdot g \qquad 4.4$$

Table 4.1 gives the deformation coefficients , determined from equation 4.4, which represent the contribution of each square to the total uplift.

The displacement of each square in West Antarctica can then be evaluated using a computer by considering the change in load on all the 48 surrounding squares and multiplying each by the corresponding deformation coefficient. The resulting uplift of the central square is the sum of the contributions from all 49 squares in the array.

The calculation of ice and water loads within each square was performed by computer. The mean surface elevation, mean bedrock elevation and its standard deviation were calculated for each square and the distribution of bedrock elevations was assumed to conform to a normal distribution. This is supported by fig. 4.10a which shows the distribution of all bedrock elevations used. A statistical Chi^2 test revealed a better than 95% confidence level. The calculation of water burden is less direct and a similar method to Steed (1980) was adopted. The squares for which RES data and traverse data were available are shown shaded in fig. 4.9. For the remaining squares values for the ice load had to be estimated from other sources. Many squares actually lie over floating ice and therefore have no ice burden on them. The others were either extrapolated or interpolated from neighbouring squares containing data. For several, however, values were estimated from topographic maps. Many of these areas were mountainous with a comparatively small ice load. Most of the squares without data fortunately lie on the periphery of the area of interest. The squares in the southern Transantarctic Mountains occur inside the inner area of interest and were carefully examined on large scale topographic maps. Each 100 km square in question was overlain on 1:250 000 USGS reconnaissance maps of the Transantarctic Mountains and then divided into 64 smaller squares. The mean surface and bedrock elevation was estimated for each small square with the average of all 64 being used in the final calculation of uplift.

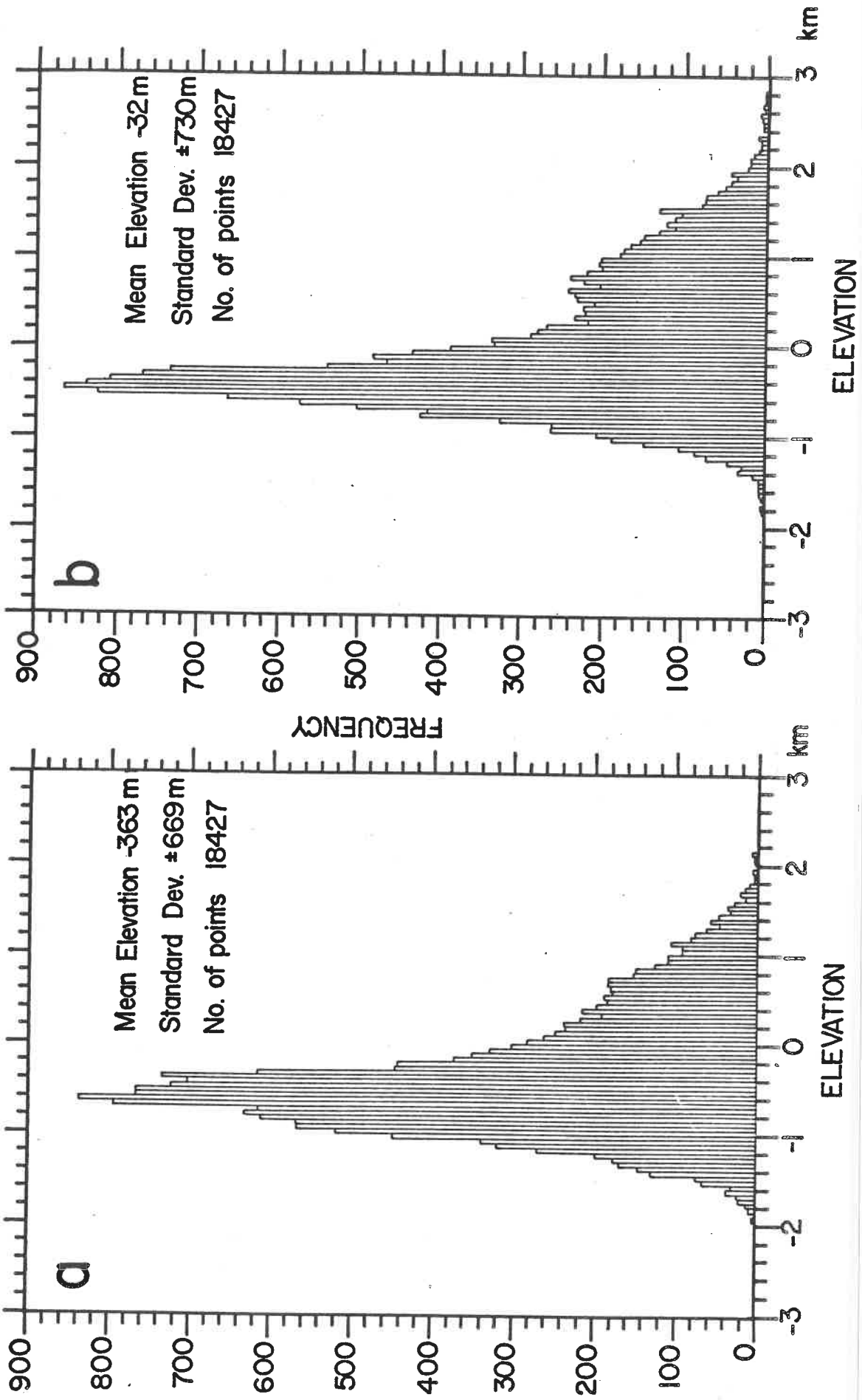


Fig. 4.10 Distribution of bedrock elevations in West Antarctica a)present b) after isostatic adjustment.

The amount of uplift as calculated in West Antarctica is shown in figs. 4.11 and 4.12. A surface was fitted to the calculated values of uplift for each 100 km square and a more closely spaced array of values of uplift produced. This new array of values was then applied to the bedrock elevations in West Antarctica and the data recontoured (see fig. 4.13). A contour interval of 500 m (cf. 250 m for bedrock map, see fig. 2.8) was chosen because of the limitations of the method used. The time constant invloved in the isostatic response is not of interest to this work and fig. 4.13 represents the final result of isostatic uplift. Although no account of glacial erosion is taken, fig. 4.13 is nevertheless a good, large-scale representation of the topography of West Antarctica prior to continental glaciation.

4.3.3 LIMITATIONS OF METHOD

The calculation of isostatic uplift by the method described is subject to several limitations:

1) The thickness of lithosphere has been assumed to be 110 km. There have been no direct measurements of lithospheric thickness made in Antarctica. The value of 110 km has been suggested by Walcott (1970) for continental crust in Canada. This value may be applicable for East Antarctica but may be in error for West Antarctica. The relationship between the MOHO and the lithosphere/asthenosphere boundary is also unclear. Those squares lying close to the continental edge on the Amundsen/Bellingshausen Sea coasts may also be in error due to the transistion from a continental to oceanic environment. The only alternative would be to assume a thickness somewhere between that of oceans and continents.

2) The method is limited by having to define a continuous function as a series of discrete values. An improved method might determine the

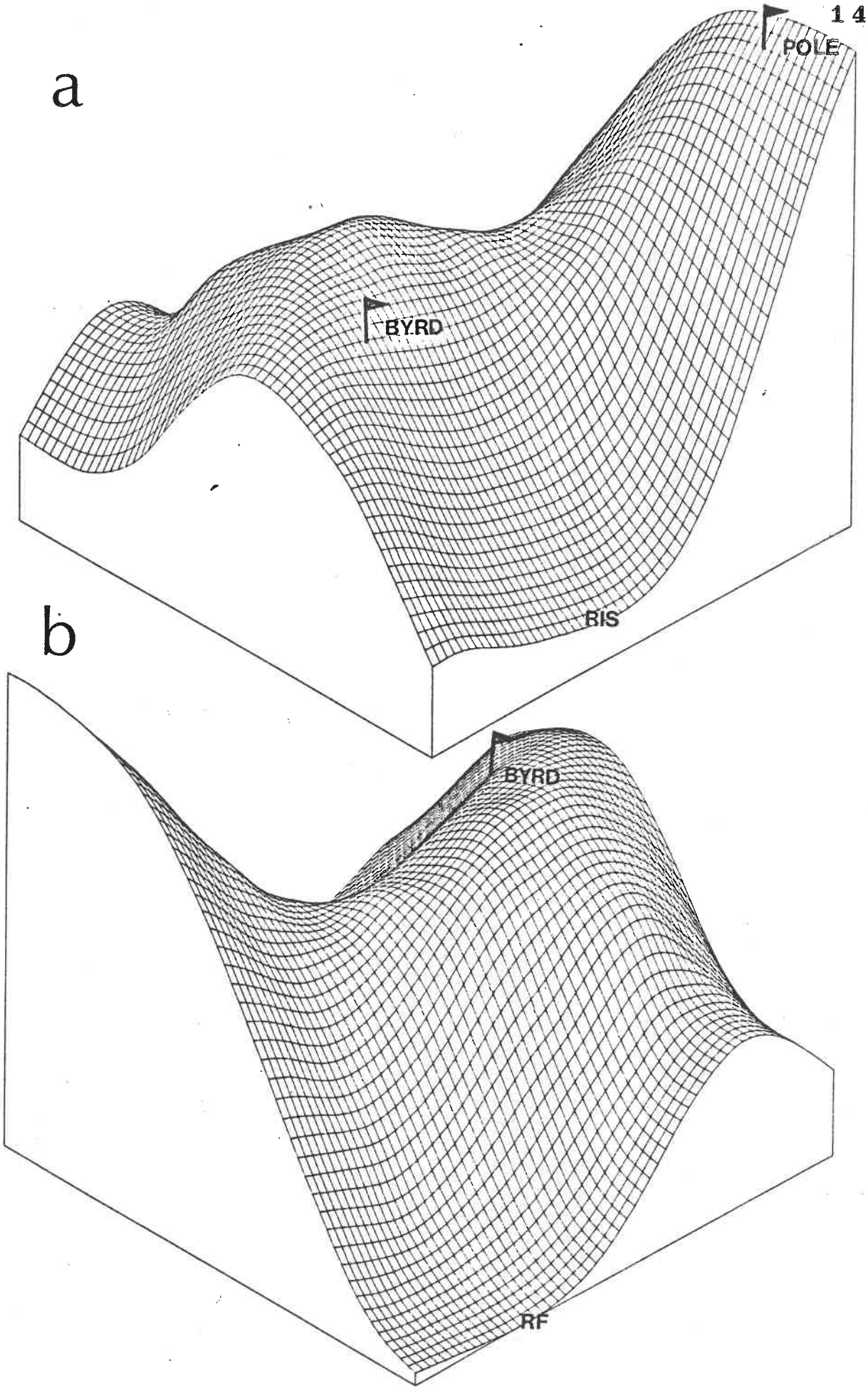


Fig. 4.12 3-D view of isostatic uplift in West Antarctica.
(RIS-Ross Ice Shelf, RF-Ronne-Filchner Ice Shelf).

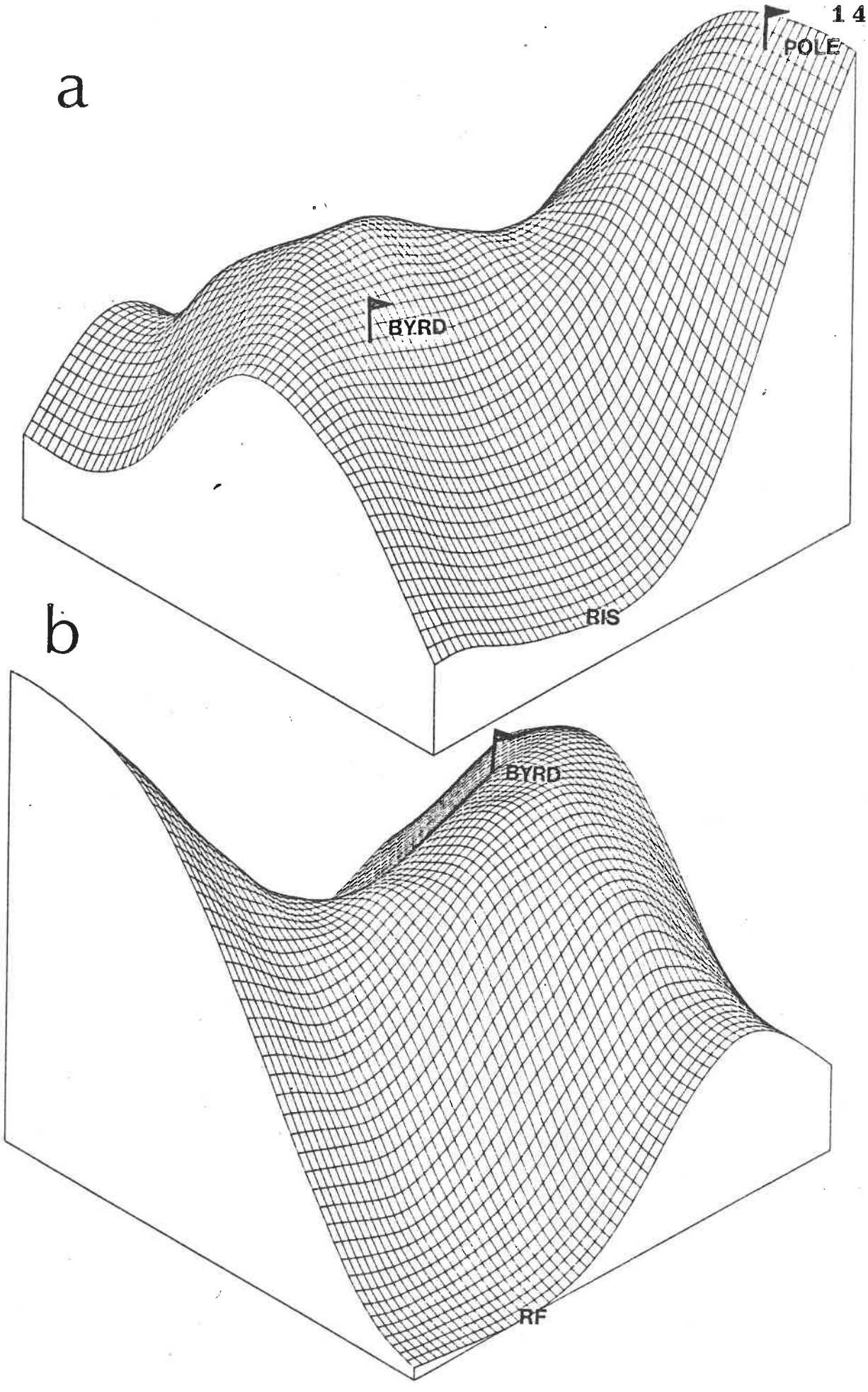


Fig. 4.12 3-D view of isostatic uplift in West Antarctica. (RIS-Ross Ice Shelf, RF-Ronne-Filchner Ice Shelf).

values for an array of smaller cell size, eg. 50 km. This would have involved, however, considerably more computation. As a compromise the value of the function was obtained by averaging several values over the area of each 100 km square.

3) Treating the crust as an array of 100 km square blocks that respond to loading as defined by the deformation function is also an oversimplication and associated with point (2). 100 km was thought to be adequate for the elemental cell size because it is less than the radius of relative stiffness (130 km) over which the displacment due to a point load is approximately linear (Brotchie and Silvester,1969). Reducing the cell size would have resulted in fewer points within each cell for calculation of the load. Rather than treat the problem as a collection of concentrated loads it might have been more applicable to consider the body as one and the problem as that of variable loading (Brotchie and Silvester,1969). As the exact dimensions of the ice sheet are unknown this prevents a more rigorous approach.

4) The statistical approximation for calculating the ice and water burdens may also be a limiting factor because although the distribution of bedrock elevations as a whole are close to a normal distribution individual squares may not conform as closely.

5) The assumption that West Antarctica is in isostatic equilibrium may not be entirely correct. Although Bentley and Robertson (in press) show that large areas of West Antarctica are in equilibrium 2 positive anomalies, one at the base of the Peninsula and the other on the NW flank of the Ellsworth Mountains, are taken to represent uncompensated crustal thinning. These two anomalies are fortunately on the edge of the area of main interest.

6) The load in many squares has had to be estimated by various methods as already described. Most of these squares lie around the periphery

of the area and consequently only affect the margins of the map. The results presented are taken only from the inner area of interest (see fig. 4.9).

4.3.4 DISCUSSION

The pattern of uplift in West Antarctica is shown in fig. 4.11 and 4.12. The effect of isostatic uplift on the distribution of bedrock elevations can be seen in fig. 4.10b. The mean elevation in West Antarctica has risen by ~330 m. As expected the amount of uplift decreases towards the continental ice sheet margin (ie. the Ronne Ice Shelf, Ross Ice Shelf and Amundsen Sea). Uplift increases to over 400 m in the centre of West Antarctica and corresponds to the deepest ice of the Byrd Subglacial Basin. The pattern of contours changes as the Transantarctic Mountains are approached where the contours are seen to swing around to parallel the mountains. Uplift increases steadily towards central East Antarctica reaching 700 m at the South Pole. Similar studies in Wilkes Land, East Antarctica, have shown that uplift is ~900-1000 m in the centre of East Antarctica (Steed, 1980).

A representation of bedrock topography in West Antarctica prior to glaciation is shown in fig. 4.13 and was compiled from the RES data and the same additional sources as fig. 2.8 (Bentley and Ostenso, 1961; Behrendt, 1964a; Robinson, 1964a; Bentley and Chang, 1971; Bentley, pers. commun.). Adjusted sea level is shown by a solid black line.

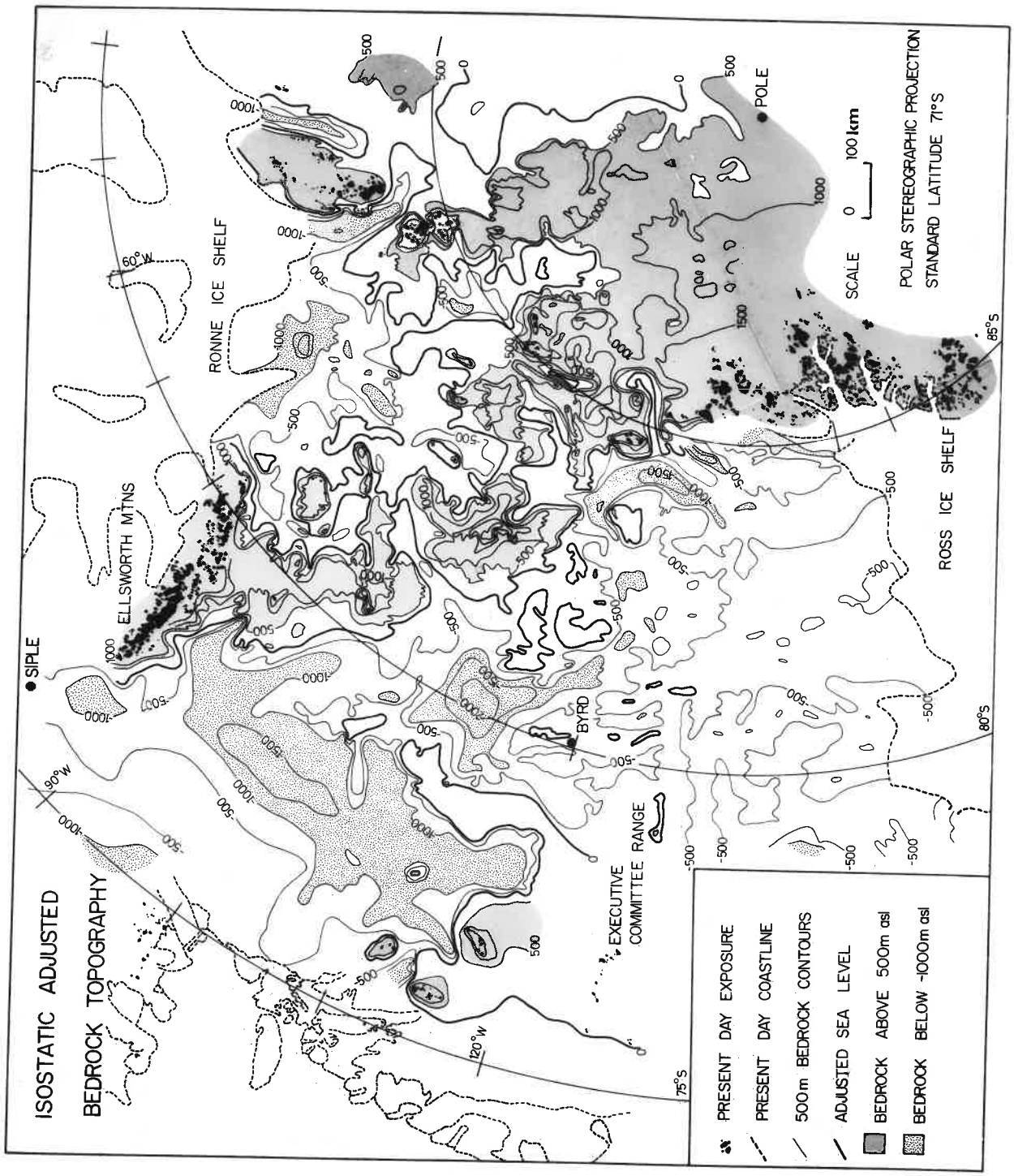


Fig. 4.13 Isostatic adjusted bedrock topography.

Although the area of present day exposure is small it is clear that large areas associated with these exposures would lie above sea level after isostatic uplift. A land bridge extends from the present day Ellsworth Mountains across the Whitmore Mountains and joins the main part of the Transantarctic Mountains in the vicinity of the Horlick Mountains. There is no major seaway between the Ross and Weddell Seas. Another major land area is formed by the volcanic outcrops of Marie Byrd Land. LeMasurier and Rex (in press) consider the bulk of the volcanics to post date the formation of the West Antarctic Ice Sheet. Consequently such areas should be ommitted from a preglacial reconstruction of West Antarctica. Marie Byrd Land is however a separate continental fragment in West Antarctica (Sharnberger and Scharon, 1972, in press) and so probably would still have formed an island in preglacial times, although of smaller dimensions than indicated in fig. 4.13. The sinuous ridge, prominent on fig. 2.8, nows forms a narrow peninsula of land extending eastwards from the volcanic area. This peninsula cuts across the Byrd Subglacial Basin, which still forms a very prominent feature, separating two of its deepest areas. Again this feature may have to be ommitted from the reconstruction if it is of a similar age and origin as the Marie Byrd Land Volcanics.

Apart from a few small, and possibly insignificant islands, a clear submarine connection exists between the Ross Sea and the Amundsen/Bellingshausen Seas. The area of low elevations to the east of Byrd Station is joined by a series of lows to a large trough lying along the front of the Horlick Mountains. This low is probably, in part, structurally related to large scale faulting along the front of the Horlick Mountains but must also reflect a certain amount of overdeepening by glacial erosion. Two smaller lows to the west are almost certainly the result of glacial erosion and reflect an earlier direction of ice flow since present day glacier flow out of the Transantarctic Mountains is at an angle to the trend of these lows (Drewry, 1978), which are probably fjords in origin.

The area at the head of the Ross Ice Shelf is very smooth and lies close to 500 m below adjusted sea level. This reflects recent sedimentation and probably masks continuation of the deeper parts of the Byrd Subglacial Basin (Rose, in press). At the head of the Ronne Ice Shelf elevations are well below adjusted sea level. The northern end of the Pensacola Mountains are bounded by two narrow troughs (as first indicated by fig. 2.8). These troughs have obviously been heavily eroded by major ice streams but may nevertheless still reflect some structural control. A major low extends southwards between the Patuxent Range of the Pensacola Mountains and the main part of the Transantarctic Mountains. The two deep valleys on fig. 2.8 that almost sever the Horlick Mountains from the rest of the Transantarctic Mountains are still visible.

The general impression of West Antarctica prior to glaciation is one of a series of islands and deep marine embayments. Extreme variations in elevation from 2000 m below adjusted sea level in the Byrd Basin to over 5000 m above adjusted sea level in the Ellsworth Mountains are observed. An area at the present day, exhibiting similar variations in elevation and with a similar distribution of land and sea areas is Japan and the Japan Sea. The Japan Sea represents a marginal basin developed as a result of extension between the Asian plate and the crustal fragment of Japan behind an active subduction zone (Wyllie, 1971). The possible tectonic environment in West Antarctica prior to continental glaciation will however be discussed in a later chapter.

CHAPTER 5 ANALYSIS OF MAGNETIC DATA

5.1 INTRODUCTION

The spacing of flight lines was generally seldom less than 50 km making an areal approach to the analysis of the data virtually impossible. As a consequence much emphasis has been placed on studying the magnetic data in profile form. A major improvement on previous aeromagnetic studies in West Antarctica (Behrendt and Wold, 1963) is the simultaneous recording of RES and magnetic data. This allows direct correlation of the magnetics with subglacial topography. Where magnetic basement is found to occur at the ice/rock interface anomalies can be modelled to obtain quantitative estimates of bedrock magnetisation using the RES profile as an upper limit to the models. The first part of this chapter outlines the theory behind the methods of analysis used in studying the profiles and the final part of the chapter briefly describes possible methods of obtaining a spatial pattern from the data. The computer programs used in this chapter were all developed by staff of the Branch of Regional Geophysics at the USGS in Denver and have been used with the kind permission of the authors, who are acknowledged at the appropiate points within the text. The author spent several weeks at the USGS learning methods of analysing aeromagnetic data. Each program has however been extensively modified in Cambridge to allow operation on the Cambridge IBM 370/165 and to accept a different data format. In all cases new plotting routines were written.

5.2 MAGNETIC PROFILE ANALYSIS

Magnetic data as described in chapter 2 were concatenated with reduced RES data to give profiles containing simultaneous magnetic and ice thickness measurements. All data were plotted by computer to allow visual

inspection. Behrendt and Wold (1963) selected short wavelength anomalies that were sufficiently symmetrical and undisturbed by neighbouring anomalies to permit calculations of depths to their sources. Using Peters' (1949) graphical half-slope method they obtained an estimate of maximum depth to magnetic basement on ~58 anomalies in West Antarctica. This method of analysis is extremely slow and in this analysis a rapid computer method for determining depth to magnetic basement has been used which allows a certain amount of interference between neighbouring anomalies (Werner, 1953; Hartman, Teskey and Friedberg, 1971; Jain, 1976); thus overcoming a constraint that limited the interpretations of Behrendt and Wold (1963).

The need to compare anomalies on different segments of a flight or anomalies on a completely different flight recorded at different orientations or altitude has necessitated the use of a computer program which can transform profiles permitting change in direction of magnetisation, direction of the regional field and height of the survey (Blakely, 1975). Selected portions of profile were then analysed using a linear least-squares inversion program (Cady, 1977) to obtain quantitative estimates of rock magnetisation.

5.2.1 SMOOTHING OF DATA

The data recorded in the field suffers from the problem of random high frequency noise (see fig. 5.1a). The exact cause of the noise was not ascertained. Possible sources were charge build-up due to flying through low cloud or operation of the de-ic ing circuits for aircraft engines. The noise must be removed before further analyses (ie. the depth determination) can be performed. High frequency anomalies resulting from random noise, for example, may mask completely the signal from deeper bodies (Jain, 1976).

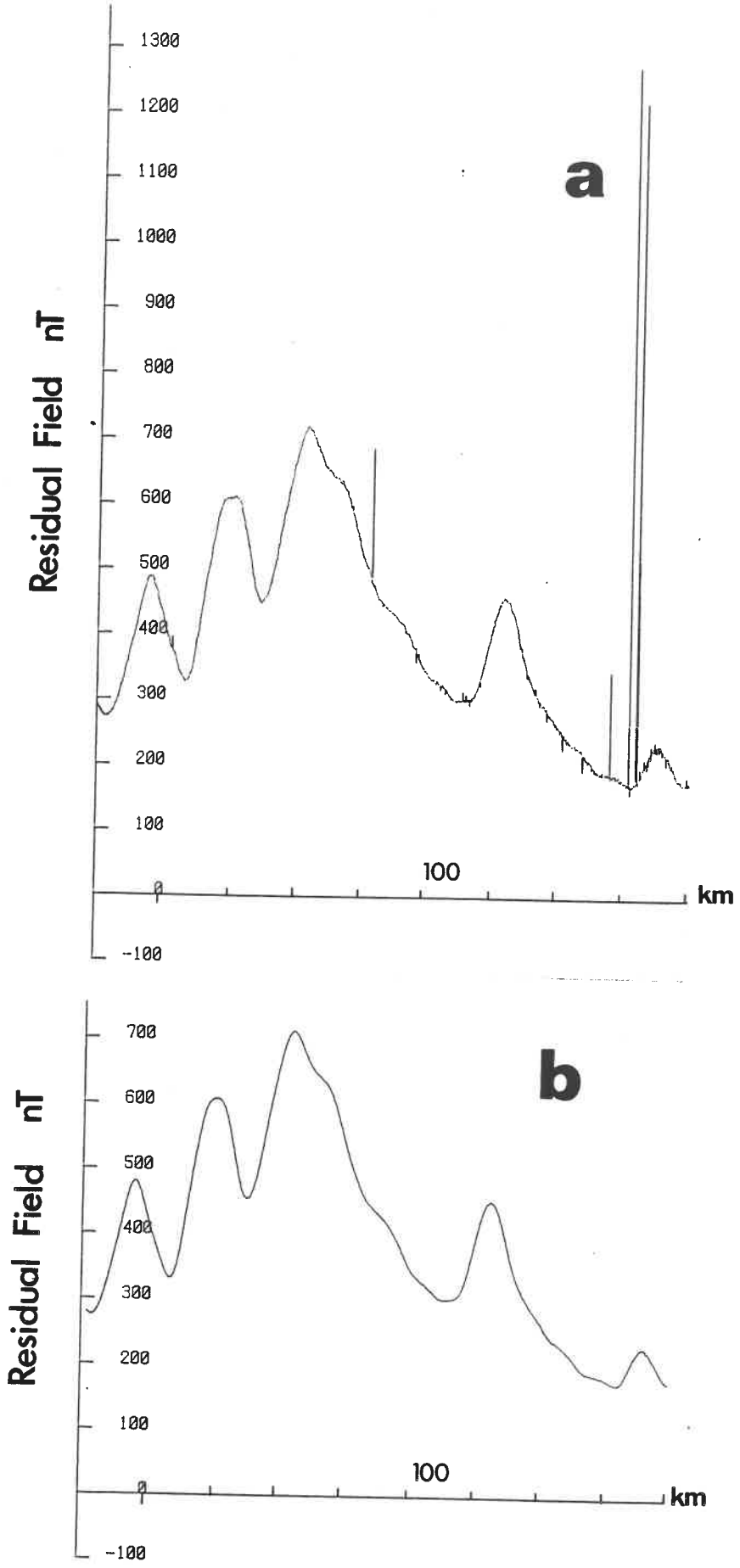


Fig. 5.1 Filtering of magnetic data a) raw data
b) smoothed data

The method adopted is straightforward. A first stage involved the use of a computer program to read through input data checking the slope between successive points. If the slope exceeded a predetermined value the point was rejected and the value replaced by one obtained by linear interpolation. This has the effect of removing large spikes. The data were then, in the second stage, run through a low band-pass filter consisting of a 7-point running mean. Determination of the Nyquist frequency is not possible since the input data are already the result of sampling of a continuous function. A cycle rate of 0.75 s for the magnetometer is however unlikely to produce aliasing of anomalies, nor is the effect of the filter. The result of these two smoothing stages are shown in fig 5.1b.

5.2.2 DEPTH TO MAGNETIC BASEMENT

The analysis is based on an idea proposed by Werner in 1953 which is described in Hartman, Teskey and Friedberg (1971). The method was adapted for computer analysis by Anderson and Cordell (1973). Their program was modified in Cambridge and new plotter routines added to display solutions on a RES profile. This allows quick comparison between the bedrock elevation and the elevation indicated by the program for magnetic basement.

The technique assumes that an observed magnetic field can be referred to a system of magnetically homogeneous fault- and dyke-like sources that trend in directions perpendicular to the profile for a distance many times greater than their depth. The magnetisation can be in any arbitrary direction so long as its direction and intensity are constant. The method is commonly referred to as Werner's Deconvolution method (Hartman et al, 1971). The measured field h(x,z) can be regarded as the two-dimensional convolution of the two-dimensional spatial 'impulse' response of a single hypothetical body f(x,z) with a geological distribution g(x,z), comprising

identical bodies with that spatial 'impulse' response.

$$h(x,z) = \iint_{-\infty}^{\infty} f(x - \alpha, z - \beta)\ g(\alpha,\beta)\ d\alpha d\beta$$

Given the recorded field h(x,z), with a knowledge of the source geometry, f(x,z), the determination of the geological source distribution g(x,z) is properly referred to as deconvolution.

Werner (1953) showed that for a simple dyke (thin sheet) with infinite strike length and depth extent the total field can be written in the form

$$f(x) = \frac{A(x - x_o) + Bz}{(x - x_o)^2 + z^2} \qquad 5.1$$

where x represents the distance along the profile, f(x) is the total field intensity at x, x_o is the horizontal distance along the traverse to the point immediately above the top of the dyke and z is the depth to the top of the dyke (see fig. 5.2). A and B are functions of the field strengh, susceptibility, dip, strike, magnetic inclination, and declination etc. Rearranging 5.1 and collecting terms yields

$$B_o + B_1 x + B_2 f(x) + B_3 xf(x) = x^2 f(x) \qquad 5.2$$

where $B_o = -Ax_o + Bz$

$B_1 = A$

$B_2 = -(x_o^2 + z_o^2)$

$B_3 = 2x_o$

Since there are four unknowns, 5.2 can be solved for B_o, B_1, B_2 and B_3 at four x-values and hence it is possible to obtain the values x_o and z, where

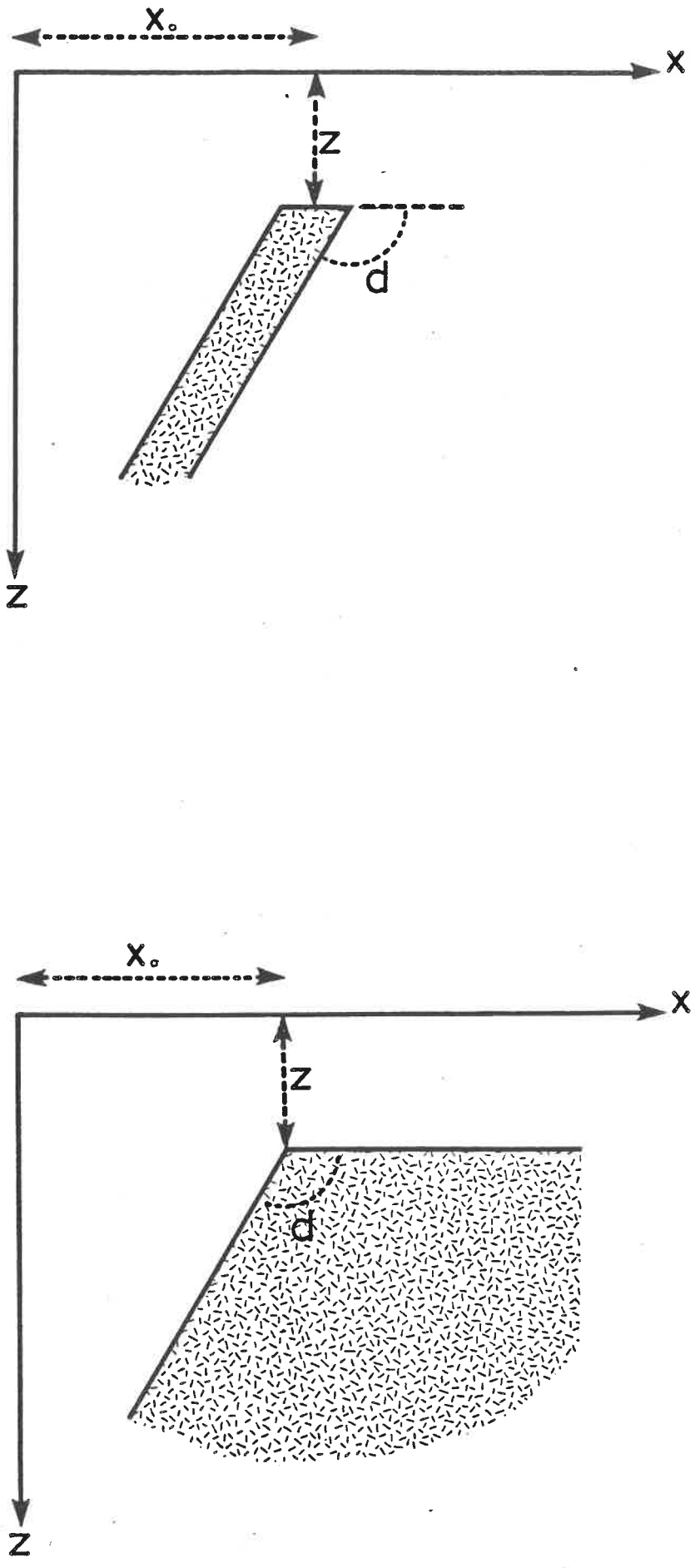


Fig. 5.2 Geometry of dyke-like and fault-like bodies.

$$x_o = \frac{B_3}{2} \quad \text{and} \quad z = \pm \frac{1}{2} \sqrt{-4B_2 - B_3^2}$$

Consider, now, the observed data function h(x) comprising the effect of a nearby target source plus interference from the superimposed effects of all other adjacent sources, and assume that the interference can be represented by a polynomial of order n. Thus

$$h(x) = f(x) + \sum_{k=o}^{n} a_k x^k \qquad 5.3$$

substituting for f(x) into 5.2 and collecting terms yields

$$x^2 h(x) = A_o + A_1 x + A_2 x^2 + A_3 x^3 + \ldots\ldots\ldots$$

$$\ldots\ldots\ldots A_{n+2} x^{n+2} + A_{n+3} h(x) + A_{n+4} x\, h(x) \qquad 5.4$$

where $A_o = B_o - a_o B_2$

$A_1 = B_1 - a_1 B_2 - a_o B_3$

$A_2 = a_o - a_1 B_3 - a_2 B_2$

.
.
.
.

$A_k = a_{k-2} - a_{k-1} B_3 - a_k B_k$ where $k = 3 \ldots\ldots n$

.
.
.
.

$A_{n+1} = a_{n+1} - a_n B_3$

$A_{n+2} = a_n$

$A_{n+3} = B_2$

$A_{n+4} = B_3$

Equation 5.4 is linear in A and the system can be solved for the A's given at least n+5 observations leading to solutions for x_o and z, where

$$x_o = \frac{A_{n+4}}{2} \quad \text{and} \quad z = \sqrt{-A_{n+3} - x_o^2}$$

In practice a first or second order polynomial for the interference is sufficient (Hartman et al, 1971), so that 6 or 7 points are required for solution of the system.

A dyke or thin sheet is actually two interfaces that are too close together for their anomalies to be separated. When, however, the width of the body exceeds the depth of burial the recognition of two interfaces becomes possible. Werner (1953) showed that the anomaly of a dyke has the same form as the horizontal derivative of the anomaly of an interface (fault-like body). Thus by performing Werner based deconvolution on both the total field and on the calculated horizontal derivative we are able to identify both dyke-like and fault-like bodies.

The computer program takes specified segments of a flight and first, as described in the previous section, removes high frequency noise with a low band pass filter. As input data is equally spaced in time (every 0.75 s) the program produces an array of data from the input that is equally spaced in distance using either linear or cubic spline interpolation methods. The degree of the interference polynomial can be varied but was usually set at n=2. The program then cycles through the data with a window of length n+5 where the spacing between points is again variable, but usually set to 1. For each position of the window n+5 equations like 5.4 are formed and then solved using Gauss' Elimination method. Each position of the window will give a solution for x_o and z, which, if within certain limits is plotted at the same scale on to a previously drawn RES profile.

The spacing between points is then incremented, usually by 1, and the data cycled through the new, wider window. This is repeated many times for larger and larger window sizes. This is necessary since the sensitivity of equation 5.4 for the detection of an anomalous geological source will be strongly related to the horizontal distance subtended by the window (Hartman et al, 1971). In other words, the broader a given anomaly the larger must be the dimension of the window required to recognise it. With wider window lengths aliasing of the anomalies can become a problem. Jain (1976) suggested filtering the data with a appropiate anti-alias filter for successive passes through the data. The effect of omitting this filtering process is to produce a 'noisey' looking plot of depth solutions. Typically the plot produced will comprise many isolated points, together with a few clusters of points. By inspection the centre of each cluster is accepted as being a relatively strong solution and the isolated points rejected (see fig. 5.5).

In the next stage of calculation the program takes the total field data and by Lagrange interpolation produces the horizontal derivative of the total field. The whole procedure is then repeated producing a new plot containing solutions for fault-like bodies (see fig. 5.6). Most of these will be found to coincide with solutions for dyke-like bodies. The correct solution is a matter of interpretation but the magnetic anomaly itself or the relative compactness of the two clusters may be diagnostic in some cases. Examples for theoretical data are given in a later section and the result of the analysis of the real data is given in Appendix 2.

The method described above has some obvious limitations. The technique assumes that the profile is normal to the strike of the bodies and that the bodies extend to large distances on either side of the profile. The extent of the bodies is not a difficult constraint to meet as the distance need only be a few times the depth to the source (Jain, 1976). The angle at which the profile crosses the body is a more severe constraint but oblique

trending bodies are admissible if their strike is known. Unfortunately the flights are too widely spaced in most areas to determine the strike of particular anomalies. A normal crossing would produce the narrowest anomaly and consequently the shallowest depth. In nature, however, most bodies are irregular and the effect of irregularities at oblique angles would be to magnify the distortion of the magnetic anomaly (Behrendt and Wold, 1963). Consequently the most symmetrical anomaly would result from the most nearly normal crossing. Small departures from normal crossing can be tolerated as the effect varies inversely as the cosine of the angle; a crossing 25^{o} to normal would give a calculated depth only 10% too great (Behrendt and Wold, 1963). Generally these errors tend to give anomaly sources that are too deep.

Hartman et al (1971) suggest that, ultimately, all geological structures can be considered to be a distribution of homogeneous bodies bounded by interfaces. Thus if a body or a contact or a slope change is even slightly two-dimensional it is susceptible to analysis by Werner based deconvolution (Hartman et al, 1971). The great advantage of the method is that the equations used permit solution even when only parts of an anomaly are available for study. Solutions can be obtained from any set of equally spaced points and those points do not need to be predetermined or be critical points such as inflection points, maxima or minima.

5.2.3 COMPUTER MODELLING

In areas where depth estimates indicated magnetic basement lies at the ice-rock interface, computer modelling methods were used to provide quantitative estimates of rock magnetisation. A computer program, written by Cady (1977) was used which performs, along a profile perpendicular to strike. for one or more bodies, both forward and inverse calculations for the gravity and magnetic anomaly fields and independent gravity and

magnetic inverse calculations for density and susceptibility or vector magnetisation. The program can perform two-dimensional calculations for infinitely long prismatic bodies using the equations of Talwani, Worzel and Landisman (1959) as well as applying end corrections for the 2 - dimensional case using the equations of Shuey and Pasquale (1973) and Cady (1980). Shuey and Pasquale (1973) coined the term '$2\frac{1}{2}$-dimensional' body to represent bodies invariant in cross-section but terminated at finite distance along strike. The '$2\frac{1}{2}$-dimensional' approach has the convenience and speed of the 2-dimensional approach but with much of the generality of the complete 3-dimensional approach of Talwani (1965).

The main steps in the derivation of the equations used will briefly be given.

In fig. 5.3a consider the semi-infinite prism KLMN, with magnetisation J, that extends to infinity along the positive x-axis and along both the positive and negative y-axes. Talwani and Heirtzler (1964) show that the components of the field for such a body are;

$$Hz = 2 \sin\phi \left[J_x \left\{ (\theta_2 - \theta_1) \cos\phi + \sin\phi \ln\left(\frac{r_2}{r_1}\right) \right\} \quad \ldots\ldots \right.$$
$$\left. \ldots - J_z \left\{ (\theta_2 - \theta_1) \sin\phi - \cos\phi \ln\left(\frac{r_2}{r_1}\right) \right\} \right] \qquad 5.5$$

$$H_x = 2 \sin\phi \left[J_x \left\{ (\theta_2 - \theta_1) \sin\phi - \cos\phi \ln\left(\frac{r_2}{r_1}\right) \right\} \ldots\ldots \right.$$
$$\left. \ldots + J_z \left\{ (\theta_2 - \theta_1) \cos\phi + \sin\phi \ln\left(\frac{r_2}{r_1}\right) \right\} \right] \qquad 5.6$$

$$H_y = 0$$

magnetic inverse calculations for density and susceptibility or vector magnetisation. The program can perform two-dimensional calculations for infinitely long prismatic bodies using the equations of Talwani, Worzel and Landisman (1959) as well as applying end corrections for the 2 - dimensional case using the equations of Shuey and Pasquale (1973) and Cady (1980). Shuey and Pasquale (1973) coined the term '$2\frac{1}{2}$-dimensional' body to represent bodies invariant in cross-section but terminated at finite distance along strike. The '$2\frac{1}{2}$-dimensional' approach has the convenience and speed of the 2-dimensional approach but with much of the generality of the complete 3-dimensional approach of Talwani (1965).

The main steps in the derivation of the equations used will briefly be given.

In fig. 5.3a consider the semi-infinite prism KLMN, with magnetisation J, that extends to infinity along the positive x-axis and along both the positive and negative y-axes. Talwani and Heirtzler (1964) show that the components of the field for such a body are;

$$Hz = 2 \sin\phi \left[J_x \left\{ (\theta_2 - \theta_1) \cos\phi + \sin\phi \ln\left(\frac{r_2}{r_1}\right) \right\} \ldots\ldots \right.$$
$$\left. \ldots - J_z \left\{ (\theta_2 - \theta_1) \sin\phi - \cos\phi \ln\left(\frac{r_2}{r_1}\right) \right\} \right] \qquad 5.5$$

$$H_x = 2 \sin\phi \left[J_x \left\{ (\theta_2 - \theta_1) \sin\phi - \cos\phi \ln\left(\frac{r_2}{r_1}\right) \right\} \ldots\ldots \right.$$
$$\left. \ldots + J_z \left\{ (\theta_2 - \theta_1) \cos\phi + \sin\phi \ln\left(\frac{r_2}{r_1}\right) \right\} \right] \qquad 5.6$$

$$H_y = 0$$

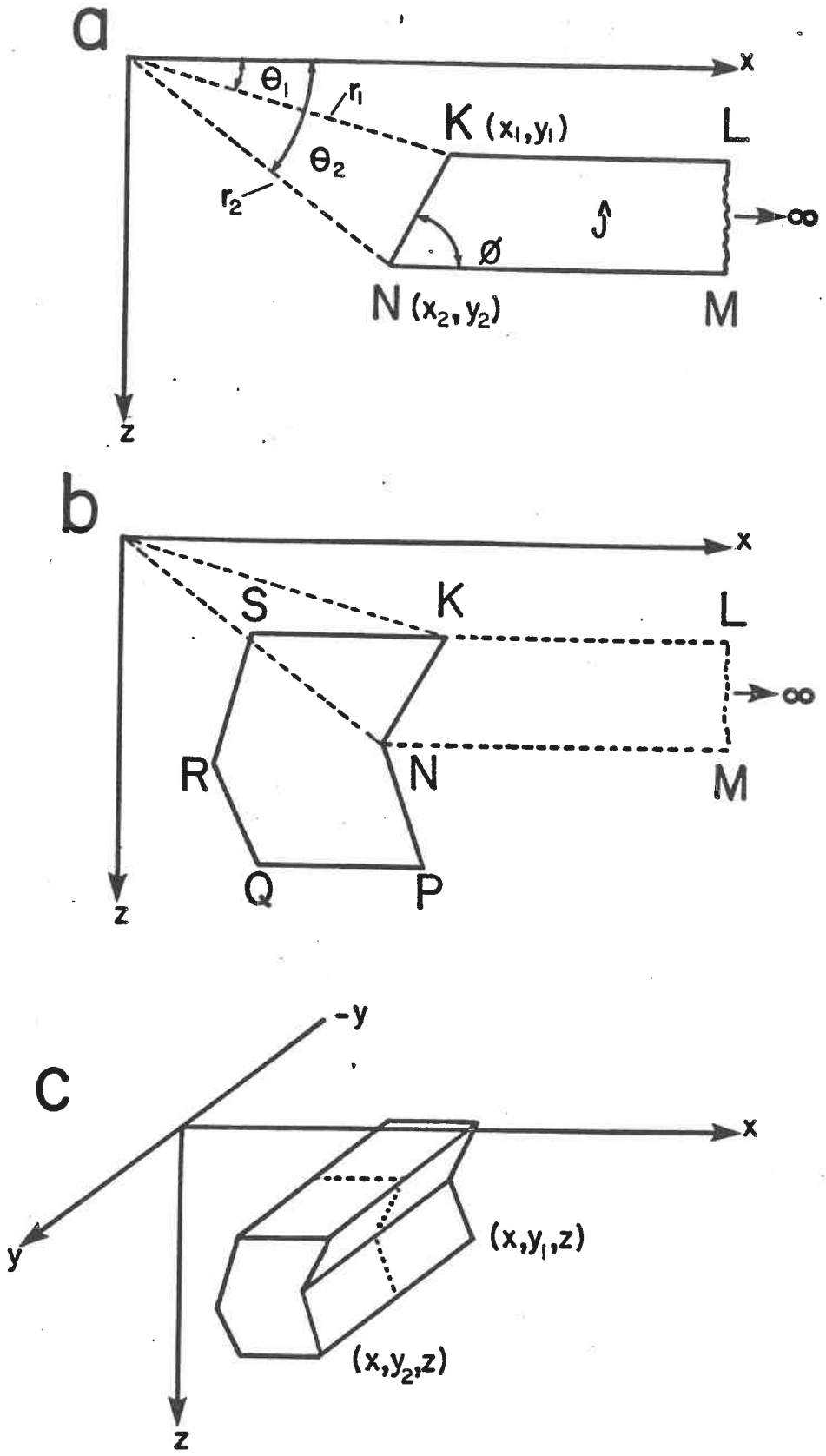


Fig. 5.3 Geometry of bodies used for modelling studies.
a) and b) 2-dimensional.
c) $2\frac{1}{2}$-dimensional.

where $r_2 = \sqrt{x_2^2 + z_2^2}$

$r_1 = \sqrt{x_1^2 + z_1^2}$

J_x, J_y, J_z are components of magnetisation $\hat{J}$

and H_x, H_y, H_z are components of the earths field

Now consider a body with polygonal cross-section KNPQRS (fig. 5.3b). The magnetic anomaly for such a body can be evaluated by obtaining the anomalies for prisms such as KLMN and taking regard of the sign. The procedure adopted by Talwani and Heirtzler (1964) was to proceed around the prism from K in a clockwise direction. For segments like KN, in which increases, the anomaly is given a negative sign while segments like RS are assigned a positive sign. The resulting sum around the body for all the segments is the anomaly caused by the body KNPQRS. Equations 5.5 and 5.6 can be rewritten in more general terms

$$H_z = 2\ (J_x B - J_z A) \qquad 5.7$$

$$H_x = 2\ (J_x A + J_z B) \qquad 5.8$$

where $A = \dfrac{\Delta z^2}{\Delta z^2 + \Delta x^2}\ \Delta\theta + \dfrac{\Delta z\ \Delta x}{\Delta z^2 + \Delta x^2}\ \ln\left(\dfrac{r_{i+1}}{r_i}\right)$

$B = \dfrac{\Delta z \Delta x}{\Delta z^2 + \Delta x^2}\ \Delta\theta - \dfrac{\Delta z^2}{\Delta z^2 + \Delta x^2}\ \ln\left(\dfrac{r_{i+1}}{r_i}\right)$

where $\Delta z = z_{i+1} - z_i$

$\Delta x = x_i - x_{i+1}$

$\Delta\theta = \theta_i - \theta_{i+1}$

$$r_{i+1} = \sqrt{x_{i+1}^2 + z_{i+1}^2}$$

$$r_i = \sqrt{x_i^2 + z_i^2}$$

Shuey and Pasquale (1973) extended the derivation of Talwani and Heirtzler (1964) and introduced end corrections to the calculation, thus avoiding both the unreasonable assumption of infinite strike length and the complexity of the complete 3-dimensional interpretation. The modelling studies presented later in this thesis make use only of the simpler 2D equations. However, for completeness the derivation of the $2\frac{1}{2}$D equations will be outlined.

With the geometry defined in fig. 5.3c the magnetic field $\hat{H}(r)$ can be written;

$$\hat{H}(r) = \nabla \int_V (\hat{J} \cdot \nabla) \frac{d^3 \hat{r}_o}{|\hat{r} - \hat{r}_o|} \qquad 5.9$$

and if the body is uniformly magnetised then;

$$H_x = 2 J_x P_x + 2 J_z Q \qquad 5.10$$

$$H_y = -2 J_y R \qquad 5.11$$

$$H_z = 2 J_x Q - 2 J_z P_z \qquad 5.12$$

where $P_x = \frac{\partial^2 U}{\partial x^2}$ 5.13

$P_z = -\frac{\partial^2 U}{\partial z^2}$ 5.14

$R = -\frac{\partial^2 U}{\partial y^2}$ 5.15

$Q = \frac{\partial^2 U}{\partial x \partial z}$ 5.16

where U = Newtonian Potential $= \frac{1}{2} \int_v \frac{d^3 \hat{r}_o}{|\hat{r} - \hat{r}_o|}$

To simplify the calculation Shuey and Pasquale (1973) constrained the bodies to be symmetrical about the x-z plane and, moving the origin to the point of observation

$$\frac{\partial^2 U}{\partial x \partial y} = 0 \quad \text{and} \quad \frac{\partial^2 U}{\partial y \partial z} = 0$$

Using La Places' equation $\frac{\partial^2 U}{\partial x^2} + \frac{\partial^2 U}{\partial y^2} + \frac{\partial^2 U}{\partial z^2} = 0$

then $P_x - P_z - R = 0$ 5.17

Following the derivation of Shuey and Pasquale (1973)

$P_z = -\oint \frac{Y}{r} \frac{z}{x^2 + z^2} dx$ 5.18

$P_x = -\oint \frac{Y}{r} \frac{x}{x^2 + z^2} dz$ 5.19

$Q = -\oint \frac{Y}{r} \frac{z}{x^2+z^2} dz = \oint \frac{Y}{r} \frac{x}{x^2+z^2} dx$ 5.20

$R = -\oint \frac{Y}{r} \frac{x}{z^2+y^2} dz = -\oint \frac{Y}{r} \frac{z}{x^2+y^2} dx$ 5.21

where $r^2 = x^2 + Y^2 + z^2$

Y = strike length of body

At this point the limiting case of 2-dimensional behaviour can be checked by setting $Y=\infty$ and $Y/r=1$, then $R=0$ and $P_x=P_z=P$. The formulae for P and Q then reduce to equations 5.7 and 5.8, the 2-dimensional equations of Talwani and Heirtzler (1964).

Shuey and Pasquale (1973) simplify the theory further by introducing complex variables and equation 5.18 - 5.21 become

$$Q+iP_z = \oint \frac{Y}{r} \frac{dx}{x + iz} \qquad 5.22$$

$$-(Q + iP_x) = \oint \frac{Y}{r} \frac{idz}{x + iz} \qquad 5.23$$

$$R = \mathrm{Im} \oint \frac{z}{r} \frac{dx}{x + iY} = -\mathrm{Im} \oint \frac{x}{r} \frac{dz}{z + iY} \qquad 5.24$$

The final formulae are obtained by integrating equations 5.22 - 5.24 along each side of the polygon from x_i,z_i to x_{i+1},z_{i+1}, for all N sides.

$$Q+i P_z = \sum^{N} \frac{-\Delta x}{\Delta x + i\Delta z} \ln\left(\frac{F_{i+1}}{F_i}\right) \qquad 5.25$$

$$(Q + iP_x) = \sum^{N} \frac{i\Delta z}{\Delta x + i\Delta z} \ln\left(\frac{F_{i+1}}{F_i}\right) \qquad 5.26$$

$$iR = \sum^{N} \ln\left(\frac{F_{i+1}}{F_i}\right) \qquad 5.27$$

$$\text{where } F_n = \frac{\Delta x + i\Delta z}{x_n + iz_n}\left(1 + \frac{r_n}{Y}\right) + \frac{i}{Y^2}\left(x_n \Delta z - z_n \Delta x\right) \qquad 5.28$$

Combining the geometrical factors in equations 5.25 - 5.27 with the components of magnetisation as given by Shuey and Pasquale (1973) in

equations 5.10 - 5.12, allows the determination of the components of the anomalous field H_x, H_y and H_z from which it is possible to calculate ΔT, the total field anomaly.

Let $\hat{T}_o$ be the total field measured at a point far from anomalous bodies and then introduce an anomalous magnetic body which produces disturbing field components H_x, H_y, H_z at the magnetometer. The total field $\hat{T}$ that is measured is the vector sum of $\hat{T}_o$ and the disturbing field (Cady, 1980).

$$\hat{T} = \left[(T_o x + H_x)^2 + (T_o y + H_y)^2 + (T_o z + H_z)^2 \right]^{\frac{1}{2}} \qquad 5.29$$

where $T_o x = T_o \cos I \cos A$

$T_o y = T_o \cos I \sin A$

$T_o z = T_o \sin I$

and I=inclination of $\hat{T}_o$, A=declination of $\hat{T}_o$ (which for the case of purely induced magnetisation reduces to D, the declination of the earths field).

Since a proton precession magnetometer is insensitive to field direction the anomalous field ΔT is simply the scalar difference of $\hat{T}$ and $\hat{T}_o$.

$$\Delta T = |\hat{T}| - |\hat{T}_o| = \left[(T_o \cos I \cos A + H_x)^2 + (T_o \cos I \sin A + H_y)^2 + (T_o \sin I + H_z)^2 \right]^{\frac{1}{2}} - |\hat{T}_o| \qquad 5.30$$

If the anomalous field is much less than the earths field then equation 5.30 reduces to the approximation

$$\Delta T \simeq H_z \sin I + H_x \cos I \cos A + H_y \cos I \sin A \qquad 5.31$$

In the program (Cady, 1977) forward calculations are made using either the exact equation 5.30 or the approximation given in equation 5.31. Inverse solutions, however, must make use of equation 5.31 for the least squares calculations of susceptibility and remanent magnetisation since it is linear in H_x,H_y and H_z.*

Tests of the program are given in a later section of this chapter and results presented in Appendix 2. Unless otherwise stated interpretations were made using the simpler 2-dimensional equations.

5.2.4 TRANSFORMATION OF PROFILES

The magnetic data presented were collected on many separate flights spanning two seasons work in the Antarctic. The nature of the terrain and other constraints, such as weather conditions meant that many adjacent legs in the grid were flown at different altitudes. In order to directly compare anomalies a capability to transform profiles was essential. A computer program originally written by Blakely (1975) was used which could transform a total field anomaly $h_1(x)$ into a new anomaly $h_2(x)$, but either 1) is at a different elevation, or 2) has a different direction of the regional field, and/or has a different direction of source magnetisation. Transforming the profile to one at a new elevation is most important for the work in this thesis while point 2 is more useful when comparing anomalies over large distances, for eg. oceanic magnetic anomalies. Also data collected in this thesis were generally recorded in one of two directions being in a square grid form. The mathematical background is dealt with in Blakely and Cox (1972) and Schouten and McCamy (1972) and is only briefly outlined here.

*see note at end of Appendix 3

Consider an arbitrary 2-dimensional source which is parallel to the y-axis with magnetisation J(x,z) and let the anomaly due to this source be $h_1(x)$. Blakely and Cox (1972) showed that without requiring knowledge of the shape or magnetisation of the source, we can assume $h_1(x)$ is produced by an infinitely thin plane with magnetisation m(x).

$$h_1(x) = g_1(x) * m(x)$$

where * represents convolution and $g_1(x)$ is the earth filter for the plane. The new anomaly $h_2(x)$ is given by a similar equation;

$$h_2(x) = g_2(x) * m(x)$$

where m(x) remains the same but $g_1(x)$ and $g_2(x)$ are different. Let $H_1(k)$ represent the Fourier transform of $h_1(x)$ such that

$$H_1(k) = \int_{-\infty}^{\infty} h_1(x)\, e^{-ikx}\, dx$$

$$\text{and } h_1(x) = \frac{1}{2\pi} \int_{-\infty}^{\infty} H_1(k)\, e^{ikx}\, dk$$

where k = wave number

and similary for $g_1(x)$,$g_2(x)$ and m(x).

The Fourier convolution theorem states that two functions convolved in space and two functions multiplied in the wave number domain are transform pairs. Therefore;

$$H_1(k) = G_1(k)\, M(k) \qquad 5.32$$

$$H_2(k) = G_2(k)\, M(k) \qquad 5.33$$

and from 5.32 and 5.33

$$H_2(k) = H_1(k) \frac{G_2(k)}{G_1(k)} \qquad 5.34$$

which in the space domain is

$$h_2(x) = \frac{1}{2\pi} \int_{-\infty}^{\infty} H_2(k) \, e^{ikx} \, dk$$

Hence, the transformed anomaly is determined by a filtering operation where the wave number domain representation of the filter is $G_2(k)/G_1(k)$. No knowledge is required about the true source of $h_1(x)$ so long as it is 2-dimensional (Blakely and Cox, 1972).

Upward and downward continuation filters are purely real filters of the form

$$\frac{G_2(k)}{G_1(k)} = e^{-|k|\Delta z} \qquad 5.35$$

(Dean, 1958, Schouten and McCamy, 1972), where Δz is the amount of elevation change (positive for upward continuation). The upward continuation filter attenuates high wave numbers and has the effect of smoothing the anomaly (see fig. 5.7). The downward continuation filter amplifies high wave numbers and increases the resolution of the anomaly (see fig. 5.8).

To change the direction of either the regional field or the magnetisation Blakely and Cox (1972) showed that

$$\frac{G_2(k)}{G_1(k)} = \theta \ \text{sgn}\ k \qquad 5.36$$

where θ is a constant depending only on the inclinations and declinations of both the old and new directions of regional field and magnetisation.

The computer program uses the fast Fourier transform algorithm, FORK, developed at Stanford University by J. Claerbout (1976). The program accepts the input anomaly and takes the fast Fourier transform of it. The transformed data are then filtered in the wave number domain by either the filter defined in equation 5.35 or that in equation 5.36. The resulting complex array is then inverse-Fourier transformed and plotted out. Downward continuation is a very unstable calculation and it is generally necessary to low-band pass filter $h_1(x)$ first (Blakely, 1975). Consequently the program includes a wave number domain filter as described by Schouten and McCamy (1972) to eliminate the highest wave numbers before downward continuation is performed.

5.2.5 THEORETICAL TESTS OF PROGRAMS

As mentioned earlier the programs described in this chapter were developed at the USGS in Denver. Each program had to be modified in Cambridge to run on a different computer, to accept data in a different format, and required plotter routines to be written. Consequently as a check on the successful adaption of each program and also as a guide to understanding the internal running of each program, theoretical data were used.

The computer modelling routine was tested first using theoretical 3-dimensional data (Aero Service, undated) so as to test the working of every subroutine. After testing, the modelling program was used to generate the total field anomaly across 2-dimensional models of dyke- and fault-like bodies. The data were then analysed using the Werner deconvolution method of determining maximum depth to magnetic basement. The depths determined were then compared with known depths to the tops of the bodies. The data were then, first upward continued and then downward continued before being again analysed by the Werner deconvolution program to check the new depths to the bodies.

Test of Modelling Program

The first test uses a 8x8x3 prism from a book of magnetic type curves developed by Aero Service (undated). The observed values were obtained from Cady (1977) who had measured the values directly from the total field curves. The rectangular prism is divided into two bodies by a diagonal in order to test the program on a sloping side. Bodies 1 and 2 have susceptibility of 1.0×10^{-5} (cgs) and no remanent magnetisation. The profile azimuth is 0^{o} and the regional field inclination 60^{o} and declination 0^{o}. The result of a forward calculation for the two bodies is shown in fig. 5.4a. The mean error between the observed and calculated fields is 5.26×10^{-4} nT with a RMS deviation of 3.62×10^{-2} nT. Fig. 5.4b shows a successful inverse calculation for susceptibility and remanent magnetisation giving values very close to the nominal values. The least squares solutions are listed in table 5.1. The mean error between the observed field and that determined by least squares solution for susceptibility is 2.93×10^{-3} nT with RMS deviation 2.65×10^{-2} nT and for remanent magnetisation 3.04×10^{-3} nT with RMS deviation 2.17×10^{-2} nT.

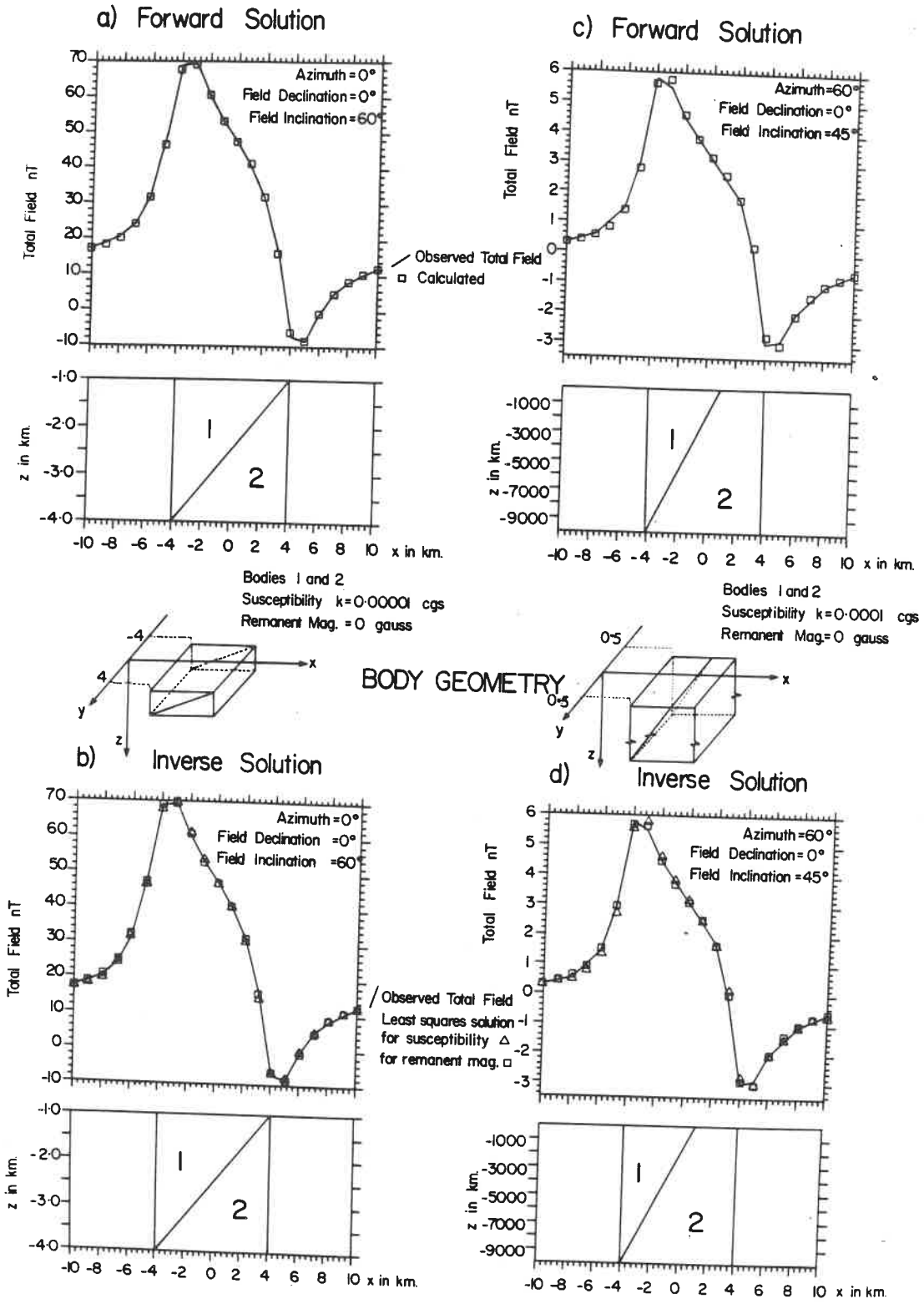


Fig. 5.4 Theoretical tests of modelling program.

FORWARD SOLUTION	Bodies	1	2	Errors (nT)
Susceptibility (cgs)		1	1	0.00053±0.036
Remanent Mag. (gauss)		0	0	
INVERSE SOLUTION	Bodies	1	2	Errors (nT)
Susceptibility (cgs)		1.02	1.01	0.0029±0.026
Remanent Mag.	Amplitude (gauss)	1.02	1.01	0.0030±0.021
	Inclination	60.0	60.1	
	Declination	0.0	0.0	

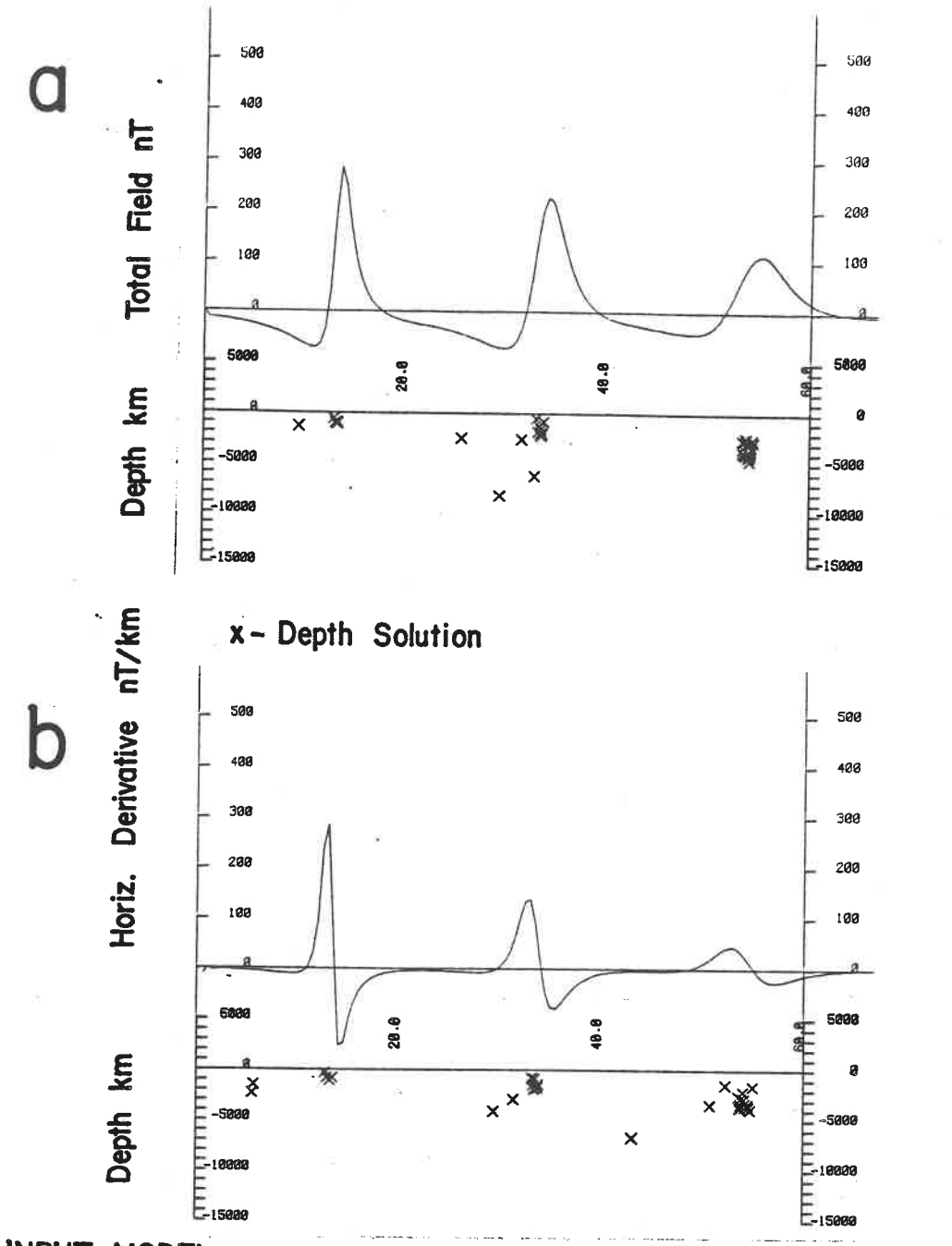
FORWARD SOLUTION	Bodies	1	2	Errors (nT)
Susceptibilty (cgs)		10	10	0.017±0.13
Remanent Mag. (gauss)		0	0	
INVERSE SOLUTION	Bodies	1	2	Errors (nT)
Susceptibility (cgs)		10.1	9.79	0.014±0.12
Remanent Mag.	Amplitude (gauss)	9.7	9.46	0.013±0.082
	Inclination	43.9	44.4	
	Declination	4.3	7.4	

Table 5.1 Forward and Inverse solutions for theoretical models used for testing modelling program (see also fig. 5.4).

The second test uses an 8x1x∞ prism again from Aero Service (undated) (see fig. 5.4). The azimuth of the profile is 60° compared to 0° in the first test and the regional field inclination 45° and declination 0°. A bottom depth of -9999 km was used to approximate minus infinity. Again the body was divided into 2 to test the program on sloping sides. The prism was not divided along a simple diagonal because with bodies with a near infinite bottom the triangle with its base near the surface would have a much greater effect than the triangle with its base at depth. Bodies 1 and 2 have susceptibility of $1x10^{-4}$ cgs and again no remanent magnetisation. The result of forward and inverse calculation are shown in fig. 5.4c and fig. 5.4d respectively. The mean error between observed and calculated fields in the forward solution is $1.71x10^{-2}$ nT with RMS deviation $1.29x10^{-1}$ nT. In the inverse solution for susceptibility the mean error between observed and calulated fields is $1.4x10^{-2}$ nT with RMS deviation $1.21x10^{-1}$ nT, while for remanent magnetisation the mean error between observed and calculated fields is $1.3x10^{-2}$ nT with RMS deviation $8.23x10^{-2}$ nT (see Table 5.2).

Test of Depth to Magnetic Basement Program

In the first test the modelling program was used to generate the total field anomaly over 3 2-dimensional dykes ie. bodies whose width is less than the depth to their upper surfaces. The depths to the tops of the dykes are 1 km, 2 km, and 4 km respectively (see fig. 5.5). The total field anomalies and the depth solutions on the total field data using Werners' deconvolution method are shown in fig. 5.5a. The program then took the horizontal derivative of the total field and solved for fault- like bodies (see fig. 5.5b). As would be expected, knowing the nature of the bodies, solutions on the total field for dyke-like bodies gives more accurate depth solutions with tighter clusters (see fig. 5.5a). The centres of each cluster can be seen in fig. 5.5a to lie very close to the actual depths.



INPUT MODEL

Azimuth = 45° Inclination = -72°

Declination = 60° Susceptibility = 0·007 cgs

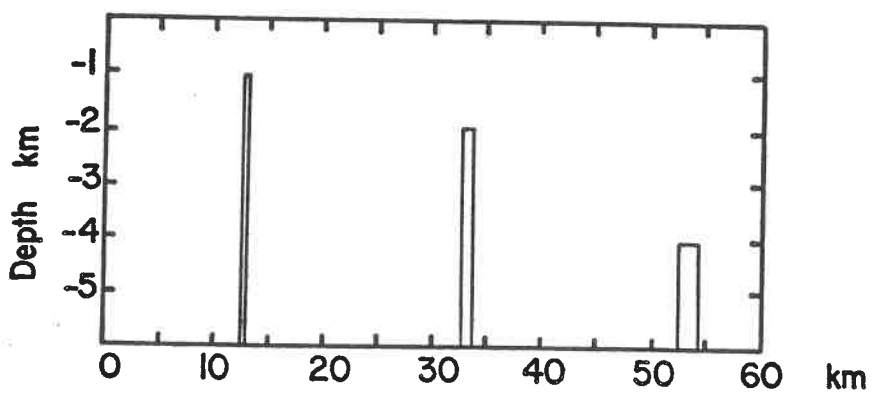
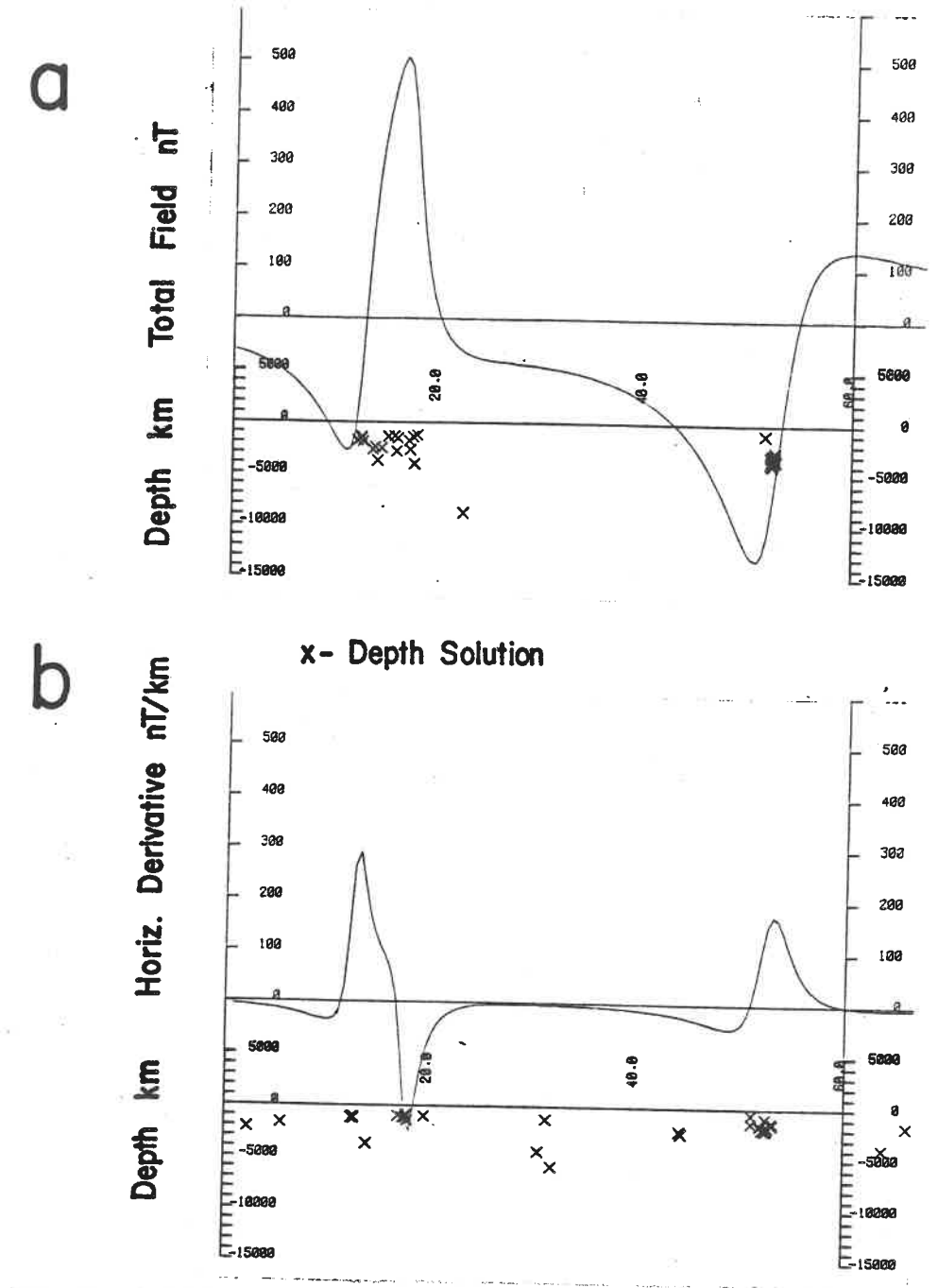


Fig. 5.5 Werner Deconvolution for 3 theoretical dyke-like bodies.



INPUT MODEL

Azimuth = 45° Inclination = -72°

Declination = 60° Susceptibility k_1 = 0·003 cgs

k_2 = 0·005 cgs

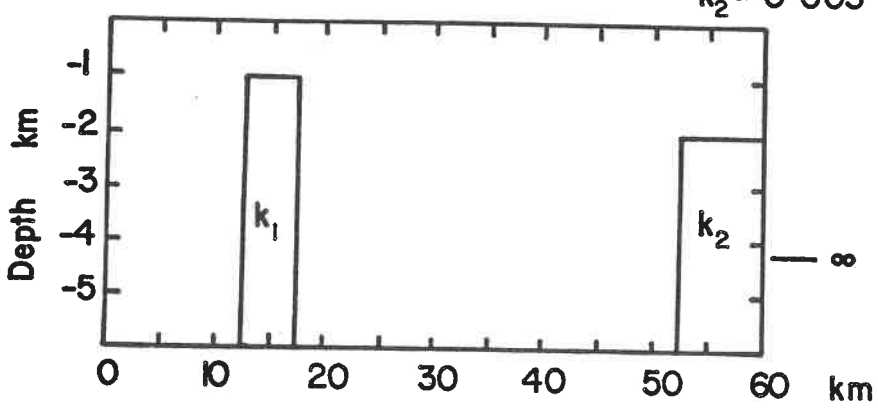


Fig. 5.6 Werner Deconvolution for theoretical fault-like bodies.

For the second test the total field anomaly across 2-dimensional fault-like bodies was produced. The first body consisted of two vertical interfaces 5 km apart at a depth of 1 km such that the body has the appearance of a fat dyke and the second body consisted of a single vertical interface at a depth of 2 km. In this case the solution for fault-like bodies on the horizontal derivative of the total field gave the best results (see fig. 5.6b). The solutions for the total field data tend to be too deep and are not in such tight clusters (fig. 5.6a).

Test of Upward amd Downward Continuation

The total field anomalies for the fault-like bodies in fig. 5.6a were continued upward by 1 km for the first test. The effect of upward continuation was to change the depths to the bodies to 2 km and 3 km (see fig. 5.7). The total field anomaly can be seen to be attenuated as expected. The transformed data were then passed to the Werner deconvolution program which solved the total field and its horizontal derivative for dyke- and fault-like bodies (see fig. 5.7). The depth solutions on the horizontal derivative again give the best results with values close to the actual solutions (see fig. 5.7b).

For the second test the profile in fig. 5.7a was continued downward by 1.0 km so as to bring it back to the original level, depths to the bodies again becomes 1.0 and 2.0 km. The process of downward continuation correctly amplifies the anomalies (see fig. 5.8). Analysis of the transformed total field data by Werner deconvolution is shown on fig. 5.8. Depth solutions are more scattered because downward continuation has the effect of amplifying the highest wave numbers which causes the Werner deconvolution program to identify shallow sources. Nevertheless apart from edge effects of the FFT used in the calculation, the anomalies in fig. 5.8a are very similar to those on 5.6a which were generated by the modelling program.

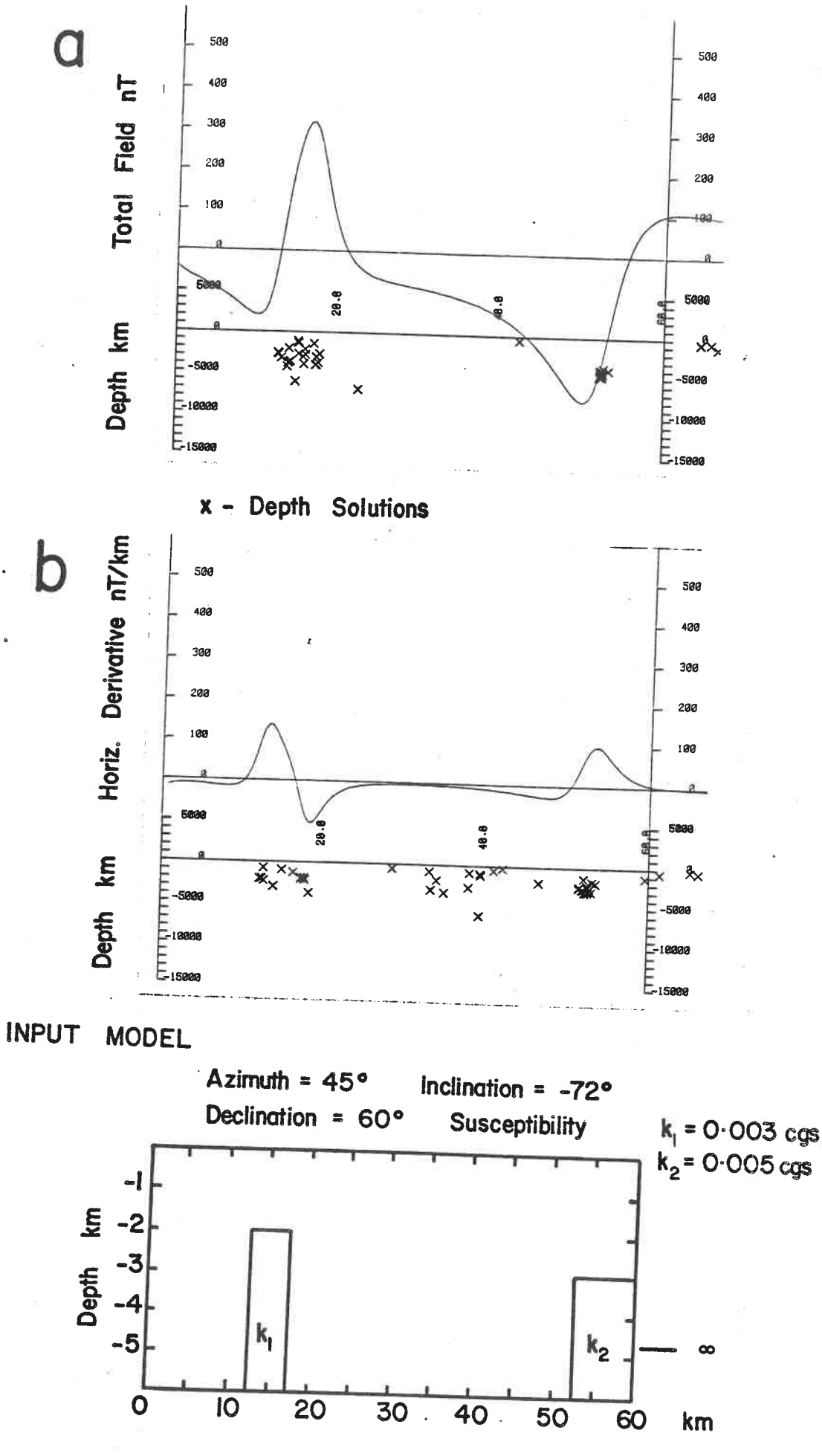


Fig. 5.7 Test of upward continuation using Werner Deconvolution program.

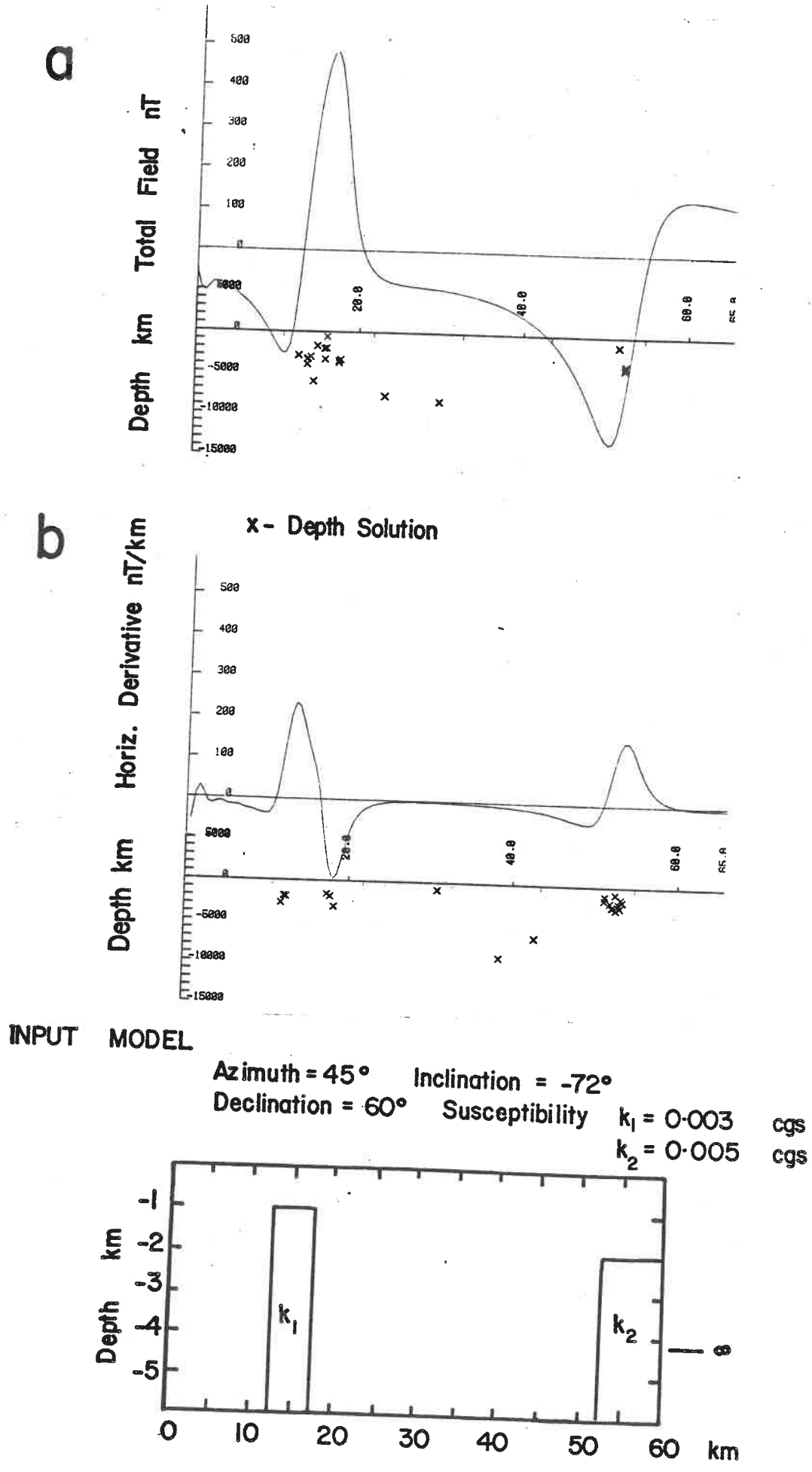


Fig. 5.8 Test of downward continuation using Werner Deconvolution program.

5.3 AREAL APPROACH

An areal approach to the analysis of the data has not been practical due to the large separation between flight lines. The residual magnetic however have been plotted along flight lines (figs. 5.9 and 5.10). Using such a presentation it is possible to identify broad regional magnetic trends or patterns that may exist in West Antarctica. Several boundaries between areas of different field characteristics can be recognised (fig. 5.11). At the northern edge of the map numerous large amplitude (~1000 nT) short wavelength anomalies (~10-20 km) occur. This area is terminated to the south by an area in which the field is more subdued with only isolated anomalies. Towards the South Pole the field shows no anomalies of narrow width but only broad low amplitude anomalies. Just north of the position of the Thiel Mountains several anomalies of wavelength ~40-50 km and amplitude ~400 nT occur in a small area.

The quietest field is seen in the area at the head of the Ronne-Filchner Ice Shelf between the Ellsworth and Pensacola Mountains. The possible geological significance of all these observations will be discussed in the next chapter.

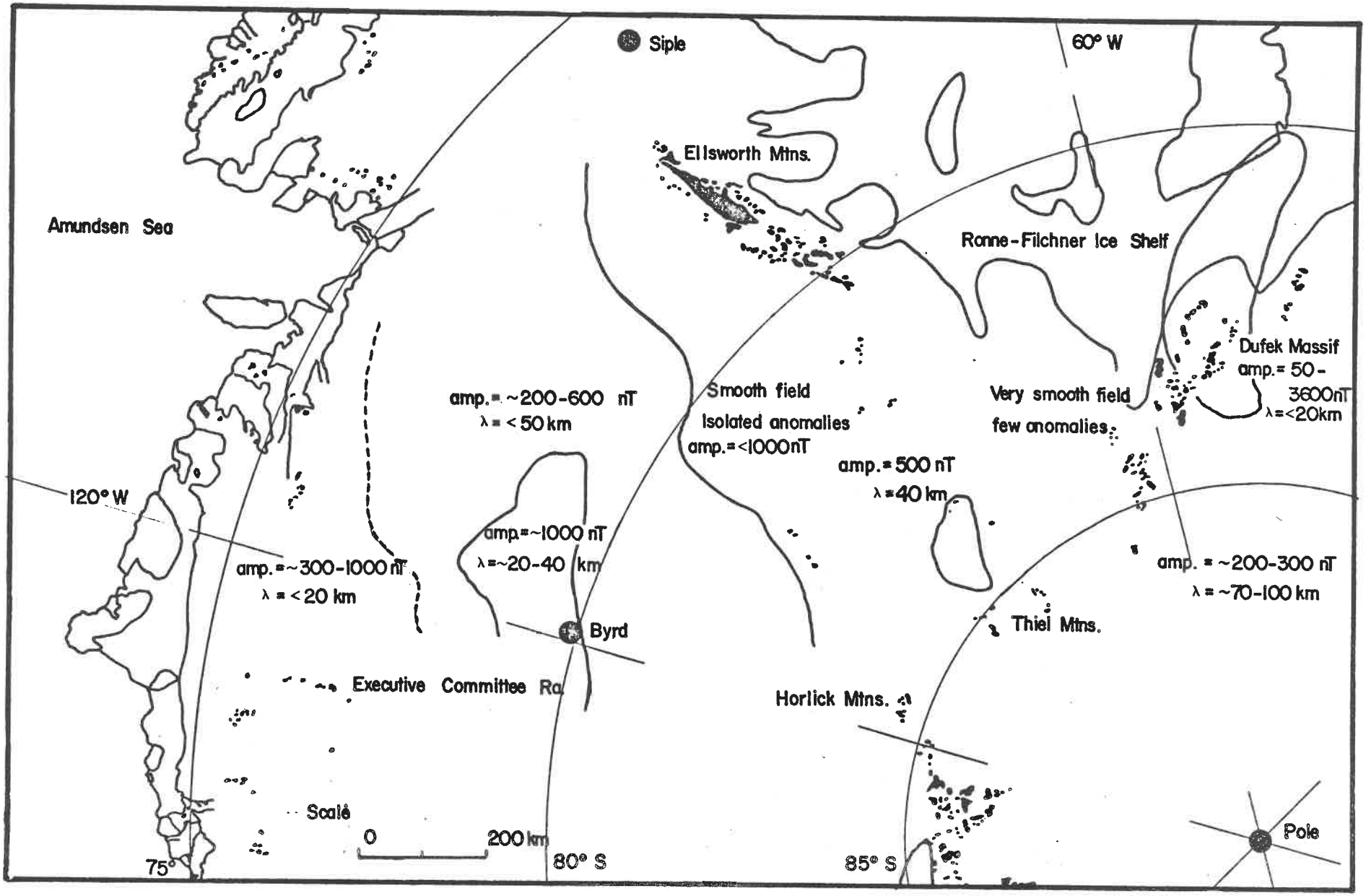


Fig. 5.11 Characteristics of the residual magnetic field in West Antarctica.

CHAPTER 6 GEOLOGICAL AND TECTONIC INTERPRETATIONS

6.1 INTRODUCTION

Following compilation of a detailed topographic bedrock map from RES in chapter 4, West Antarctica was crudely divided into seven units. In this chapter these units are discussed and refined further drawing not only on topographic information but also the results of the isostatic reconstruction, depths to magnetic basement and all other pertinent geophysical measurements. Where appropriate anomalies are modelled as described in chapter 5 to give quantitative estimates of bedrock magnetisation.

The current understanding of the subglacial geology and structure of West Antarctica was discussed in chapter 1. Further interpretations of the geophysical, geological and tectonic characteristics of the ice-covered areas of West Antarctica are presented. Discussion will concentrate on the identification of the boundary zone between East and West Antarctica and the identification of major structural units. Each structural unit will be discussed in turn. The boundary between East and West Antarctica will be dealt with last following discussion of the two units lying on either side of it.

The implications of these interpretations to current views of the tectonic evolution of West Antarctica will be outlined, and the chapter concludes with a brief discussion of the role of West Antarctica in Gondwanaland.

6.2.1 CENOZOIC VOLCANIC PROVINCE

The Cenozoic volcanic province is known from exposures to occur in a relatively narrow zone along the Pacific coast of Antarctica from the Antarctic Peninsula and sub-Antarctic islands to Marie Byrd Land. Further Cenozoic volcanics crop out in the McMurdo Sound area and at Cape Adare (Hamilton, 1972). In Marie Byrd Land Cenozoic volcanic outcrops extend some 350 km inland from the coast to the Crary Mountains and Executive Committee Range (see fig. 6.2). Data were not collected over a large part of the volcanic province except in the area between the Crary Mountains and Thwaites Glacier.

The Cenozoic volcanics in West Antarctica have been divided into two units comprising a basal unit of alkali basalt flows and palagonitized tuffs and breccias overlain by stratovolcanoes with parasitic cones (LeMasurier, 1972). The stratovolcanoes consist mainly of felsic flows and pyroclastics of alkaline composition while the parasitic cones are largely alkali basalt. The differential vertical displacement of the pre-volcanic erosion surface, the rectilinear alignment of the stratovolcanoes and the bimodal and alkaline character of the volcanism suggests that the volcanic activity is related to extensional tectonics (LeMasurier and Rex, in press).

Source depths within this area suggest that magnetic basement lies mainly close to the ice/rock interface indicating lack of a thick sedimentary section, a feature noted by Behrendt and Wold (1963). Several depth solutions in this area indicate magnetic basement may, however, in some places lie 2.5-3 km below the ice/rock interface (see fig. 6.1). The 2.5-3 km of non-magnetic material overlying basement is likely to be low susceptibility volcanics rather than sedimentary strata bearing in mind the variation in magnetic susceptibility noted for these rocks by Bentley

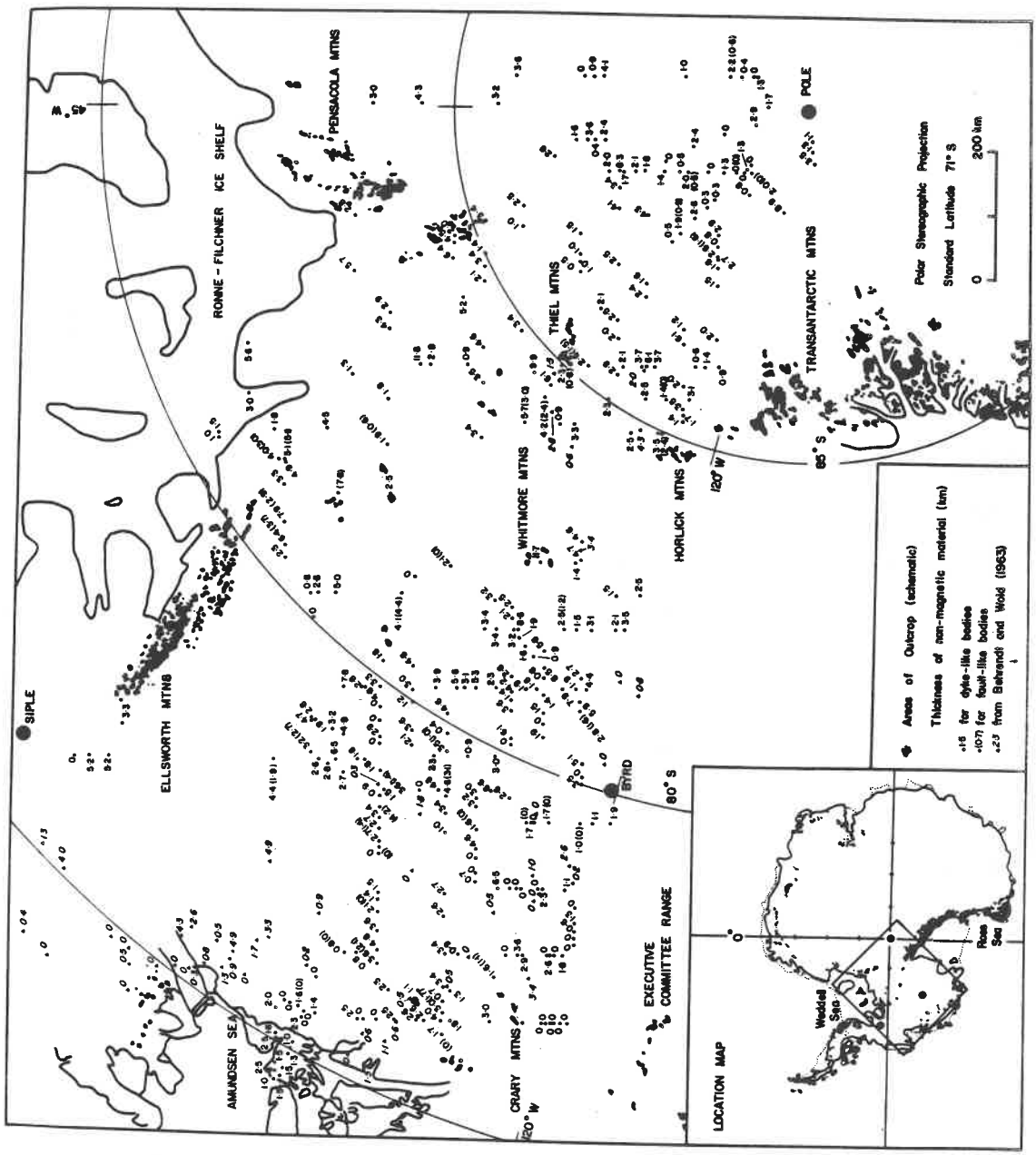


Fig. 6.1 Thickness of non-magnetic material overlying magnetic 'basement' in West Antarctica.

and Chang (1971). This is supported by seismic refraction data on a flank of Toney Mountain in which 3 km of andesitic-basaltic flows, similar to those exposed, are seen overlying the basement surface (Bentley and Clough,1972). Bentley and Chang (1971) report, however, no significant anomaly from Toney Mountain indicating lower susceptibilities for the rocks as compared to other parts of the volcanic province.

The Crary Mountains, meanwhile, were found by Bentley and Chang (1971) to be associated with a striking anomaly of at least 1400 nT amplitude. Such large amplitude anomalies were not recorded on a flight that passed close to the Crary Mountains even after continuing the observed field downward to the level of the ground traverse. The observed anomalies have a peak-peak amplitude of only 450-600 nT (see A-A' on fig. 6.2). Bentley and Chang (1971) had estimated the susceptibility of the subglacial rock in the vicinity of the Crary Mountains to be 0.05 cgs from their magnetite content as measured by Doumani and Ehlers (1962). The anomalies on profile A-A' in fig. 6.2 were modelled using the least squares inversion program (see fig. A3.1). In order to fit the data both normal and reversed remanent magnetisations were required. Susceptibilities are at least 2 orders of magnitude lower than that estimated by Bentley and Chang (1971) ranging from 0.00015 to 0.00354 cgs. Normal and reversed remanent magnetisations vary in amplitude from 0.006 to 0.027 gauss. Bentley and Chang (1971) also noted that an important degree of remanent magnetisation with a direction significantly different from the present field is suggested by the large size of the negative part of the anomaly associated with the Crary Mountains. The anomalies in A-A' on fig. 6.2 can be seen to be strongly negative. The difference in anomaly amplitudes between Bentley and Chang (1971) and this work again illustrate how varied the magnetic susceptibility of such volcanic rock may be.

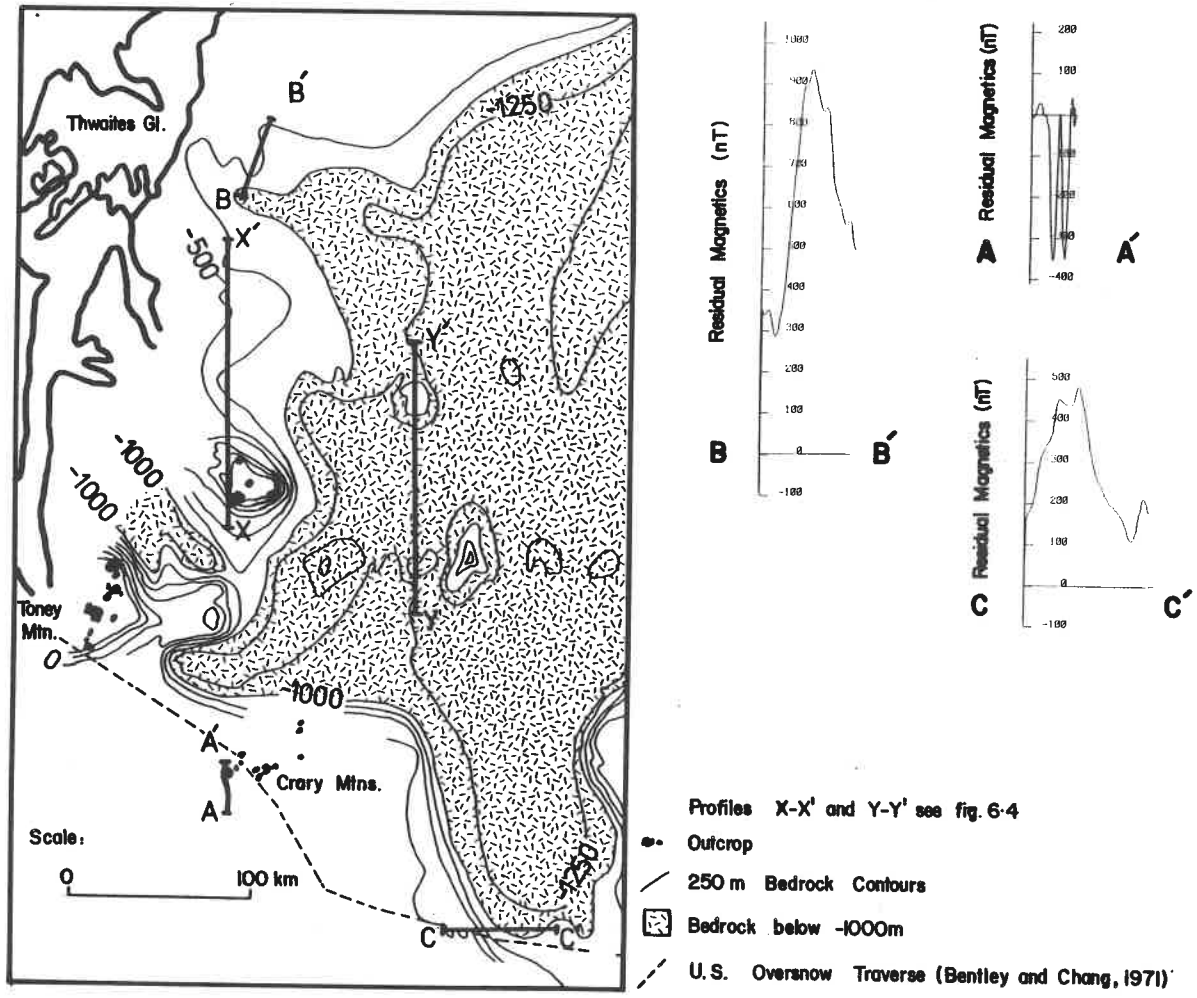


Fig. 6.2 Cenozoic Volcanic Province.

Fig. 6.2 Cenozoic Volcanic Province.

The low susceptibilities and reversed magnetisations obtained from anomalies near the Crary Mountains contrast with those obtained from modelling the anomalies on profile B-B' which runs across the Thwaites Glacier (see fig. 6.2). Susceptibilities vary from 0.011 to 0.017 cgs while remanent magnetisations are all normal ranging in amplitude from 0.006 to 0.009 gauss (see fig. A3.2). The model was modified to take into account depth solutions given in appendix 2 resulting in a slightly higher value of susceptibility (0.02 cgs) and remanent magnetisation (0.014 gauss) near the start of the profile (see fig. A3.3). The nature of the rock forming the magnetic source is unknown but the high values are consistent with values for the Cenozoic volcanics elsewhere. What is clear is that the volcanics beneath the Thwaites Glacier are likely to be more basic in composition than those in A-A' near the Crary Mountains.

A third profile was modelled (C-C' on fig. 6.2) and resulted in similar susceptibilities and intensities of remanent magnetisation as the profile across the Thwaites Glacier (fig. A3.4). However the inclinations for the remanent magnetisation are significantly different than the present regional field. In model 2 (fig. A3.5) reversed magnetisations were required to fit the observed data.

The boundary between the volcanic province and the Byrd Subglacial Basin on topographic grounds probably coincides with the steep subglacial slopes between the two. There is no clear break in the character of the magnetic field between the Cenozoic volcanic province of Marie Byrd Land and the Byrd Subglacial Basin (see figs. 5.9 and 5.10).

6.2.2 BYRD SUBGLACIAL BASIN

A major feature in West Antarctica is undoubtably the Byrd Subglacial Basin extending from the northern end of the Ellsworth Mountains in the east as far west as Byrd Station and then probably continuing southwards towards the front of the Transantarctic Mountains (see fig. 2.8). The basin is divided into two deep areas, each reaching elevations of over 2000 m below sea level, by a sinuous topographic ridge. The basin separates the essentially Cenozoic volcanic areas of the Marie Byrd Land coast from the older Ellsworth Mountains province. Even allowing for complete isostatic recovery this basin still forms a deep submarine connection between the Ross and Amundsen Seas (see fig. 4.9) and probably represents a major tectonic lineament in West Antarctica.

The basin is characterised by numerous large amplitude, 500-1000 nT, anomalies (see figs. 5.9 and 5.10). The source depths indicate, on the whole, that the magnetic basement lies close to the ice/rock interface and conicides with it in many places (fig. 6.1). This is consistent with seismic refraction data which indicates ~0.5 km of Cenozoic sediments overlying ~2.5 km of probable Cenozoic flows and pyroclastics (Bentley and Clough, 1972).

Bentley and Chang (1971) found that susceptibility of the volcanics exposed in the outcrops of Marie Byrd Land varied greatly, some having a value as high as 0.05 cgs while others gave rise to virtually no magnetic anomaly. This observation is supported by the spread of measured susceptibilities for volcanics in appendix 1 although none recorded a value as high as 0.05 cgs. The variation in susceptibility can clearly be seen in the RES and magnetic data where in places there is positive correlation between bedrock peaks and magnetic anomalies while in other bedrock areas highs have no significant magnetic signature. Fig. 6.3 shows

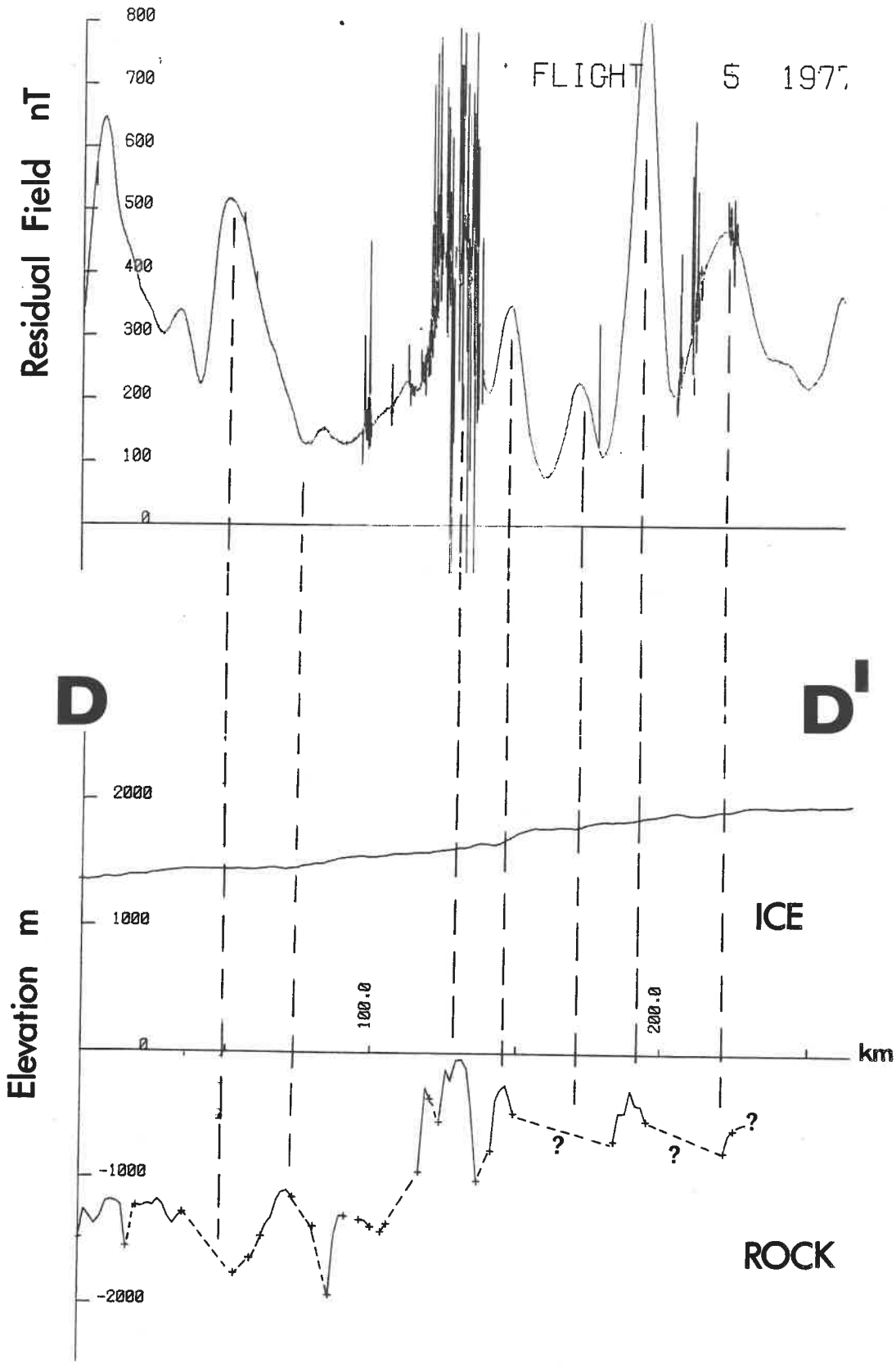


Fig. 6.3 RES and magnetic profile over volcanics illustrating variation in bedrock magnetisation.
(see fig. 6.5 for locations)

this well. On the basis of the magnetics and seismic evidence the floor of the basin would seem to be almost entirely volcanic in origin with the volcanics overlain by a variable but thin amount of Cenozoic sediment.

The magnetic anomalies over the basin appear to be lower in amplitude and longer in wavelength than the anomalies recorded near the exposed volcanics in Marie Byrd Land. This is probably the result, over the basin, of the greater distance between magnetometer and source of the anomalies. Taking into account different elvations of the data (~500 m), the thicker ice in the basin (~1500 m) and allowing for ~1000 m of recent sediment in the basin the anomalies over outcrops and the basin appear very similar. Fig. 6.4 is an example of two profiles, one near the exposed volcanics, which has been upward continued by 3 km to allow comparison with the other profile on a parallel line ~100 km south over the Byrd Subglacial Basin.

A feature not previously described during any of the oversnow traverses is the sinuous ridge on fig. 2.8 seen cutting across the Byrd Subglacial Basin. It can be seen to extend out of the volcanic area of Marie Byrd Land and is associated with magnetic signatures up to ~1000 nT (see fig. 6.5) which combined with its appearence on RES records (see fig. 4.3) would suggest a similar volcanic origin. Source depths indicate that in many places on the ridge the magnetic basement lies close to the ice/rock interface while in others the causal body lies well below this level. Again this is probably the result of the wide variation in susceptibility already noted.

The profiles shown on fig. 6.5 were modelled using the 2-D least squares inversion program (Cady,1977,1980) in order to obtain quantitative estimates of bedrock magnetisations (see appendix 3). Profile A-A' on fig. 6.5 is taken from the central portion of this ridge. Using the RES determined ice/rock interface as the upper surface of the model

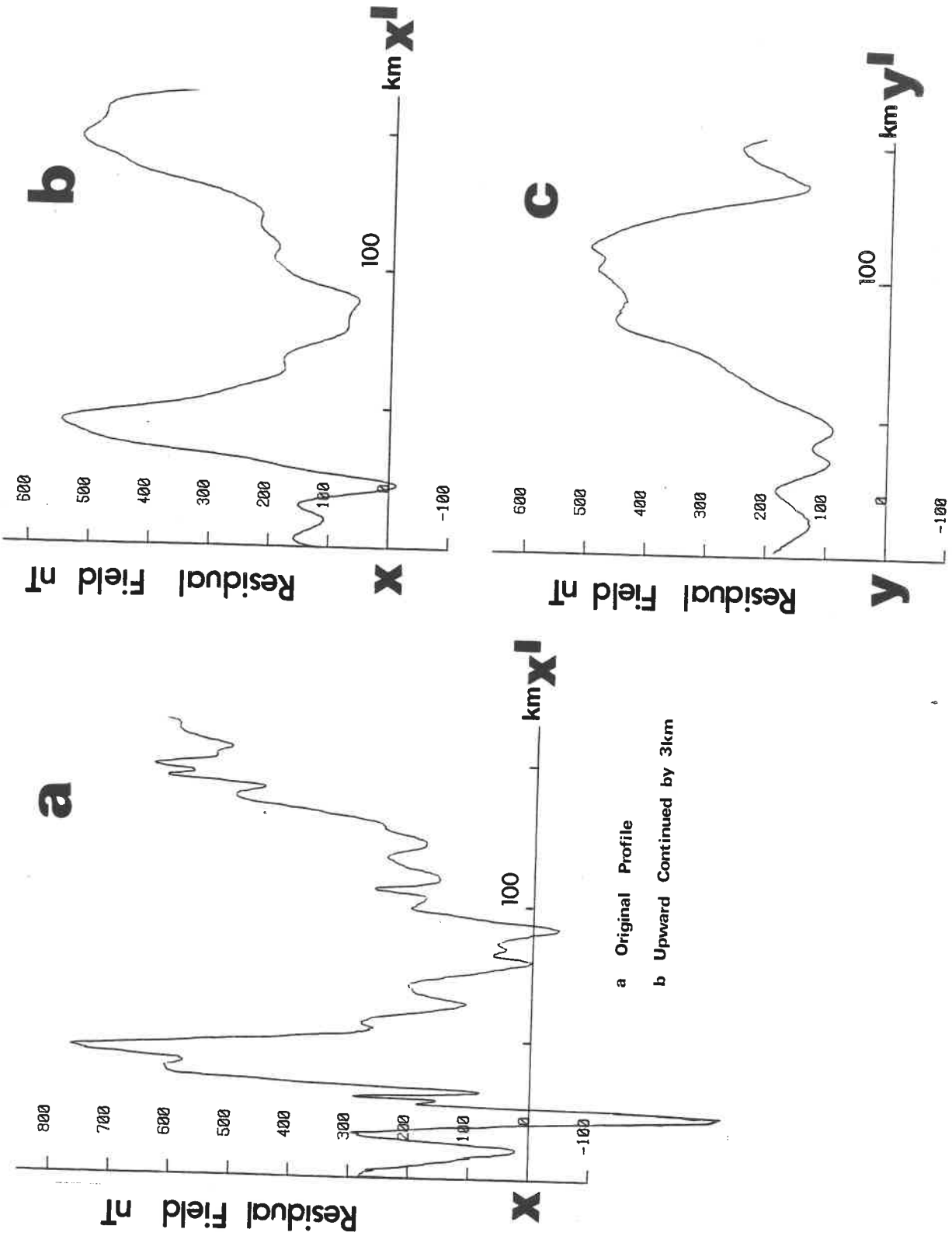


Fig. 6.4 Comparison of anomalies over exposed Cenozoic Volcanics and the Bryd Subglacial Basin.
(see fig 6.2 for locations)

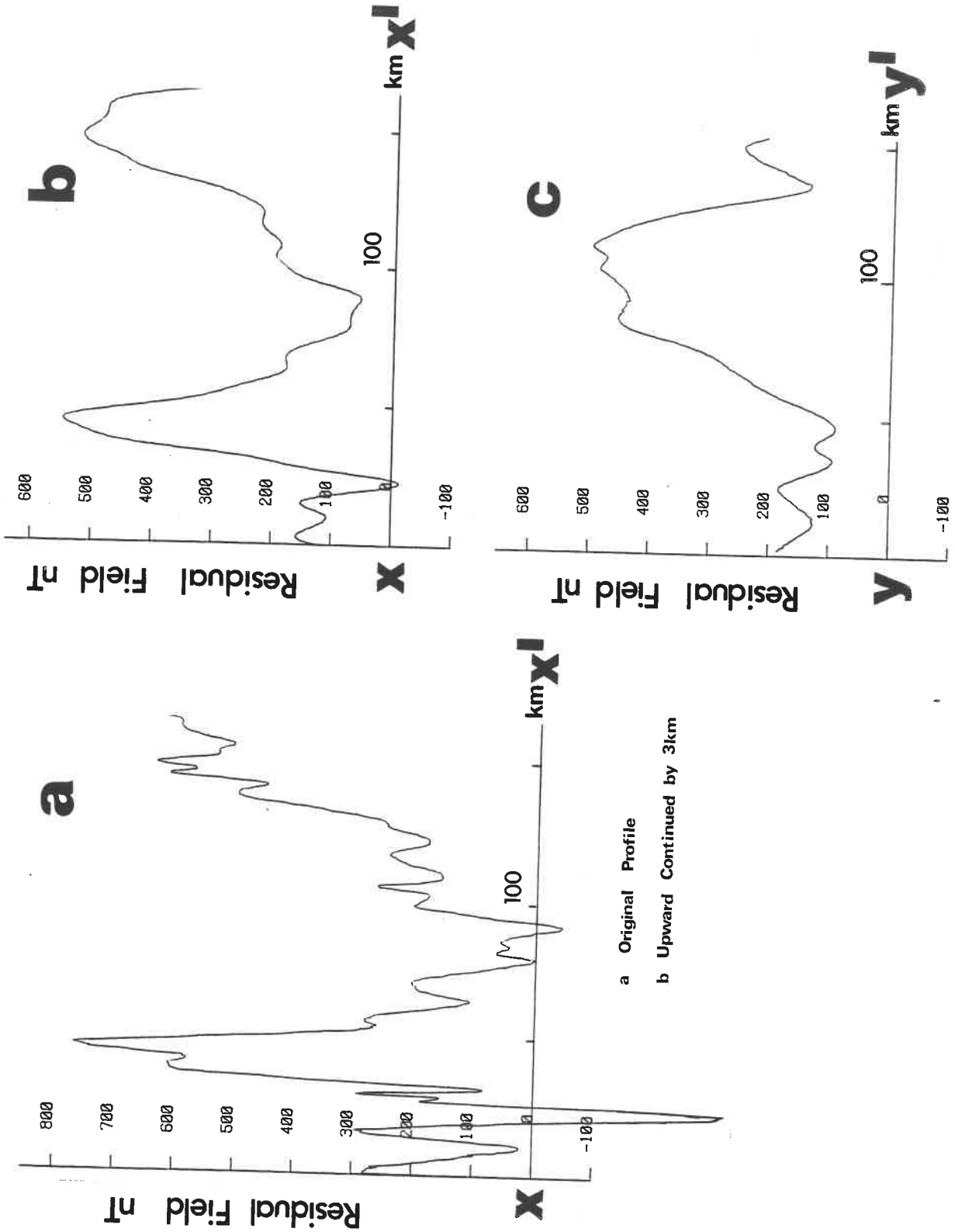


Fig. 6.4 Comparison of anomalies over exposed Cenozoic Volcanics and the Bryd Subglacial Basin.
(see fig 6.2 for locations)

susceptibilities required to fit the observed anomalies are relatively low, in the range 0.002 to 0.005 cgs. Both normal and reversed remanent magnetisations were required with amplitudes ranging from 0.0001 to 0.003 gauss (see fig. A3.6). The model was altered to take into account the maximum depth to magnetic basement as indicated in appendix 2. The maximum susceptibility required rose to 0.0133 cgs and the remanent magnetisation to 0.012 gauss (fig. A3.7). None of the volcanics sampled in appendix 1 had a value of susceptibility this high but they are still well within the value estimated by Bentley and Chang (1971) for the volcanics near the Crary Mountains (0.05 cgs). Profile B-B' is at 90° to A-A' and roughly perpendicular to a spur on the side of the ridge. Susceptibilities for fig. A3.8 are in the same range as those for the previous model (fig. A3.7) with values 0.006 to 0.0172 cgs. (see fig. 6.5) Remanent magnetisations however are all normal and in the range 0.002 to 0.007 gauss. Again the model was altered to take into account depth to magnetic basement. The resulting solutions however for susceptibility and remanent magnetisation are very high, maximum values being 0.09 cgs and 0.177 gauss respectively (see fig. A3.9). Either the magnetic basement is very basic in composition or the true magnetic basement is shallower than the maximum given by appendix 2. The latter would seem more reasonable. C-C' is similarly on a spur on the side of the ridge but further to the west. Susceptibilities in fig. A3.10 range from 0.007 to 0.019 cgs and remanent magnetisations from 0.003 to 0.011 gauss. No blocks have reversed magnetisations but the inclinations of the remanent magnetisation are significantly different from the present field directions suggesting that remanent magnetisation is still important. The result of modifying the model to fit the maximum depths to magnetic basement were to raise the maximum susceptibility to 0.0654 cgs and the remanent magnetisation to 0.09 gauss (see fig. A3.11). Completely reversed magnetisations were now needed to fit the observed data. Such high values of susceptibility would imply magnetite contents in excess of 10% for the causal body. Only very basic igneous rock is likely to have such a magnetite content. The values here are very similar to those from C-C' on fig. 6.2 and is further support for a similar origin for both the Cenozoic Volcanic Province of Marie Byrd Land and the ridge cutting

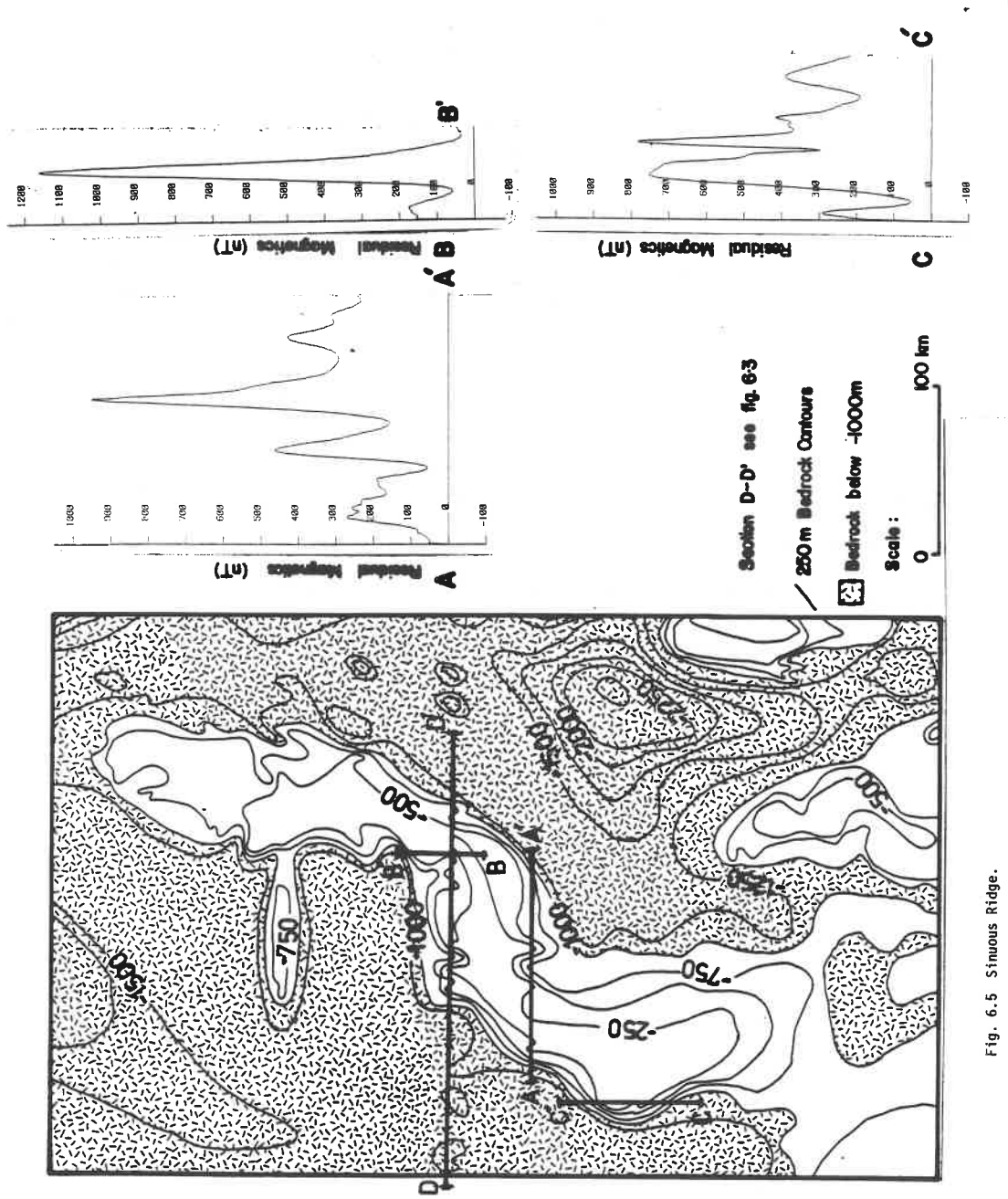


Fig. 6.5 Sinuous Ridge.

Fig. 6.5 Sinuous Ridge.

across the Byrd Subglacial Basin.

The formation of the Byrd Basin is a subject of much debate, although there is support for the basin having formed in an extensional tectonic environment (Elliot, 1974; LeMasurier and Rex, in press). Elliot (1974) envisages a tectonic environment in the mid-Mesozoic, somewhat similar to that of back-arc spreading within a continental plate, as responsible for the formation of the Byrd Basin. A problem, however, lies in the great distance between rifted zone and inferred trench lying along the edge of the continent (Elliot,1974). Ford and Kistler (1980) support the idea of a rift environment at this time but attribute it to a short lived intracontinental, incipient rift belt related to opening of the Weddell Sea during the initial development of the south-west Indian ridge. LeMasurier and Rex (in press), however, believe the basin to be much younger and to have formed since the development of the West Antarctic ice sheet citing much evidence from the exposed Cenozoic volcanics in Byrd Land and Ellsworth Land. Evidence for rifting during the Cenozoic is supported by the character of the volcanics (LeMasurier and Rex, in press) and also from studies of sea floor spreading in the south Pacific Ocean (Molnar et al,1975).

LeMasurier and Rex (in press) believe that the lack of a considerable thickness of recent sediment in the deep subglacial troughs in Marie Byrd Land indicates that they and the entire Byrd Basin have formed largely or entirely since the development of the continental ice sheet. However, the example of a linear subglacial trough in Marie Byrd Land used by LeMasurier and Rex was based on free air gravity anomalies given by Bentley and Chang (1971) (discussed in chapter 4) and considered speculative. Although seismic refraction data indicate only 0.5 km of recent sediment in the Byrd Subglacial Basin (Bentley and Clough,1972) source depths in fig. 6.1 suggest that in places the thickness of non-magnetic material, which need not necessarily be all volcanic in origin, is

much greater. Some block faulting during the Cenozoic, as seen in the displacement of the very flat pre-volcanic erosion surface in Marie Byrd Land is clearly apparent (LeMasurier and Rex,in press). The dissected appearence of the volcanic outcrops of Toney Mountain and Mount Takahe on fig. 2.8 on RES records does not rule out any vertical displacment but it is hard to believe that the entire Byrd Subglacial Basin could have formed in the same way. It is more reasonable to believe that the Byrd Subglacial Basin originally developed as a result of rifting and major tectonics in the middle to late Mesozoic but then underwent further rifting and modification during Cenozoic times.

6.2.3 ELLSWORTH - WHITMORE MOUNTAINS

Limited geological evidence available at present (Craddock and Webers, in press) suggest similarity between the Whitmore and Ellsworth Mountains. For this reason they will be discussed together.

The exposed Ellsworth Mountains are known to consist of several km of late Precambrian - Palaeozoic sedimentary and metasedimentary strata. A highland area exhibiting rugged relief was described in chapter 4 as extending westwards beneath the ice from the exposed ranges. This extension of the exposed, essentially non-magnetic sequence, into West Antarctica is supported by the magnetic data which shows the area having few anomalies and a generally smooth field (see figs. 5.9 and 5.10). This was also noted in previous magnetic work (Behrendt,1964b). Seismic evidence from Bentley and Clough (1972) indicates a relatively constant thickness of Ellsworth Mountains type Palaeozoic rock and/or granitic intrusives along the northern margin of the highland area from the western foothills of the Sentinel Range to south of Byrd Station. Source depths within this area nearly all indicate a combined thickness of non-magnetic material overlying basement in the range 3.5-8 km (see fig. 6.1). The

isolated outcrops of the Nash and Pirrit Hills, although topographically isolated from the main highland area, are considered nevertheless to be geologically related to the Mesozoic Ellsworth orogen. The thickness of sediment indicated by the source depths in the vicinity of the Pirrit Hills is consistent with those occurring at the southern end of the Ellsworth Mountains. Thicknesses near the Nash Hills are much less but these outcrops can be seen on fig. 2.8 to be a minor and more isolated feature.

The exposed Whitmore Mountains are surrounded by a large highland area and source depths from close to the exposed peaks give a thickness of non-magnetic material of 11.7 km (see fig. A2.2). In contrast seismic refraction data from a few km north of the Whitmore Mountains indicates a combined thickness of sediments and intrusives of only 0.7 km overlying basement (Bentley and Clough,1972). This of course can be explained for ascoustic basement need not always correspond to the magnetic basement. These workers however, did report a high velocity layer (~7 km) at an elevation of ~4 km below sea level which also appears on several profiles near the Transantarctic Mountains and concluded that apart from some massive limestones and marbles only mafic igneous rocks exhibit such high velocities. This layer is either the result of lower crustal rocks at an extremely shallow depth or is the result of a dolerite intrusion within the basement (Bentley and Clough,1972). Clearly this deep seated anomaly in the Whitmore Mountains could be related to such a layer, but only if it occurs at much greater depth beneath the exposed mountains. Other possible sources within the lower crust are unknown.

Separating the Whitmore Mountains block from the highland area extending south from the exposed Ellsworth Mountains is a deep and narrow trough reaching elevations of 1000 m below sea level. This feature has not been described previously and we can only speculate on its structural significance. The feature may represent a boundary between two different

areas or be the result of erosion. From the RES and magnetic evidence in this thesis, however, there is no good reason to suggest that the Whitmore Mountains belong to a separate tectonic unit.

The northern margin of this highland area abutting the Byrd Subglacial Basin is well defined topographically on fig. 2.8. Jankowski and Drewry (1981) showed that this margin also marks a distinct change in the pattern of magnetics from high amplitude anomalies to the north to a much more subdued field to the south that is consistent with subglacial extension of the exposed sediments in the Ellsworth Mountains. Fig. 6.6 shows example of topographic and magnetic profile across this boundary. This boundary also exhibits, as would be expected, a marked change in the depth to magnetic basement. To the south, in the Ellsworth block, magnetic basement lies 3-8 km below the ice/rock interface while to the north it is generally less than 2 km and at many places coincides with it. The seismic evidence, magnetics and RES all suggest that this margin represents the boundary between two distinctly different geological provinces.

To the west, in the area south of Byrd Station, the boundary becomes less well defined. RES data suggests that the boundary follows the edge of the deep subglacial basin around to the west side of the Whitmore Mountains before passing into the complex area between the Whitmore and Thiel Mountains. The change in the magnetic field described however can be seen in fig. 6.7 to depart significantly from the position of the boundary as suggested by the RES data. The high amplitude anomalies to the north, associated with volcanics in the Byrd Subglacial Basin seem to continue without break very close to the Whitmore Mountains. What is impossible to distinguish is the age of the sources of the magnetic anomalies. The anomalies near the Whitmore Mountains, although similar in appearance to those associated with the Cenozoic volcanics, may be older and related to activity when the Ellsworth-Whitmore Mountains were in their original position in Gondwanaland.

areas or be the result of erosion. From the RES and magnetic evidence in this thesis, however, there is no good reason to suggest that the Whitmore Mountains belong to a separate tectonic unit.

The northern margin of this highland area abutting the Byrd Subglacial Basin is well defined topographically on fig. 2.8. Jankowski and Drewry (1981) showed that this margin also marks a distinct change in the pattern of magnetics from high amplitude anomalies to the north to a much more subdued field to the south that is consistent with subglacial extension of the exposed sediments in the Ellsworth Mountains. Fig. 6.6 shows example of topographic and magnetic profile across this boundary. This boundary also exhibits, as would be expected, a marked change in the depth to magnetic basement. To the south, in the Ellsworth block, magnetic basement lies 3-8 km below the ice/rock interface while to the north it is generally less than 2 km and at many places coincides with it. The seismic evidence, magnetics and RES all suggest that this margin represents the boundary between two distinctly different geological provinces.

To the west, in the area south of Byrd Station, the boundary becomes less well defined. RES data sugests that the boundary follows the edge of the deep subglacial basin around to the west side of the Whitmore Mountains before passing into the complex area between the Whitmore and Thiel Mountains. The change in the magnetic field described however can be seen in fig. 6.7 to depart significantly from the position of the boundary as suggested by the RES data. The high amplitude anomalies to the north, associated with volcanics in the Byrd Subglacial Basin seem to continue without break very close to the Whitmore Mountains. What is impossible to distinguish is the age of the sources of the magnetic anomalies. The anomalies near the Whitmore Mountains, although similar in appearance to those associated with the Cenozoic volcanics, may be older and related to activity when the Ellsworth-Whitmore Mountains were in their original position in Gondwanaland.

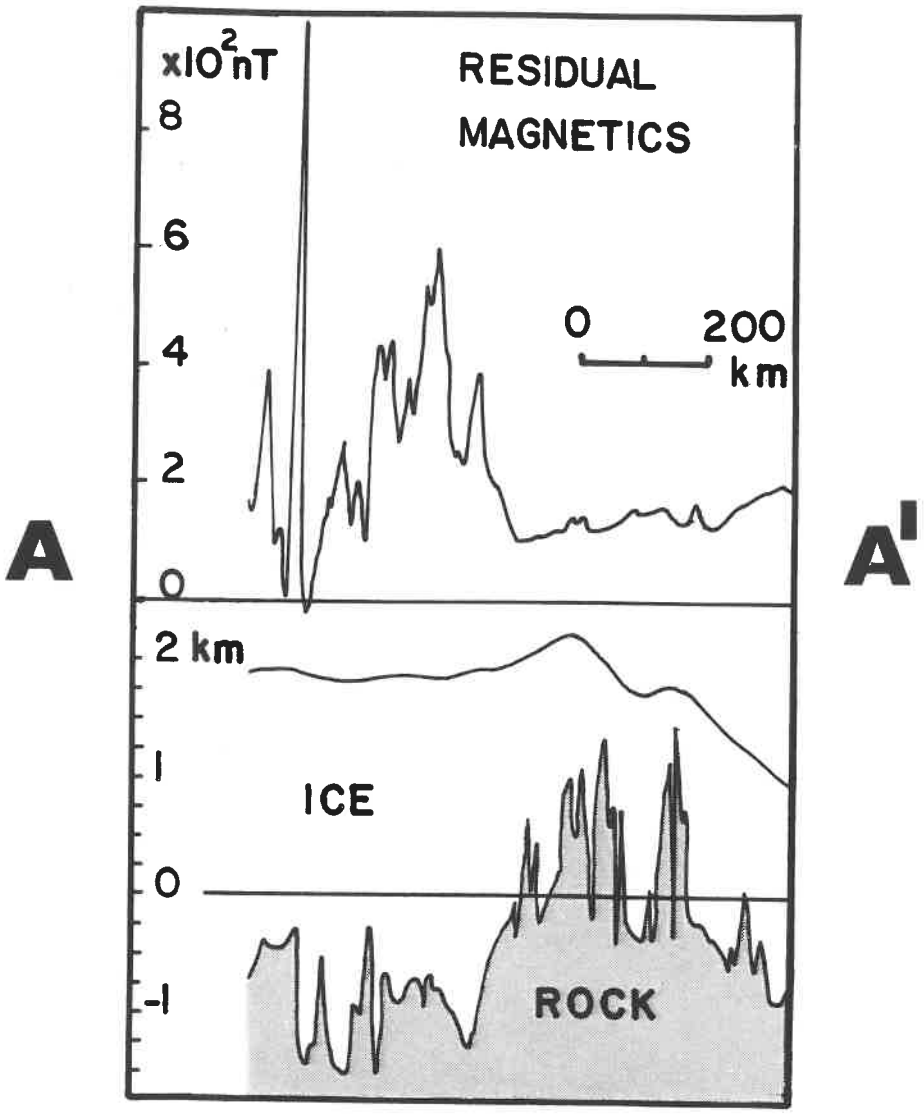


Fig. 6.6 RES and magnetic profile across boundary between Byrd Subglacial Basin and Ellsworth Mtns.

In contrast to the northern flank of the Ellsworth-Whitmore Mountains area which is well defined the southern flank is more complex and problematic. The location of the boundary zone between the Whitmore and Thiel Mountains will be discussed in a later section following discussion of the Transantarctic Mountains.

Bedrock at the head of the Ronne-Filchner Ice Shelf forms a deep depression (up to 2000 m below sea level) which appears to widen out towards the ice shelf. Behrendt et al (1974) report a substantial thickness of sediment in this area on the basis of the very smooth magnetic field. This is supported by the magnetic data presented here (see figs. 5.9 and 5.10) and isolated source depths indicate that magnetic basement lies well below the ice/rock interface (see fig. 6.1). Speculations on the significance if this bedrock low can be given. Hochstein calculated depth to MOHO at 83° S 70° W, on the southern edge of this basin, reporting thin crust of 24 km (Bentley,1973). The idea that the Ellsworth Mountains and any associated subglacial area is 'out of place' in West Antarctica is not new (eg. Schopf, 1969; Stump, 1973; Elliot,1975; Clarkson and Brook, 1977; Dalziel, in press). It is therefore possible that the bedrock low, underlain by thin crust and infilled with several km of sediment is related to rifting that would have accompanied any displacment of the Ellsworth Mountains block.

The eastern boundary of the Ellsworth Mountains, beneath the Ronne-Filchner Ice Shelf is unknown. No data were collected from this region, but Clarkson and Brook (1977) have, however, analysed gneisses and schists from the Haag Nunataks (77° 02 S 78° 20 W) and conclude that they represent an up-faulted slice of the metamorphic basement underlying the Ellsworth Mountains. Apart from a deep subglacial trough between the Ellsworth Mountains and the Orville Coast, which may continue eastward to the north of the Haag Nunataks, there are insufficient data to delimit the margins of this fragment of continental crust (Clarkson and Brook,1977).

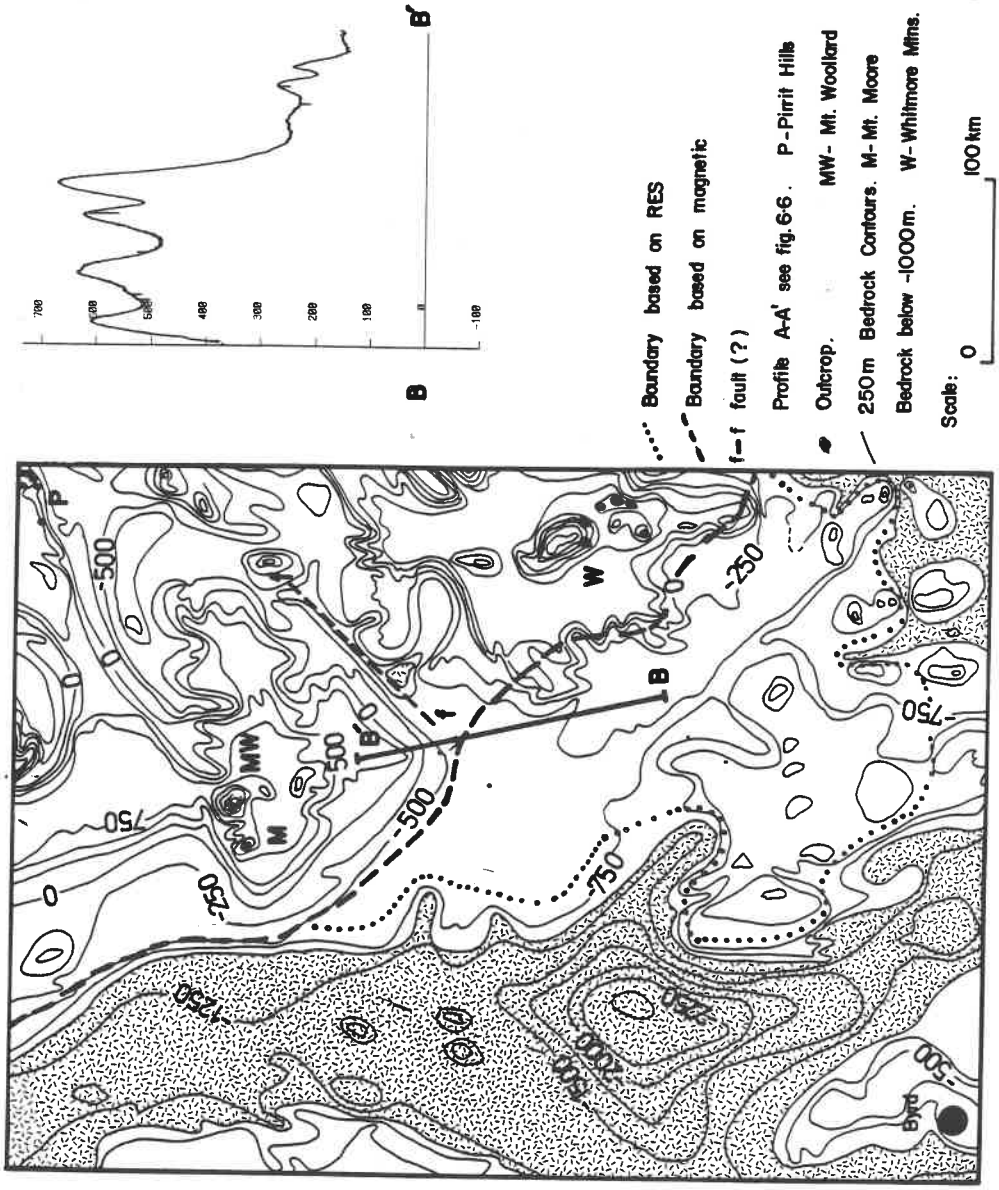


Fig. 6.7 Boundary between Byrd Subglacial Basin and Ellsworth Mtns.

Fig. 6.7 Boundary between Byrd Subglacial Basin and Ellsworth Mtns.

6.2.4 TRANSANTARCTIC MOUNTAINS

Previous geophysical investigations (Robinson,1964a) have shown that the ranges forming the block faulted Transantarctic Mountains continue for several hundred kilometres beneath the East Antarctic ice sheet. RES studies in the main part of the Transantarctic Mountains from the Horlick Mountains to Cape Adare by Drewry (1973) and Steed (1980) supported this view and showed that there is a generally uniform transition between the exposed ranges and the continental interior with no evidence of major structural discontinuities. The RES studies presented in this thesis confirm this structure for the isolated ranges forming the continuation of the Transantarctic Mountains from the Ross Ice Shelf to the Ronne-Filchner Ice Shelf. High elevations related to the mountain chain continue beneath the ice linking the Horlick Mountains to the Thiel Mountains (see fig. 2.8). The only breaks to an otherwise continuous mountain chain are the narrow troughs bounding the Pensacola Mountains and the roughly N-S trending trough between the Thiel Mountains and the Patuxent Range of the Pensacola Mountains. Whether these troughs have any structural significance is uncertain, they are discussed in a later section of this chapter.

The geology of the Transantarctic Mountains, outlined in detail in chapter 1, comprises of a basement complex of late-Precambrian to lower Palaeozoic meta-sedimentary and meta-volcanic rocks intruded by numerous calc-alkaline lower Palaeozoic plutons. This basement complex is overlain unconformably by a relatively flat lying Upper Palaeozoic - Mesozoic non-marine sedimentary sequence that has been intruded and overlain by Jurassic tholeiitic rocks.

Source depths for magnetic anomalies from this work and Behrendt and Wold (1963) show in places evidence of a substantial non-magnetic, presumably sedimentary sequence, overlying magnetic basement in the ice covered areas surrounding the exposed parts of the Transantarctic Mountains (see fig. 6.1). Around the Horlick, Thiel and southern end of the Pensacola Mountains source depths indicate thicknesses of non-magnetic material in the range 2.5-6.5 km with a few isolated solutions falling outside this range. The data suggests a general shallowing of the magnetic basement towards the interior of East Antarctica. Seismic refraction studies from south of the Horlick Mountains (column 29 on Table 1.3) would indicate only 300 m of sediment overlying basement (Bentley and Clough,1972) and thus corroborate this conclusion. No significant anomalies were recorded over the East Antarctic basement south of the Transantarctic Mountains. The subdued field is likely to be, in part, due to the large separation between magnetometer and source (~3 km). The source depths exhibit no consistent pattern but vary in the range 0 km to 4 km below the ice/rock interface. However, this is expected for a metamorphic terrain that has undergone a long and complex history of deformation and thermal events.

The Transantarctic Mountains have zones of numerous anomalies of narrow width and other areas with an essentially smooth field (Behrendt, 1964b). The narrow width anomalies are probably associated with the McMurdo Volcanics. Abundant tholeiitic sills and dykes that occur in the Transantarctic Mountains are unlikely to be the cause of the narrow width anomalies as susceptibilities reported by Bull et al (1962) for the Ferrar Dolerites are quite low (<0.002 cgs). The McMurdo Volcanics do not extend into the area surveyed and consequently no anomalies of narrow width were recorded. The majority of the sources within the area seem likely to be related to the metamorphic basement complex, although possible sources within the basement are unknown.

The source of the very high amplitude anomalies recorded in the Pensacola Mountains is however now well known (Behrendt et al, 1974; Behrendt et al, 1980, 1981). These anomalies occur in the vicinity of the Forrestal Range and Dufek Massif which form only part of a large (>50000 km^2) layered mafic intrusion in which measured susceptibilities range from 0.1 to 0.0007 cgs. The bedrock data in fig. 2.8 indicated a slight depression in the bedrock surface between the exposed sections in the Forrestal Range and Dufek Massif. Jankowski and Drewry (1981) attribute this to the lopolith-synclinal form of the intrusion that is not primary but has developed as the result of weak folding after emplacement (Behrendt et al,1974). The possible tectonic setting of this large intrusion is of importance to the evolution of this part of Gondwanaland and is discussed in a later section.

6.2.5 BOUNDARY BETWEEN EAST AND WEST ANTARCTICA

The nature of the boundary zone between East and West Antarctica is not well understood. Information on the deep structure is beyond the RES and magnetic data available to this thesis. The only contribution to the discussion involves the position and near surface manifestations of this boundary zone. Unlike the East Antarctic margin of the Transantarctic Mountains the West Antarctic margin is in places abrupt. Long (1965) reported a boundary fault system of ~3000 m displacement, between the Ohio Range of the Transantarctic Mountains and the bedrock of West Antarctica (see fig. 1.3). Further north Barrett (1965) reported a similar fault of ~5000 m throw at Cape Surprise in the Beardmore Glacier area. A steeply dipping fault has also been mapped in the Pensacola Mountains separating the Neptune Range from the Schmidt Hills (Behrendt et al, 1974). The abrupt margin to the Transantarctic Mountains appears a logical position for the transistion between East and West Antarctica across which the depth to MOHO is believed to decrease by ~10 km (Adams,1972). The cause of the marked bouguer gravity gradient across the boundary is a matter of debate

but is further evidence that the Transantarctic Mountains overlie an important and major tectonic transistion. A steep fault-like boundary would seem reasonable if the Transantarctic Mountains marked the edge of the continent at the time of separation of Gondwanaland (Behrendt et al,1974). The steep margin to the Transantarctic Mountains observed on RES records in the ice covered areas around the Horlick Mountains and southern Pensacola Mountains (fig. 6.8) appears consistent with a fault interpretation. The depth to which a fault zone may extend is however a matter of conjecture.

The precise location of the boundary zone in the area between the end of the Horlick Mountains and the Patuxent Range of the Pensacola Mountains, as mentioned, is difficult to ascertain. The Thiel Mountains lying roughly half-way between the two would seem on topographic grounds and geological similarities (Ford and Sumsion,1971) to belong to the same tectonic province as the Transantarctic Mountains in this area. Source depths between the Horlick and Thiel Mountains (see fig. 6.1) are fairly constant giving a thickness of non-magnetic material in the range 2-4 km indicating no major changes in structure. The Whitmore Mountains lie ~250 km to the north of the Thiel Mountains and show geological similarities to the Ellsworth Mountains, a separate tectonic province (Craddock and Webers,in press). The scattered outcrops of the Stewart Hills, Hart Hills and Pagano Nunatak are more problematic. Pagano Nunatak consists entirely of felsic plutonic rocks and like those of the Whitmore Mountains gives isotopic ages in the range 163-190 Ma BP (Craddock and Webers,in press), and are, therefore, related to the early Mesozoic Ellsworth orogen. The Stewart Hills consist of tightly folded meta-sedimentary rocks with a radiometric age of 508 Ma BP and like the Thiel Mountains, retain a record of the older lower Palaeozoic Ross orogeny (Craddock and Webers,in press). The Hart Hills are a problem as their tectonic position is as yet unknown, consisting of deformed meta-sediments and probably younger altered gabbroic rocks.

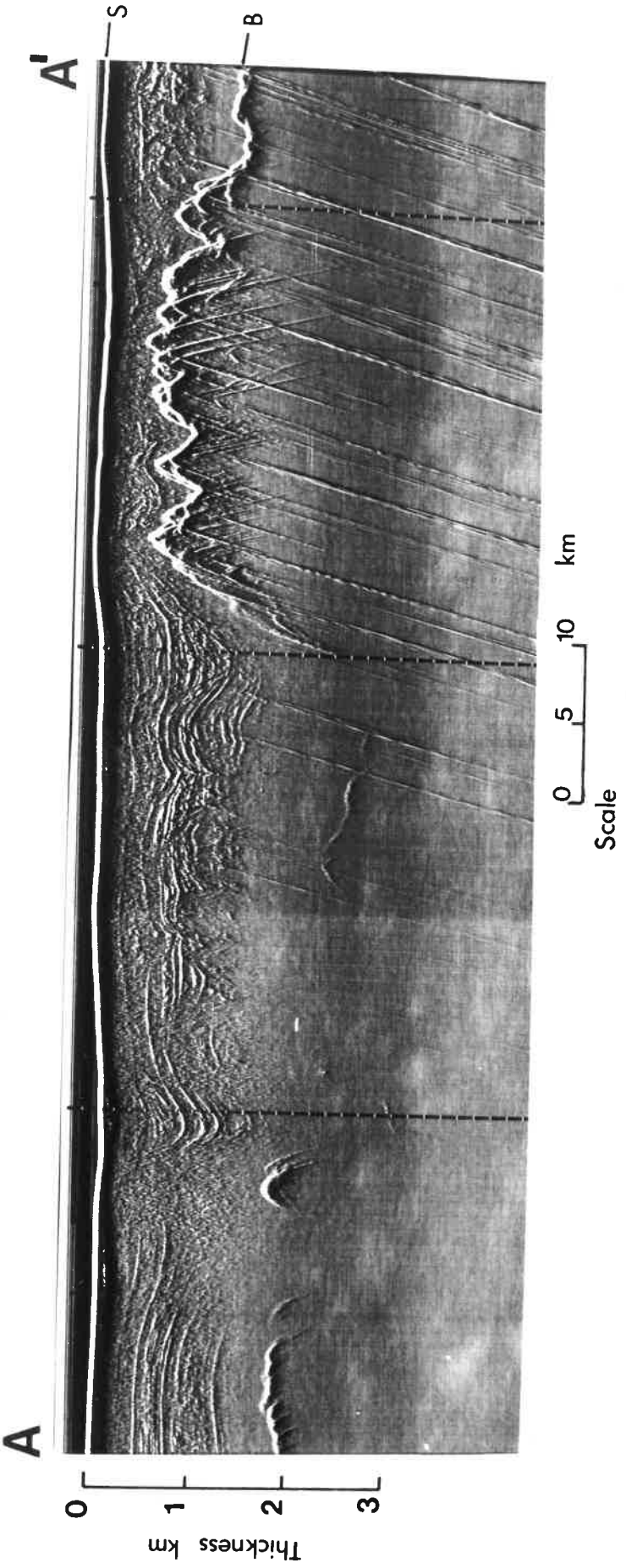


Fig 6.8 RES profile over margin of Transantarctic Mtns.

The boundary zone between the two different tectonic provinces of the Ellsworth Mountains and Transantarctic Mountains must pass through this complex area. Lying between the scattered outcrops and the Thiel Mountains is an area of highland (see fig. 6.9) connected to the Whitmore Mountains by a series of upstanding blocks but separated from the Thiel Mountains by a narrow trough. There does not appear to be any logical topographic boundary between the provinces. The tectonic position of this highland area between the Thiel Mountains and the Hart Hills is uncertain. This area lies close to the boundary zone and may therefore show affinities to either tectonic province or even both.

The area of highland between the scattered outcrops and the Thiel Mountains is associated with a pronounced magnetic anomaly of ~350 nT which occurs on two adjacent lines (see fig. 6.9). Source depths on these two anomalies plus solutions 96 and 327 in appendix 2 are all significantly deeper than those surrounding the Thiel Mountains giving a thickness of non-magnetic material in the range 4.2-9.9 km. The two anomalies in fig. 6.9 would appear to be due to the same causal body. If this is the case then the strike of the causal body is ~40° off perpendicular reducing the depths by ~23%. What is clear, however, is that the magnetic basement beneath the highland area is significantly different from that beneath the Transantarctic Mountains or that around Hart Hills and Pagano Nunatak. The nature of the causal body is unknown. Altered gabbros in the Hart Hills were sampled but their susceptibility is too low to give rise to these anomalies (0.00007 cgs, see appendix 1) nor the felsic intrusives of Pagano Nunatak (0.00004 cgs) or the granites of the Thiel Mountains (0.00205- 0.00236 cgs). If the causal body is associated with the Transantarctic Mountains then it is necessary to infer a major fault on the northern side of the Thiel Mountains downthrowing this block. Another possibility is that the Thiel Mountains block is underlain by basement that is not exposed in the surrounding nunataks. The evidence would tend to suggest that

1) The Whitmore Mountains and Pagano Nunatak are formed partially or

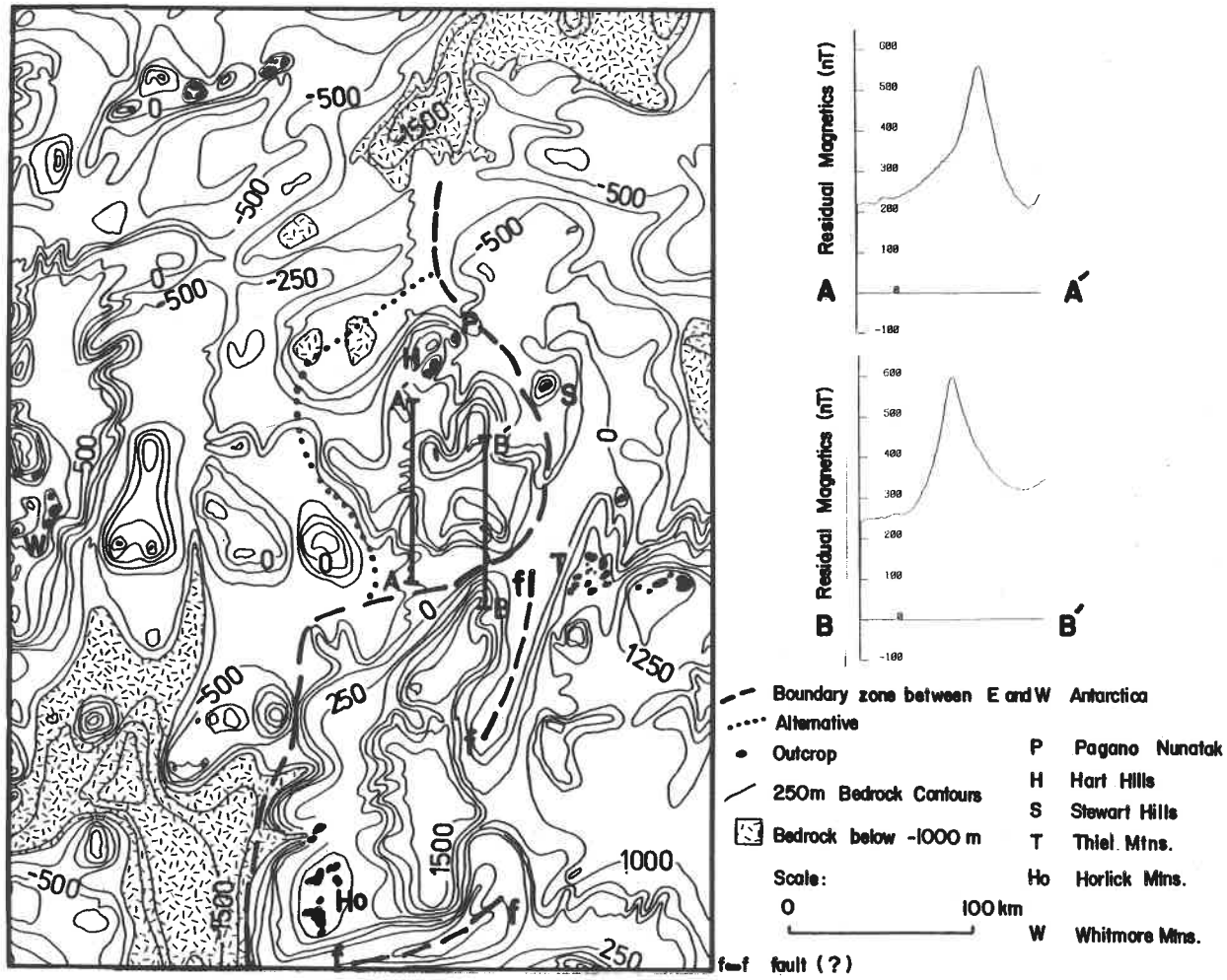


Fig. 6.9 Boundary between East and West Antarctica.

Fig. 6.9 Boundary between East and West Antarctica.

wholly of felsic plutons that are isot opically younger than those of the Stewart Hills and Thiel Mountains.

2) There appears to be a change in depth to magnetic basement between the Thiel Mountains and the scattered outcrops of the Hart Hills and Pagano Nunatak with a corresponding increase in the thickness of non-magnetic rocks overlying the basement.

It seems likely that the boudary zone between East and West Antarctica passes through this area between the Thiel Mountains, Stewart Hills and the Hart Hills and Pagano Nunatak. Until the tectonic position of the Hart Hills and the highland area between them and the Thiel Mountains can be determined more precisely then the boundary zone could follow either one of two lines shown on fig. 6.9.

6.3 IMPLICATIONS TO THE TECTONIC HISTORY OF ANTARCTICA

In chapter 1 the tectonic history of Antarctica was briefly outlined, dividing it into two regions comprising a stable Precambrian continental shield area (East Antarctica) and a series of younger orogenic belts lying along the margin of the shield and extending Pacific wards to form West Antarctica. These orogenic belts become progressively younger away from the shield area and in places there is considerable overlap (Elliot,1975). In such a complex area as West Antarctica, where rock exposure is very small, the structural division into areas belonging to different periods of orogenic activity is a major problem but of considerable interest for regional tectonic interpretations. The preceding sections of this chapter described the structure of West Antarctica in terms of major units. Those conclusions can now be discussed in the context of the tectonic evolution of Antarctica as we understand it.

The Transantarctic Mountains lie along the margin of the East Antarctic shield area and mark the site of repeated deformation and intrusive activity. The earliest deformation may have occurred ~1000 Ma BP in the Nimrod orogeny, recognised along the Shackleton Coast (Grindley and McDougal,1969) although recent work has cast some doubt on the existence of a separate orogeny (Adams et al, in press). The first well documented orogeny, the Beardmore orogeny, occurred in the late Precambrian in the central Transantarctic Mountains and was accompanied by large batholithic intrusions (Elliot,1975). The lower Palaeozoic Ross orogeny is the most widespread in the Transantarctic Mountains. A 500 Ma BP thermal event is recorded over a wide area in East Antarctica (Elliot,1975). A younger mid-Palaeozoic event, the Borchgrevink orogeny of Craddock (1970) and Elliot (1975) is described in North Victoria land but this now seems to be limited to granitic intrusive activity alone (Wright,1980). It is possible that this intrusive activity is a late phase of activity related to the Ross event.

This history of deformation along the margin of the East Antarctic shield area has resulted in the rugged and complex struture exhibited by the Transantarctic Mountains at the present day. RES has shown the elevated and rugged terrain of the exposed mountains to extend beneath the ice cover into East Antarctica for several hundred kilometers gradually decreasing in relief with no marked inland boundary. The magnetic data confirm this with a general shallowing of the magnetic basement inland. This contrasts sharply with an abrupt margin on the West Antarctic side of the Transantarctic Mountains.

The isolated ranges in West Antarctica marking the continuation of the Transantarctic Mountains chain (eg. Pensacola Mountains, Thiel Mountains) have undergone further deformation during the late Palaeozoic - early Mesozoic. The dissected nature of this part of the Transantarctic Mountains may reflect the more complex tectonic history. In mid-Jurassic times vast amounts of mafic magma were generated as seen in the Dufek Intrusion of the Pensacola Mountains and throughout the Transantarctic Mountains as the Ferrar Dolerites and Kirkpatrick Basalts. Although these Jurassic tholeiitic rocks have been associated with an extensional tectonic regime (Elliot,1974) new data has shown that the Dufek Intrusion now ranks almost alongside the Bushveld Intrusion in size (Behrendt et al, 1980,1981) and has prompted new interpretations. Ford and Kistler (1980) suggest that the Transantarctic Mountains lie along a failed rift system related to opening of the Weddell Sea. Considerable disruption of the crust might be expected in this area if the Dufek Intrusion lay close to an active triple junction in Mesozoic times. The troughs bounding two sides of the Pensacola Mountains although now occupied by major ice streams, and the trough between the Patuxent Range and the Thiel Mountains may reflect this disruption.

A major problem in Antarctic tectonics has been reconciliation of the trend of late Palaeozoic - early Mesozoic deformation in the Ellsworth Mountains with that of a similar age in the Pensacola Mountains. This discordant trend and the similarities in stratigraphy led to the idea that the Ellsworth Mountains are 'out of place' in West Antarctica (Schopf, 1969; Stump, 1973; Elliot, 1975; Clarkson and Brook, 1977). This is now well supported by recent palaeomagnetic data which have shown ~90^{o} difference between mean declinations of palaeomagnetic vectors from late Cambrian and early Ordovician rocks in the Ellsworth Mountains and the East Antarctic Craton (Watts and Bramall,1980). An original position for the Ellsworth Mountains westward of the Littlewood Nunataks at ~35^{o} W on the edge of the Ronne-Filchner Ice Shelf is suggested (Clarkson and Brook,1977). With the Ellsworth Mountains in this position there is

continuity between the Cape Fold Belt, the Ellsworth Mountains and the Transantarctic Mountains. Also the early Mesozoic intrusives of the Whitmore Mountains would no longer occur within West Antarctica many hundreds of kilometres from the continental edge. They would lie in much closer proximity to similar Gondwanide plutons in South America and the Peninsula which are related to active subduction and must occur relatively close to the active Pacific continental margin of Gondwanaland. Exact timing of displacement of the Ellsworth Mountains is difficult to fix, although it would seem likely that it was associated with the opening of the Weddell Sea in middle to late Jurassic (Elliot,1972).

Naturally the original position and timing of displacment are impossible to reassess here but the extent of the Ellsworth Mountains continental fragment and signs in West Antarctica of large scale movements can be commented upon. The boundaries of the Ellsworth Mountains structural unit were discussed earlier and include a large part of West Antarctica. The bedrock low at the head of the Ronne-Filchner Ice Shelf has already been attributed to possible rifting associated with the displacement of the Ellsworth Mountains. Geological evidence would include the Whitmore Mountains in the same structural unit (Craddock and Webers,in press). This is supported by the RES data (Jankowski and Drewry,1981) but the deep narrow trough between the Whitmore Mountains and the subglacial extension of the Ellsworth Mountains may represent secondary disruption of this continental fragment. This might be expected, for the Whitmore Mountains would lie on the leading, compressional edge of this continental fragment.

At the time of displacement of the Ellsworth Mountains and injection of large volumes of tholeiitic magmas into the Transantarctic Mountains the Pacific coast areas of West Antarctica were intruded by calc-alkaline intrusives in a compressive tectonic environment related to possible subduction of Pacific oceanic crust. A spreading centre is thought to have been active in the South Pacific at this time (Molnar et al, 1975). The

Byrd Subglacial Basin probably formed contemporaneously as a result of extension perhaps in the form of back-arc spreading while the Weddell Sea was being opened and the Ellsworth mountains were being rotated into position. The amount of extension in the Byrd Subglacial Basin is unknown but must have been several hundred kilometers.

The last major tectonic event in West Antarctica involves Cenozoic volcanism and associated extensional tectonics. The magnetic data indicate that volcanic rocks probably underlie most of the Byrd Subglacial Basin and extend close to the Whitmore Mountains. However it is not possible to ascertain whether the volcanic sources are all of the same age. Those close to the Whitmore Mountains may be older and related to volcanic activity at an active continental margin prior to displacement of the Ellsworth-Whitmore Mountains. The Marie Byrd Land volcanics of Cenozoic age are related to extensional tectonics (LeMasurier and Rex, in press) but this tectonic regime is not thought responsible for the formation of the entire Byrd Subglacial Basin, although it may have resulted in some vertical faulting and modification of the features. Near the head of the Ross Ice Shelf recent sedimentation has infilled the continuation of this basin producing the subdued topography seen on RES records. The Transantarctic Mountains underwent vertical tectonics in the Cenozoic ,the Victoria orogeny.

6.4 WEST ANTARCTICA AND GONDWANALAND

Antarctica has long been considered the 'key-stone' of Gondwanaland and many attempts (fig. 1.14) made to reassemble the southern continents around Antarctica. Probably due to the lack of exposed bedrock in Antarctica, which has hindered understanding of the geology and structure, its position remains a problem in such reconstructions. Whereas for the fit of many of the other continents arguments about positions are related

to scales of tens of kilometers, in Antarctica there is still considerable debate as to whether one plate or more, and if more than one the number of microcontinental fragments and their relative movement remain major questions. Many of the answers to these problems are thought to lie beneath the ice-covered regions of West Antarctica. A better understanding of the structure of West Antarctica and its sub-division into crustal fragments provided by this thesis helps to reduce several of the many degrees of freedom in Gondwana reconstructions. For completeness a model for the breakup of Gondwanaland, concentrating on events affecting West Antarctica, is presented based largely on previous work but incorporating the better understanding of the structure of West Antarctica.

6.4.1 GONDWANALAND RECONSTRUCTION

As described in chapter 1 Antarctica appears in Gondwanaland reassemblies either as a single unit retaining its present day outline or is broken into a variable number of fragments each able to move independently. In the former type of reconstruction, (eg. Smith and Hallam, 1970; Dietz and Holden, 1970; Tarling, 1973; Norton and Sclater, 1979) distortion of the Scotia Sea region is produced or there is unacceptable overlap between the Antarctic Peninsula and South America or South Africa. Most of these reconstructions were made before the establishment of continental crust beneath the Falkland Plateau (DSDP,1977) which effectively ruled out any overlap. Harrison et al (1979) overcame this constraint for a single plate Antarctica by placing the Antarctic Peninsula along the Pacific side of South America, a position strongly criticised by Dalziel (1980). The pre-Jurassic basement in both South America and the Antarctic Peninsula consists of forearc and arc terrains which would be doubled up in an improbable manner in the reconstruction of Harrison et al (1979).

The weight of evidence from study of the oceanic magnetic anomalies in the southern oceans, from careful study of the exposed Antarctic geology, from palaeomagnetic evidence and from the geophysical work presented here suggests that Antarctica consists of at least 2, if not more, separate plates (eg. Schopf, 1969; Scharnberger and Scharon, 1972; Stump, 1973; Barker and Griffiths, 1972,1977; Herron and Tucholke, 1976; Molnar et al, 1975; DSDP, 1977; Dalziel, 1980; Kellogg, 1980; Watts and Bramall, 1980; Gordon and Cox, 1980).

Such evidence leads this writer to believe that prior to breakup of Gondwanaland Antarctica consisted of 5 crustal plates comprising the East Antarctic Craton, the Ellsworth - Whitmore Mountains, Marie Byrd Land, the Antarctic Peninsula and Thurston Island/Eights Coast. A recent reconstruction presented at the Fifth Gondwana symposium included a sixth plate, termed the Filchner plate (de Wit, 1979). The existence of continental crust beneath the Ronne-Filchner Ice Shelf is unknown and this extra plate is considered highly speculative, a view shared by Dalziel (pers. comm.)

In fig. 6.10 the East Antarctic plate is drawn using the present outline of the East Antarctic continental shelf with its Pacific margin drawn along the abrupt western margin of the Transantarctic Mountains. This margin passes to the north of the Thiel Mountains and then just to north of the Dufek Intrusion following the boundary discussed in section 6.2.5. The Dufek Intrusion is now known to extend as far east as Berkner Island and lies along the edge of the East Antarctic craton (Behrendt et al, 1981). This would imply that part of Berkner Island is underlain by continental crust of the East Antarctic plate. However, it is preferred that the Dufek intrusion lies along a major tectonic boundary and that not all of it was intruded into continental crust but may have infilled a void created during the opening of the Weddell Sea. The Ellsworth plate is drawn so as to include the Whitmore Mountains and following the boundaries discussed

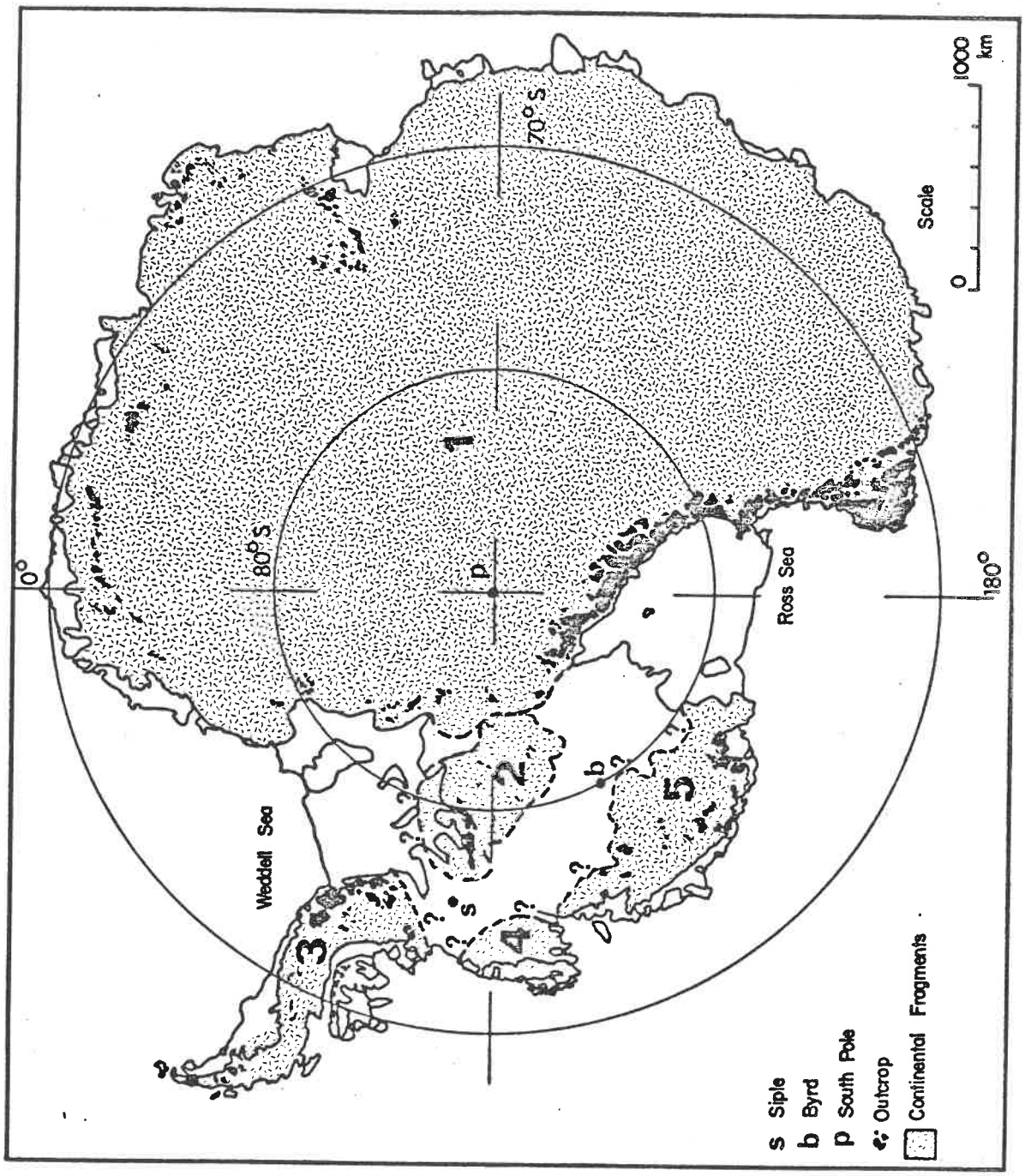


Fig. 6.10 Micro-continental fragments of West Antarctica.

in 6.2.4. The Marie Byrd Land plate is drawn using the present continental edge and so as to include the Palaeozoic basement rocks of the Kohler Range and the Ruppert Coast. The inland margin is drawn around the high terrain surrounding the Cenozoic volcanics . The Byrd Subglacial Basin is considered a post breakup feature and is thus eliminated. A separate plate is drawn around Thurston Island and the Eights Coast so as to include the exposed Palaeozoic intrusives and high grade metamorphic rock, and because this area of older continental crust appears to be isolated from the Peninsula and Marie Byrd Land. The RES data does not show the Eights Coast being connected topographically to the high areas of Marie Byrd Land. The Antarctic Peninsula plate is drawn as shown in de Witt (1979).

Supported by palaeomagnetic evidence the Ellsworth plate has been rotated clockwise through ~90^{o} to a position just westward of Littlewood Nunataks (Clarkson and Brook, 1977). This brings the trend of folds in the Ellsworth Mountains into line with those of a similar age in the Transantarctic Mountains. Dalziel (in press) believes in the general continuity of fold belts across Gondwanaland from the Sierra de la Ventana of NE Argentina to the Cape Fold Belt of South Africa and continuing through the Transantarctic Mountains into New Zealand and Australia (fig. 6.11a). The gap left by removal of the Ellsworth Mountains is closed by moving the Peninsula, Marie Byrd Land and the Eights Coast into proximity with the East Antarctic craton. Marie Byrd Land in this position would suggest a close link with the geology of New Zealand (not shown if fig. 6.11a). This is supported by Grindley and Davey (in press), who suggest that the basement geology of Marie Byrd Land resembles that of SW New Zealand. A direct relationship has also been suggested between the Swanson Formation of the Ford Ranges, Marie Byrd Land, and the Robertson Bay Group of North Victoria Land although the evidence is not conclusive (Wade and Long, in press). Marie Byrd Land in a position shown in fig. 6.11a would however lend support to these ideas.

The shape of the Peninsula is a matter of debate. The cuspate form of the southernmost Andes and the northern end of the Peninsula was attributed by Dalziel and Elliot (1971) to fragmentation of an originally continuous rectilinear cordillera. More recently Dalziel (in press) has rejected this idea although he does not think the shape need be original (ie pre-Cretaceous) as shown by Barker and Griffiths (1972). The shape of the Peninsula used here is the present shape and that used in Barker and Griffiths (1972, 1977) and de Witt (1979). In the Barker and Griffiths (1972) reconstruction the Antarctic Peninsula is placed alongside the Caird Coast of East Antarctica based on their reconstructions of the Scotia Sea. In such a position the Peninsula however would not allow the Ellsworth Mountains to be in their original position as interpreted here. Barker and Griffiths (1977) illustrate two alternative positions for the Peninsula representing two possible extremes. Their model B is preferred in which the Peninsula is allowed to lie much more nearly perpendicular to the East Antarctic craton. The position of the Peninsula adopted in fig. 6.11 is that proposed by Dalziel (in press) and Barker and Griffiths (1977) and also de Witt (1979) adjacent to the East Antarctic craton but in a more southernly position than Barker and Griffiths (1972). The fit of the remaining continents is from de Witt (1979) and Norton and Sclater (1979).

6.4.2 BREAKUP OF GONDWANALAND

The discussion concentrates on the initial breakup of Gonwanaland and events leading to the present day structure of West Antarctica.

The initial fragmentation of Gondwanaland probably occurred in late Jurassic to early Cretaceous times (Elliot, 1972; Barron et al, 1978; Craddock, in press; Norton and Sclater, 1979). The result of the initial fragmentation was the separation of West Gondwanaland (Africa and South

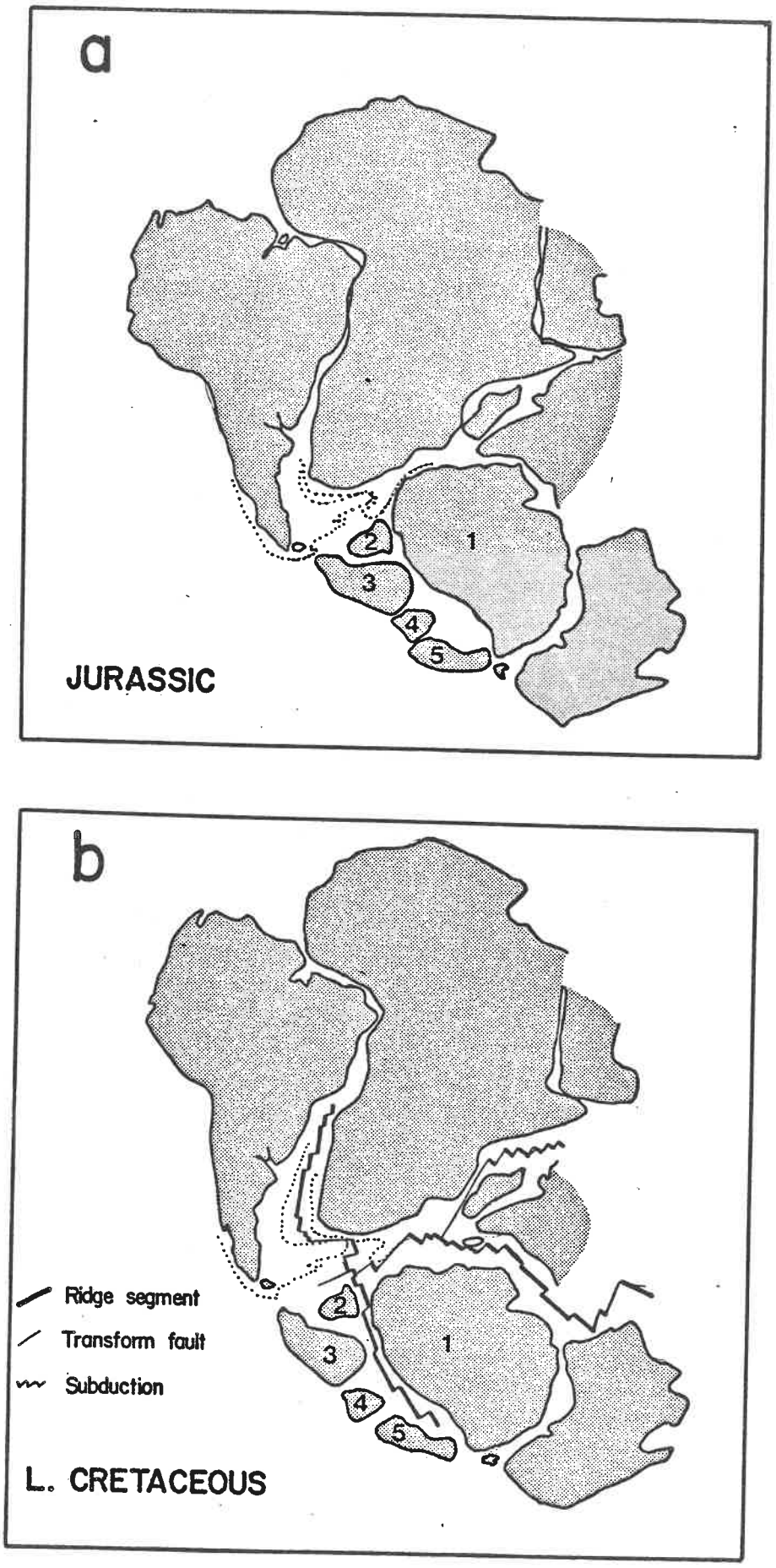
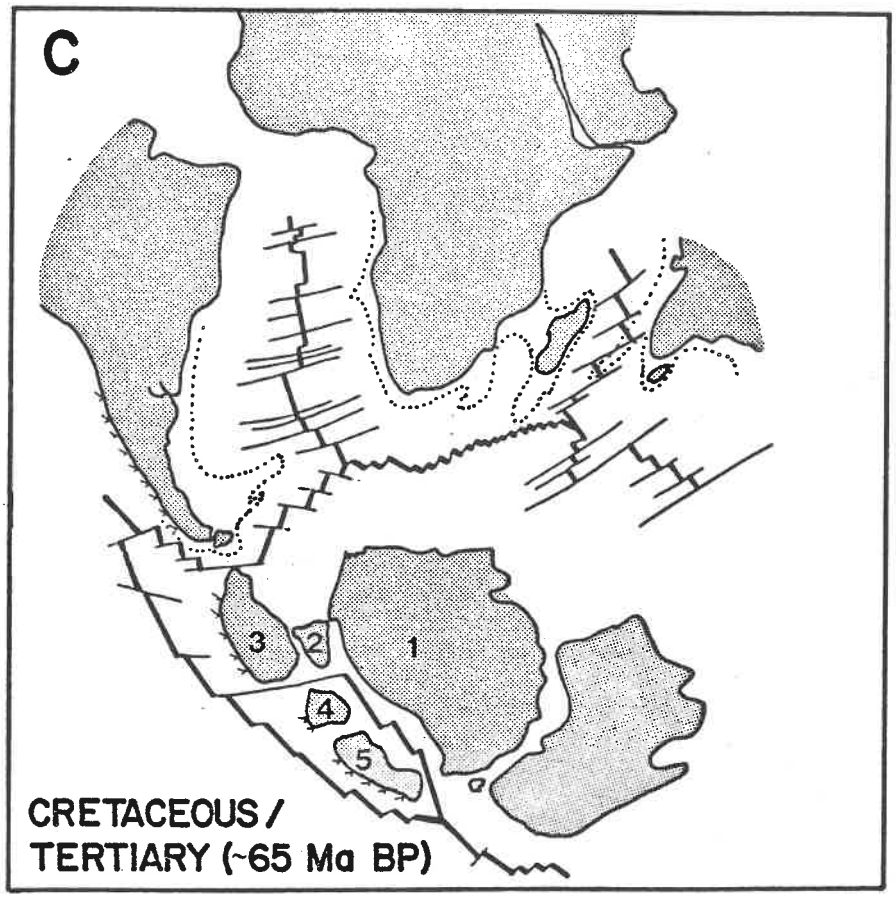


Fig. 6.11 West Antarctica and Gondwanaland.



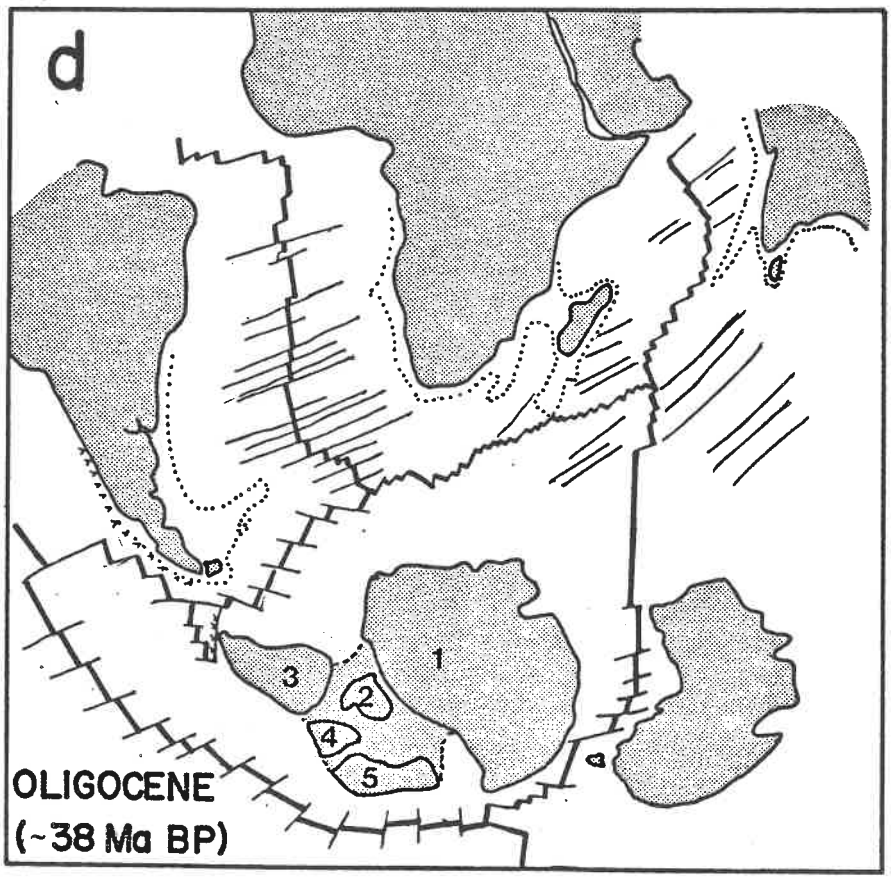


Fig. 6.11 continued.

America) from East Gondwanaland (Antarctica, India, Madagascar, Australia and New Zealand). This fragmentation is associated with basic volcanism in the Parana, Rajmahal and Deccan traps (Kyle et al, 1980). In Antarctica rifting of Gondwanaland is probably related to the large volume of tholeiitic magmas generated in mid-Jurassic times. Kyle et al (1980) believe most of the Transantarctic Mountain tholeiites were emplaced in a short time span at about 179±7 Ma BP. Ford and Kistler (1980) have divided these Antarctic tholeiitic rocks into two provinces. The Weddell Sea province tholeiites are related to opening between Africa and Antarctica, while the Transantarctic Mountains tholeiites are related to a failed rift zone. This activity in Antarctica lies within the same time period as the Karroo magmatism of South Africa but both predate the Parana, Rajmahal and Deccan traps.

The separation of East and West Gondwanaland was followed rapidly by the commencement of spreading between South America and Africa. Indeed Barker and Griffiths (1977) find it hard to imagine motion of Africa away from the remainder of Gondwanaland before opening of the South Atlantic had commenced. The initial split between the Ellsworth Mountains and East Antarctica is likely to have occurred at this time. This was probably caused by the failed rift proposed by Ford and Kistler (1980) which may also have initiated extension between East Antarctica and the microplates of West Antarctica (fig. 6.11b). This short lived rift was replaced by a situation depicted in Barker and Griffiths (1977) in which the third arm of the Antarctic/Africa triple junction extended westward as far as the marginal basin of the southern Andes, and responsible for creating the floor of the Weddell Sea. The date of opening of the Weddell Sea is uncertain. Barker and Jahn (1980) report magnetic lineations and small offset fracture zones in the eastern Weddell Sea but are unable to provide an unambiguous age for the Weddell Sea. The time at which rifting along the Transantarctic Mountains ceased is also unknown. It is possible that a 380 km westward ridge jump in the south Atlantic at ~98 Ma BP (Barker, 1979) may represent a change in the spreading pattern in this part of

Gondwanaland associated with failure of this rift.

By the late Cretaceous Madagascar and India began to separate and this event resulted in a major reorientation of spreading in the Indian Ocean (Norton and Sclater, 1979). A triple junction is thought to have become active in the Tasman Sea in the period 81-63 Ma BP (Molnar et al, 1975). Spreading occurred in the Tasman Sea and the South Pacific with the third arm of the triple junction separating East and West Antarctica. Rifting between Marie Byrd Land, Eights Coast and East Antarctica was probably connected to spreading in the Pacific by a series of transform faults and ridge sections passing between the Eights Coast and the southern end of the Peninsula similar to the situation envisaged by Herron and Tucholke (1976). Strike slip motion along a transform fault at the southern end of the Peninsula probably resulted in oroclinal bending as proposed by Kellogg (1980). The Weddell Sea was probably still being opened at this time while ahead of it the Ellsworth Mountains continued to rotate into position. Space for the Ellsworth Mountains was being made by rotation of East Antarctica away from the Peninsula which at this time was still attached to South America, and by rifting between Marie Byrd Land, Eights Coast and East Antarctica. This rifting probably resulted in development of the Byrd Subglacial Basin. This point in time, around the early Tertiary, is summarised in fig. 6.11c.

By 60 Ma BP spreading in the Tasman Sea had stopped and at ~55 Ma BP Australia separated from Antarctica (Molnar et al, 1975). They require convergence of ~500 km between East and West Antarctica in the period 63 - 38 my. No major deformation is recorded in the Antarctic at this time. In fact Cenozoic volcanism in Marie Byrd Land in the period 26-46 Ma BP is believed to have occurred in an extensional tectonic regime (LeMasurier and Rex, in press). A possible result of this convergence required by Molnar et al (1975) may have been the consolidation of the micro continental fragments of West Antarctica (fig. 6.11d).

The last major event in the breakup of Gondwanaland involved the separation of South America from the Antarctic Peninsula. The Peninsula became attached to East Antarctica which continued to rotate clockwise thereby opening the Scotia Sea (Barker and Griffiths, 1972). By this time West Antarctica had probably completely consolidated and any further events in the breakup of Gondwanaland most likely did not affect the structural configuration attained by West Antarctica.

CHAPTER 7 CONCLUSIONS

This thesis presents the results of the first major survey of West Antarctica involving simultaneous measurements of ice thickness and magnetics. A comphrehensive review of subglacial geology, structure and tectonic history of West Antarctica highlighted many problems. The results of this study have been:

West Antarctic Ice Sheet

1) Improved resolution of ice sheet surface features.
2) Delineation of major drainage basins in West Antarctica.
3) Identification of the inland boundaries of the Foundation Ice Stream.
4) Modification of the grounding line of the Ronne-Filchner Ice Shelf in the area between the Pensacola and Ellsworth Mountains (below 80° S).

Bedrock

1) Compilation of the first detailed map depicting the subglacial topography of West Antarctica.
2) Major improvement in the resolution of subglacial features and the identification of many that were unknown (eg. sinuous ridge in Byrd Subglacial Basin, deep subglacial basin at head of Ronne-Filchner Ice Shelf).
3) Calculations of the depression of the crust in West Antarctica by the ice sheet have been made and a map compiled to show the bedrock topography after complete isostatic recovery.
4) In preglacial times a major land bridge extended from the Ellsworth Mountains across the Whitmore Mountains and joined the Transantarctic

Mountains in the vicinity of the Thiel Mountains. There is therefore no major connection between the Ross and Weddell Seas.

5) A major submarine connection existed, however, via the Byrd Subglacial Basin, between the Ross and Amundsen Seas.

6) The Cenozoic volcanic areas of Marie Byrd Land form a major island in preglacial West Antarctica (although of reduced dimensions if the volcanics postdate the formation of the ice sheet).

Subglacial Geology

1) Cenozoic volcanic rocks lie close to the ice/rock interface in a large part of the subglacial areas of Marie Byrd Land.

2) Magnetisation of these rocks varies greatly and remanent magnetisations in a direction significantly different from the present are important.

3) There is no clear break in the magnetic field across the boundary between the Cenozoic Volcanic Province of Marie Byrd Land and the Byrd Subglacial Basin.

4) The floor of the basin would seem to be volcanic in origin with the volcanics overlain by a variable, but thin, cover of Cenozoic sediment.

5) The basin is cut by a prominent sinuous ridge. This ridge, too, is believed volcanic in origin and related to the Marie Byrd Land volcanics.

6) The Byrd Basin is a major subglacial feature of West Antarctica and probably represents a tectonic lineament.

7) The origin of the basin is believed related to extensional tectonics during breakup and subsequent evolution of Gondwanaland in upper Mesozoic times.

8) The thick late-Precambrian to Palaeozoic metasedimentary sequence exposed in the Ellsworth Mountains is believed to continue beneath the ice into West Antarctica and to include the scattered outcrops of the Nash, Pirrit, Martin Hills etc. and the Whitmore Mountains.

9) The northern margin of the Ellsworth-Whitmore Mountains area with the Byrd Subglacial basin is well defined both topographically and magnetically. The boundary becomes less well defined to the west and south.

10) The Ellsworth Mountains and associated subglacial area are believed out of place in West Antarctica. Palaeomagnetic evidence suggests that they have been rotated ~90^{o} (Watts and Bramall,1980).

11) Evidence of rifting, that would have accompanied rotation and displacement of the Ellsworth Mountains, is thought to occur in the bedrock low at the head of the Ronne-Filchner Ice Shelf.

12) The boundary between East and West Antarctica is a major problem. Depth to MOHO is known to decrease by ~10 km from east to west and the boundary is associated with a steep Bouguer gravity gradient. Suggestions of a major fault between East and West Antarctica are supported by the abrupt boundary to the Transantarctic Mountains on the West Antarctic side. The depth to which a fault zone may extend is a matter of conjecture.

13) The subglacial topography between the Whitmore Mountains and the Thiel Mountains is extremely rugged and the boundary between East and West Antarctica is more problematic in this area. Limited geological information and the results of this study suggest that the boundary zone passes close to the Thiel Mountains in the area between them and the outcrops of the Stewart and Hart Hills and Pagano Nunatak.

West Antarctica and Gondwanaland

1) Antarctica is believed to comprise of at least 5 separate plates which have moved independently to each other during the breakup of Gondwanaland.

2) The present day structure of West Antarctica is the result of

movements between the East Antarctic craton and the microplates of West Antarctica. Initial fragmentation of Antarctica is possibly related to a failed rift system along the Transantarctic Mountains in upper Jurassic times.

APPENDIX 1 MAGNETIC SUSCEPTIBILITY OF ANTARCTIC ROCKS

The degree to which a magnetic body, placed in an external field, becomes magnetised is determined by its magnetic susceptibility. Susceptibility is a dimensionless ratio, buts its magnitude depends on the units of measurement, the susceptibility in SI units being larger than the susceptibility in cgs units by the factor 4π . Susceptibility is defined by the equation:

$$I = kH \qquad \text{A1.1}$$

where I=Intensity of magnetisation (or polarisation)
and H=Magnetic field strengh (Oe)

The magnetic poles induced in a material by an external field H will produce a field of their own, H'. The total field within the body is defined as the magnetic induction B and can be written:

$$B = H+H' = H+4\pi I \qquad \text{A1.2}$$

combining A1.1 and A1.2 leads to

$$B = (1+4\pi k)\, H \qquad \text{A1.3}$$

The ratio of induction B to magnetising force H is known as the magnetic permeability μ.

$$\mu = (1+4\pi k) \qquad \text{A1.4}$$

It follows that since in the cgs system B is measured in gauss and as u is dimensionless that the gauss is dimensionally the same as the oested.

In total, 31 samples of rocks from West Antarctica belonging to the collection of C. Craddock at the University of Wisconsin were examined by Dr. D.J. Drewry and their magnetic susceptibility measured using a Bison 3101 magnetic susceptibility measuring system. The Bison magnetic susceptibility system is based on a fundamental design by Mooney (1952) involving a three coil induction balance. An important feature of the instrument is that it measures susceptibility in a field approximately equal to that of the earth's magnetic field. Magnetic susceptibility for ferrimagnetic materials depends strongly upon field strength (Dobrin, 1976). 24.5 mm (1 inch) cores were taken from all samples for measurement of susceptibility. Results are listed in table A1.1 and susceptibilities are quoted in cgs units $x10^{-5}$.

TABLE A1.1

SUSCEPTIBILITY MEASUREMENTS OF WEST ANTARCTIC ROCKS FROM COLLECTION OF C CRADDOCK, UNIVERSITY OF WISCONSIN

SAMPLE LOCATION	SAMPLE	DESCRIPTION	CGS $x10^{-5}$
THIEL MTNS	60-H-1	Basement 'Monzonite'	205-236
	60-H-2	Altered 'Beacon'?	15-20
	6-H-46	Basement 'Monzonite'	50
	60-H-52	'Beacon'	5-6
STEWART HILLS	60-6-17	Quartzite	5
	60-6-30	Quartzite	5
PIRRIT HILLS	60-8-27	Granite	10
HART HILLS	W-65-35	Quartzite	2-3
	W-65-8	Gabbro	7-8
PAGANO NUNATAK	W-64-3	Granite	2-4
	W-64-6	Granite	
WHITMORE MTNS	W-65-53	Phyllite Quartzite	3-4
MT Seelig	W-65-48	Pegmatite Gneiss-granite	4-5
Linck Nunatak	W-65-75	Granite	3-4

SAMPLE LOCATION	SAMPLE	DESCRIPTION	CGS $\times 10^{-5}$
ELLSWORTH MTNS			
Polarstar Point	TB-64-68	Polarstar Formation	4
Mucks Hills	64-TB-51F	Crashsite Quartzite?	7
Heritage Range	62-A-1	"	1
" "	64-HH-61C	"	3
(Marble Hills)	TB-64-47	Minaret Group	0
HUDSON MTNS	68-10-2	Vesicular Basalt	25
	60-12-19	"	10
RUPPERT COAST			
Kinsey Ridge	67-C-12	'Felsic intrusive'	80-100
Lambert Nunatak	67-C119		150-320
Mt Vance	67-C-23A	Metavolcanic	275-315
THURSTON ISLAND	60-9-14	Granite-Gneiss	300+
	60-9-6	"	220+
JONES MTNS	61-13-9	Dark green serpentenized Basalt dyke	5
	61-1-45	Basalt	5
	61-203	Porphyritic olivine Basalt	140-150+
	61-7-14?	Olivine basalt	11

SAMPLE LOCATION	SAMPLE	DESCRIPTION	CGS $x10^{-5}$
Runner Ridge D	61-11-37	Porphyritic basalt	140-150+
N-Dome E Peak	61-12-44	Porphyritic basalt	20-25

APPENDIX 2 MAXIMUM DEPTH TO MAGNETIC BASEMENT

Table A2.1 lists all depth solutions obtained on anomalies in West Antarctica using Werners' Deconvolution method of calculating maximum depth to magnetic basement for dyke-like and fault-like bodies. Table A2.1 is accompanied by fig A2.1 which shows all flights on which magnetic data were collected and the location of all depth estimates. In most cases a bedrock elevation was obtained directly from the RES records, or, where there were no bedrock return at that point, a bedrock elevation was interpolated from the bedrock topography map (see Fig. 2.8 and map in back pocket). Solutions 181,182 and 183 occur over ice-shelf and no bedrock elevation is available. The ice-shelf thickness is ~1000 m and therefore an estimate for the elevation of the sea bottom of -1500 m has been used which allows for a certain amount of overdeepening by the ice stream that feeds the ice shelf in this vicinity. Solutions 253-262 all occur on the Thwaites Glacier tongue and likewise no data are available on the submarine contours. However recent bathymetric maps (GEBCO,1980) show that the -500 m isobath lies close to the grounding line in other areas along the coast of West Antarctica, and this figure has been used. Depth estimates obtained from the horizontal derivative are shown by an asterisk in table A2.1 and are placed in brackets on Fig. 6.1.

Sections of flight track do not have many depth estimates because;

1) there were no significant anomalies (which is significant in itself).
2) the data were excessively 'nois y' such that the data were unreliable even after filtering.
3) to a lesser extent the aircraft was changing altitude rapidly or manoeuvring as discussed in chapter 2 thus rendering the data unreliable.

Figs. 5.9 and 5.10 can be used to show which sections of flight track were 'nois y' as opposed to showing no significant anomalies.

The quality of the depth solutions has been graded either 1, 2 or 3 depending on the tightness and number of points in each cluster that signifies a depth solution. Grade 1 was assigned to solutions obtained from tight clusters, comprising numerous points with little vertical spread in the points. Examples of all solutions can not be given but figs. A2.2 - A2.5 show some examples of grade 1 solutions. Grade 2 solutions were obtained from good clusters of points but unlike the clusters for grade 1 solutions the grade 2 clusters were well spread vertically or horizontally making it more difficult to pick off a depth (see Figs. A2.4 - A2.9). The centre or the point where there were the tightest grouping of points was used as the depth solution. Grade 3 solutions were obtained from small groupings of points but which are related to observed anomalies (see Figs. A2.8 - A2.10).

Unless otherwise stated no vertical exaggeration has been used on the examples shown in this appendix. The actual analyses were done on large scale plots, never with any vertical exaggeration, but which obviously cannot be reproduced in this thesis. The examples given in this appendix are merely to indicate the quality of the solutions used in chapter 6.

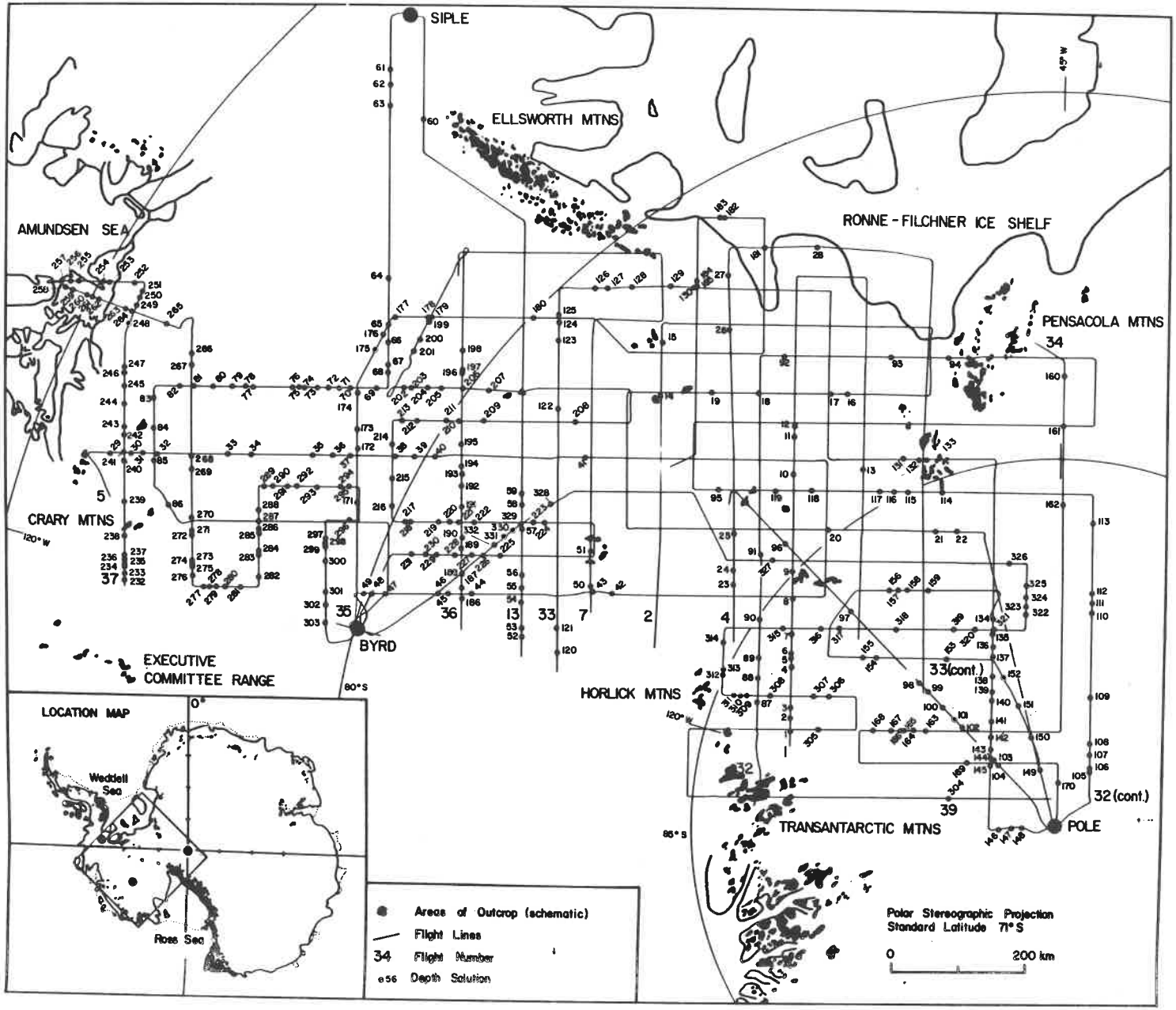


Fig. A2.1 Location of depth solutions.

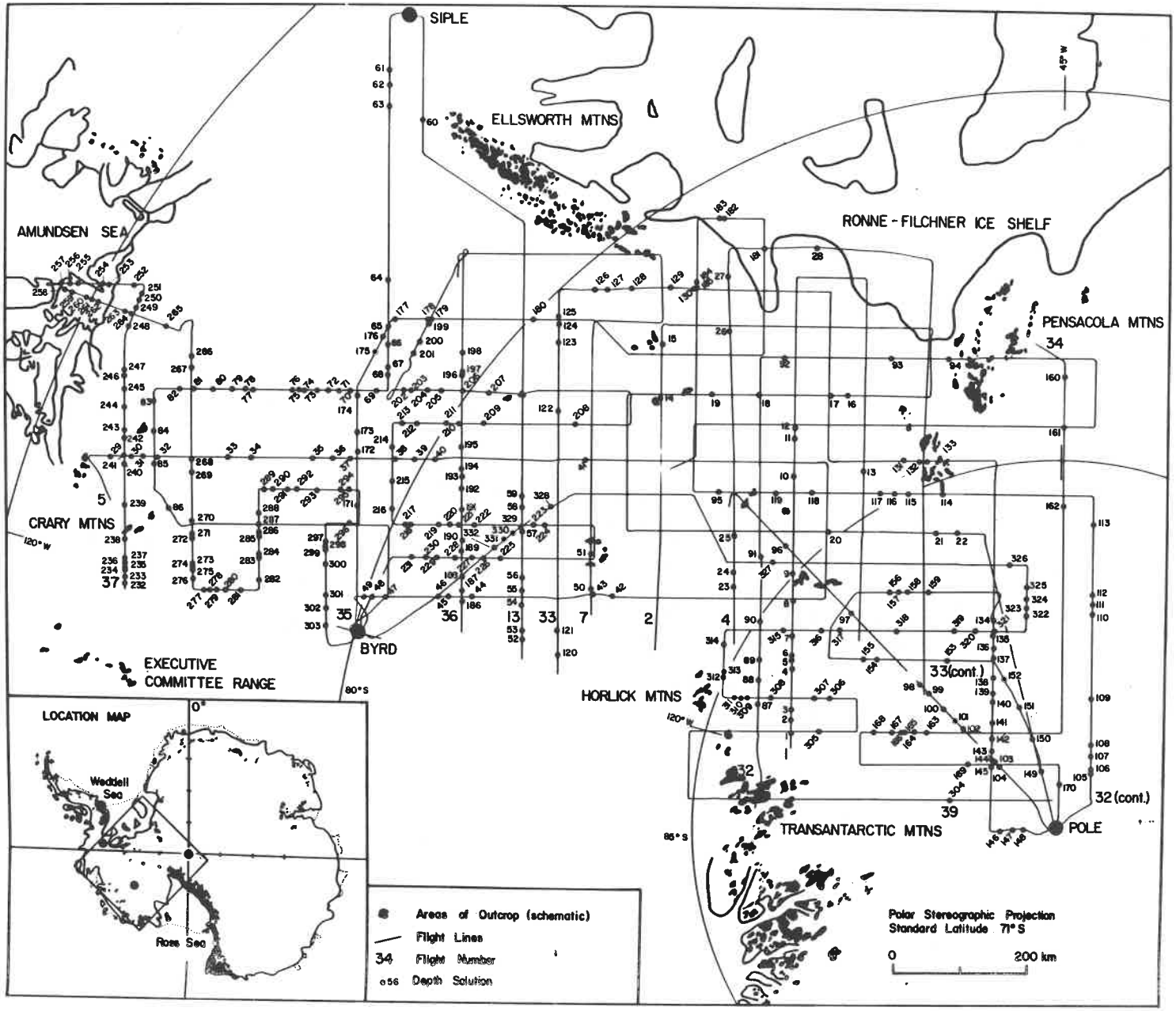


Fig. A2.1 Location of depth solutions.

TABLE A2.1

NUMBER	FLT	YR	CBD	LAT	LONG	DEPTH (km asl)	BED m	DIFF km	
1	1	1977	705.0	-86.0912	-114.8847	0.0	874	0.9	1
2	1	1977	711.0	-86.0573	-113.5373	0.0	1368	1.4	1
3	1	1977	720.0	-85.9999	-111.6158	0.0	624	0.6	2
4	1	1977	755.0	-85.7487	-104.7307	-2.5	1175	3.7	2
5	1	1977	762.0	-85.6949	-103.4846	-5.0	1084	6.1	2
6	1	1977	766.0	-85.6612	-102.7913	-2.5	1151	3.7	2
7	1	1977	783.0	-85.5083	-99.8044	-0.8	2050	2.1	1
8	1	1977	814.0	-85.1911	-95.7831	-1.5	1080	2.6	2
8	1	1977	814.0*	-85.1911	-94.7831	0.0	1500	1.5	1
9	1	1977	833.0	-84.9716	-91.9443	-1.5	800	2.3	1
9	1	1977	833.0*	-84.9716	-91.9443	0.0	800	0.8	1
10	1	1977	906.0	-83.9958	-82.7027	-1.5	-572	0.9	1
11	1	1977	937.0	-83.5660	-79.8057	-4.0	-1000	2.9	3
12	1	1977	948.0	-83.4690	-79.2173	-12.3	-410	11.8	3
13	1	1977	1292.0	-84.4631	-74.4401	-5.5	-300	5:2	3
14	2	1977	853.0	-82.0243	-88.5049	-2.5	0	2.5	2
15	2	1977	894.0*	-81.4728	-85.0776	-8.3	-424	7.8	1
16	2	1977	1275.0	-83.4561	-71.5779	-3.0	-81	2.9	1
17	2	1977	1290.0	-83.3430	-73.4594	-5.0	-700	4.3	1
18	2	1977	1351.0	-82.8218	-80.3833	-2.5	-700	1.8	2
19	2	1977	1390.0	-82.4352	-84.3437	-2.3	-383	1.9	2
19	2	1977	1390.0	-82.4352	-84.3437	-1.0	-383	0.6	2
20	2	1977	1766.0	-84.8779	-83.4666	-4.0	-600	3.4	2
21	2	1977	1865.0	-85.6444	-68.0684	0.0	949	0.9	3
22	2	1977	1887.0	-85.7570	-64.3013	-1.3	1248	2.5	3
23	4	1977	753.0	-84.4570	-99.1200	-3.0	324	3.3	3
24	4	1977	767.0	-84.3371	-97.4186	-1.5	-608	0.9	2
25	4	1977	800.0	-84.0258	-93.5533	-5.3	461	5.7	1
25	4	1977	800.0*	-84.0258	-93.5533	-2.5	461	3.0	1
26	4	1977	975.0	-81.8690	-79.2138	-5.0	-529	4.5	1
27	4	1977	1018.0	-81.2726	-76.6945	-3.3	-1450	1.8	2
28	4	1977	1123.0	-81.4528	-68.4554	-6.5	-938	5.6	3
29	5	1977	886.0	-76.1163	-114.1948	-2.5	-826	1.7	1
29	5	1977	886.0*	-76.1163	-114.1948	-0.8	-826	0.0	1
30	5	1977	903.0	-76.3848	-113.7405	-3.5	-529	3.0	1
30	5	1977	903.0*	-76.3848	-113.7405	-2.3	-529	1.7	2
31	5	1977	912.0	-76.5249	-113.5260	-2.0	-1266	0.7	1
32	5	1977	923.0	-76.6984	-113.2487	-5.0	-1640	3.4	3
33	5	1977	983.0	-77.6042	-111.4713	-4.0	-1374	2.6	2
34	5	1977	1003.0	-77.9045	-110.9137	-4.0	-1300	2.7	1
35	5	1977	1056.0	-78.6838	-109.1234	-2.0	-1011	1.0	1
36	5	1977	1074.0	-78.9175	-108.5107	-3.8	-400	3.4	1
37	5	1977	1088.0	-79.1211	-107.9789	-5.0	-400	4.6	1
37	5	1977	1088.0*	-79.1211	-107.9789	-3.5	-400	3.1	2

38	5	1977	1124.0	-79.6671	-106.4407	-4.8	-1300	3.5	1
38	5	1977	1124.0*	-79.6671	-106.4407	-2.3	-1300	1.0	2
39	5	1977	1139.0	-79.8908	-105.7499	-2.3	-1700	0.4	2
40	5	1977	1156.0	-80.1464	-104.9152	-6.0	-1400	4.6	1
41	5	1977	1279.0	-81.8446	-97.7373	-2.5	-364	2.1	1
41	5	1977	1279.0*	-81.8446	-97.7373	-0.4	-364	0.0	2
42	5	1977	1769.0	-83.0995	-108.1310	-5.0	-371	4.6	3
43	5	1977	1785.0	-82.8789	-108.8909	-4.3	400	4.7	3
44	5	1977	1895.0	-81.3862	-113.8737	-3.0	-279	2.7	2
45	5	1977	1919.0	-81.0454	-114.6645	-6.0	-69	5.9	2
46	5	1977	1924.0	-80.9752	-114.8444	-3.3	-408	2.8	1
46	5	1977	1924.0*	-80.9752	-114.8444	-2.0	-408	1.6	2
47	5	1977	1973.0	-80.2851	-116.5912	-6.0	-908	5.1	1
48	5	1977	1984.0	-80.1248	-116.9226	-0.4	-403	0.0	2
49	5	1977	1992.0	-80.0096	-117.1317	-4.0	-500	3.5	1
50	7	1977	720.0	-82.8086	-108.5400	-0.8	600	1.4	1
51	7	1977	749.0	-82.5811	-105.1393	-10.5	1200	11.7	1
52	13	1977	707.0	-82.2115	-116.1243	-4.0	-539	3.5	3
53	13	1977	714.0	-82.1751	-115.4069	-2.5	-440	2.1	1
54	13	1977	739.0	-82.0496	-112.9013	-3.5	-427	3.1	3
55	13	1977	752.0	-81.9752	-111.6455	-1.8	-289	1.5	1
56	13	1977	762.0	-81.9124	-110.6186	-3.0	-550	2.5	1
56	13	1977	762.0*	-81.9124	-110.6186	-1.8	-550	1.2	1
57	13	1977	804.0	-81.6163	-106.5042	-9.0	-400	8.6	2
58	13	1977	822.0	-81.4691	-104.7592	-4.0	-600	3.4	1
59	13	1977	831.0	-81.3963	-103.9157	-4.0	-650	3.4	2
60	13	1977	1178.0	-77.0973	-87.6233	-4.0	-750	3.3	1
61	13	1977	1343.0	-76.2922	-87.1279	-1.0	-1250	0.0	1
62	13	1977	1358.0	-76.4545	-87.7605	-6.5	-1300	5.2	1
63	13	1977	1374.0	-76.6369	-88.4882	-6.5	-1300	5.2	1
64	13	1977	1526.0	-78.2357	-96.4521	-5.5	-1144	4.4	2
64	13	1977	1526.0*	-78.2357	-96.4521	-3.0	-1144	1.9	2
65	13	1977	1567.0	-78.6150	-98.8932	-3.3	-700	2.6	2
66	13	1977	1587.0	-78.7889	-100.1290	-7.3	-800	6.5	2
67	13	1977	1603.0	-78.9247	-101.1587	-2.5	-700	1.8	2
68	13	1977	1610.0	-78.9860	-101.6171	-2.5	-701	1.8	2
69	13	1977	1633.0	-78.9767	-102.9159	-4.0	-400	3.6	1
69	13	1977	1633.0*	-78.9767	-102.9159	-1.8	-400	1.4	1
70	13	1977	1655.0	-78.6844	-103.8569	-1.8	-900	0.9	1
71	13	1977	1666.0*	-78.5341	-104.3035	-4.8	-597	4.2	2
72	13	1977	1674.0	-78.4222	-104.6303	-4.0	-600	3.4	2
73	13	1977	1683.0	-78.3003	-104.9849	-3.3	-600	2.7	2
74	13	1977	1695.0	-78.1334	-105.4397	-3.3	-600	2.7	1
74	13	1977	1695.0*	-78.1334	-105.4397	-2.0	-600	1.4	1
75	13	1977	1700.0*	-78.0666	-105.6252	-0.7	-697	0.0	2
76	13	1977	1708.0	-77.9548	-105.9240	-1.1	-1101	0.0	2
77	13	1977	1740.0	-77.5075	-107.0602	-3.0	-1500	1.5	2
78	13	1977	1747.0	-77.4091	-107.2950	-3.0	-1600	1.4	1
79	13	1977	1758.0	-77.2573	-107.6529	-3.5	-1389	2.1	1
79	13	1977	1758.0*	-77.2573	-107.6529	-1.5	-1389	0.1	1
80	13	1977	1773.0	-77.0538	-108.1207	-5.0	-1421	3.6	2

81	13	1977	1792.0	-76.7936	-108.6919	-6.0	-1194	4.8	3
82	13	1977	1803.0	-76.6418	-109.0152	-4.8	-1177	3.6	2
82	13	1977	1803.0*	-76.6418	-109.0152	-3.3	-1177	2.1	2
83	13	1977	1838.0	-76.3798	-110.3932	-3.8	-1433	2.3	1
84	13	1977	1863.0	-76.5376	-111.8990	-2.0	-900	1.1	2
85	13	1977	1892.0	-76.7072	-113.6933	-2.8	-1500	1.3	3
86	13	1977	1935.0	-77.1187	-115.8741	-2.5	-900	1.6	2
86	13	1977	1935.0*	-77.1187	-115.8741	-2.0	-900	1.1	3
87	32	1978	723.0	-85.5447	-112.8987	-3.5	-382	3.1	2
88	32	1978	745.0	-85.4165	-109.2795	-1.5	-110	1.4	1
88	32	1978	745.0*	-85.4165	-109.2795	0.0	-110	0.0	1
89	32	1978	765.0	-85.2852	-106.1520	-1.5	1544	3.0	2
90	32	1978	801.0	-85.0215	-101.0811	-2.0	300	2.3	1
91	32	1978	857.0	-84.4772	-93.2593	-3.0	1162	4.2	1
91	32	1978	857.0*	-84.4772	-93.2593	-1.3	1162	2.4	1
92	32	1978	1038.0	-82.5797	-75.9807	-2.0	-706	1.3	2
93	32	1978	1135.0	-83.2184	-65.2593	-6.0	-338	5.7	1
94	32	1978	1187.0	-83.4512	-58.6270	-3.0	-235	2.8	1
95	32	1978	1780.0	-83.4613	-91.0344	-3.3	132	3.4	3
96	32	1978	1859.0	-84.6316	-89.6672	-10.0	-100	9.9	2
97	32	1978	1940.0	-85.9158	-89.5842	-1.0	1126	2.1	3
98	32	1978	2025.0	-87.2883	-89.3489	0.0	540	0.5	2
99	32	1978	2035.0	-87.4536	-89.3228	-1.0	931	1.9	1
99	32	1978	2035.0*	-87.4536	-89.3228	0.0	931	0.9	1
100	32	1978	2053.0	-87.7492	-89.2285	-2.5	84	2.6	2
101	32	1978	2067.0	-87.9896	-89.1572	0.0	267	0.3	3
102	32	1978	2075.0	-88.1248	-89.0942	-0.3	3	0.3	3
103	32	1978	2112.0	-88.7542	-88.6509	-1.5	-166	1.3	2
104	32	1978	2117.0	-88.8376	-88.5498	0.0	-93	-0.1	3
105	32	1978	2405.0	-89.1116	-12.2039	-1.3	0	1.3	3
106	32	1978	2408.0	-89.0681	-13.9695	0.0	-28	0.0	2
107	32	1978	2419.0	-88.9012	-19.1631	-0.8	-351	0.4	2
108	32	1978	2427.0	-88.7728	-22.1018	-2.5	-361	2.2	2
108	32	1978	2427.0*	-88.7728	-22.1018	-1.0	-361	0.6	1
109	32	1978	2462.0	-88.1841	-29.9338	-1.5	-500	1.0	1
110	32	1978	2530.0	-87.0369	-35.9668	-5.0	-878	4.1	3
111	32	1978	2538.0	-86.9002	-36.3911	-1.5	-623	0.9	2
112	32	1978	2545.0	-86.7801	-36.7451	-0.5	-445	0.0	2
113	32	1978	2600.0	-85.8312	-38.7180	-4.3	-610	3.6	3
114	32	1978	2739.0	-85.1719	-64.8586	-2.5	936	3.4	2
115	32	1978	2765.0	-85.0064	-69.6753	-1.5	-140	1.4	2
116	32	1978	2776.0	-84.9264	-71.5774	-3.8	-345	3.4	3
117	32	1978	2789.0	-84.8247	-73.7249	-2.5	-439	2.1	2
118	32	1978	2843.0	-84.3253	-81.9438	-5.0	-400	4.6	2
119	32	1978	2872.0	-84.0092	-85.8025	-4.0	-503	3.5	2
120	33	1978	763.0	-82.7488	-116.5056	-3.0	-488	2.5	1
121	33	1978	786.0	-82.6305	-114.1025	-2.3	-800	1.5	3
122	33	1978	975.0*	-81.1205	-95.8999	-4.0	398	4.4	1
122	33	1978	976.0	-81.1105	-95.8230	-3.3	815	4.1	1
123	33	1978	1032.0	-80.5087	-91.5354	-4.0	1025	5.0	3
124	33	1978	1047.0	-80.3369	-90.4597	-3.0	-239	2.8	3

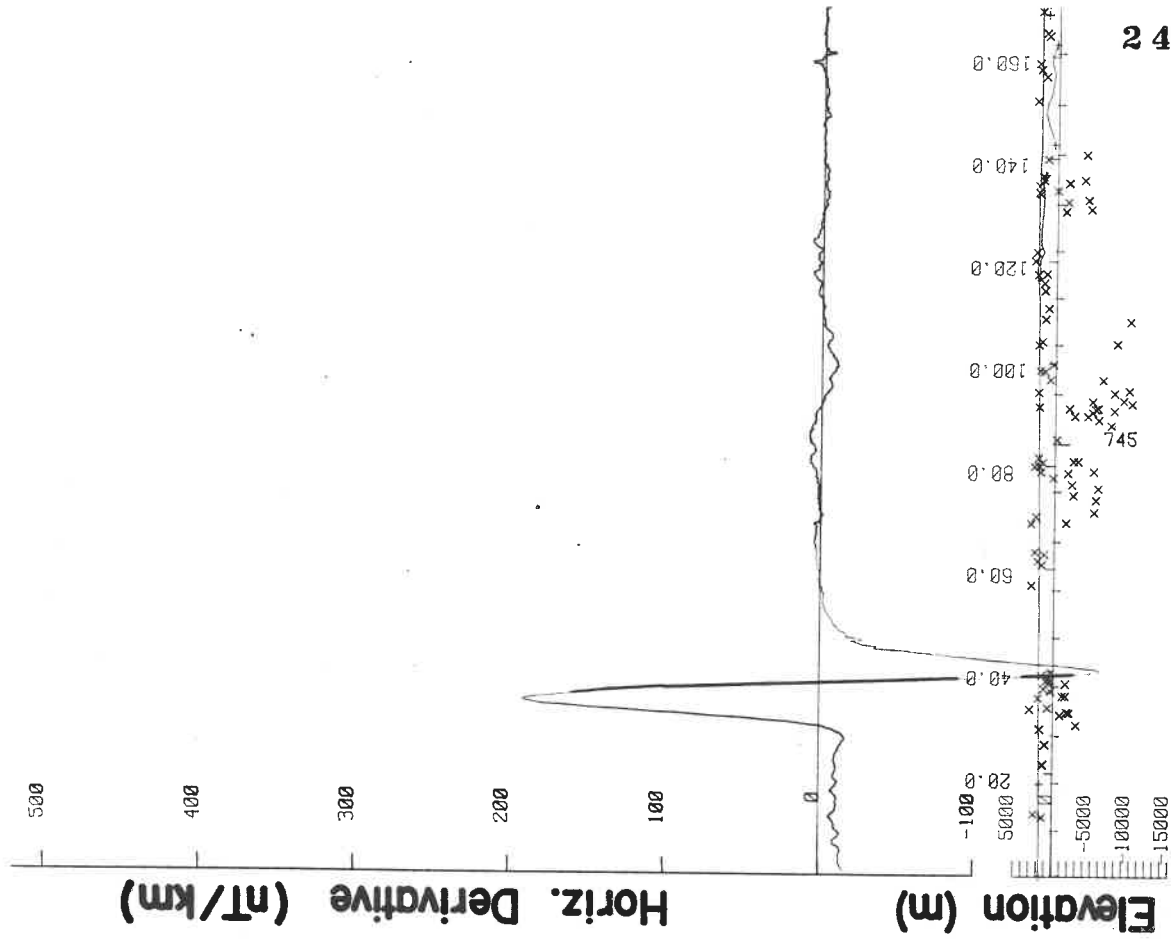
125	33	1978	1052.0	-80.2803	-90.1045	-1.3	-445	0.8	3
126	33	1978	1104.0	-80.3333	-86.4438	-2.5	-240	2.3	3
127	33	1978	1114.0	-80.4416	-85.6538	-7.0	-599	6.4	3
127	33	1978	1114.0*	-80.4416	-85.6538	-4.3	-599	3.7	2
128	33	1978	1133.0	-80.6348	-84.0977	-8.5	-600	7.9	2
128	33	1978	1133.0*	-80.6348	-84.0977	-3.5	-600	2.9	2
129	33	1978	1167.0	-80.9597	-81.3467	-3.5	-184	3.3	3
130	33	1978	1187.0	-81.1529	-79.7305	-6.0	-1129	4.9	1
131	33	1978	1510.0	-84.5618	-68.5366	-6.5	-78	6.4	3
132	33	1978	1523.0	-84.6484	-66.5444	-4.0	459	4.5	3
133	33	1978	1527.0	-84.6767	-65.9685	-1.5	521	2.0	1
134	33	1978	1725.0	-87.0333	-62.7297	-1.0	978	2.0	3
135	33	1978	1737.0	-87.2287	-63.9929	-1.0	724	1.7	2
136	33	1978	1748.0	-87.4091	-65.2649	-1.3	864	2.1	3
137	33	1978	1755.0	-87.5277	-66.0615	-1.5	297	1.8	2
138	33	1978	1770.0	-87.7718	-68.5671	-1.0	432	1.4	3
139	33	1978	1782.0	-87.9626	-71.1509	0.0	513	0.5	1
140	33	1978	1788.0	-88.0564	-72.6436	-1.5	472	2.0	1
140	33	1978	1788.0*	-88.0564	-72.6436	0.0	472	0.5	1
141	33	1978	1804.0	-88.3045	-77.1929	0.0	134	0.0	1
142	33	1978	1817.0	-88.4943	-82.0183	-1.0	301	1.3	2
143	33	1978	1827.0	-88.6308	-86.5430	0.0	92	0.0	3
143	33	1978	1827.0*	-88.6308	-86.5430	0.0	92	0.0	2
144	33	1978	1832.0	-88.6982	-89.0662	0.0	-260	0.0	3
145	33	1978	1838.0	-88.7743	-92.4963	-2.3	-223	2.0	1
145	33	1978	1838.0*	-88.7743	-92.4963	0.0	-223	0.0	2
146	33	1978	1896.0	-89.2406	-138.5850	-3.5	-42	3.5	3
147	33	1978	1907.0	-89.4229	-137.7354	-1.0	285	1.3	1
148	33	1978	1916.0	-89.5636	-138.6816	-0.8	363	1.1	1
149	33	1978	2157.0	-89.1998	-59.9961	-3.0	-100	2.9	3
150	33	1978	2185.0	-88.7535	-60.7100	0.0	-250	0.0	1
151	33	1978	2213.0	-88.2968	-62.7981	-2.5	-100	2.4	2
152	33	1978	2241.0	-87.8405	-65.2151	0.5	478	0.0	2
153	33	1978	2293.0	-87.2773	-78.5615	-4.0	292	4.3	3
154	33	1978	2350.0	-86.6184	-92.7678	-1.0	568	1.6	2
155	33	1978	2360.0	-86.4851	-94.6428	-2.0	356	2.4	2
156	33	1978	2479.0	-86.0466	-80.8699	-1.0	-505	0.5	2
157	33	1978	2487.0	-86.1156	-79.3430	-1.5	-488	1.0	2
158	33	1978	2492.0	-86.1605	-78.3752	-1.5	-519	1.0	1
159	33	1978	2512.0	-86.3185	-74.3701	-1.3	250	1.5	1
160	34	1978	1739.0	-83.8632	-44.6824	-3.0	27	3.0	2
161	34	1978	1782.0	-84.5305	-44.6392	-4.3	0	4.3	1
162	34	1978	1851.0	-85.5970	-44.4380	-4.0	-800	3.2	2
163	34	1978	2180.0	-87.7853	-99.3706	-2.0	905	2.9	3
164	34	1978	2190.0	-87.6559	-101.6218	0.0	847	0.8	1
165	34	1978	2200.0	-87.5215	-103.6523	-2.0	571	2.6	3
165	34	1978	2200.0*	-87.5215	-103.6523	-1.0	571	1.6	1
166	34	1978	2203.0	-87.4817	-104.2323	-2.0	721	2.7	2
167	34	1978	2210.0	-87.3870	-105.4502	-1.0	798	1.8	2
168	34	1978	2225.0	-87.1793	-107.8507	-1.3	206	1.5	2
169	34	1978	2352.0	-88.3677	-103.6584	-0.5	346	0.8	1

170	34	1978	2463.0	-89.3941	-40.8555	-2.0	-282	1.7	1
171	35	1978	930.0	-79.4605	-110.8972	-8.0	-1400	6.6	2
172	35	1978	977.0	-79.1477	-107.4142	-4.8	-500	4.3	1
173	35	1978	994.0	-79.0222	-106.1867	-1.3	-1300	0.0	1
174	35	1978	1026.0	-78.7714	-103.9236	-2.3	-800	1.5	1
175	35	1978	1068.0	-78.6568	-100.7036	-3.5	-800	2.7	1
176	25	1978	1087.0	-78.6229	-99.5452	-3.5	-739	3.8	3
177	35	1978	1103.0	-78.6323	-98.1045	-4.0	-844	3.2	3
177	35	1978	1103.0*	-78.6323	-98.1045	-3.5	-844	2.7	2
178	35	1978	1128.0	-78.9435	-96.8772	-6.0	-1259	4.7	1
179	35	1978	1130.0	-78.9668	-96.7766	-4.0	-1200	2.8	2
180	35	1978	1222.0	-80.0562	-91.5969	1.0	1006	0.0	2
181	35	1978	1513.0	-81.1712	-72.7053	-4.5	-1500	3.0	2
182	35	1978	1570.0	-80.5670	-74.4482	-3.0	-1500	1.5	1
183	35	1978	1574.0	-80.5339	-74.7976	-2.5	-1500	1.0	1
184	35	1978	1650.0	-81.0798	-79.2307	-4.5	-504	4.0	1
184	35	1978	1650.0*	-81.0798	-79.2307	-3.5	-504	3.0	1
185	35	1978	1657.0	-81.1650	-79.6050	-6.0	-894	5.1	2
185	35	1978	1657.0*	-81.1650	-79.6050	-6.0	-894	5.1	2
186	36	1978	755.0	-81.2759	-114.8025	-4.5	-123	4.4	1
187	36	1978	766.0	-81.2137	-113.7619	-2.0	-127	1.9	2
188	36	1978	777.0	-81.1532	-112.7500	-8.0	-100	7.9	3
189	36	1978	800.0	-81.0120	-110.6598	-2.5	-708	1.8	2
190	36	1978	807.0	-80.9666	-110.0306	-3.0	-1100	1.9	2
191	36	1978	838.0	-80.7515	-107.3501	-3.0	-700	2.3	1
192	36	1978	855.0	-80.6287	-105.9737	-6.0	-747	5.3	1
193	36	1978	865.0	-80.5547	-105.1724	-4.0	-900	3.1	1
194	36	1978	871.0	-80.5093	-104.6986	-6.3	-700	5.6	3
195	36	1978	892.0	-80.3462	-103.0784	-4.8	-900	3.9	2
196	36	1978	956.0	-79.7965	-98.4204	-6.0	-1200	4.8	2
197	36	1978	963.0	-79.7726	-97.9412	-4.0	-1200	2.8	2
198	36	1978	975.0	-79.6184	-97.1138	-10.0	-1200	7.8	2
199	36	1978	1133.0	-79.0079	-96.9302	-3.5	-1600	1.9	2
200	36	1978	1150.0	-79.0608	-98.3909	-4.5	-1267	3.2	2
201	36	1978	1160.0	-79.0872	-99.2607	-6.0	-1100	4.9	1
202	36	1978	1227.0	-79.2760	-101.8132	-1.4	-1376	0.0	2
203	36	1978	1232.0	-79.3457	-101.5645	-4.0	-1100	2.9	2
204	36	1978	1246.0	-79.5364	-100.8687	-1.3	-1298	0.0	2
205	36	1978	1259.0	-79.7088	-100.2014	-1.2	-1157	0.0	2
206	36	1978	1276.0	-79.9343	-99.3242	-4.5	-1200	3.3	3
207	36	1978	1298.0	-80.2327	-98.2278	-1.5	250	1.8	2
208	36	1978	1497.0	-81.4125	-95.8279	-25.0	-250	0.0	1
209	36	1978	1580.0	-80.4231	-100.4961	-5.0	-176	4.8	2
210	36	1978	1603.0	-80.1307	-101.6450	-4.0	-1000	3.0	1
211	36	1978	1612.0	-80.0153	-102.0771	-2.5	-1300	1.2	2
212	36	1978	1640.0	-79.6576	-103.3528	-5.0	-1400	3.6	2
213	36	1978	1651.0	-79.5139	-103.8330	-3.5	-1400	2.1	2
214	36	1978	1681.0	-79.5230	-105.7465	-3.5	-1240	2.3	1
215	36	1978	1706.0	-79.7041	-107.6699	-2.3	-1400	0.9	1
216	36	1978	1735.0	-79.9184	-109.9963	-4.8	-1750	3.0	2
217	36	1978	1758.0	-80.1625	-110.6539	-2.0	-2300	0.0	1

218	36	1978	1763.0	-80.2388	-110.4518	-8.5	-2400	6.1	2
219	36	1978	1786.0	-80.5806	-109.4806	-5.5	-1900	3.6	3
220	36	1978	1795.0	-80.7133	-109.0867	-3.0	-1600	1.4	2
221	36	1978	1801.0	-80.8012	-108.8274	-5.5	-1300	4.2	2
222	36	1978	1816.0	-81.0168	-108.1357	-3.5	-750	2.8	1
223	36	1978	1867.0	-81.7298	-105.5749	-2.5	-400	2.1	1
224	36	1978	1876.0	-81.8524	-105.0838	-2.5	29	2.5	1
225	36	1978	2033.0	-81.5312	-109.7623	-6.5	-728	5.8	3
226	36	1978	2050.0	-81.3073	-110.4537	-9.5	-1045	8.5	2
227	36	1978	2060.0	-81.1770	-110.8303	-2.0	-1200	0.8	2
228	36	1978	2077.0	-80.9564	-111.4678	-2.0	-609	1.4	2
229	36	1978	2093.0	-80.7425	-112.0334	-2.0	-500	1.5	1
230	36	1978	2103.0*	-80.6089	-112.3780	-0.5	-1400	0.0	1
231	36	1978	2116.0	-80.4267	-112.8298	-4.0	-2100	1.9	3
232	37	1978	786.0	-76.8030	-120.9726	0.1	132	0.0	2
233	37	1978	792.0	-76.7797	-120.5466	0.0	9999	0.0	1
234	37	1978	797.0	-76.7581	-120.1975	0.0	9999	0.0	2
235	37	1978	800.0	-76.7465	-119.9870	0.0	9999	0.0	1
236	37	1978	803.0	-76.7332	-119.7649	0.0	9999	0.0	2
237	37	1978	806.0	-76.7199	-119.5594	0.0	9999	0.0	2
238	37	1978	822.0	-76.6434	-118.4151	-1.5	1049	2.6	1
239	37	1978	852.0	-76.5037	-116.5004	-4.0	-1000	3.0	1
240	37	1978	886.0	-76.3223	-114.3184	-2.0	-235	1.8	2
241	37	1978	892.0	-76.2857	-113.9075	-5.0	-997	4.0	1
242	37	1978	907.0	-76.1908	-112.9051	-3.0	-437	2.6	2
243	37	1978	912.0	-76.1609	-112.5860	-3.0	-362	2.6	2
244	37	1978	938.0	-76.0310	-111.3008	-2.8	-218	2.5	2
245	37	1978	955.0	-75.9378	-110.4168	-0.9	-922	0.0	1
246	37	1978	968.0	-75.8595	-109.7450	-0.6	-623	0.0	1
247	37	1978	972.0	-75.8345	-109.5278	-3.0	-487	2.5	2
248	37	1978	1017.0	-75.6230	-107.2316	-2.3	-885	1.4	3
249	37	1978	1039.0	-75.5897	-106.1418	-2.3	-644	1.6	2
249	37	1978	1039.0*	-75.5897	-106.1418	-0.6	-644	0.0	2
250	37	1978	1047.0	-75.5764	-105.7473	-0.8	-809	0.0	2
251	37	1978	1053.0	-75.5681	-105.4531	-0.7	-659	0.0	1
252	37	1978	1072.0	-75.4282	-105.2150	-2.5	-500	2.0	1
253	37	1978	1091.0	-75.1302	-105.8468	-2.3	-500	1.8	2
254	37	1978	1096.0	-75.0536	-105.9986	-3.0	-500	2.5	1
255	37	1978	1117.0	-74.7440	-106.6187	-2.0	-500	1.5	2
256	37	1978	1124.0	-74.6375	-106.8271	-3.0	-500	2.5	2
257	37	1978	1130.0	-74.5459	-106.9987	-1.5	-500	1.0	2
258	37	1978	1165.0	-74.6247	-107.1726	-2.0	-500	1.5	1
259	37	1978	1173.0	-74.7364	-107.1131	-2.0	-500	1.5	2
260	37	1978	1188.0	-74.9483	-106.9943	-1.8	-500	1.3	2
261	37	1978	1194.0	-75.0350	-106.9451	-1.5	-500	1.0	1
262	37	1978	1200.0	-75.1183	-106.8976	-2.8	-500	2.3	1
263	37	1978	1227.0	-75.4936	-106.6784	-0.8	-824	0.0	2
264	37	1978	1233.0	-75.5687	-106.6325	-0.8	-771	0.0	3
265	37	1978	1271.0	-76.0574	-106.3264	-1.0	-1014	0.0	2
266	37	1978	1332.0	-76.5633	-107.0377	-2.0	-1175	0.8	1
266	37	1978	1332.0*	-76.5633	-107.0377	-1.2	-1175	0.0	2

267	37	1978	1342.0	-76.6386	-107.6707	-2.0	-1240	0.8	1
268	37	1978	1417.0	-77.1578	-112.6013	-5.0	-1600	3.4	1
269	37	1978	1427.0	-77.2215	-113.2896	-2.3	-1359	0.9	3
270	37	1978	1466.0	-77.4445	-116.0286	-0.5	-488	0.0	2
271	37	1978	1477.0	-77.5032	-116.8090	-4.0	-431	3.6	2
272	37	1978	1481.0	-77.5234	-117.0924	-3.5	-600	2.9	2
273	37	1978	1502.0	-77.6275	-118.6216	-0.6	-613	0.0	2
274	37	1978	1503.0	-77.6308	-118.6984	-2.5	57	2.6	2
275	37	1978	1506.0	-77.6443	-118.9168	0.1	120	0.0	3
276	37	1978	1514.0	-77.6796	-119.4789	-2.0	-227	1.8	2
277	37	1978	1533.0	-77.8700	-120.0390	-0.4	-408	0.0	1
278	37	1978	1538.0	-77.9484	-119.9329	-0.5	-485	0.0	2
279	37	1978	1544.0	-78.0435	-119.8114	-1.0	-400	0.6	2
280	37	1978	1550.0	-78.1419	-119.6799	-2.0	-740	1.3	3
281	37	1978	1563.0	-78.3503	-119.3932	-0.9	-944	0.0	3
282	37	1978	1588.0	-78.5588	-118.3534	-2.0	-900	1.1	1
283	37	1978	1608.0	-78.4720	-116.9487	-3.5	-1200	2.3	1
284	37	1978	1613.0	-78.4469	-116.6009	-1.1	-1077	0.0	1
285	37	1978	1629.0	-78.3734	-115.4989	0.2	153	0.0	1
286	37	1978	1633.0	-78.3501	-115.2280	0.0	-200	0.0	1
287	37	1978	1640.0	-78.3150	-114.7666	-0.2	-217	0.0	1
288	37	1978	1650.0	-78.2582	-114.0310	-7.5	-1000	6.5	1
289	37	1978	1675.0	-78.2280	-112.4701	-2.0	-1300	0.7	2
290	37	1978	1682.0	-78.3380	-112.2428	-1.1	-1108	0.0	2
291	37	1978	1694.0	-78.5213	-111.8521	-0.2	-176	0.0	2
292	37	1978	1701.0	-78.6347	-111.6096	-5.0	-400	4.6	1
293	37	1978	1718.0	-78.8946	-111.0152	-2.0	-405	1.6	2
293	37	1978	1718.0*	-78.8946	-111.0152	-0.4	-405	0.0	1
294	37	1978	1737.0	-79.1896	-110.3178	-3.8	-600	3.2	1
295	37	1978	1742.0	-79.2696	-110.1175	-3.8	-750	3.0	1
296	37	1978	1782.0	-79.4944	-112.2927	-4.0	-1400	2.6	2
297	37	1978	1817.0*	-79.2507	-114.1724	0.0	-1250	0.0	3
298	37	1978	1821.0	-79.2776	-114.5276	-2.8	-1100	1.7	2
299	37	1978	1823.0*	-79.2877	-114.7078	0.0	-1100	0.0	2
300	37	1978	1835.0	-79.3600	-115.8005	-2.8	-1104	1.7	2
300	37	1978	1835.0*	-79.3600	-115.8005	-1.1	-1104	0.0	2
301	37	1978	1859.0	-79.4962	-117.9964	-1.0	-1037	0.0	2
301	37	1978	1859.0*	-79.4962	-117.9964	-2.0	-1037	1.0	3
302	37	1978	1868.0	-79.5434	-118.8492	-2.0	-900	1.1	3
303	37	1978	1882.0	-79.6141	-120.1763	-2.8	-900	1.9	2
304	39	1978	197.0	-88.4552	-121.0934	-8.5	417	8.9	3
305	39	1978	585.0	-86.4751	-113.6040	-1.3	700	2.0	2
306	39	1978	667.0	-86.3997	-106.0311	-0.5	736	1.2	3
307	39	1978	677.0	-86.2278	-107.4634	-5.5	585	6.1	3
308	39	1978	701.0	-85.8042	-110.4358	-1.3	761	2.0	2
309	39	1978	723.0	-85.4158	-112.6294	-2.0	1501	3.5	2
310	39	1978	729.0	-85.3141	-113.1435	0.0	1687	1.7	2
311	39	1978	734.0	-85.2341	-113.5493	0.0	1381	1.4	2
312	39	1978	767.0*	-84.9590	-110.9558	-1.0	1374	2.4	2
313	39	1978	770.0	-84.9426	-110.5436	-3.0	461	3.5	2
314	39	1978	797.0	-84.7759	-106.7542	-1.0	1534	2.5	2

315	39	1978	866.0	-85.3760	-99.7373	-1.0	1944	2.9	1
316	39	1978	900.0	-85.7760	-95.8037	-0.8	1235	2.0	1
317	39	1978	915.0	-85.9551	-93.6975	-1.0	1462	2.5	1
318	39	1978	965.0	-86.5246	-84.8188	-3.0	-500	2.5	1
319	39	1978	1016.0	-86.9774	-72.9919	-3.5	589	4.1	2
320	39	1978	1035.0	-87.1033	-67.8154	-2.3	1115	3.4	2
321	39	1978	1050.0	-87.1857	-63.3943	-7.5	776	8.3	3
322	39	1978	1090.0	-87.0851	-53.9036	-2.0	392	2.4	1
323	39	1978	1098.0	-86.9568	-53.5225	0.0	413	0.4	2
324	39	1978	1103.0	-86.8701	-53.2756	-2.8	827	3.6	2
325	39	1978	1114.0	-86.6951	-52.8357	-1.3	310	1.6	1
326	39	1978	1146.0	-86.3530	-55.6113	-2.5	296	2.8	1
327	39	1978	1325.0	-84.6706	-92.6936	-6.0	107	6.1	2
328	39	1978	1530.0	-81.7977	-103.2534	-3.0	200	3.2	2
329	39	1978	1557.0	-81.5869	-106.1973	-3.5	-300	3.2	1
330	39	1978	1563.0	-81.5400	-106.8975	-2.5	-600	1.9	1
331	39	1978	1572.0	-81.4713	-107.8520	-2.3	-700	1.6	1
332	39	1978	1583.0	-81.4043	-108.8988	-1.8	-900	0.9	2



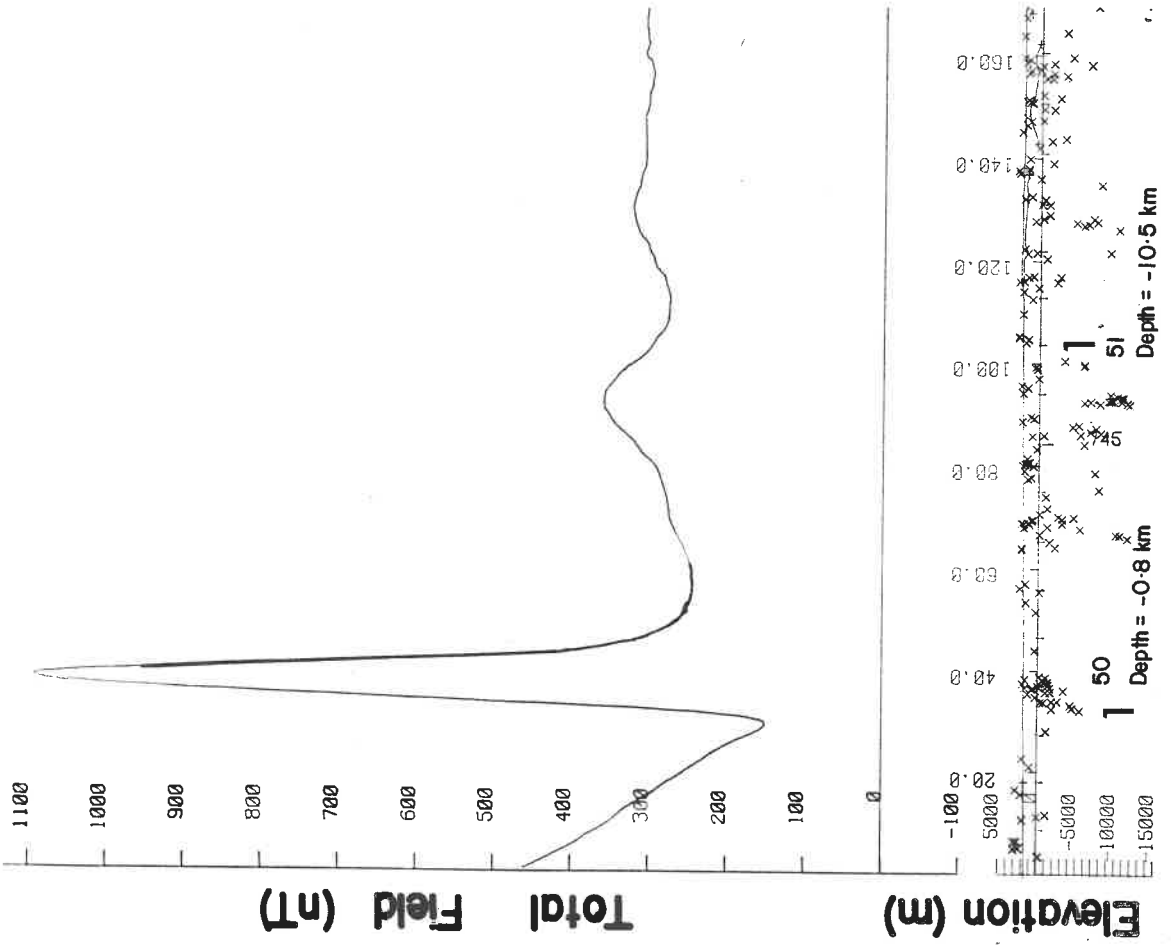


Fig. A2.2 Example of grade 1 solution.

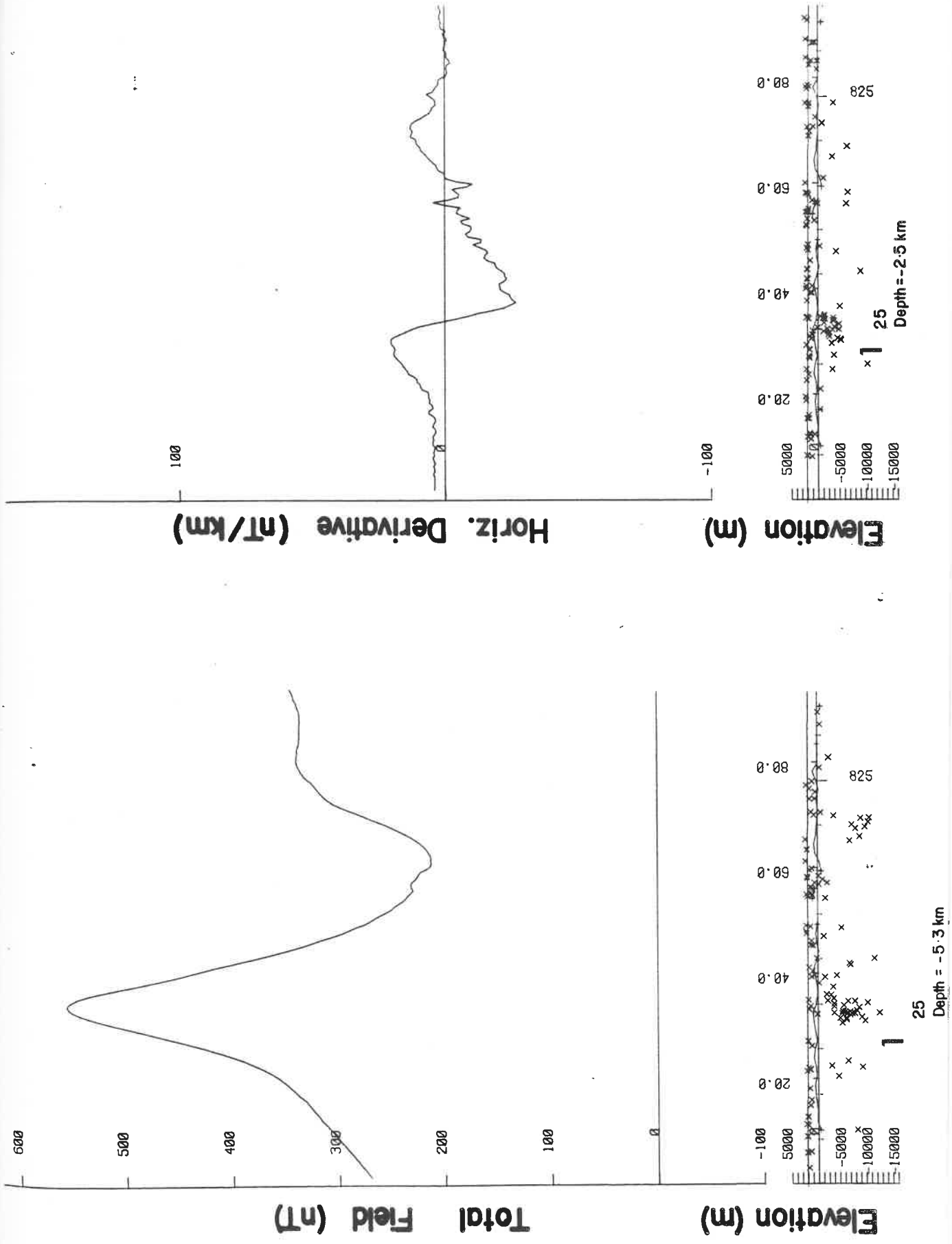


Fig. A2.3 Example of grade 1 solution.

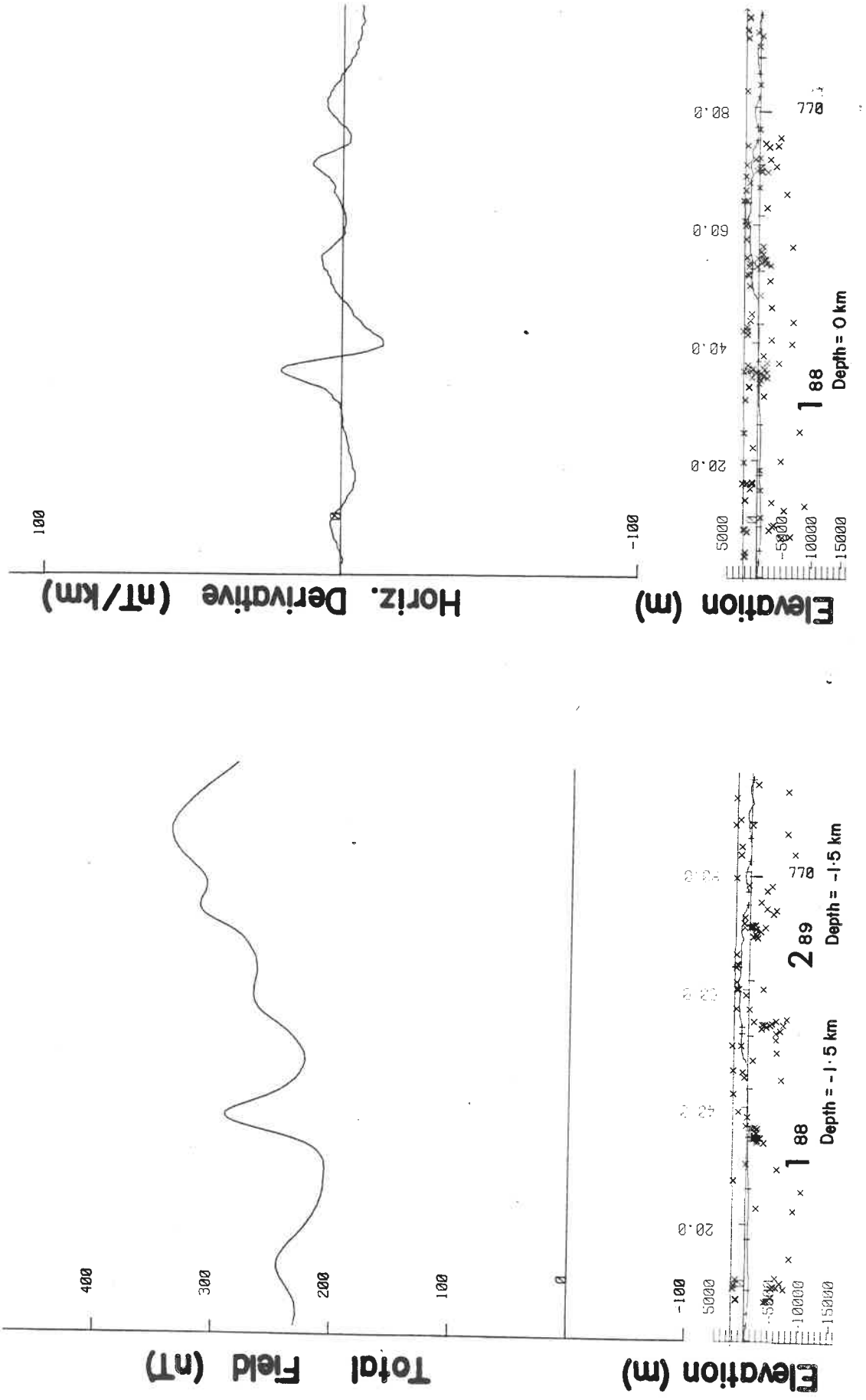
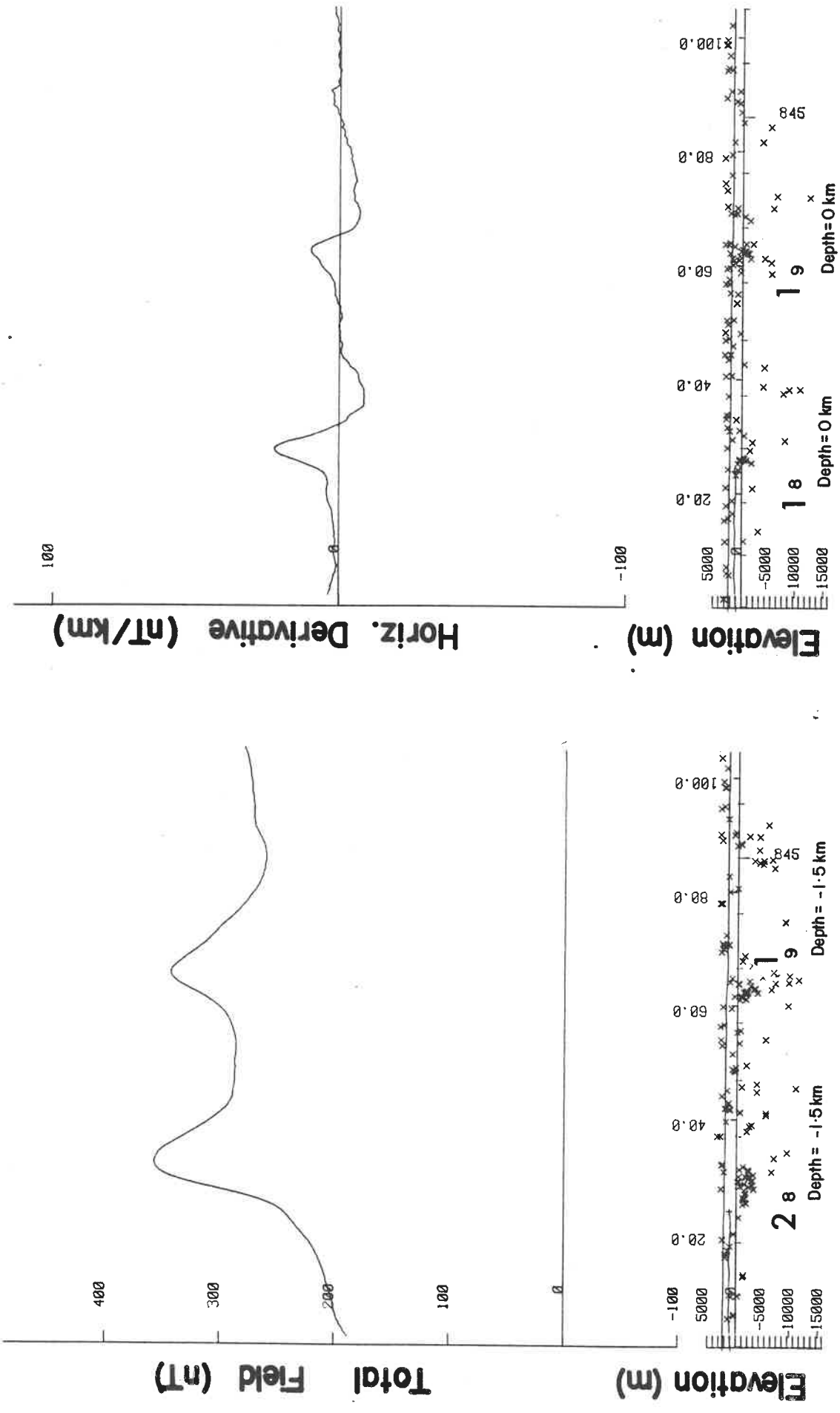


Fig. A2.4 Example of grade 1 solution.



Fig, A2.5 Example of grade 1 and grade 2 solutions.

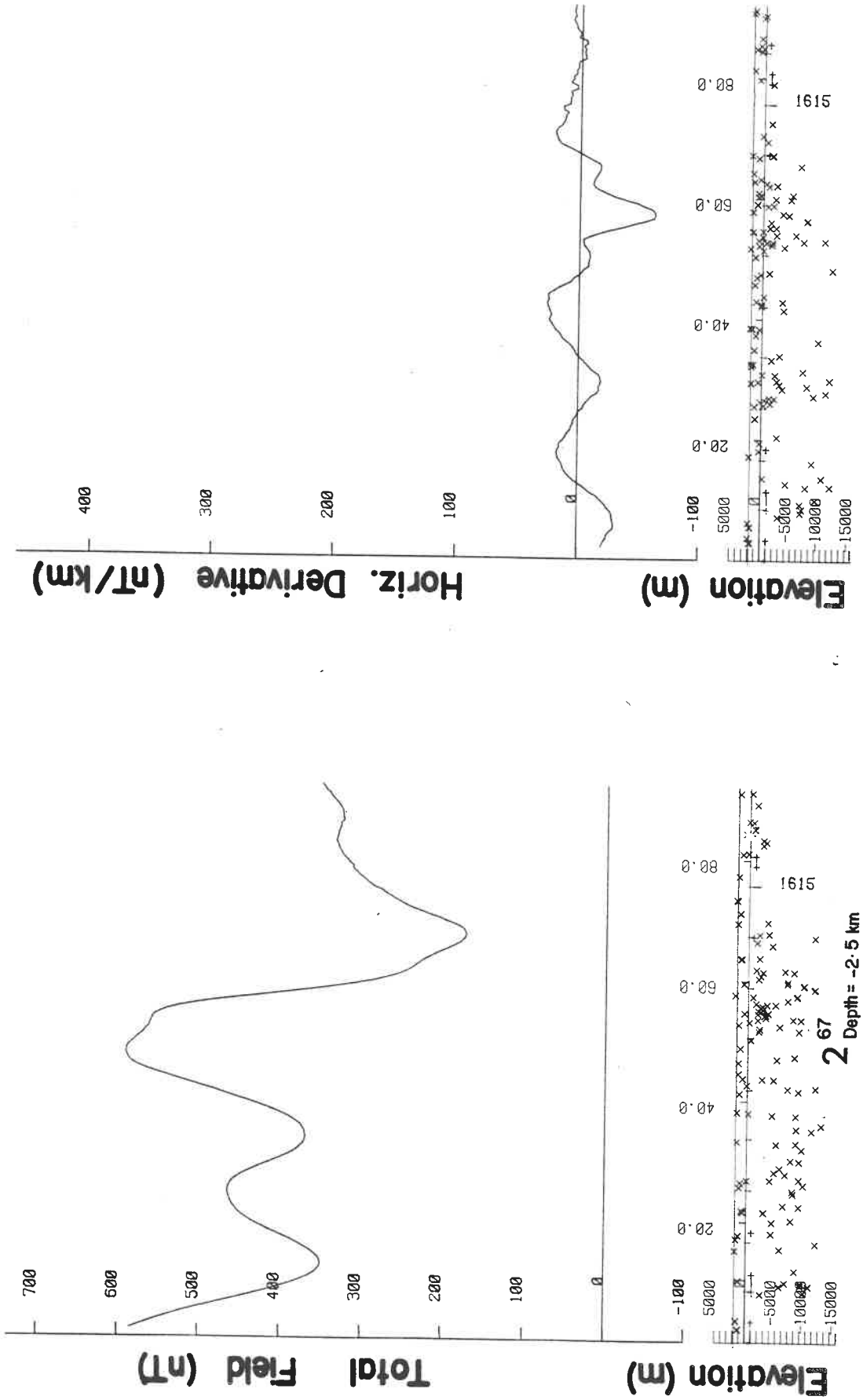


Fig. A2.6 Example of grade 2 solution.

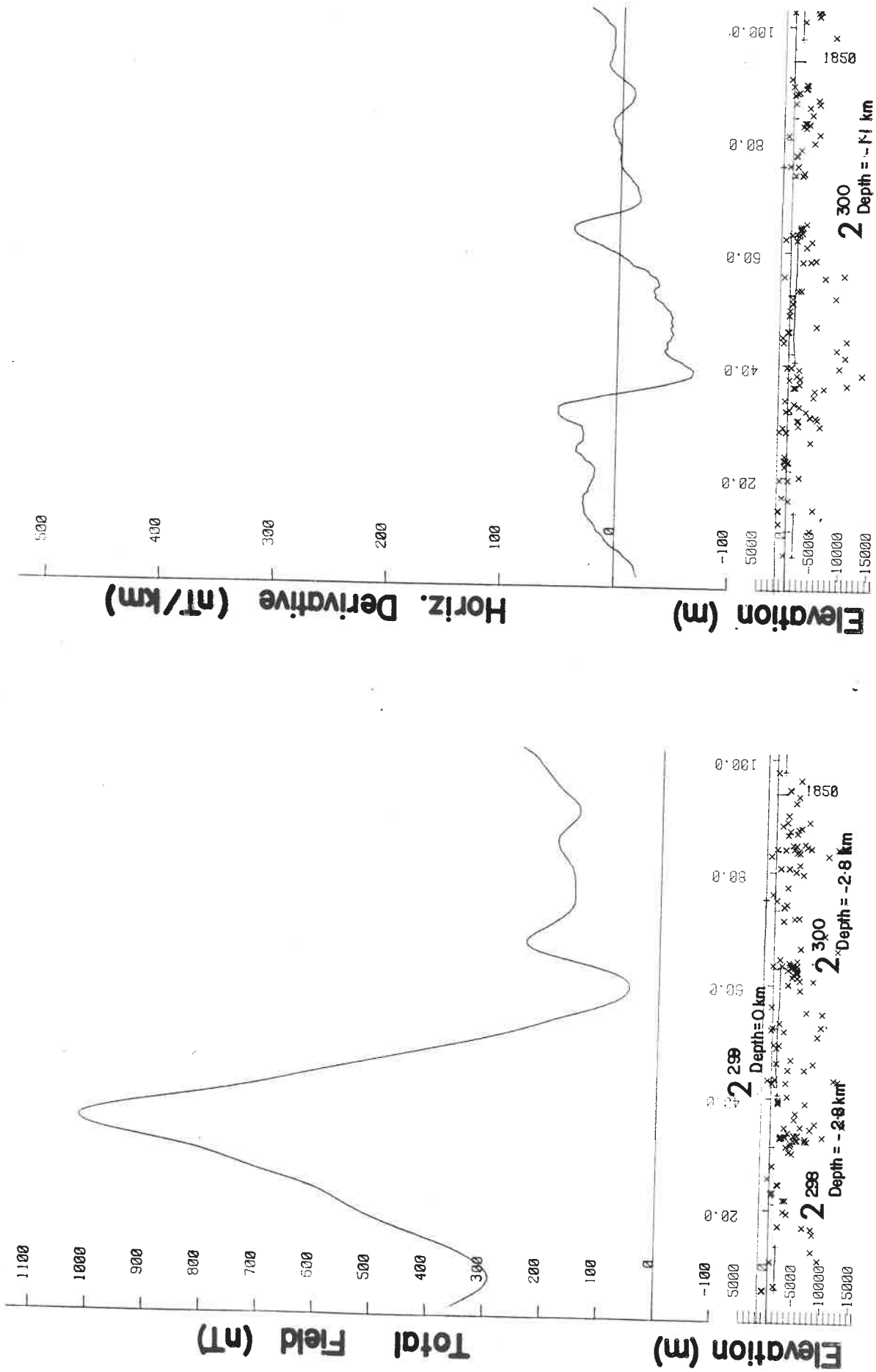


Fig. A2.7 Example of grade 2 solution.

Fig. A2.8 Example of grade 2 and grade 3 solutions.

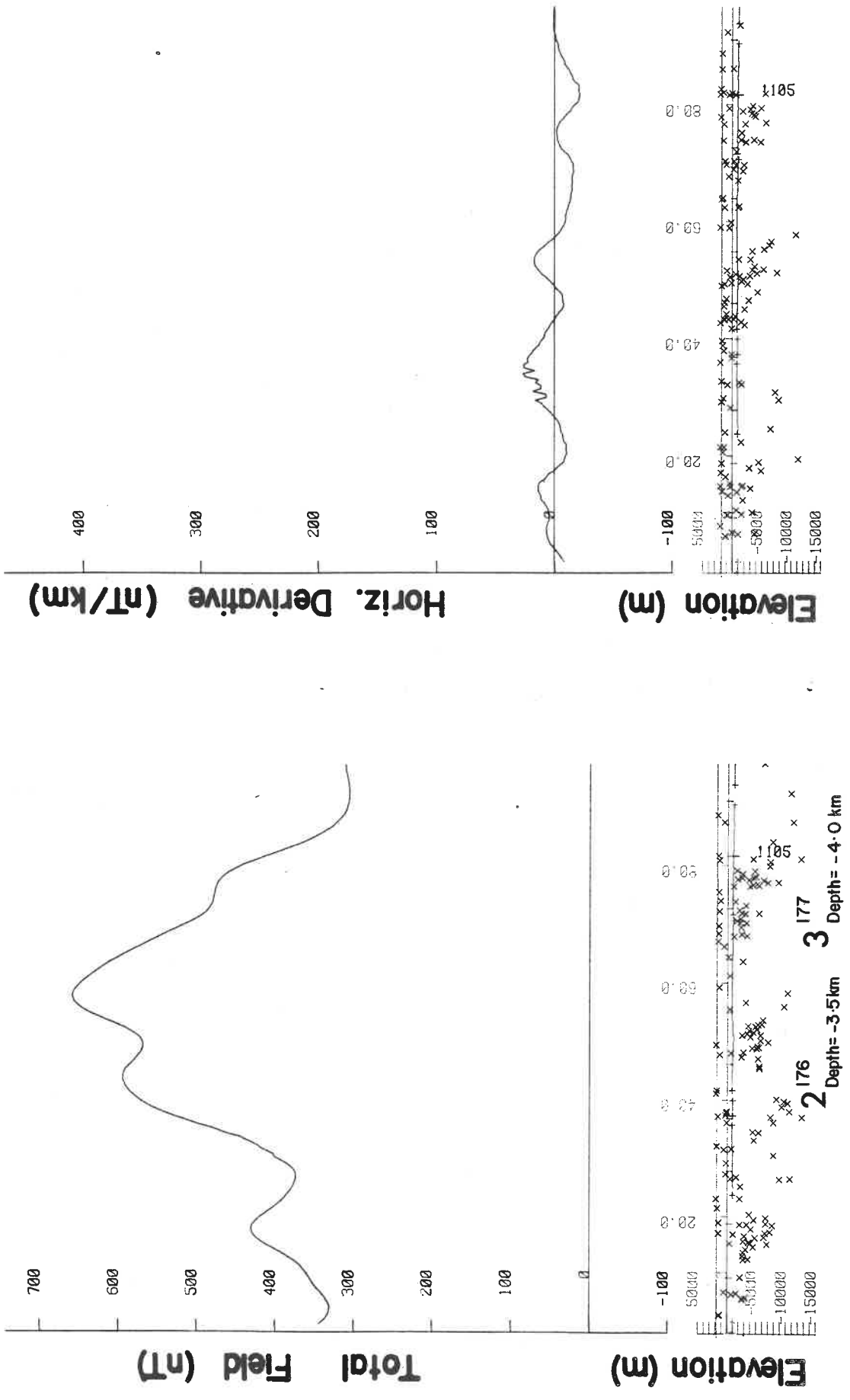


Fig. A2.9 Example of grade 2 and grade 3 solutions.

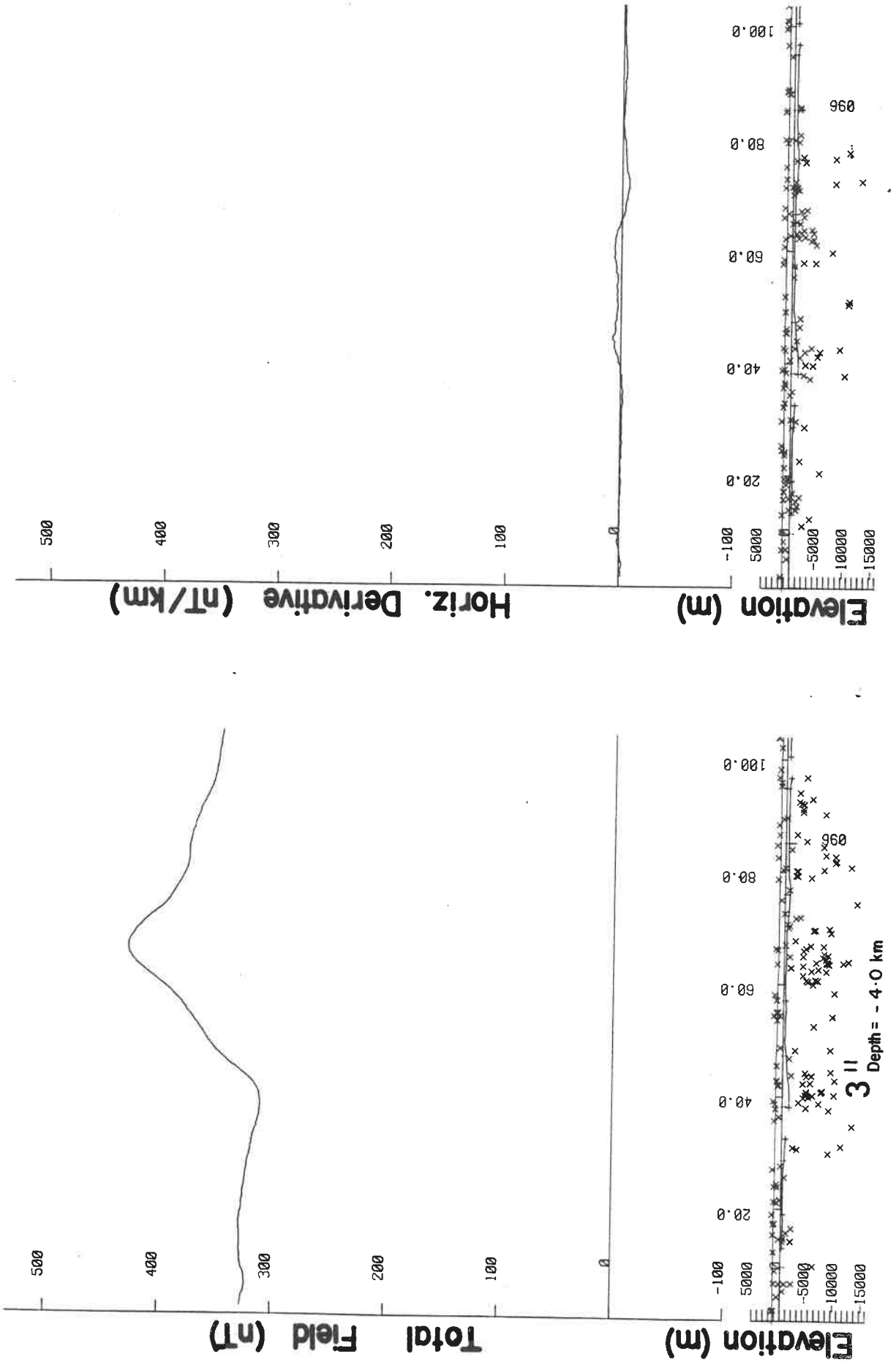


Fig. A2.10 Example of grade 3 solution.

APPENDIX 3 COMPUTER MODELLING OF ANOMALIES

The results of the 2D modelling are presented here. In model A for each profile the upper limit of the bodies is taken to be the ice/rock interface as determined by RES. The crust has been arbitrarily divided into vertical sided, flat bottomed blocks several kilometers thick. Boundaries between blocks were placed beneath steep gradients and changes in gradient in the total field observations as necessary in a method similar to Behrendt et al (1981). The models are obviously geologically unrealistic but in the absence of any knowledge of the bedrock geology and upper crustal structure this method provides a quantitative estimate of the magnetic properties of the bedrock.

The models where appropriate were then modified to take into account the maximum depth to magnetic basement as indicated by Appendix 2. In this way two extremes are modelled. In the first instance using the minimum depth to basment (ie. the ice/rock interface) and then the maximum depth to basment. For each model inverse solutions were obtained for susceptibility and remanent magnetisation using Cady's (1980) inversion method.

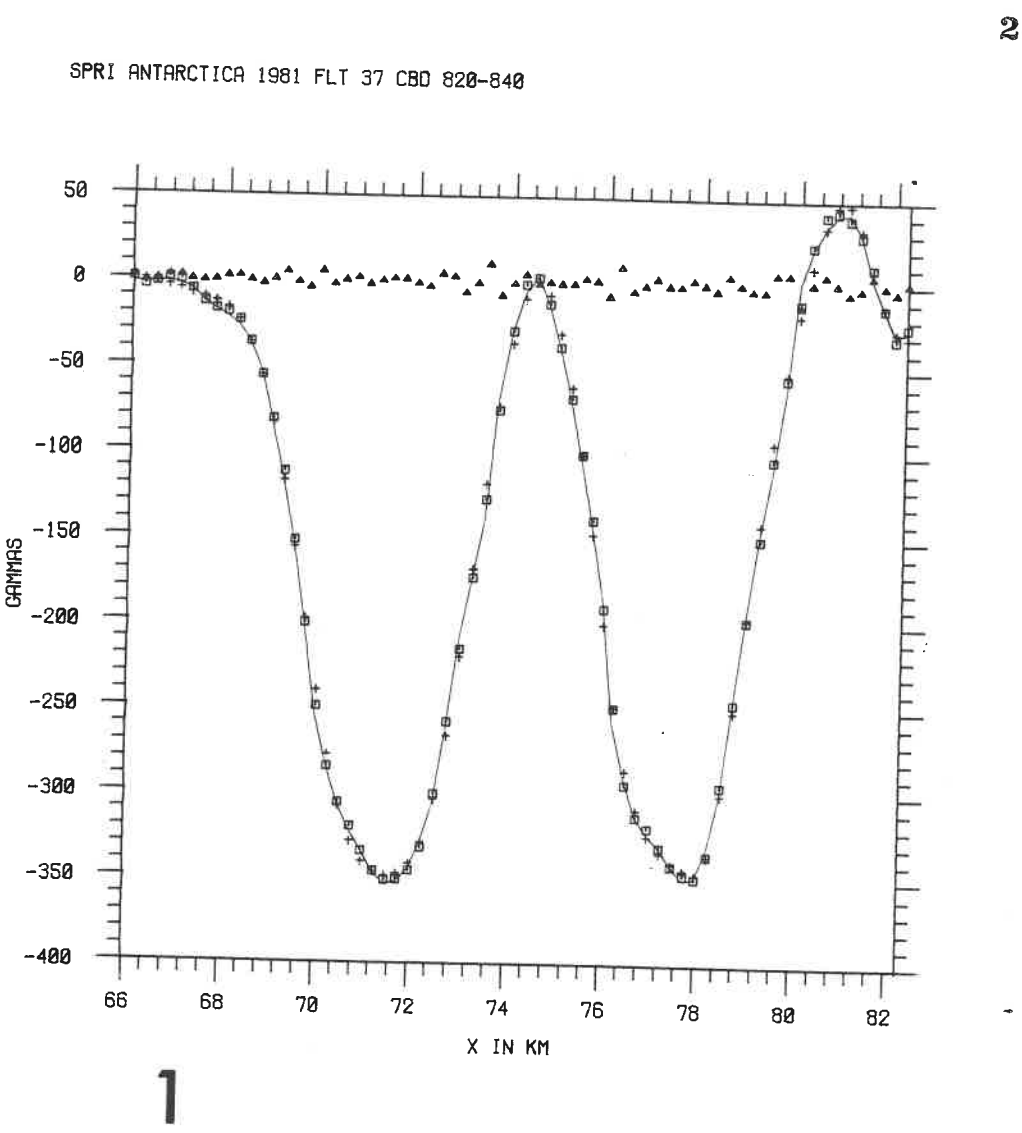
The observed field is shown by a continuous line in all the models. Inverse solutions for susceptibility are shown by crosses and inverse solutions for remanent magnetisation by open squares. Open triangles plotted represent the residual between the observed total field and the inverse solution for remanent magnetisation. In general the inverse solution for remanent magnetisation gives a better fit to the observed field because of the extra degree of freedom available. All bodies are numbered and correspond to body numbers in the tables of results. The line drawn on all body plots above the top of the vertical bodies represents the absolute elevation of the measurements. The ice sheet surface has not been plotted as this is considered to be irrelevant to the modelling. Dotted lines in

the body plots indicate the changes imposed on the models by maximum depths to magnetic basement. All results are given in table form following the models for each profile. Susceptibilities are given in cgs units $x10^{-5}$. Remanent magnetisations are also given in cgs units of gauss $x10^{-5}$.

ADDENDUM

The inverse solutions presented in this thesis represent separate solutions for susceptibility and for vector magnetisation. Solutions for susceptibility are obtained by assuming that all bodies have zero remanence. Each body is then assumed by the computer program to have zero susceptibility and inverse calculations are made for remanent magnetisations. In reality, however, this represents the vector magnetisation resulting from the combined effect of susceptibility and remanence. All mentions of inverse solutions for remanent magnetisation therefore properly refer to the vector magnetisation.

All bodies have been constrained to have vertical sides. This however represents only one possible model and is not a unique solution.



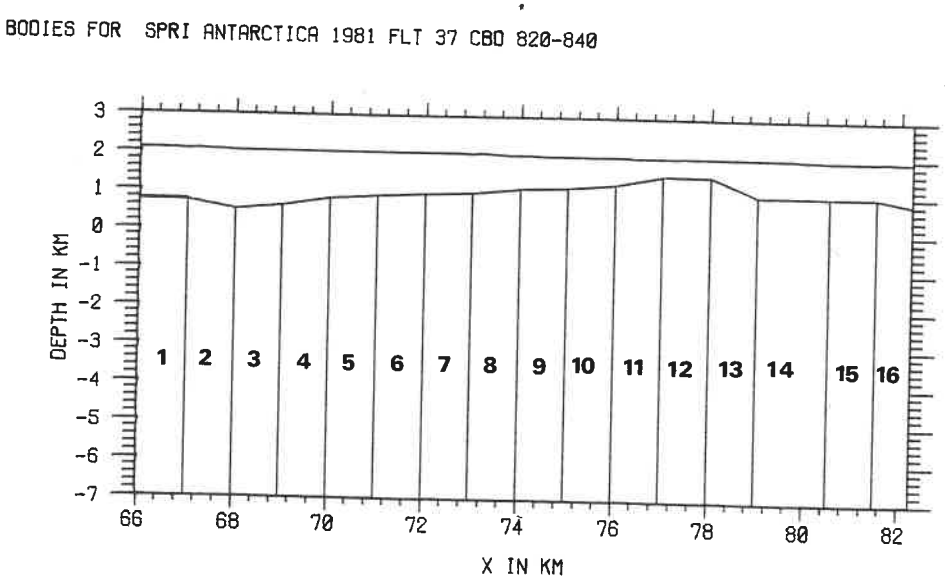
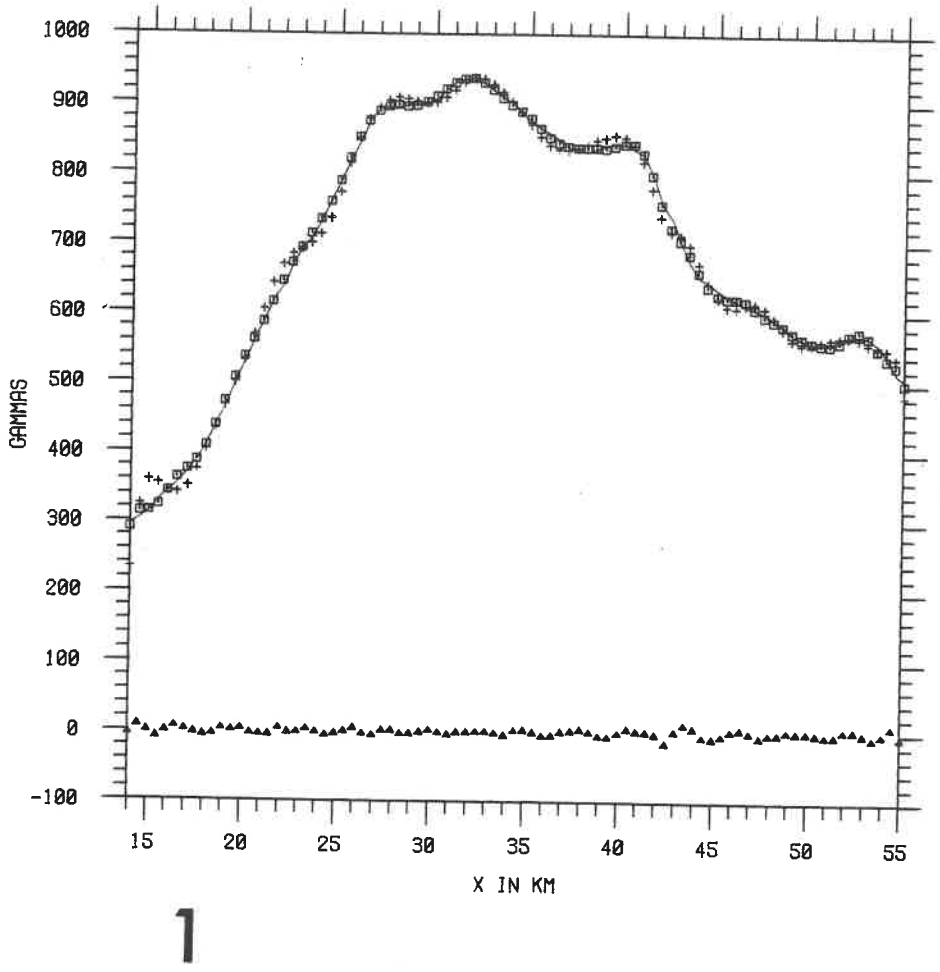


Fig. A3.1 Cenozoic Volcanic Province Profile A-A' Model 1
Profile Azimuth = 315° Field Declination = 63°
Field Inclination = -73°

			Bodies	1	2	3	4	5	6	7	8	9	10	11	12	13	14	15	16	Errors
1	Susceptibility (cgs)			203	171	354	187	-46	33	-54	148	255	167	20	15	-43	165	273	92	-0.018±6.5
	Remanent Mag.	Amplitude (gauss)		626	1280	2470	2720	2340	1920	1640	1230	906	847	788	719	836	691	678	670	-0.021±3.82
		Inclination		-13.4	-13.4	-31.7	-68.4	-17.5	-7.4	-1.2	1.7	2.2	3.0	3.8	9.0	24.8	13.6	29.0	43.8	
		Declination		135	135	135	315	315	315	315	315	315	315	315	315	315	315	315	135	

Fig. A3.1 (continued) Table of results.



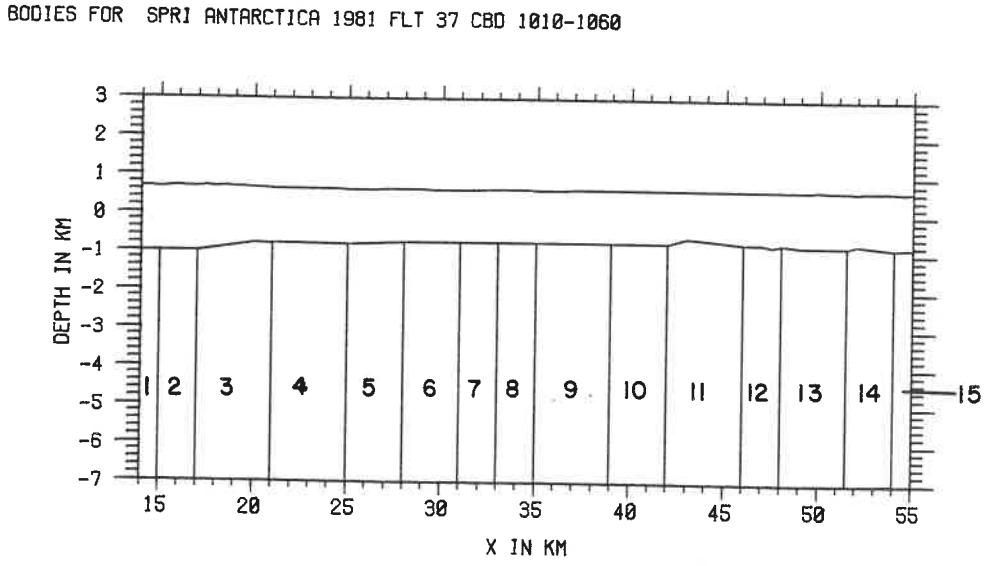
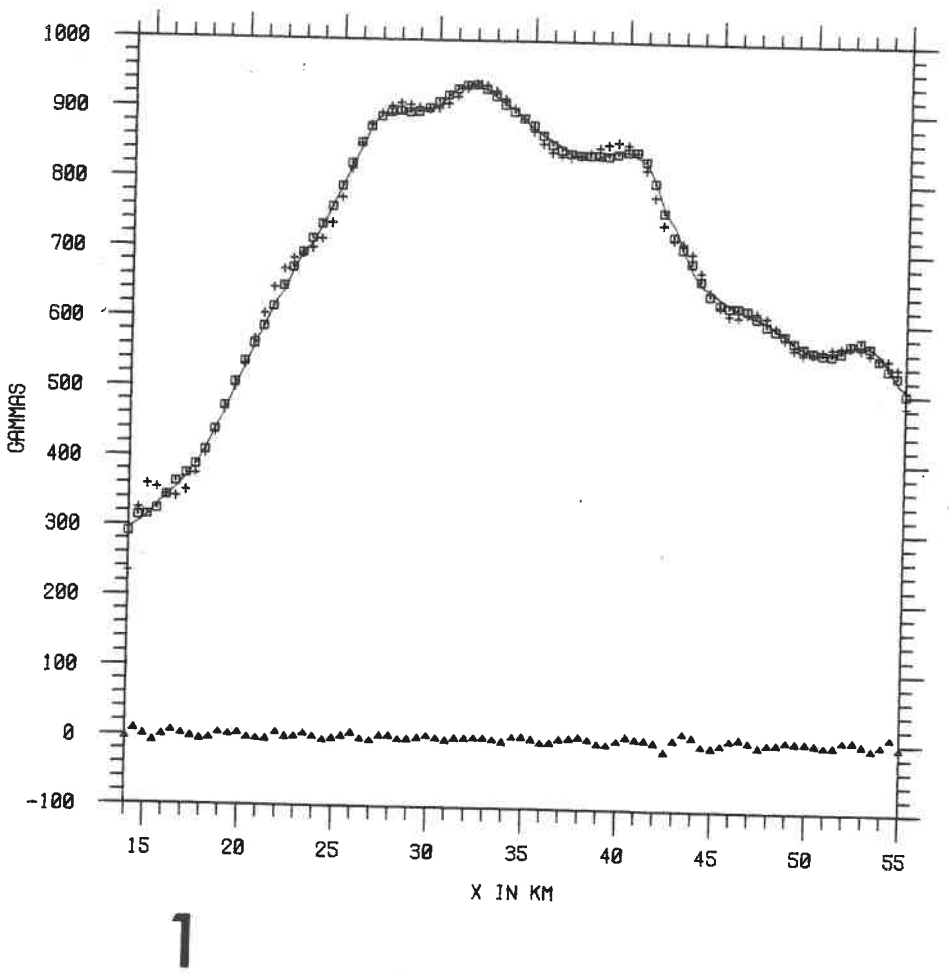


Fig. A3.2 Cenozoic Volcanic Province Profile B-B' Model 1
Profile Azimuth = 335° Field Declination = 53°
Field Inclination = -70.7°



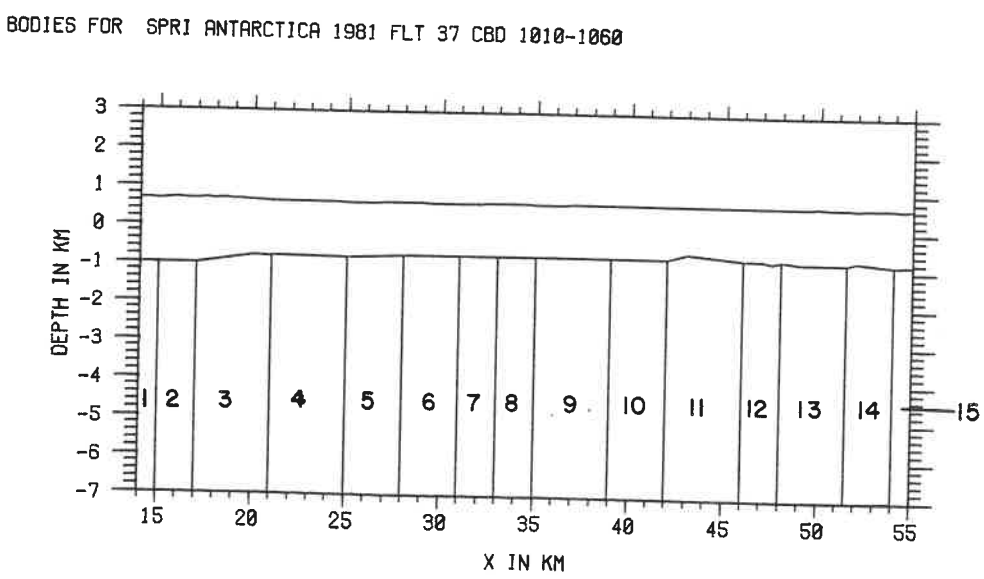
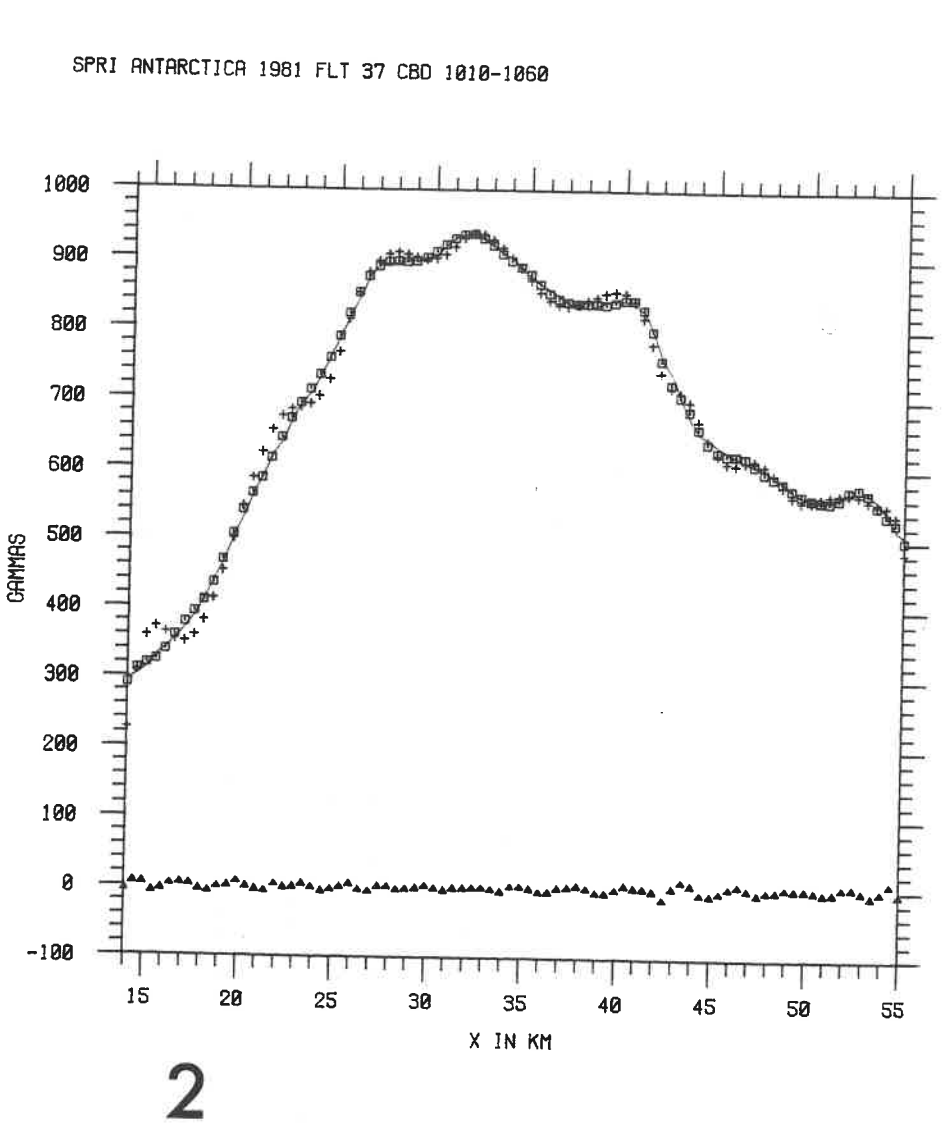


Fig. A3.2 Cenozoic Volcanic Province Profile B-B' Model 1
Profile Azimuth = 335° Field Declination = 53°
Field Inclination = -70.7°



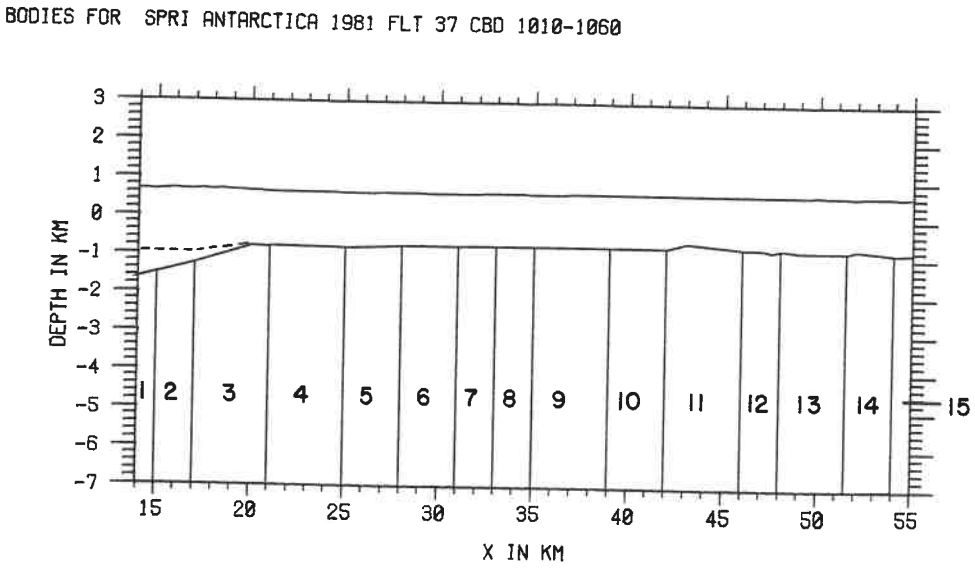
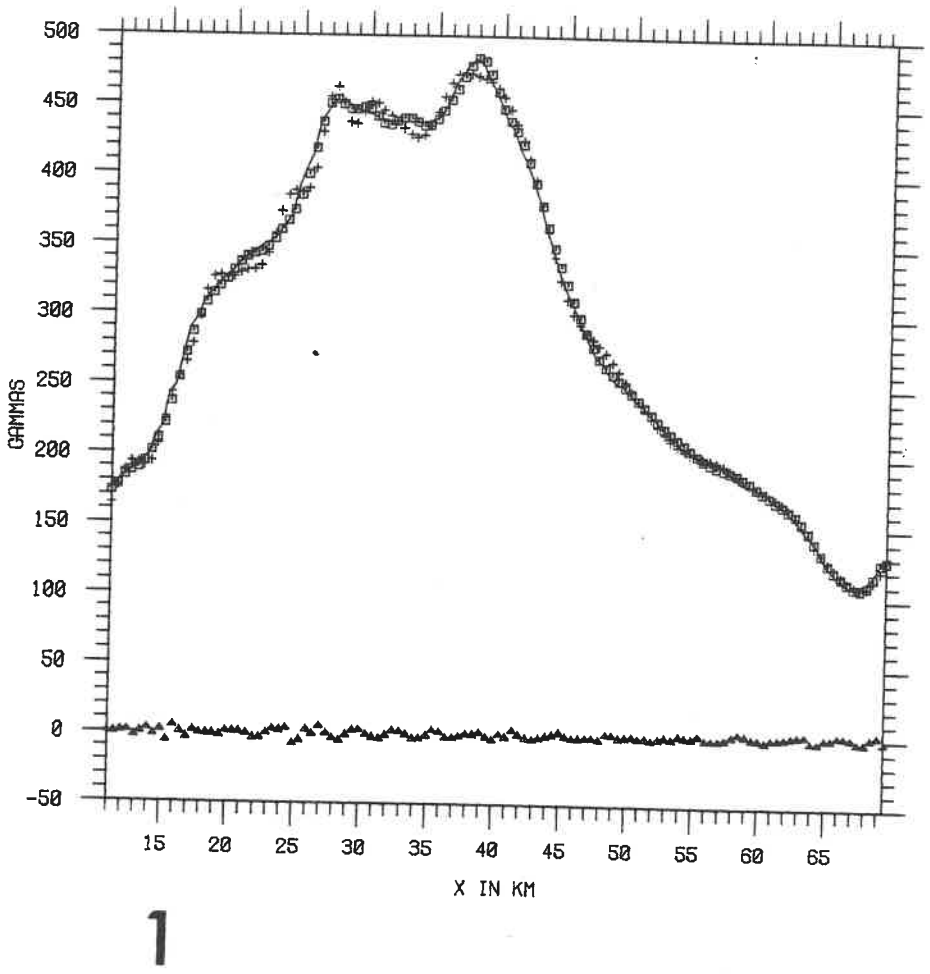


Fig. A3.3 Cenozoic Volcanic Province Profile B-B' Model 2
Profile Azimuth = 335° Field Declination = 53°
Field Inclination = -70.7°

			Bodies	1	2	3	4	5	6	7	8	9	10	11	12	13	14	15	Errors
1	Susceptibility (cgs)			1470	1210	1340	1520	1670	1650	1700	1660	1600	1600	1330	1360	1240	1130	1240	-0.346±14.6
	Remanent Mag.	Amplitude (gauss)		925	939	853	904	944	910	904	866	834	818	644	653	654	633	610	-0.021±4.26
		Inclination		-38.2	-58.0	-51.0	-43.8	-45.0	-42.6	-44.6	-44.6	-48.5	-45.2	-50.7	-70.0	-68.2	-53.9	-38.2	
		Declination		155	335	335	335	335	335	335	335	335	335	335	335	335	335	335	
2	Susceptibility (cgs)			2150	1180	1270	1460	1630	1610	1670	1630	1570	1580	1310	1340	1220	1120	1220	-0.549±17.8
	Remanent Mag.	Amplitude (gauss)		1400	967	817	892	934	901	898	860	828	813	640	651	653	633	611	-0.025±4.35
		Inclination		-28.5	-43.7	-60.1	-46.0	-47.0	-44.3	-46.4	-46.3	-50.2	-46.6	-52.4	-72.4	-70.4	-55.5	-39.0	
		Declination		155	335	335	335	335	335	335	335	335	335	335	335	335	335	335	

Figs. A3.2 and A3.3 (continued) Table of results.



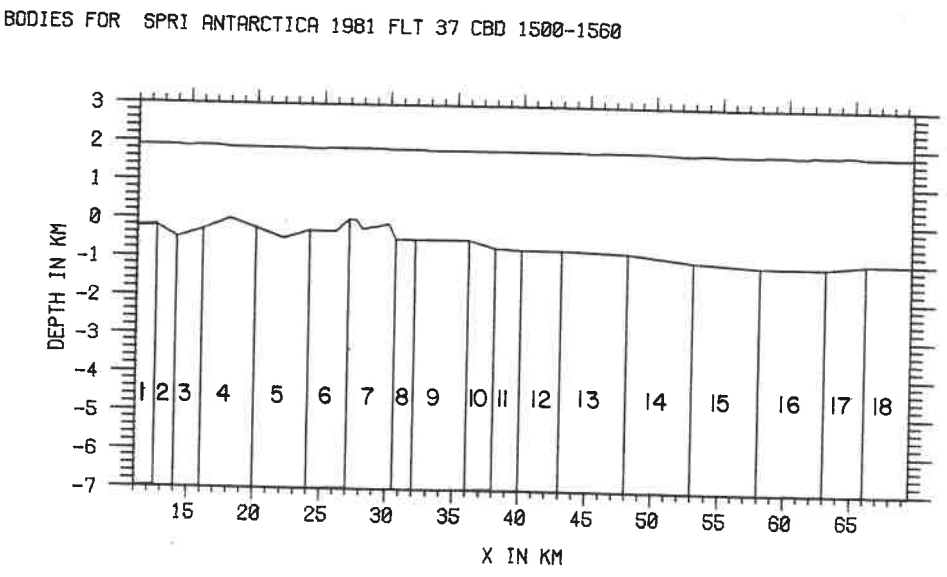
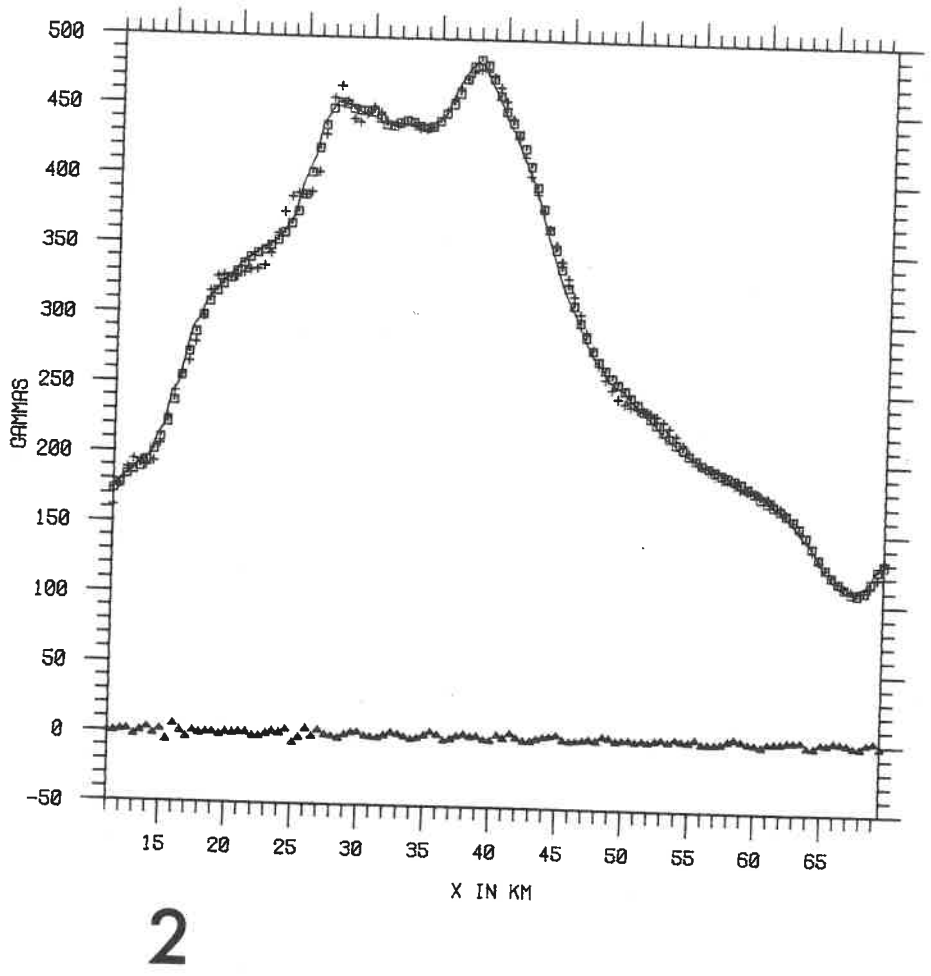


Fig. A3.4 Cenozoic Volcanic Province Profile C-C' Model 1
Profile Azimuth = 45° Field Declination 64.5°
Field Inclination = -73.5°



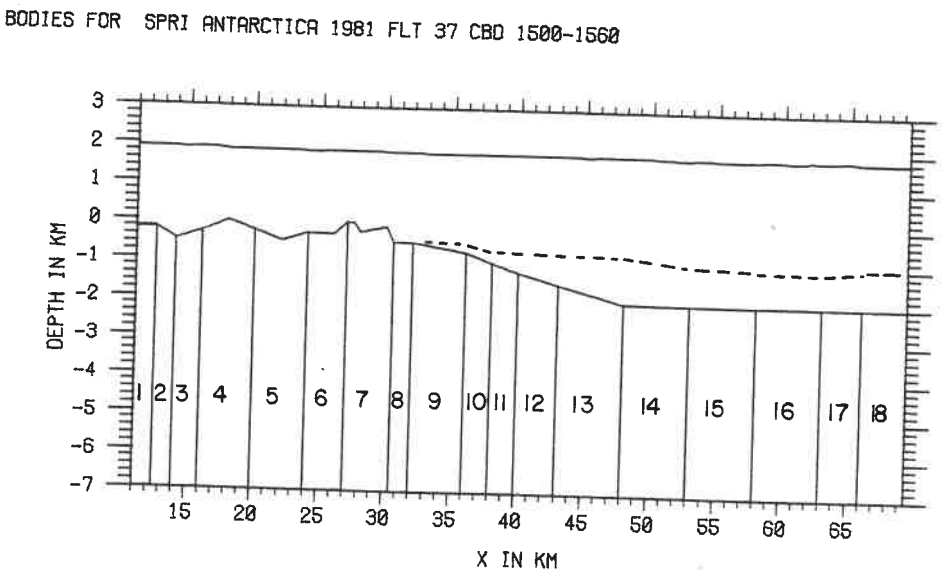
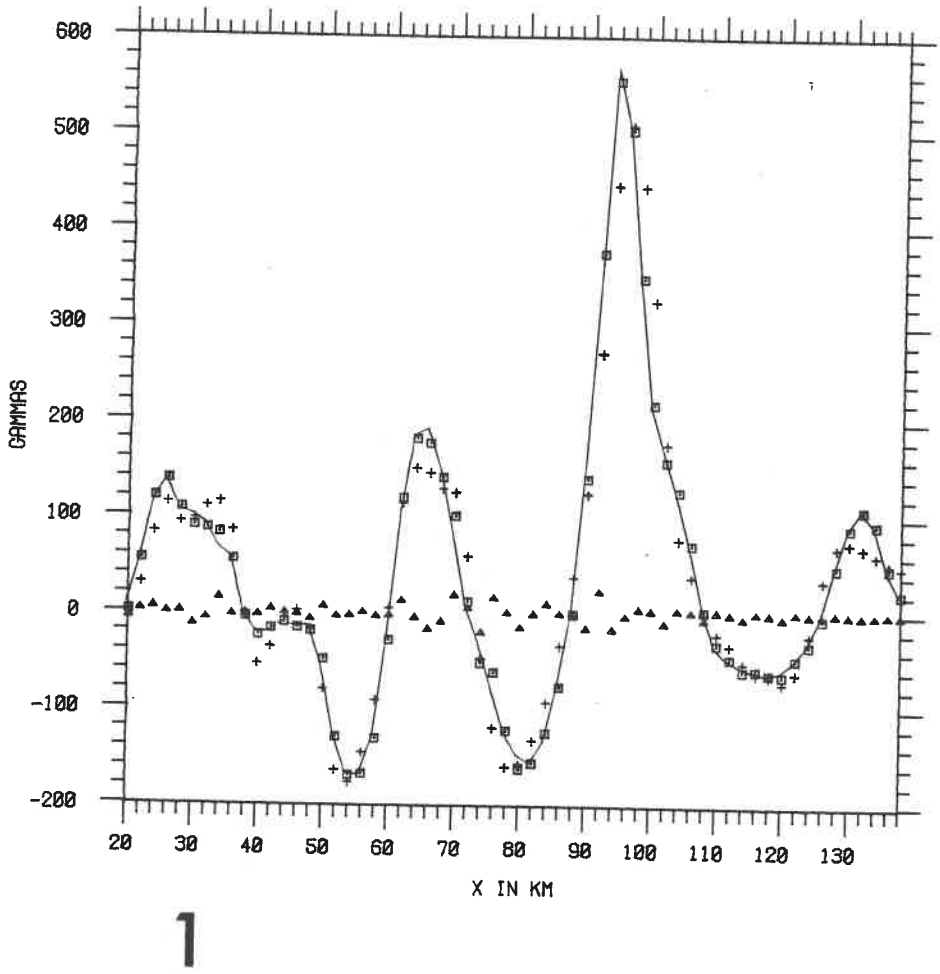


Fig. A3.5 Cenozoic Volcanic Province Profile C-C' Model 2
Profile Azimuth = 45° Field Declination = 64.5°
Field Inclination = -73.5°

			Bodies	1	2	3	4	5	6	7	8	9	Errors
1			Susceptibility (cgs)	1030	1320	1630	1230	1530	1380	1240	1640	1360	
	Remanent Mag.		Amplitude (gauss)	808	699	317	247	320	256	135	81	277	
			Inclination	-45.8	-11.3	-23.7	-62.2	-71.9	-64.4	-75.2	50.8	-8.4	
			Declination	45	45	45	45	45	45	45	225	225	
(continued)			Bodies	10	11	12	13	14	15	16	17	18	
1			Susceptibility (cgs)	1390	1460	1340	1200	1160	1130	1070	977	911	-0.011±6.88
	Remanent Mag.		Amplitude (gauss)	413	755	762	675	684	695	726	798	915	-0.007±2.09
			Inclination	-2.3	-11.9	-29.9	-34.0	-38.6	-38.3	-36.8	-32.0	-36.8	
			Declination	225	225	225	225	225	225	225	225	225	

			Bodies	1	2	3	4	5	6	7	8	9	Errors
2			Susceptibility (cgs)	1310	1320	1640	1240	1540	1380	1250	1550	1390	
	Remanent Mag.		Amplitude (gauss)	832	746	361	244	297	254	131	285	254	
			Inclination	-44.0	-9.2	-15.4	-47.5	-53.3	-35.8	-10.6	58.3	49.1	
			Declination	45	45	45	45	45	45	45	45	225	
(continued)			Bodies	10	11	12	13	14	15	16	17	18	
2			Susceptibility (cgs)	1470	1570	1520	1550	1520	1370	1330	1210	1250	-0.012±6.15
	Remanent Mag.		Amplitude (gauss)	515	1050	981	905	931	958	1040	1270	1570	-0.005±1.77
			Inclination	52.9	18.0	-10.2	-18.0	-18.2	-19.4	-19.6	-17.3	-27.9	
			Declination	225	225	225	225	225	225	225	225	225	

Figs. A3.4 and A3.5 (continued) Table of Results.



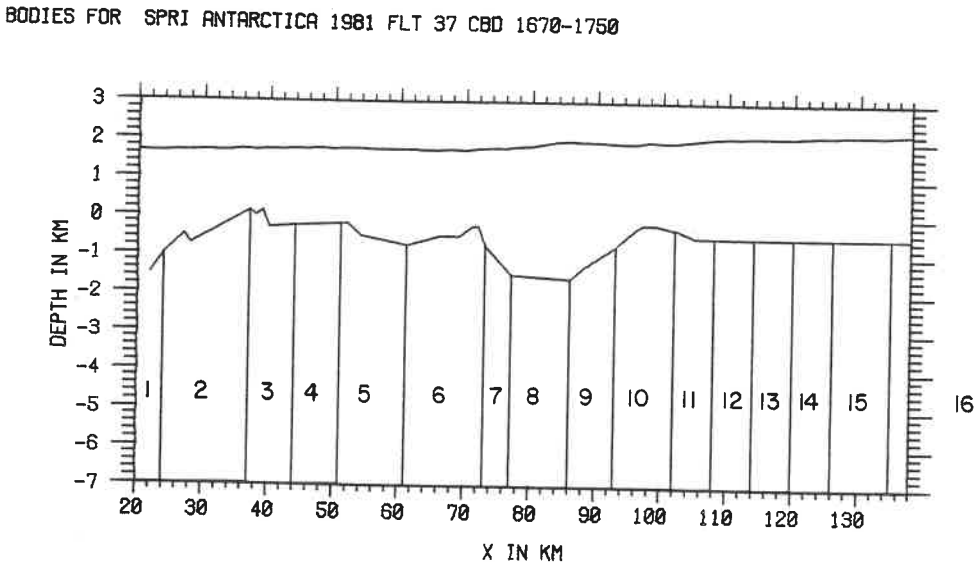
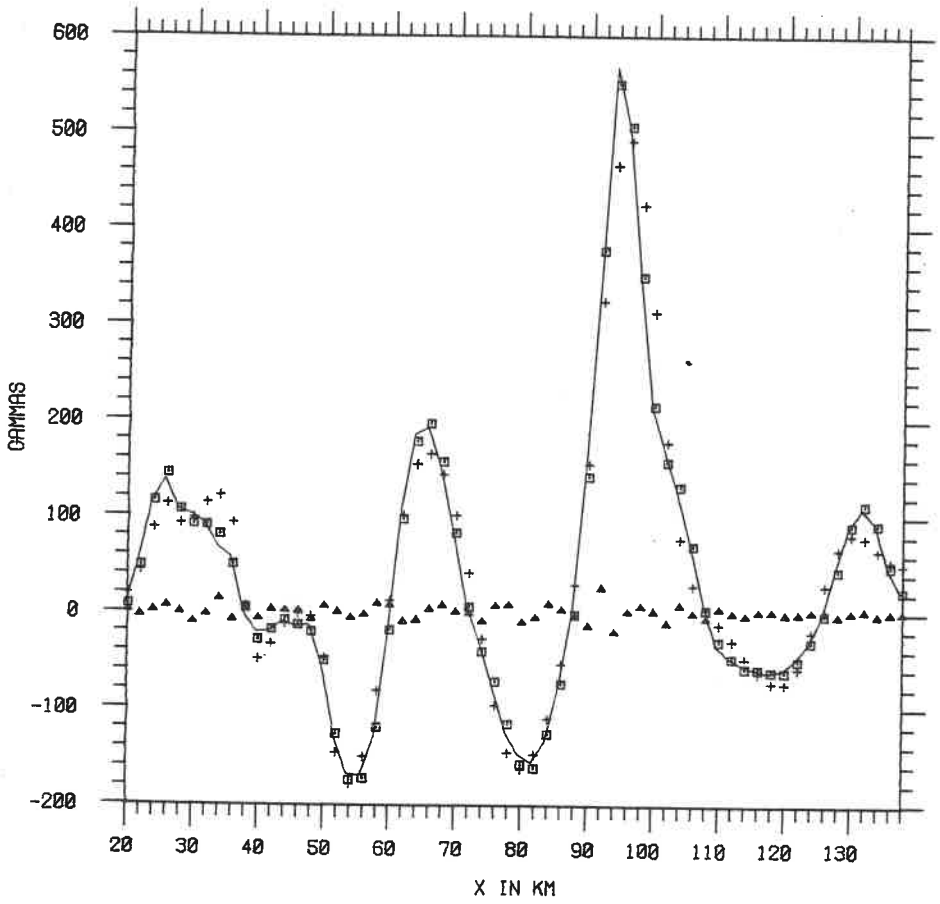


Fig. A3.6 Sinuous Ridge Profile A-A' Model 1
Profile Azimuth = 45° Field Declination = 62°
Field Inclination = -72.5°

SPRI ANTARCTICA 1981 FLT 37 CBD 1670-1750



2

BODIES FOR SPRI ANTARCTICA 1981 FLT 37 CBD 1670-1750

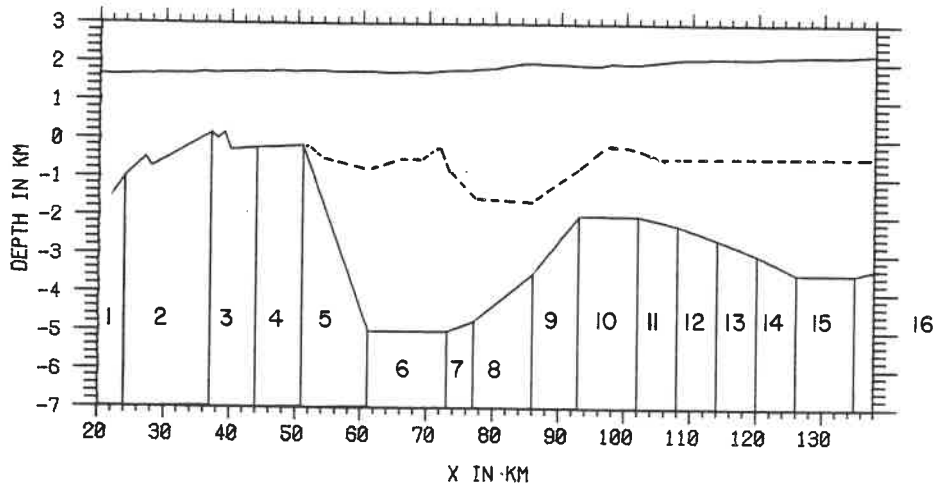
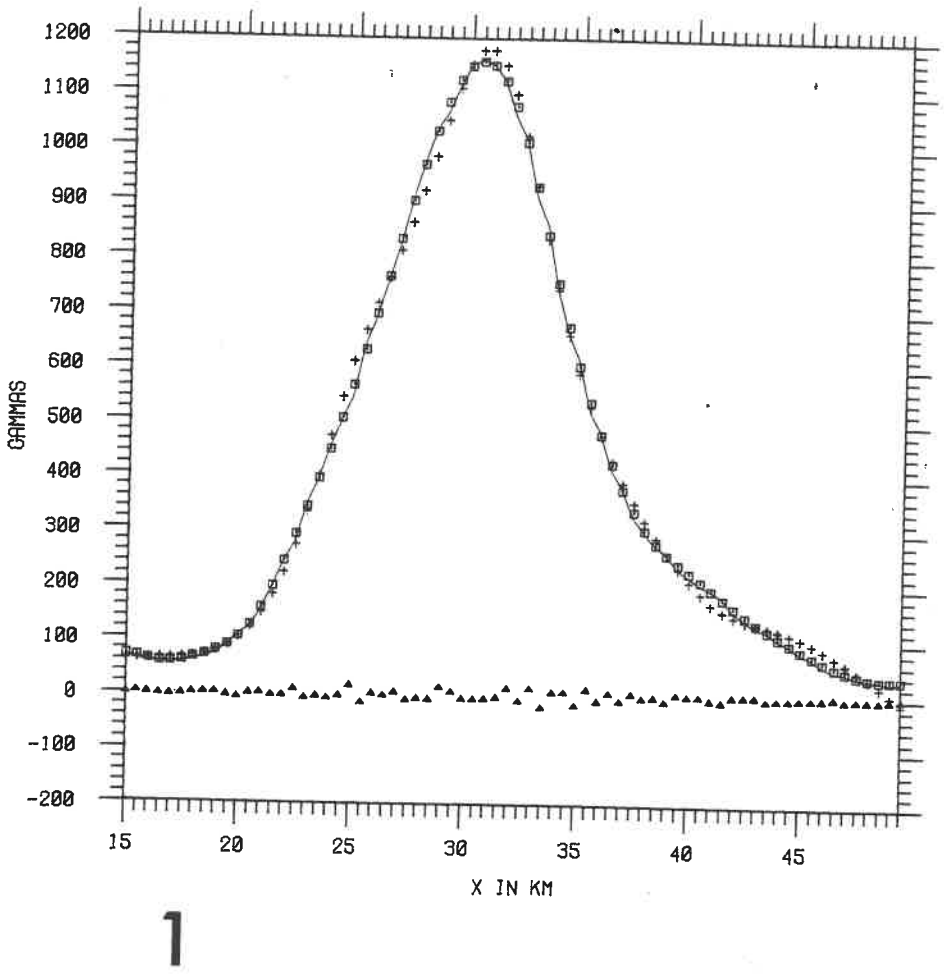


Fig. A3.7 Sinuous Ridge Profile A-A' Model 2
Profile Azimuth = 45° Field Declination = 62°
Field Inclination = -72.5°

			Bodies	1	2	3	4	5	6	7	8	Errors
1	Susceptibility (cgs)			281	298	231	249	137	301	312	199	
	Remanent Mag.	Amplitude (gauss)		112	109	74	59.9	11.3	138	142	37	
		Inclination		-51.0	-84.4	-70.4	-75.4	-48.8	-87.4	-40.4	47.8	
		Declination		225	225	225	225	45	45	225	225	
(continued)			Bodies	9	10	11	12	13	14	15	16	
1	Susceptibility (cgs)			271	537	424	351	298	252	331	317	-0.043±37.4
	Remanent Mag.	Amplitude (gauss)		32	252	274	218	201	189	194	144	-0.013±7.9
		Inclination		66.9	-42.2	-54.5	-58.1	-64.1	-73.8	-88.4	-79.6	
		Declination		225	45	45	45	45	45	45	45	

			Bodies	1	2	3	4	5	6	7	8	Errors
2	Susceptibility (cgs)			311	308	240	237	171	1330	1020	291	
	Remanent Mag.	Amplitude (gauss)		169	192	168	157	139	1080	1160	296	
		Inclination		-84.4	-77.3	-89.0	-87.3	-78.3	-84.1	-23.7	38.2	
		Declination		45	45	45	45	225	225	225	225	
(continued)			Bodies	9	10	11	12	13	14	15	16	
2	Susceptibility (cgs)			290	811	523	509	456	382	668	554	2.13±30.5
	Remanent Mag.	Amplitude (gauss)		204	586	671	595	603	626	658	344	-0.025±6.97
		Inclination		71.9	-40.4	-65.3	-83.5	-81.7	-63.8	-49.5	-30.7	
		Declination		45	45	45	45	45	45	225	225	

Figs. A3.6 and A3.7 (continued) Table of results.



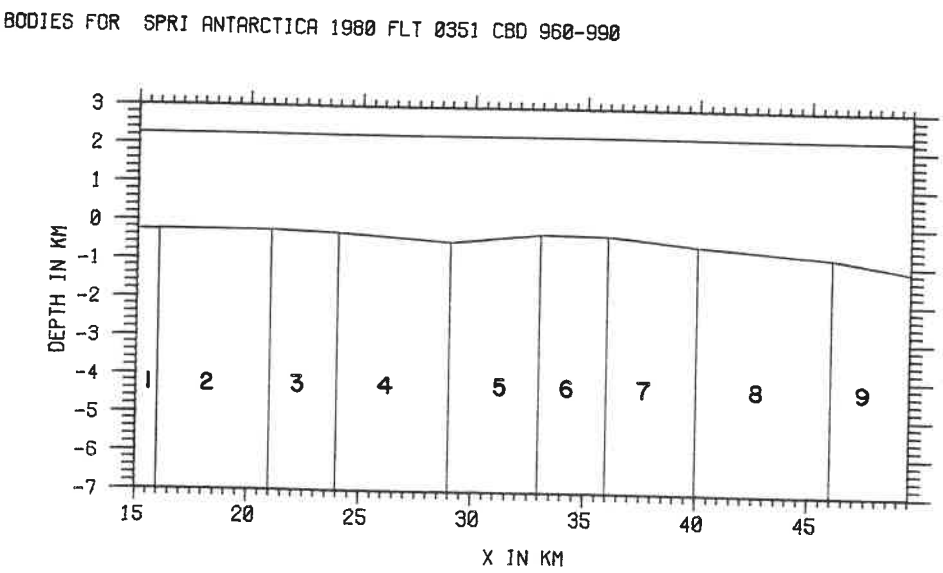
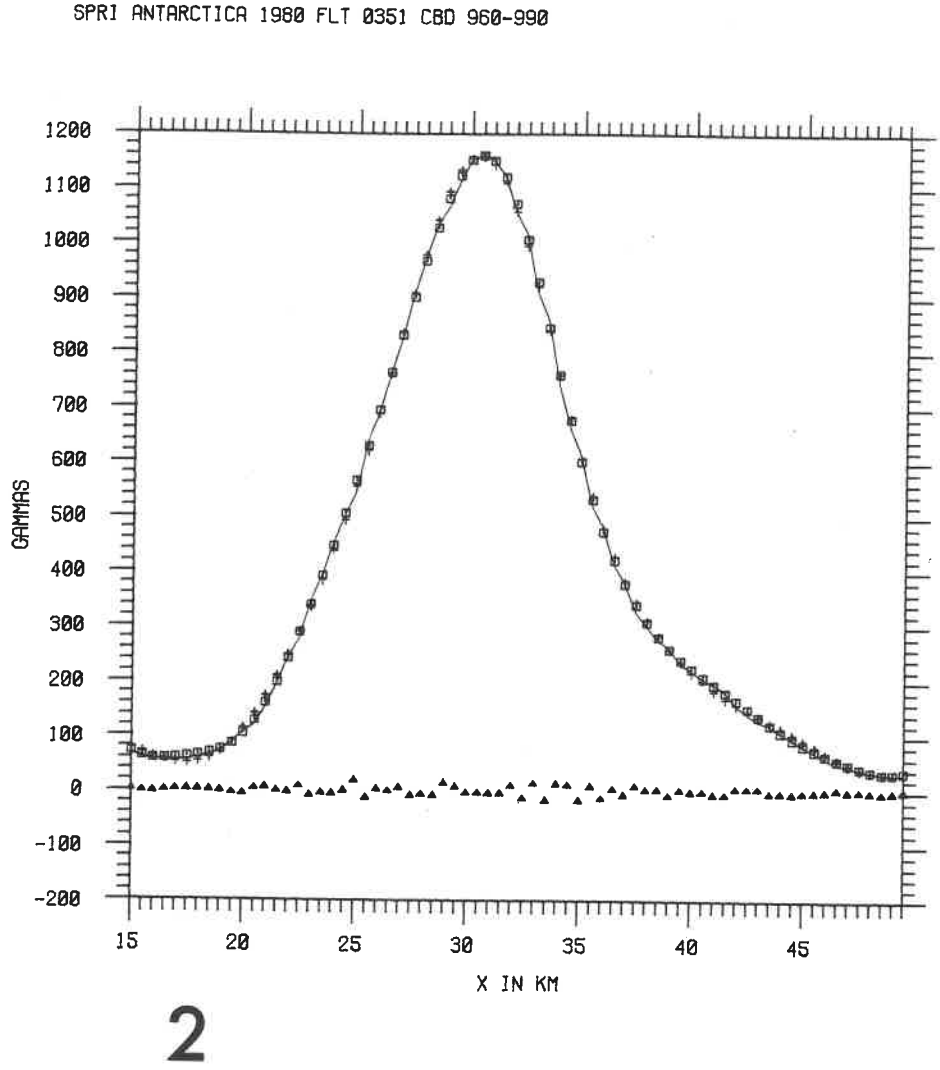


Fig. A3.8 Sinuous Ridge Profile B-B' Model 1
Profile Azimuth = 315° Field Declination = 60°
Field Inclination = -72°



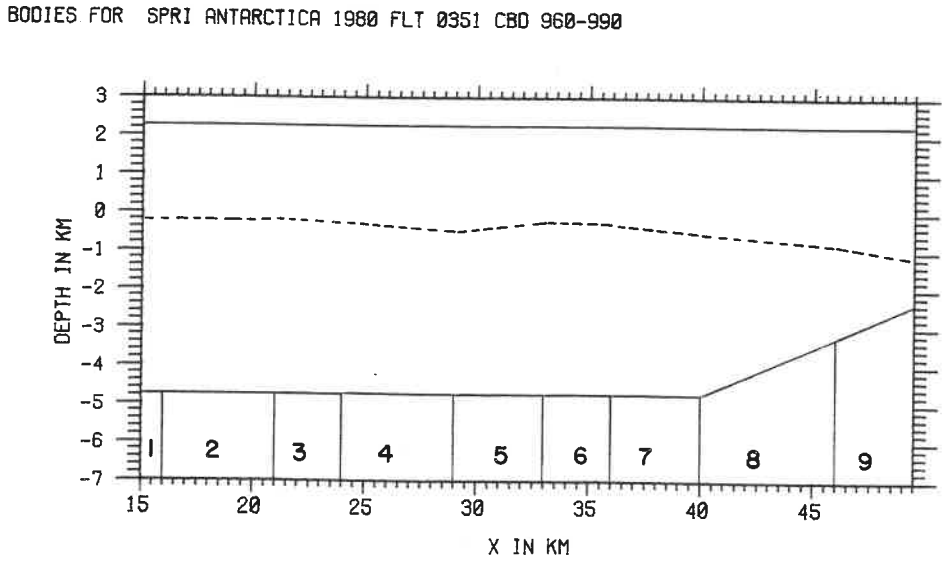
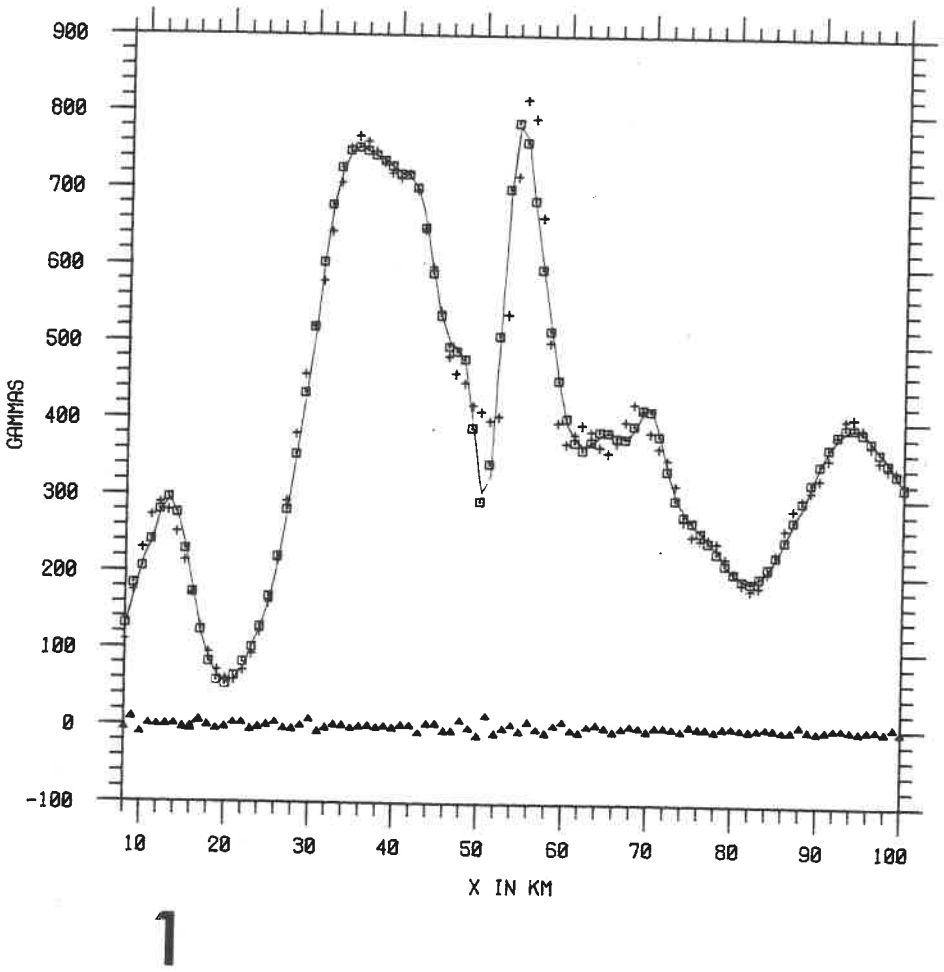


Fig. A3.9 Sinuous Ridge Profile B-B' Model 2
Profile Azimuth = 315° Field Declination = 60°
Field Inclination = -72°

Bodies			1	2	3	4	5	6	7	8	9	Errors
1	Susceptibility (cgs)		643	656	691	1150	1720	1050	979	850	783	0.046±20.8
	Remanent Mag.	Amplitude (gauss)	631	603	720	737	750	408	293	284	256	-0.001±6.66
		Inclination	-60.0	-32.7	-22.3	-17.7	-32	-23.6	-27.2	-52.3	-46.2	-
		Declination	315	315	315	315	315	315	315	315	315	
2	Susceptibility (cgs)		2500	463	2570	1700	9290	353	3220	1650	754	-0.025±10.3
	Remanent Mag.	Amplitude (gauss)	7430	7520	17700	13700	17500	15100	5410	975	262	-0.006±6.84
		Inclination	7.5	-11.9	-81.7	-22.6	-9.4	11.3	51.2	35.7	45.2	
		Declination	135	135	135	315	315	315	315	315	315	

Figs. A3.8 and A3.9 (continued) Table of results.



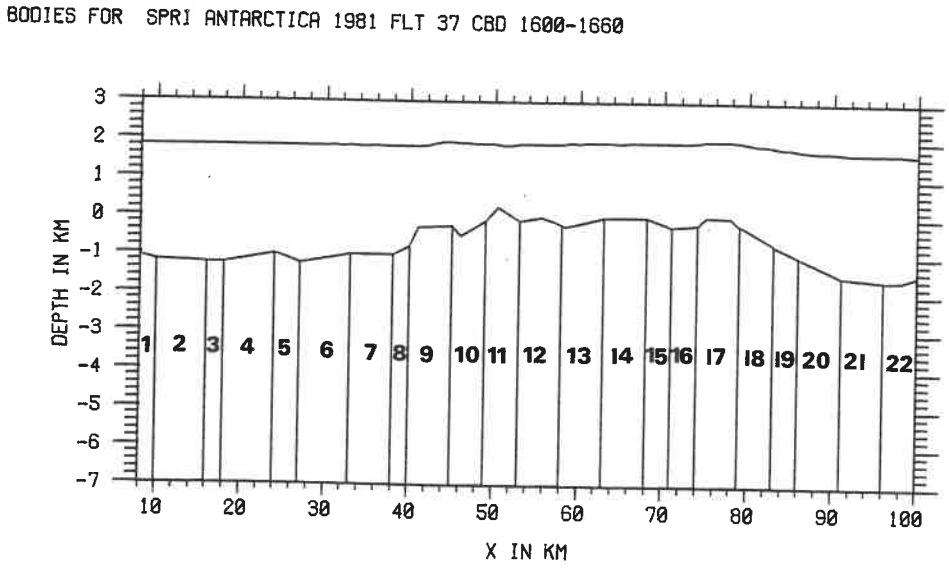
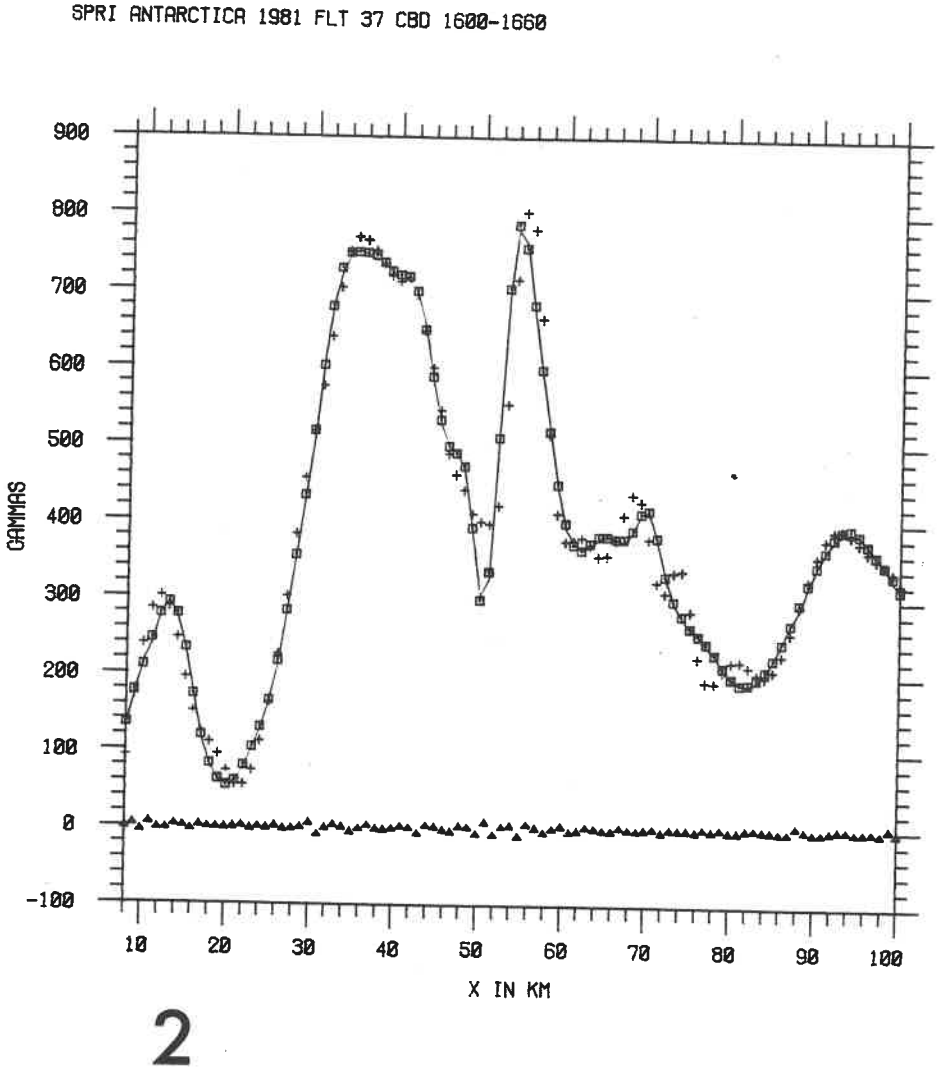


Fig. A3.10 Sinuous Ridge Profile C-C' Model 1
Profile Azimuth = 315° Field Declination = 60°
Field Inclination = -72°



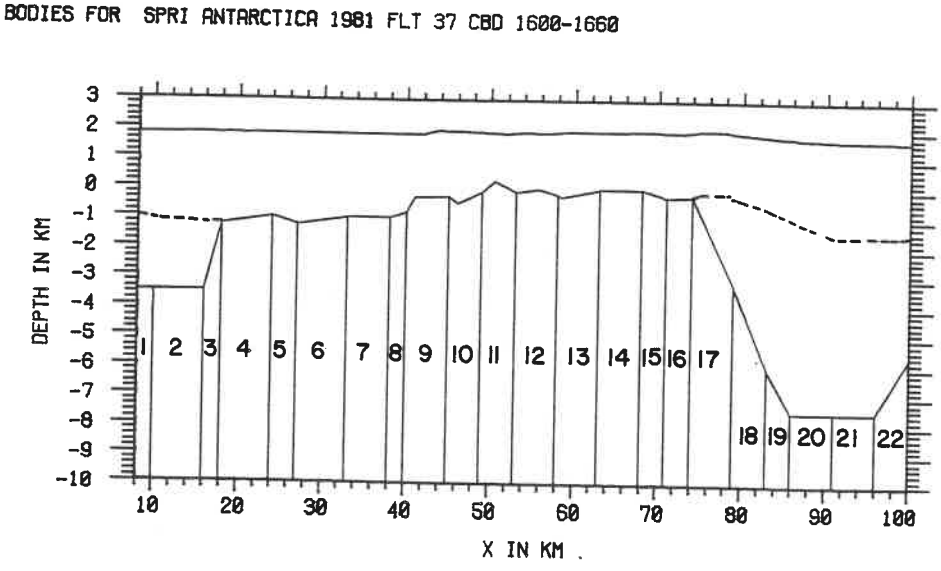


Fig. A3.11 Sinuous Ridge Profile C-C' Model 2
Profile Azimuth = 315° Field Declination = 60°
Field Inclination = -72°

			Bodies	1	2	3	4	5	6	7	8	9	10	11	Errors
1			Susceptibility (cgs)	710	1010	966	944	1040	1460	1760	1980	1450	1600	1170	
	Remanent Mag.		Amplitude (gauss)	998	1130	1190	1040	1080	1090	975	971	695	733	349	
			Inclination	-77.1	-37.6	-25.6	-21.2	-14.8	-17.3	-18.2	-17.1	-20.9	-14.7	-2.80	
			Declination	315	315	315	315	315	315	315	315	315	315	315	
(continued)			Bodies	12	13	14	15	16	17	18	19	20	21	22	
1			Susceptibility (cgs)	1690	1440	1340	1450	1510	1180	1320	1390	1570	1750	1590	-0.883±33.3
	Remanent Mag.		Amplitude (gauss)	368	418	481	537	464	421	497	567	620	678	681	-0.019±4.17
			Inclination	-71.4	-85.3	-86.8	-64.5	-86.0	-80.5	-83.1	-83.5	-83.0	-77.2	-65.4	
			Declination	315	315	315	315	315	135	135	135	315	135	135	

			Bodies	1	2	3	4	5	6	7	8	9	10	11	Errors
2			Susceptibility (cgs)	657	1460	615	586	743	1070	1330	1470	1110	1220	873	
	Remanent Mag.		Amplitude (gauss)	1480	1680	1360	821	755	696	516	408	283	353	255	
			Inclination	-54.4	-27.9	-28.3	-7.90	-3.20	-6.90	-6.8	-4.7	-13.1	-4.3	21.0	
			Declination	315	315	315	315	315	315	315	315	315	315	315	
(continued)			Bodies	12	13	14	15	16	17	18	19	20	21	22	
2			Susceptibility (cgs)	1340	1090	1010	1100	808	1030	2730	3100	5620	6540	3130	-1.02±34.5
	Remanent Mag.		Amplitude (gauss)	102	117	146	105	146	253	1080	7330	9880	8260	2150	-0.005±3.06
			Inclination	-13.5	-4.6	-10.2	-20.9	14.4	3.7	26.7	8.5	-13.7	-86.6	-86.2	
			Declination	135	135	135	135	135	135	135	135	135	135	315	

Figs. A3.10 and A3.11 (continued) Table of results.

REFERENCES

MERICAN GEOG. SOC. OF NEW YORK, 1970, "Antarctica, 1:5,000,000", sheet B

DAMS C.J., WODZICKI A., BRADSHAW J.D., LAIRD M.G., in press. "K-Ar ages of the Wilson, Robertson Bay, Sledgers and Mariners Groupes, North Victoria Land, Antarctica". in: Craddock, C. (ed), Antarctic Geoscience, Madison, University of Wisconsin Press

)AMS R.D., 1972. "Dispersion wave studies in Antarctica". in: Adie, R.J. (ed), Antarctic Geology and Geophysics, Oslo, Universitetsforlaget, p473-483

IE R.J., 1955. "The Petrology of Graham Land: II, The Andean granite-gabbro suite". Falkland Islands Dependencies Survey Scientific Report, no.12, p39

E R.J., 1964. "Geological History". in: Priestley, R., Adie, R.J., and Robin, G. de Q., (eds), Antarctic Research, Butterworths, London, p118-162.

)SERVICE, undated. "Magnetic fields and gradients over vertical prisms and dipping sheets". Aero Service, Houston, Texas, 318pp

G.B., 1855. "On the computation of the effect of the attraction on mountains masses, as disturbing the apparent astronomical latitude of stations in geodetic surveys". Phil. Trans. Royal Society, London, vol.145, p101-104

)FU S.I., 1978. "Recent progress in Antarctic auroral studies". Antarctic Research Series, vol.29, p157-199

FU S.-I., CHAPMAN S., 1961. "New theory of the Aurora Polaris". American Rocket Society, p775-783

SON W.L., CORDELL L., 1973. "Digital magnetic interpretation system". JSGS unpub. report, 32pp

BAUGH N.B., 1961. "Preliminary report on the geology of the Dufek assif". IGY, World Data Center A, Glaciology, Glaciology Report 4, 155-193

P.F., 1979. "The history of ridge-crest offset at the Falkland-gulhas fracture Zone from a small circle geophysical profile". ophysical Journal of the Royal Astronomical Society, vol.59, p131-

145

BARKER P.F., BUCKLEY F., REX D.C., 1977. "Cenozoic volcanism in the Antarctic". Phil. Trans. Royal Society, London, B, vol. 279, p131-142

BARKER P.F., GRIFFITHS D.H., 1972. "The evolution of the Scotia Ridge and Scotia Sea". Phil. Trans. Royal Society, London, A, vol. 271, p151-183

BARKER P.F., GRIFFITHS D.H., 1977. "Towards a more certain reconstruction of Gondwanaland". Phil. Trans. Royal Society, London, B, vol. 279, p143-159

BARKER P.F., HILL I.A., WEAVER S.D., PANKHURST R.J., in press. "The origin of the Eastern South Scotia Ridge as an intra-oceanic island arc". in: Craddock, C. (ed), Antarctic Geoscience, Madison, University of Wisconsin Press, abstract only

BARKER P.F., JAHN R.A., 1980. "A marine geophysical reconnaissance of the Weddell Sea". Geophysical Journal of the Royal Astronomical Society, vol.63, p271-283

BARRETT P.J., 1965. "Geology of the area between the Axel Heiberg and Shackleton Glaciers, Queen Maud Range, Antarctica". NZ Journal of Geology and Geophysics, vol.8, no.2, p344-363

BARRETT P.J., GRINDLEY G.W., WEBB P.N., 1972. "The Beacon Supergroup of East Antarctica". in: Adie, R.J. (ed), Antarctic Geology and Geophysics, Oslo, Universitetsforlaget, p319-332

BARRON E.J., HARRISON C.G.A., HAY W.W., 1978. "A revised reconstruction of the southern continents". Trans. American Geophysical Union, vol. 59, no.5, p436-449

BECK M.E., FORD A.B., BOYD W.W., 1968. "Palaeomagnetism of a stratiform intrusion in the Pensacola Mountains, Antarctica". Nature, vol. 217, no.5128, p534-535

BEHRENDT J.C., 1963. "Seismic measurements on the ice sheet of the Antarctic Peninsula". Journal of Geophysical Research, vol.68, no.21, p5793-88

BEHRENDT J.C., 1964a. "Antarctic Peninsula Traverse geophysical results relating to glaciological and geological studies". Wisconsin, report 64-1

BEHRENDT J.C., 1964b. "Distribution of narrow width magnetic anomalies in Antarctica". Science, vol. 144, p993-994

BEHRENDT J.C., DREWRY D.J., JANKOWSKI E.J., GRIM M.S., 1980. "Aeromagnetic and Radio Echo ice-sounding measurments show much greater area of the Dufek Intrusion, Antarctica". Science, vol. 299, p1014-1017.

BEHRENDT J.C., DREWRY D.J., JANKOWSKI E.J., GRIM M.S., 1981. "Aeromagnetic and Radio Echo ice-sounding measurments over the Dufek Intrusion, Antarctica.". Journal of Geophysical Research, vol. 86, B4, p3014-3020

BEHRENDT J.C., HENDERSON J.R., MEISTER L., RAMBO W.L., 1974. "Geophysical Investigations of the Pensacola Mountains and adjacent glaciated areas of Antarctica". US Geological Survey Professional Paper, no.844.

BEHRENDT J.C., MEISTER L., HENDERSON J.R., 1966. "Airborne geophysical study in the Pensacola Mountains of Antarctica". Science, vol. 153, no.3742, p1373-1376

BEHRENDT J.C., WOLD R.J., 1963. "Depth to Magnetic 'Basement' in West Antarctica". Journal of Geophysical Research, vol.68, no4, p1145-1153

BENTLEY C.R., 1962. "Glacial and subglacial geography of Antarctica". Geophysical Monograph 7: Antarctic Research, American Geophysical Union, p11-25

BENTLEY C.R., 1964. "The structure of Antarctica and its ice cover". in: Odishaw, H. (ed), Research in Geophysics, 2, Solid Earth and Interface Phenomena, M.I.T. Press, Cambridge, Mass., p335-389.

BENTLEY C.R., 1973. "Crustal structure of Antarctica". Tectonophysics, vol. 20, p229-240

BENTLEY C.R., CHANG F.K., 1971. "Geophysical exploration in Marie Byrd Land, Antarctica". Antarctic Research Series, vol. 16, p1-38

BENTLEY C.R., CLOUGH J.W., 1972. "Antarctic subglacial structure from seismic refraction measurments". in: Adie, R.J. (ed), Antarctic Geology and Geophysics, Oslo, Universitetsforlaget, p683-691

BENTLEY C.R., OSTENSO N.A., 1961. "Glacial and subglacial topography of West Antarctica.". Journal of Glaciology, vol. 3, p882-911

BENTLEY C.R., ROBERTSON J.D., in press. "Isostatic gravity anomalies in West Antarctica". in: Craddock, C. (ed), Antarctic Geoscience, Madison, University of Wisconsin Press

BIBBY J.S., 1966. "The stratigraphy of part of NE Graham Land and the James Ross Island Group". British Antarctic Survey Scientific Report, no.53,

p37.

BLAKELY R.J., 1975. "Documentation on program REDUCE". USGS internal report

BLAKELY R., COX A., 1972. "Identification of short polarity events by transforming marine magnetic profiles to the pole". Journal of Geophysical Research, vol.77, no.23, p4339-4349

BLUNDELL D.J., 1962. "Palaeomagnetic investigations in the Falkland Island Dependencies". British Antarctic Survey Scientific Report, no.39, 24pp

BLUNDELL D.J., STEPHENSON P.J., 1959. "Palaeomagnetism of some dolerite intrusions from the Theron Nunataks and Whichaway Nunataks, Antarctica.". Nature, vol. 184, p1860-1862

BOTT M.H.P., 1971. "The Interior of the Earth". Edward Arnold, London

BOUCET A.J., JOHNSON J.G., DOUMANI G.A., WEBERS G.F., 1967. "Devonian of Antarctica". in Oswald, D.H. (ed), International Symposium on the Devonian System, Calgary 1967, Alberta Society of Petroleum Geologists, p639-648.

BOYER S.J., 1979. "Glacial geologic observations in the Dufek Massif and the Forrestal Range, 1978-79". Antarctic Journal of US, vol.14, no.5, p46-47

BRIDEN J.C., OLIVER R.L., 1963. "Palaeomagnetic results from the Beardmore Glacier region, Antarctica". New Zealand Journal of Geology and Geophysics, vol. 6, p388-394

BROTCHIE J.F., SILVESTER R., 1969. "On Crustal Flexure". Journal of Geophysical Research, vol. 74, no.22, p5240-5252

BULL C., IRVING E., WILLIS I., 1962. "Further palaeomagnetic results from S. Victoria Land, Antarctica". Geophysical Journal of the Royal Astronomical Society, vol.6, no.3, p320-336

BURMESTER R.F., SHERIFF S.D., 1980. "Palaeomagnetics of the Dufek Intrusion, Pensacola Mountains, Antarctica". Antarctic Journal of the US, vol. 15, no.5, p43-45

CADY J.W., 1977. "Calculation of gravity and magnetic anomalies along profiles with end corrections and inverse solutions for density and magnetization". USGS open file report, 77-463

CADY J.W., 1980. "Calculation of gravity and magnetic anomalies of finite-length right polygonal prisms". Geophysics, vol.45, no.10, p1507-1512

CASTLE J.W., CRADDOCK C., 1975. "Deposition and metamorphism of the Polarstar Formation (Permian), Ellworth Mountains". Antarctic Journal of the US, vol. 10, no.5, p239-241

CHANG F.K., 1964. "Seismic wave studies in NW Marie Byrd Land, Antarctica". Bulletin of the Seismological Society of America, vol.54, no.1, p51-65

CHRISTENSEN E.L., 1970. "Radioglaciology - 300 MHz radar". TUD, Laboratory of Electromagnetic Theory, Report 93, Lyngby, 45pp

CLAERBOUT J.F., 1976. "Fundamentals of Geophysical Data Prospecting with Applications to Petroleum Prospecting". Mcgraw Hill, New York

CLARKSON P.D., in press. "Tectonic significance of the Shackleton Range". in: Craddock, C. (ed), Antarctic Geoscience, Madison, University of Wisconsin Press

CLARKSON P.D., BROOK M., 1977. "Age and position of the Ellsworth Mountains crustal fragment, Antarctica". Nature, vol. 265, no.5595, p615-616

CRABTREE R.D., DOAKE C.S.M., 1980. "Flow lines on Antarctic ice shelves". Polar Record, vol.18, p259-299

CRADDOCK C., 1969. "Geology of the Ellsworth Mountains". in: Bushnell V.C., and Craddock, C. (eds), Antarctic Map Folio Series, Folio 12, American Geog. Soc. of New York, Sheet 4

CRADDOCK C., 1970. "Tectonic map of Gondwanaland". in: Bushnell V.C., and Craddock, C. (eds), Antarctic Map Folio Series, Folio 12, American Geog. Soc. of New York, Sheet 23

CRADDOCK C., 1972. "Antarctic Tectonics". in: Adie, R.J. (ed), Antarctic Geology and Geophysics, Oslo, Universitetsforlaget, p449-455

CRADDOCK C., in press. "Antarctica and Gondwanaland". in: Craddock, C. (ed), Antarctic Geoscience, Madison, University of Wisconsin Press

CRADDOCK C., BASTIEN T.W., RUTFORD R.H., 1964. "Geology of the Jones Mountains area". in: Adie, R.J. (ed), Antarctic Geology, Amstedam, North Holland Pub. Co., p171-187

CRADDOCK C., WEBERS G.F., 1964. "Fossils from the Ellsworth Mountains, Antarctica". Nature, vol. 201, p174-175

CRADDOCK C., WEBERS G.F., in press. "Geology of the Ellsworth Mountains-Thiel Mountains Ridge". in: Craddock, C. (ed), Antarctic Geoscience, Madison, University of Wisconsin Press

CRARY A.P., 1963a. "Marine sediment thickness in the Eastern Ross Sea area, Antarctica". Geological Society of America Bulletin, vol.72, no.5, p787-790

CRARY A.P., 1963b. "Results of the US traverses in East Antarctica, 1958-61". IGY Glaciological Report, no.7, American Geog. Soc. of New York, 144pp

CRARY A.P., ROBINSON E.S., BENNETT H.F., BOYD W.W., 1962. "Glaciological studies of the Ross Ice Shelf, Antarctica, 1957". IGY Glaciological Report, no.6, American Geographical Society of New York

CRARY A.P., VAN der HOEVEN F.G., 1961. "Sub-ice topography of Antarctica, longitude 160° Wto 130° E". in: Symposium on Antarctic Glaciology, General Assembly of Helsinki, International Association of Scientific Hydrology, IUGG, (IASH publication no.55) p125-131

DALZIEL I.W.D., 1980. "Comments and Reply on Mesozoic evolution of the Antarctic Peninsula and the Southern Andes". Geology, p260-262

DALZIEL I.W.D., in press. "Pre-Jurassic history of the Scotia Arc region". in: Craddock, C. (ed), Antarctic Geoscience, Madison, University of Wisconsin Press

DALZIEL I.W.D., ELLIOT D.H., 1971. "Evolution of the Scotia Arc". Nature, vol.233, p246-252

DALZIEL I.W.D., ELLIOT D.H., 1973. "The Scotia Arc and Antarctic margin". in: Stehli, F.G. and Nairn, A.E.M. (eds), The Ocean Basins and Continental Margins: vol.1 The South Atlantic, Plenum, New York, p171-246

DEAN W.C., 1958. "Frequency analysis for gravity and magnetics interpretation". Geophysics, vol.23, p97-127

De WITT M., 1979. "Gondwanaland reassembly". Result of the reunite Gondwanaland workshop at the Univ. of Witwatersrand, Johannesberg, 1979, in: Cresswell M.M. and Vella, P. (eds), Gondwana Five, Proceedings of the 5th International Gondwana Symposium, Wellington, New Zealand, 1980, Balkema

DIETZ R.S., HOLDEN J.C., 1970. "Reconstruction of Pangaea; its breakup and dispersion of continents - Permian to Present". Journal of Geophysical Research, vol.75, no.26, p4939-4956

DIETZ R.S., HOLDEN J.C., SPROLL W.P., 1972. "Antarctica and continental

drift". in: Adie, R.J. (ed), Antarctic Geology and Geophysics, Oslo, Universitetsforlaget, p837-842

DOBRIN M.B., 1976. "Introduction to Geophysical Prospecting". McGraw Hill, 630pp

DOUMANI G.A., EHLERS E.G., 1962. "Petrology of rocks from mountains in Marie Byrd Land, West Antarctica". Geological Society of America Bulletin, vol.73, p877-882

DOUMANI G.A., et al, 1965. "Lower Devonian fauna of the Horlick Formation, Ohio Range Antarctica". in: Hadley J.B. (ed), Geology and Palaeontology of the Antarctic, Antarctic Research Series, vol.6, p241-81

DOW J.A.S., NEALL V.E., 1972. "Summary of the geology of Lower Rennick Glacier, North Victoria Land.". in: Adie, R.J. (ed), Antarctic Geology and Geophysics, Oslo, Universitetsforlaget, p339-345

DREWRY D.J., 1973. "Sub-ice relief and geology of East Antarctica". unpub PhD thesis in the University of Cambridge

DREWRY D.J., 1975a. "Initiation and growth of the East Antarctic ice sheet". Journal of the Geological Society, vol.131, p255-273

DREWRY D.J., 1975b. "Radio Echo Sounding Map of Antarctica". Polar Record, vol.17, no.109, p359-374

DREWRY D.J., 1976. "Deep sea drilling from Glomar Challenger in the southern ocean". Polar Record, vol.18, no.112, p47-77

DREWRY D.J., 1978. "Aspects of the early evolution of West Antarctic ice". in: Van Zinderen Bakker, E.M. (ed), Antarctic glacial history and world palaeoenvironments, A.A. Balkema, Rotterdam, p25-32

DREWRY D.J., MELDRUM D.T., 1978. "Antarctic airborne radio echo sounding 1977-78". Polar Record, vol.19, no.120, p267-273

DREWRY D.J., MELDRUM D.T., JANKOWSKI E.J., 1980. "Radio echo and magnetic sounding of the Antarctic ice sheet 1978-79". Polar Record, vol.20, no.124, p43-57

DREWRY, D.J., JORDAN, S.R., JANKOWSKI, E.J., to be published, "Measured properties of the Antarctic ice sheet: surface configuration, ice thickness, volume and bedrock characteristics". Annals of Glaciology, vol.3

DSDP, 1977. "Evolution of the SW Atlantic Ocean Basin: results of leg 36, DSDP". in: Initial Reports of the Deep Sea Drilling Project, vol.36, p993-1014

DU TOIT A.L., 1937. "Our Wandering Continents". Oliver and Boyd, Edinburgh, 366pp

ELLIOT D.H., 1972. "Major oxide chemistry of the Kirkpatrick Basalt, Central Transantarctic Mountains". in: Adie, R.J. (ed), Antarctic Geology and Geophysics, Oslo, Universitetsforlaget, p413-418

ELLIOT D.H., 1974. "The tectonic setting of the Jurassic Ferrar Group, Antarctica". in: Proceedings of the Symposium on Andean and Antarctic Volcanology Problems, International Assoc. of Volcanology and Chemistry of the Earth's Interior, p357-372

ELLIOT D.H., 1975. "Tectonics of Antarctica: A review". American Journal of Science, vol.275-A, p45-106

EVANS S., 1963. "Radio techniques for the measurement of ice thickness". Polar Record, vol.11, no.73, p406-410

FAURE G., HILL R.L., JONES L.M., ELLIOT D.H., 1972. "Isotope composition of strontium and silica content of Mesozoic basalt and dolerite from Antarctica". in: Adie, R.J. (ed), Antarctic Geology and Geophysics, Oslo, Universitetsforlaget, p617-24

FERRAR H.T., 1907. "Report on the field geology of the region explored during the 'Discovery' Antarctic expedition 1901-04". in: National Antarctic Expedition 1901-04, Natural History, vol.1 Geology, British Museum (Natural history), London, p1-100

FINKEL A., 1978. "Magnetic Compensation of the National Science Foundation's LC-130 Aircraft". APL report, S2R/78/194

FLINT R.F., 1971. "Glacial and Quaternary Geology". Wiley, London

FORD A.B., 1964. "Cordierite bearing hypersthene quartz monzonite porphyry in the Thiel Mountains and its regional importance". in: Adie, R.J. (ed), Antarctic Geology, Amstedam, North Holland Pub. Co., p429-441

FORD A.B., 1970. "Development of the layered series and capping granophyre of the Dufek Intrusion of Antarctica". in: Proceedings of the Symposium on the Bushveld igneous complex and other layered intrusions, Geological Society of South Africa, special pub. 1

FORD A.B., 1972a. "Fit of Gondwana Continents - Drift reconstruction from Antarctic continental viewpoint". 24th International Geological Congress (Montreal), section 3, p113-121

FORD A.B., 1972b. "The Weddell orogeny - latest Permian to early Mesozoic deformation at the Weddell Sea margin of the Transantarctic Mountains". in: Adie, R.J. (ed), Antarctic Geology and Geophysics, Oslo, Universitetsforlaget, p419-426

FORD A.B., AARON J.M., 1962. "Bedrock geology of the Thiel Mountains, Antarctica". Science, vol.137, no.3532, p751-752

FORD A.B., BARRETT P.J., 1975. "Basement rocks of the south-central Ross Sea, site 270, DSDP leg 28". in:Initial Reports of the Deep Sea Drilling Project, vol.28, p861-868

FORD A.B., BOYD W.W. Jnr., 1968. "The Dufek Intrusion, a major stratiform gabbroic body in the Pensacola Mountains, Antarctica". in: Proceedings of 23rd International Geological Congress, section 2, Volcanism and Tectogenesis, vol.2, p213-228

FORD A.B., HIMMELBERG G.R., 1976. "Cordierite and orthopyroxene megacrysts in late precambrian volcanic rocks of the Thiel Mountains". Antarctic Journal of the US, vol.11, no.4, p260-263

FORD A.B., KISTLER R.W., 1980. "K-Ar age, composition, and origin of Mesozoic mafic rocks related to Ferrar group Pensacola Mountains, Antarctica". New Zealand Journal of Geology and Geophysics, vol.23, p371-390

FORD A.B., SUMSION R.S., 1971. "Late precambrian silicic pyroclastic volcanism in the Thiel Mountains Antarctica". Antarctic Journal of the US, vol.6, no.5, p185-186

FOSSUM B.A., MAISEY G.H., TORSEN H.O., in press. "Marine geophysical research in the Weddell Sea during the Norwegian Antarctic research expedition". in: Craddock, C. (ed), Antarctic Geoscience, Madison, University of Wisconsin Press

GAIR H.S., STURM A., CARRYER S.J., GRINDLEY G.W., 1969. "The geology of Northern Victoria Land". in: Bushnell V.C., and Craddock, C. (eds), Antarctic Map Folio Series, Folio 12, American Geog. Soc. of New York, sheet 13

GEBCO, 1980. "Antarctica (1:6,000,000)". General Bathymetric Maps of the

Oceans, Canadian Hydrographic Service, Ottawa, Canada

GLEN J.W., PAREN J.G., 1975. "The electrical properties of snow and ice". Journal of Glaciology, vol.15, no.73, p15-38

GORDON R.G., COX A., 1980. "Palaeomagnetic test of the early Tertiary plate circuit between the Pacific Basin plates and the Indian plate". Journal of Geophysical Research, vol.85, B11, p6534-6546

GRIFFITHS J.R., 1974. "Revised continental fit of Australia and Antarctica". Nature, vol.249, p336

GRIKUROV G.E., 1978. "Geology of the Antarctic Peninsula". Amerind, New Dehli, and NSF Office of Polar Programs, Washington DC

GRINDLEY G.W., DAVEY F.J., in press. "Some aspects of the reconstruction of New Zealand, Australia and Antarctica (review)". in: Craddock, C. (ed), Antarctic Geoscience, Madison, University of Wisconsin Press

GRINDLEY G.W., LAIRD M.G., 1969. "Geology of the Shackleton Coast". in: Bushnell V.C., and Craddock, C. (eds), Antarctic Map Folio Series, Folio 12, American Geog. Soc. of New York, sheet 15

GRINDLEY G.W., MCDOUGALL I., 1969. "Age and correlation of the Nimrod Group and other precambrian rock units in the central Transantarctic Mountains, Antarctica". NZ Journal of Geology and Geophysics, vol.12, no.2 and 3, p391-411

GRINDLEY G.W., WARREN G., 1964. "Stratigraphic nomenclature and correlation in the western Ross Sea region". in: Adie, R.J. (ed), Antarctic Geology, Amstedam, North Holland Pub. Co., p314-333

GUNN B.M., 1966. "Modal and element variation in Antarctic tholeiites". Geochim. Cosmochim. Acta., vol.30, p881-920

GUNN B.M., WARREN G., 1962. "Geology of Victoria Land between the Mawson and Mulock Glaciers, Antarctica". New Zealand Geological Survey Bulletin 71, and Transantarctic expedition 1955-58 Scientific report, no.11, 157pp

HALPERN M., 1968. "Ages of Antarctic and Argentine rocks bearing on continental drift". Earth and Planetary Science Letters, vol.5, no.3, p159-167

HALPERN M., 1972. "Rb-Sr total rock and mineral ages from the Marguerite Bay area, Kohler Range and Fosdick Mountains". in: Adie, R.J. (ed),

Antarctic Geology and Geophysics, Oslo, Universitetsforlaget, p197-204

HAMILTON W., 1964. "Tectonic map of Antarctica - a progress report". in: Adie, R.J. (ed), Antarctic Geology, Amstedam, North Holland Pub. Co., p676-680

HAMILTON W., 1972. "The Hallett volcanic province, Antarctica". USGS Professional Paper, no.456-C, 62pp

HARRINGTON H.J., WOOD B.L., MCKELLAR I.C., LENSEN G.J., 1967. "Topography and geology of the Cape Hallett district, Victoria Land Antarctica". NZ Geological Survey Bulletin, no.80, 100pp

HARRISON C.G.A., BARRON E.J., HAY W.W., 1979. "Mesozoic evolution of the Antarctic Peninsula and the southern Andes". Geology, vol.7, p374-378

HARRISON C.H., 1970. "Reconstruction of subglacial relief from radio echo sounding records". Geophysics, vol.35, no.6, p1099-1115

HARTMAN R.R., TESKEY J., FRIEDBERG J.L., 1971. "A system for rapid digital aeromagnetic interpretation". Geophysics, vol.36, no.5, p891-918

HAYES D.E., DAVEY F.S., 1975. "A geophysical study of the Ross Sea, Antarctica". in: Initial Reports of the Deep Sea Drilling Project, vol.28, p919-942

HAYES D.E. et al, 1973. "Leg 28 deep sea drilling in the southern ocean". Geotimes, vol.18, no.6, p19-24

HEEZEN B.C., THARP M., BENTLEY C.R., 1972. "Morphology of the Earth in the Antarctic and subantarctic". in: Bushnell V.C. (ed), Antarctic Map Folio Series, Folio 16, American Geog. Soc. of New York, sheet 7

HERRON E.M., TUCHOLKE B.E., 1976. "Sea-floor magnetic patterns and basement structure in the south eastern Pacific". in: Initial Reports of the Deep Sea Drilling Project, vol.35, p263-278

HERZ N., 1977. "Timing of spreading in the South Atlantic: information from Brazilian alkalic rocks". Geological Society of America Bulletin, vol.88, p101

HICKERSON R.L., 1979. "Magnetic compensation National Science Foundation Polar research aircraft no.159131 for 1978-79". APL report, S2R/79/145

HILL I.A., BARKER P.F., 1980. "Evidence for Miocene back-arc spreading in the

central Scotia Sea". Geophysical Journal of the Royal Astronomical Society, vol.63, p427-440

HJELLE A., OHTA Y., WINSES T., in press. "Geology and petrology of southern Heritage Range, Ellsworth Mountains". in: Craddock, C. (ed), Antarctic Geoscience, Madison, University of Wisconsin Press

HUFFMAN J.W., SCHMIDT D.L., 1966. "Pensacola Mountains Project". Antarctic Journal of the US, vol.1, no.4, p123-124

HUGHES T., 1977. "West Antarctic ice streams". Reviews of Geophysics and Space Physics, vol.15, no.1, 46pp

IMHOF R.K., DOOLITTLE R.C., 1966. "Mapping from oblique photographs". in: Thompson, M.M. (ed), Manual of Photogrammetry, 3rd edition, American Society of Photogrammetry, p875-917

JACOBS J.A., 1974. "A Textbook on Geonomy". Adam Hilger, London

JAIN S., 1976. "An automatic method of direct interpretation of magnetic profiles". Geophysics, vol.41, no.3, p531-541

JANKOWSKI E.J., DREWRY D.J., 1981. "The structure of West Antarctica from Geophysical Studies". Nature, vol.291, no.5810, p17-21

JOHARI G.P., CHARRETTE P.A., 1975. "Permittivity and attenuation in polycrystalline and single ice 1h at 35 and 60 Mhz". Journal of Glaciology, vol.14, no.17, p293-303

KAMINUMA K., in press. "Seismicity in Antarctica". in: Craddock, C. (ed), Antarctic Geoscience, Madison, University of Wisconsin Press

KAMINUMA K., ISHIDA M., 1971. "Earthquake activity in Antarctica". Antarctic Record, no.42, p53-60

KELLOGG K.S., 1980. "Palaeomagnetic evidence for oroclinal bending of the southern Antarctic Peninsula". Geological Society of America Bulletin, vol.91, no.1, p414-420

KELLOGG K.S., REYNOLDS R.L., 1974. "Palaeomagnetic study of igneous rocks of the Northern Lassiter Coast, Antarctic Peninsula". Antarctic Journal of the US, vol.9, p38-40

KELLOGG K.S., REYNOLDS R.L., 1978. "Palaeomagnetic results from the Lassiter Coast, Antarctica and a test for oroclinal bending of the Antarctic Peninsula". Journal of Geophysical Research, vol.83, no.B5, p2293-2299

KING-HELE D.G., 1975. "A view of earth and air". Phil. Trans. Royal Society,

London, vol.278, p67-109

KOROTKEVICH Y.E.S., KOBLENTS Y.A.P., KOSENKO N.G., 1977. "Karta Korennogo Rel'yefa Antarktidy 1:10,000,000 (Soyuzmornii proyekt)". Arctic and Antarctic Institute, Leningrad

KOROTKEVICH Y.E.S., SAVTYUGIN L.M., MOREV V.A., 1978. "Drilling through the ice shelf near Novolazarevskaya station". Inf. Byull. Sov. Antarckt. Eksped., no.98, p49-52

KOVACH R.L., PRESS F., 1961. "Surface wave dispersion and crustal structure in Antarctica and the surrounding oceans". Ann. di Geofis. vol.14, no.2, p211-214

KYLE P.R., ELLIOT D.H., 1976. "Mineral chemistry of Kirkpatrick Basalts". Antarctic Journal of US, vol.11, no.4, p253-256

KYLE P.R., ELLIOT D.H., SUTTER J.F., 1980. "Jurassic Ferrar Supergroup tholeiites from the Transantarctic Mountains Antarctica and their relationships to the initial fragmentation of Gondwana". in: Cresswell M. M. and Vella, P. (eds), Gondwana Five, Selected Parers and abtracts presented at the fifth international Gondwana Symposium, Wellington, New Zealand

LAIRD M.G., BRADSHAW J.D., WODZICKI A., in press. "Stratigraphy of the late Precambrian and early Palaeozoic Bowers Supergroup, Northern Victoria Land". in: Craddock, C. (ed), Antarctic Geoscience, Madison, University of Wisconsin Press

LAUDON T.S., 1972. "Stratigraphy of eastern Ellsworth Land". in: Adie, R.J. (ed), Antarctic Geology and Geophysics, Oslo, Universitetsforlaget, p207-214

LAUDON T.S., LACKEY L.L., QUILTY P.G., OTWAY P.M., 1969. "Geology of Eastern Ellsworth Land". in: Bushnell V.C., and Craddock, C. (eds), Antarctic Map Folio Series, Folio 12, American Geog. Soc. of New York, sheet 3

LELIAK P., 1961. "Identification and evaluation of magnetic field sources of magnetic airborne detector equipped aircraft". IRE Transactions on Aerospace and Navigational Electronics, Sept. 1961

LeMASURIER W.E., 1972. "Volcanic record of Cenozoic glacial history of Marie Byrd Land". in: Adie, R.J. (ed), Antarctic Geology and Geophysics, Oslo, Universitetsforlaget, p251-259

LeMASURIER W.E., REX D.C., in press. "Volcanic record of glacial history in Marie Byrd Land and Western Ellsworth Land: Revised chronology and evaluation of tectonic interrelationships". in: Craddock, C. (ed), Antarctic Geoscience, Madison, University of Wisconsin Press

LEVANON N., BENTLEY C.R., 1979. "Ice elevation map of Queen Maud Land Antarctica from balloon altimetry". Nature, vol.278, p842-844

LEVANON N., JULIAN P.R., SUOMI V.E., 1977. "Antarctic topography from balloons". Nature, vol.268, no.5620, p514-516

LINDSLEY D.H., ANDREASEN G.E., BALSLEY J.R., 1966. "Magnetic properties of rock and minerals". in: Clark, S.P. Jnr. (ed), Handbook of Physical Constants, Geological Society of America, Memoir 97, p543-552

LONG W.E., 1964. "The stratigraphy of the Horlick Mountains". in: Adie, R.J. (ed), Antarctic Geology, Amstedam, North Holland Pub. Co., p352-363

LONG W.E., 1965. "Stratigraphy of the Ohio Range Antarctica". Antarctic Research Series, vol.6, p71-116

LOPATIN B.G., ORLENKO E.M., 1972. "Outline of the geology of Marie Byrd Land and the Eights Coast". in: Adie, R.J. (ed), Antarctic Geology and Geophysics, Oslo, Universitetsforlaget, p245-250

MACK J.W., HAUBRICH R.A., 1961. "Gravity analysis in gas storage exploration". paper presented at 31st. International Society of Exploration Geophysicists meeting, Denver, 1961

MANZONI M., NANNI T., 1977. "Palaeomagnetism of Ordovician lamprophyres from Taylor Valley, Victoria Land, Antarctica". Pure and Applied Geophysics, vol.115, p961-978

MCGREGOR V.R., WADE F.A., 1969. "Geology of Western Queen Maud Mountains". in: Bushnell V.C., and Craddock, C. (eds), Antarctic Map Folio Series, Folio 12, American Geog. Soc. of New York, sheet 16

MCKENZIE D.P., 1967. "Some remarks on heat flow and gravity anomalies". Journal of Geophysical Research, vol.72, no.24, p6261-6273

MENARD H.W., 1971. "The late Cenozoic history of the Pacific and Indian ocean basins". in: Turekian (ed), Late Cenozoic glacial ages, New Haven, Yale University Press, p1-14

MERCER J.H., 1978. "West Antarctic Ice sheet and CO_2 greenhouse effect: a threat of diaster". Nature, vol.271, no.5643, p321-325

LeMASURIER W.E., REX D.C., in press. "Volcanic record of glacial history in Marie Byrd Land and Western Ellsworth Land: Revised chronology and evaluation of tectonic interrelationships". in: Craddock, C. (ed), Antarctic Geoscience, Madison, University of Wisconsin Press

LEVANON N., BENTLEY C.R., 1979. "Ice elevation map of Queen Maud Land Antarctica from balloon altimetry". Nature, vol.278, p842-844

LEVANON N., JULIAN P.R., SUOMI V.E., 1977. "Antarctic topography from balloons". Nature, vol.268, no.5620, p514-516

LINDSLEY D.H., ANDREASEN G.E., BALSLEY J.R., 1966. "Magnetic properties of rock and minerals". in: Clark, S.P. Jnr. (ed), Handbook of Physical Constants, Geological Society of America, Memoir 97, p543-552

LONG W.E., 1964. "The stratigraphy of the Horlick Mountains". in: Adie, R.J. (ed), Antarctic Geology, Amstedam, North Holland Pub. Co., p352-363

LONG W.E., 1965. "Stratigraphy of the Ohio Range Antarctica". Antarctic Research Series, vol.6, p71-116

LOPATIN B.G., ORLENKO E.M., 1972. "Outline of the geology of Marie Byrd Land and the Eights Coast". in: Adie, R.J. (ed), Antarctic Geology and Geophysics, Oslo, Universitetsforlaget, p245-250

MACK J.W., HAUBRICH R.A., 1961. "Gravity analysis in gas storage exploration". paper presented at 31st. International Society of Exploration Geophysicists meeting, Denver, 1961

MANZONI M., NANNI T., 1977. "Palaeomagnetism of Ordovician lamprophyres from Taylor Valley, Victoria Land, Antarctica". Pure and Applied Geophysics, vol.115, p961-978

MCGREGOR V.R., WADE F.A., 1969. "Geology of Western Queen Maud Mountains". in: Bushnell V.C., and Craddock, C. (eds), Antarctic Map Folio Series, Folio 12, American Geog. Soc. of New York, sheet 16

MCKENZIE D.P., 1967. "Some remarks on heat flow and gravity anomalies". Journal of Geophysical Research, vol.72, no.24, p6261-6273

MENARD H.W., 1971. "The late Cenozoic history of the Pacific and Indian ocean basins". in: Turekian (ed), Late Cenozoic glacial ages, New Haven, Yale University Press, p1-14

MERCER J.H., 1978. "West Antarctic Ice sheet and CO_2 greenhouse effect: a threat of diaster". Nature, vol.271, no.5643, p321-325

MIRSKY A., 1964. "Reconsideration of the 'Beacon' as a stratigraphic name in Antarctica". in: Adie, R.J. (ed), Antarctic Geology, Amstedam, North Holland Pub. Co., p364-378

MIRSKY A., 1969. "Geology of the Ohio Range-Liv Glacier area". in: Bushnell V.C., and Craddock, C. (eds), Antarctic Map Folio Series, Folio 12, American Geog. Soc. of New York, sheet 17

MOLNAR P., ATWATER T., MAMMERICKX J., SMITH S.M., 1975. "Magnetic anomalies, bathymetry and the tectonic evolution of the South Pacific since the late Cretaceous". Geophysical Journal of the Royal Astronomical Society, vol.40, p383-420

MOONEY H.M., 1953. "Magnetic susceptibility measurements in Minnesota, part 1: Technique of Measurement". Geophysics, vol.17, p351-543

NATOPS, 1975. "Performance data". Naval Air Transport Operations no.451, LC-130 F/R manual, US Navy, section 11

NEAL C.S., 1977. "Radio echo studies of the Ross Ice Shelf". unpub PhD thesis in Univ. of Cambridge, England

NETTLETON L.L., 1976. "Gravity and Magnetics in oil prospecting". McGraw Hill International Series in the Earth and Planetary Sciences

NEUBERG H.A.C., THIEL E., WALKER P.T., BEHRENDT J.C., AUGHENBAUGH N.B., 1959. "The Filchner Ice Shelf". Association of American Geographers Annals, vol.49, no.2, p110-119

NORTON I.O., SCLATER J.G., 1979. "A model for the evolution of the Indian Ocean and the breakup of Gondwanaland". Journal of Geophysical Research, vol.84, no.B12, p6803-6830

ORHEIM O., ELVERHØI A., 1981. "Model for submarine glacial deposition". Annals of Glaciology, vol.2, p123-128

PEDDIE N.W., FABIANO E.D., 1976. "Model of Geomagnetic Field for 1975". Journal of Geophysical Research, vol.81, no.14, p2539-2542

PETERS L.J., 1949. "The direct approach to magnetic interpretation and its practical applications". Geophysics, vol.14, p290-320

PRATT J.H., 1855. "On the attraction of the Himalaya Mountains and of the elevated regions beyond them , upon the plumb-line in India.". Phil. Trans. Royal Society, London, vol.145, p53-100

PRESS F., DEWART G., 1959. "Extent of the Antarctic Continent". Science,

vol.129, p462-463

RAVICH M.G., KAMENEV E.N., 1975. "Crystalline basement of the Antarctic". Halstead Press, New York

REX D.C., 1972. "K-Ar age determinations on volcanic and associated rocks from the Antarctica Peninsula and Dronning Maud Land". in: Adie, R.J. (ed), Antarctic Geology and Geophysics, Oslo, Universitetsforlaget, p133-136

REYNOLDS R.L., KELLOGG K.S., 1974. "Palaeomagnetism of igneous rocks of the central Lassiter Coast Antarctica Peninsula". Antarctic Journal of the US, vol.9, p225-226

ROBIN G. de Q., 1975. "Velocity of radio waves in ice by means of a bore-hole interferometric technique". Journal of Glaciology, vol.15, no.73, p151-160

ROBIN G. de Q., DREWRY D.J., MELDRUM D.T., 1977. "International studies of ice sheet and bedrock". Phil. Trans. Royal Society, London, B, vol.279, p185-196

ROBIN G. de Q., EVANS S., BAILEY J.T., 1969. "Interpretation of radio echo sounding in polar ice sheets". Phil. Trans. Royal Society, London, A, vol.265, no.1166, p437-505

ROBIN G. de Q., SWITHINBANK C.W.M., SMITH B.M.E., 1970. "Radio echo exploration of the Antarctic ice sheet". AIHS-IASH Publication 86, p97-115

ROBINSON E.S., 1963. "Geophysical investigations in McMurdo Sound Antarctica". Journal of Geophysical Research, vol.68, no.1, p257-262

ROBINSON E.S., 1964a. "Geologic structure of the Transantarctic Mountains and adjacent ice covered areas". unpub PhD thesis in the Univ. of Winsonsin, Madison

ROBINSON E.S., 1964b. "Some aspects of subglacial geology and glacial mechanics between the South Pole and the Horlick Mountains". Contribution 64-7 of the Department of Geology and Geophysics and Polar Research Center, Univ. of Wisconsin, 88pp

ROSE K.E., 1978. "Radio echo sounding studies of Marie Byrd Land, Antarctica". unpub PhD thesis in the Univ. of Cambridge, England

ROSE K.E., 1979. "Characteristics of ice flow in Marie Byrd Land, Antarctica". Journal of Glaciology, vol.24, no.90, p63-76

ROSE K.E., in press. "High density radio echo sounding of bedrock in Marie Byrd Land, Antarctica". in: Craddock, C. (ed), Antarctic Geoscience, Madison, University of Wisconsin Press

RUNCORN S.K., 1956. "The magnetism of the earth's body". in: Bartels, J. (ed), Handbuch der Physik, vol.47, p498-533

RUTFORD R.H., DENTON G.H., ANDERSON B.G., 1980. "Glacial history of the Ellsworth Mountains". Antarctic Journal of the US, vol.15, no.5, p56-57

SCHARNBERGER C.K., SCHARON L., 1972. "Palaeomagnetism and plate tectonics on Antarctica". in: Adie, R.J. (ed), Antarctic Geology and Geophysics, Oslo, Universitetsforlaget, p843-48

SCHARNBERGER C.K., SCHARON L., in press. "Palaeomagnetism of rocks from Graham Land and Western Ellsworth Land, Antarctica". in: Craddock, C. (ed), Antarctic Geoscience, Madison, University of Wisconsin Press

SCHMIDT D.L., FORD A.B., 1969. "Geology of the Pensacola and Thiel Mountains". in: Bushnell V.C., and Craddock, C. (eds), Antarctic Map Folio Series, Folio 12, American Geog. Soc. of New York, sheet 5

SCHOPF J.M., 1969. "Ellsworth Mountains: Position in West Antarctica due to sea-floor spreading". Science, vol.164, no.3875, p63-66

SHOUTEN H., McCAMY K., 1972. "Filtering marine magnetic anomalies". Journal of Geophysical Research, vol.77, no.35, p7089-7099

SHUEY R.T., PASQUALE A.S., 1973. "End corrections in magnetic profile interpretation". Geophysics, vol.38, no.3, p507-512

SKOU N., SONDERGAARD F., 1976. "Radioglaciology, a 60 MHz Ice Sounder System". TUD, Laboratory of Electromagnetic Theory, Lyngby, no.169

SKOU N., TEILGAARD J., 1978. "Radioglaciology. Design and construction of ice sounding antennas for LC-130". TUD, Laboratory of Electromagnetic Theory, Lyngby, 149pp

SMITH A.G., HALLAM A., 1970. "The fit of the southern continents". Nature, vol.225, p139-144

SMITHSON S.B., 1972. "Gravity interpretation in the Transantarctic Mountains near McMurdo Sound, Antarctica". Geological Society of America Bulletin, vol.83, p3437-3442

SOKOLOVICH E.V., KAMENEV E.N., KOMARISTYY A.A., RUDNIK V.A., 1976. "The oldest rocks of Antarctica (Enderby Land)". International Geology Review,

vol.18, no.4, p371-388

SPLETTSTOESSER J.F., WEBERS G.F., 1980. "Geological investigations and logistics in the Ellsworth Mountains". Antarctic Journal of the US, vol.15, no.5, p36-39

STEED R.H.N., 1980. "Geophysical Investigations of Wilkes land, Antarctica". unpub PhD thesis in the Univ. of Cambridge, England

STUIVER M., DENTON G.H., HUGHES T.J., FASTOOK J.L., 1981. "History of the marine ice sheet in West Antarctica during the last glaciation: a working hypothesis". in: Denton, G.H. and Hughes, T.J. (eds), The Last Great Ice Sheets, Wiley Interscience pub., p319-436

STUMP E., 1973. "Earth evolution in the Transantarctic Mountains and West Antarctica". in: Tarling, D.H. and Runcorn, S.K. (eds), Implications of continental drift to the earth sciences, Academic Press, vol.2, p909-923

STUMP E., in press. "The Ross Supergroup in the Queen Maud Mountains". in: Craddock, C. (ed), Antarctic Geoscience, Madison, University of Wisconsin Press

STUMP E., FAIRBRIDGE R.W., 1975. "Antarctica". in: Fairbridge, R.W. (ed), The Encyclopedia of World Regional Geology, part 1: Western Hemisphere (including Antarctica and Australia), vol.8, Halsted press, 13pp

SWITHINBANK C.W.M., CRABTREE R.D., DOAKE C.S.M., 1976. "Major changes in the map of Antarctica". Polar Record, vol.18, no.114, p295-299

TALWANI M., 1965. "Computation with the help of a digital computer of magnetic anomalies caused by bodies of arbitrary shape". Geophysics, vol.30, no.5, p797-817

TALWANI M., HEIRTZLER J.R., 1964. "Computation of magnetic anomalies caused by two dimensional structures of arbitrary shape". in: Parks, G. (ed), Computers in the Mineral Industries, Stanford University Press, p464-480

TALWANI M., WORZEL J.L., LANDISMAN M., 1959. "Rapid gravity computations for two dimensional bodies with application to the Mendocino submarine fracture zone". Journal of Geophysical Research, vol.64, p49-59

TARLING D.H., 1971. "Gondwanaland, Palaeomagnetism and continental drift". Nature, vol.29, no.5279, p17-21

FORD W.M., GELDART L.P., SHERIFF R.E., KEY D.A., 1976. "Applied Geophysics". Cambridge University Press, Cambridge, England

:L E., 1961. "Antarctica, one continent or two?". Polar Record, vol.10, no.67, p335-348

IAS R.H., SANDERSON T.J.O., ROSE K.E., 1979. "Effect of climatic warming on the West Antarctic ice sheet". Nature, vol.277, no.5695, p355-358

PSON M.R.A., 1972. "Inarticulate brachiopods from the Shackleton Range and their stratigraphical significance". British Antarctica Survey Bulletin, no.31, p17-20

PSON M.R.A., 1975. "New palaeontological and lithological observations on the Legoupil Formation North West Antarctic Peninsula". Bulletin of the British Antarctic Survey, no.41-42, p169-185

Y R., 1978. "East Antarctic Basement Shield". unpub. thesis for the Diploma of Polar Studies in the Univ. of Cambridge, England

LL A., 1959. "Some palaeomagnetic measuements in Antarctica". Arctic, vol.12, no.3, p151-157

.A., 1972. "Geologic survey of Marie Byrd Land". Antarctic Journal of JS, vol.7, no.5, p144-145

.A., WILBANKS J.R., 1972. "Geology of Marie Byrd and Ellsworth Lands". n: Adie, R.J. (ed), Antarctic Geology and Geophysics, Oslo, niversitetsforlaget, p207-214

.A., LONG D.R., in press. "The Swanson Formation, Ford Ranges, Marie yrd Land - Evidence for direct relationship with Robertson Bay roup, North Victoria Land". in: Craddock, C. (ed), Antarctic eoscience, Madison, University of Wisconsin Press

R.I., 1970. "Isostatic response to loading of the crust in Canada". inadian Journal of Earth Sciences, vol.7, p716-727

G., 1969. "Geology of the Terre Nova Bay - McMurdo Sound area, ctoria Land". in: Bushnell V.C., and Craddock, C. (eds), Antarctic Map lio Series, Folio 12, American Geog. Soc. of New York, sheet 14

.R., BRAMALL A.M., 1980. "Palaeomagnetic investigation in the lsworth Mountains". Antarctic Journal of US, vol.15, no.5, p34-35

L.F., 1966. "An upper Cambrian archaeocyathid from Antarctica". ological Society of America, Special papers 87, abtracts for 1965,

p183

WEBERS G.F., CRADDOCK C., RODGERS M.A., ANDERSON J.J., in press. "Geology of the Whitmore Mountains". in: Craddock, C. (ed), Antarctic Geoscience, Madison, University of Wisconsin Press

WEGENER A., 1915. "The Origin of Continents and Oceans". (English translation, 1966), Constable, London

WERNER W., 1953. "Interpretation of magnetic anomalies at sheet-like bodies". Sveriges Geologiska Undersoknig, Ser, C.C. Arsbok, vol.43, no.6

WOOLLARD G.P., 1968. "Continental structure of Antarctica". Contributions of the Hawaii Institute of Geophysics, no.236

WRIGHT T.O., 1980. "Sedimentology of the Robertson Bay Group, Northern Victoria Land, Antarctica". Antarctic Journal of US, vol.15, no.5, p6-7

WYLLIE P.J., 1971. "The Dynamic Earth". Wiley International Edition